DOCTOR OF PHILOSOPHY

The role of peripheral BACE1 in modulating metabolic health

Allsop, David J. P.

Award date:
2018

University of Dundee

The role of peripheral BACE1 in modulating metabolic health

David J. P. Allsop

Thesis submitted for the degree of Doctor of Philosophy

2018

Table of Contents

List of Figures

List of Tables

Acknowledgements

Firstly, I would like to thank my supervisor, Prof. Mike Ashford, for giving me the opportunity to work in his lab and providing me with excellent guidance and support throughout the whole of my project. I'd also like to thank the Medical Research Council for funding this studentship.

Thanks also to everyone in the resource unit, for their help with the *in vivo* aspects of my work. Thanks to Dr. Andy Cassidy from the Tayside Centre for Genomic Analysis for his time and help in performing gene analyses. I'd also like to acknowledge Tayside Tissue Bank, and, in particular, Dr. Susan Bray for her help with all the tissue preparation and staining.

Throughout the course of this project I have worked with a huge number of people with the division of Molecular and Clinical Medicine who have made a huge contribution towards my project. I'd like to thank Dr. Paul Meakin for his help in training me, particularly with regards to my animal work. I'd also like to thank Dr. Alison McNeilly for being an excellent extra source of advice and ideas- particularly where mice are concerned!

The rest of the Ashford lab, past and present, have always been hugely supportive. I was welcomed from the start and it would have been impossible to complete this project without this support. Thanks must go to Gemma, John, Polly, Beth and Jennie for everything they have done for me. In particular, I need to thank DC for being the co-member of team *in vivo*, and chief FACS expert. I would still be working on all of this if it wasn't for your help (and world renowned organisational skills!). To Claire and Suz, the laughs we had while you were both in the lab were brilliant, and no matter where we end up, we will always have the colour run….

I need to say thanks to all the other staff and students of MCM past and present- lunchtime cards have kept me vaguely sane, I think. And so many people have helped make the division a brilliant place to work in- so

thanks to Geoff, Fiona A, Fiona P, Jamie O, Jamie T, Moneeza and Calum to name but a few.

Outside the lab, I have to thank all my friends, and apologise for disappearing for months on end during my project- particularly as I neared the finish line. And also thanks to everyone at Norwood CC for keeping me well grounded by helpfully pointing out my sporting ineptitude every week of the summer, and in particular to Connor and Danny, the most irritating, but ultimately best, pair of the bunch.

And finally, I must say a huge thanks to my parents Jill and Mark, brother Will and whole family, whose endless support and positivity has been invaluable. I would never have got to the start, let alone the end, of this PhD without your help, and it will always be appreciated more than you could imagine.

Declarations

Student Declaration

I hereby declare that all results described in this thesis, unless otherwise stated, are entirely my own work. I further state that the composition of this thesis was performed by myself and none of the material has been submitted for any other degree. Lastly, I verify that all sources have been appropriately cited. The work was carried out in the School of Medicine, University of Dundee, under the supervision of Professor M. L. J. Ashford.

David J. P. Allsop

Supervisor Declaration

I certify that David J. P. Allsop has completed 8 terms of experimental research and has fulfilled the conditions of Ordinance 39, University of Dundee, such that he is eligible to submit the following thesis in application for the degree of Doctor of Philosophy.

Professor M. L. J. Ashford

Abbreviations

AMPK	5' AMP-activated Protein Kinase A
ADAM	A Disintegrin and metalloproteinase domain-containing protein
APPL	Adaptor protein, phospho-tyrosine interacting with PH domain and leucine zipper
ATP	Adenosine Triphosphate
Aβ	Amyloid β peptide
AD	Alzheimer's Disease
adipoQ	adiponectin
AdipoR1/2	Adiponectin Receptor 1/2
AgRP	Agouti-related peptide
AICD	APP Intracellular Domain
APS	Ammonium Persulphate
Arg1	Arginase 1
BACE1/2	Beta Site APP Cleaving Enzyme 1/2
BAD	Bcl-2 Associated Death promoter
BAT	Brown Adipose Tissue
BBB	Blood Brain Barrier
BMI	Body Mass Index
CCL2	Chemokine (C-C motif) ligand 2 (MCP1)
CCL3	Chemokine (C-C motif) ligand 3 (MIP-1a)
CCL4	Chemokine (C-C motif) ligand 4 (MIP-1b)
CCL5	Chemokine (C-C motif) ligand 5 (RANTES)
cDNA	Complimentary Deoxyribonucleic acid
CLAMS	Complete Lab Animal Monitoring System
CNS	Central Nervous system
CTF	C- Terminal Fragment
DAG	Diacylglycerol
DIO2	Deiodinase 2
ECM	Extracellular Matrix
ELISA	Enzyme-linked Immunosorbent Assay
ELK1	ETS domain-containing protein 1

Elovl3	Elongation of very long chain fatty acids protein 3
ER	Endoplasmic Reticulum
ERK	Extracellular signal-related kinase
eWAT	epididymal white adipose tissue
FACS	Fluorescence-activated Cell Sorting
FGF21	Fibroblast Growth Factor 21
FGFR1	Fibroblast Growth Factor Receptor 1
FOXO	Forkhead Box O
GGA3	Golgi-localised y-adaptin ear containing ARF-binding
GIP	Gastric Inhibitory Peptide
GKRP	Glucokinase Regulatory Protein
GLP	Glucagon-like peptide 1
GP	Glycogen Phosphorylase
GSIS	Gluscose Stimulated Insulin Secretion
GSK3	Glycogen Synthase Kinase 3
GTT	Glucose Tolerance Test
HFD	High Fat Diet
HIF-1α	Hypoxia Inducible Factor 1α
HSL	Hormone Sensitive Lipase
i.p.	Intraperitoneal
ICV	intracerebroventricular
IDE	Insulin Degrading Enzyme
IGF1	Insulin-like Growth Factor 1
IGFR	Insulin-like Growth Factor Receptor
IKKB	IkB Kinase B
IL10	Interleukin 10
IL1β	Interleukin 1β
IL6	Interleukin 6
IR	Insulin Receptor
IRS1/2	Insulin Receptor Substrate 1/2
ITT	Insulin Tolerance Test
iWAT	inguinal White Adipose Tissue
JAK2	Janus Kinase 2

JNK	c-Jun N Terminal Kinase
LTP	Long Term Potentiation
MAPK	Mitogen-activated Protein Kinase
MRI	Magnetic Resonance Imaging
NAFLD	Non-alcoholic Fatty Liver Disease
NC	Normal Chow
NEFA	Non-esterified Fatty Acid
NF-κB	Nuclear Factor κB
NOS2	Nitric Oxide Synthase 2
NPY	Neuropeptide Y
PAGE	Polyacrylamide gel electrophoresis
PAI-1	Plasminogen activator inhibitor-1
PBS	Phosphate buffered saline
PCR	Polymerase chain reaction
PDK1	phosphoinositide dependent Kinase 1
PET-CT	Positron emission tomography–computed tomography
PGC1α	Peroxisome proliferator-activated receptor- y coactivator 1-α
PI3K	Phosphoinositide 3-kinase
PKA	Protein kinase A
POMC	Pro-opiomelanocortin
PPAR	Peroxisome proliferator-activated receptor
PRDM16	PR domain containing 16
PTP1B	Protein-tyrosine phosphatase 1B
RAGE	Receptor for advanced glycation end products
RER	Respiratory Exchange Ratio
RNA	ribonucleic acid
RT	Real time
sAPPα/β	soluble amyloid precursor protein α/β
SDS	Sodium dodecyl sulphate
SH2	Src homology 2
SHC	Src homology 2 domain-containing
SHP2	Src homology 2 domain-containing phosphatase 2
SOCS3	Suppressor of Cytokine Signalling 3

STAT	Signal transducer and activator of transcription 3
SVF	Stromal vascular fraction
T2DM	Type 2 Diabetes Mellitus
TAE	Tris-acetate- EDTA
TBST	Tris-buffered saline- Tween-20
TEMED	Tetramethylenediamine
TLR4	Toll-like Receptor 4
TNF-α	Tumour necrosis factor-α
UCP1	Uncoupling Protein 1
UPR	Unfolded protein response
UTR	Untranslated region
WAT	White Adipose Tissue
WT	Wild-type
YM1	Chitinase-like 3 (Chil3)

Summary

Obesity and Type II Diabetes Mellitus (T2DM) are two of the most prevalent medical conditions in modern society, associated with increased energy intake and diminished physical activity. Obesity and T2DM correlate with several physiological perturbations, including impaired glucose homeostasis, increased inflammation and other conditions such as Alzheimer's disease (AD). These factors, accompanied with an ageing population, has generated a need to produce novel therapeutics that could prevent or delay the onset of these conditions.

One of the leading hypotheses as to the mechanism behind the neuronal death associated with AD is the production of amyloid beta (Aβ) peptides, which ultimately form plaques and are present in AD brains when examined post-mortem. The rate limiting step in the production of these peptides is the cleavage of amyloid precursor protein (APP) by β-site APP cleaving enzyme 1 (BACE1). BACE1 is an aspartyl protease which is up-regulated by a number of cellular stresses, including hypoxia and metabolic stress, such as with high fat diet (HFD). This led to the suggestion that BACE1 may play a role in energy homeostasis. Consequently, the lab found that global knock-out of BACE1 protects mice from diet induced obesity (DIO), with accompanying improvements in glucose homeostasis, leptin sensitivity, alongside reduced inflammation. Furthermore, central infusion of Aβ peptides worsened glucose homeostasis and increased body weight in mice on a high fat diet (HFD). These data suggested that APP processing plays an important role in energy homeostasis, but it remained unclear as to whether these effects were centrally or peripherally mediated.

This thesis sought to address these questions. Mice with BACE1 removed from adipocytes are protected from DIO, with improvements in glucose homeostasis, without substantial changes in adipose tissue inflammatory status. Furthermore, peripheral infusion of Aβ peptides did not replicate the central infusion experiments. These data suggest that adipocyte BACE1 plays a vital role in modulating peripheral energy homeostasis, but that this

is likely to be via BACE1 substrates than other APP, further implying that BACE1 inhibitor drugs could be repurposed to treat obesity and associated pathologies.

Chapter 1 - Introduction

1.1 Obesity

Obesity is a term used to describe individuals with an abnormally high amount of body fat. A normal body fat percentage can vary between ethnic groups and between males and females, but the condition is a growing problem worldwide, described as being of epidemic proportions with an estimated 13%, or 600 million, of the global population being considered obese in 2014 (WHO 2016b). Obesity can be measured by several means, including by waist circumference and body fat percentage, but the most prevalent method in adults is by measuring an individual's Body Mass Index (BMI). This calculation does not take body fat into account, but rather is the total body mass divided by the square of height. Individuals with a BMI between 25 and 30 are considered overweight, whilst individuals with a BMI greater than 30 are regarded as obese (NHS 2016).

Obesity develops where there is an imbalance in energy intake over output. These conditions arise in part through increasingly sedentary lifestyles and the consumption of diets which contain high levels of fats and sugars (Finer 2003). Worryingly, levels of obesity are continuing to rise globally, doubling since 1980 (WHO 2017). Obesity is considered a risk factor for a large number of other pathologies, such as cardiovascular disease, liver disease, insulin resistance, Type 2 Diabetes Mellitus (T2DM) and some forms of cancer. Specifically, obesity seems to be the first stage in the development of a condition termed as "metabolic syndrome" (O'Neill & O'Driscoll 2014), a condition which arises through a combination of risk factors that ultimately result in more serious diseases such as cardiovascular disease and T2DM. Indeed, WHO guidelines for the diagnosis of metabolic syndrome are high levels of insulin (hyperinsulinaemia), combined with either high abdominal obesity, high triglyceride levels, high blood pressure or high levels of urinary albumin.

1.2 Type 2 Diabetes Mellitus

T2DM is one of the 2 major forms of diabetes. Type 1 diabetes is often present from birth and is considered an auto-immune disease, in which the pancreatic beta cells which produced insulin are destroyed, preventing

insulin secretion. Subsequently, this leads to high levels of blood glucose (hyperglycemia) and, if left uncontrolled, results in damage to blood vessels and organs. In contrast, T2DM is often associated with an unhealthy lifestyle and makes up approximately 90% of the diabetic population (Diabetes UK 2017a).

T2DM develops either where the pancreas fails to produce enough insulin, or where enough insulin is produced, but it is unable to act to enable glucose uptake, or a combination of these two factors. The latter situation is referred to as “insulin resistance”, and is often a precursor state to the development of T2DM in itself. Worldwide, the global population with T2DM is increasing rapidly, increasing from a prevalence in adults of 4.7% in 1980 to 8.5% by 2014 (WHO 2016a). There are now estimated to be 422 million people living with T2DM, with approximately 3.5 million within the UK as of 2014 (Diabetes UK 2017b).

1.3 Insulin

1.3.1 Insulin Signalling

Insulin is a 51-amino acid protein synthesised and secreted from the pancreatic islets by beta cells. Insulin secretion in normal physiology can be triggered by changes in plasma glucose concentration being sensed by glucokinase, which phosphorylates glucose-6-phosphate and generates ATP, inducing the closure of potassium activated ATP (KATP) channels and membrane depolarisation. Through this, intracellular concentrations of calcium increase through activation of voltage gated calcium channels (Wilcox 2005), ultimately stimulating release of insulin. In pancreatic beta cells, the glucose transporter GLUT2 plays a key role in sensing glucose levels, in rodents (Unger 1991).

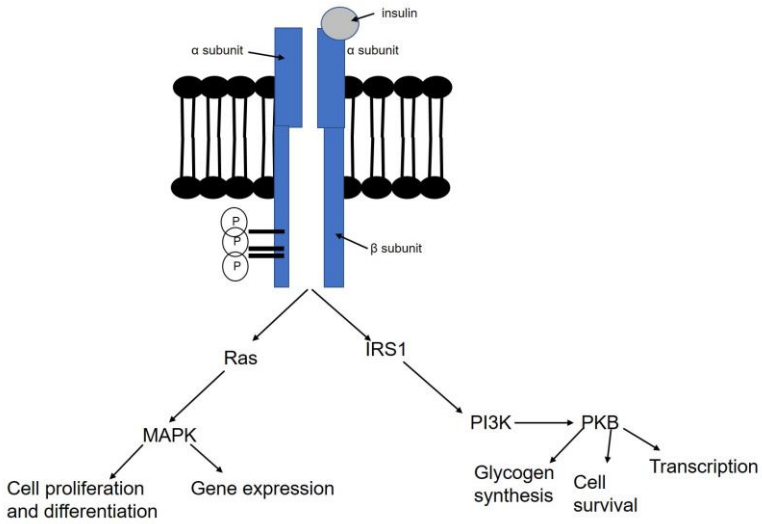

Figure 1.1 Insulin signalling pathway

Insulin binds to the insulin receptor and induces dimerization, resulting in autophosphorylation of the β subunit, and signalling via the IRS/PKB and Ras/MAPK signalling cascades

Insulin signalling occurs through the insulin receptor (IR; see figure 1.1). The IR is a glycoprotein, comprising an α subunit and a β subunit. Insulin binding on the α subunit causes the dimerization of the protein, forming a tetramer, and this $\alpha_2\beta_2$ complex autophosphorylates the β subunit at tyrosine residues 1158, 1162 and 1163- a step which results in the recruitment of substrates required for the activation of downstream pathways, mostly via Insulin Receptor Substrate 1 or 2 (IRS-1/2) (Guo 2014). There are several IRS family member proteins, of which IRS1 and IRS2 are by far the most widely studied. Indeed, double knock-out of IRS1 and 2 in the liver induces hyperglycemia, hyperinsulinemia and abolition of downstream insulin signalling (Guo 2014). There appear to be numerous tissue specific roles for these proteins. For example, IRS2 is important in lipid, but not glucose, metabolism in the muscle. In the liver, IRS1 is reported to be important in regulating gluconeogenesis, whereas IRS2 is heavily implicated in lipogenesis (Taniguchi et al. 2005). IRS3, 4 and 5 have also been characterised, but have much reduced expression levels in rodents, and apparently limited roles in insulin signalling (Boucher et al. 2014). The major 2 pathways concerned in insulin signalling are the phosphoinositide 3 kinase (PI3K) and Ras/MAPK pathways (Siddle 2011).

Upon IRS1 phosphorylation, the IRS proteins can associate with the regulatory subunits of PI3K, via SRC homology 2 (SHP2) domains. PI3K converts PIP2 to PIP3 via phosphorylation, which recruits PtdIns(3,4)P2/PtdIns(3,4,5)P3-dependent kinase 1 (PDK1), and protein kinase B (PKB- also called Akt) to the cell membrane. PKB is then activated via phosphorylation at a threonine residue. Activated PKB has multiple substrates and functions. Firstly, it deactivates glycogen synthase kinase 3 (GSK3), which serves to activate glycogen synthase and enable the production of glycogen. It also mediates translocation of GLUT4 to the cell surface to enable glucose uptake, (Bevan 2001), particularly in adipose tissue, skeletal muscle and cardiac muscle. Through phosphorylation of Forkhead Box (FOXO) transcription factors it inhibits hepatic glucose production, and promotes cells survival via phosphorylation of Bcl2-associated death promoter (BAD) (Manning & Cantley 2007). It also induces mammalian target of rapamycin (mTOR) associated protein synthesis via p70 S6 kinase and eukaryotic initiation factor (eIF) proteins (Bevan 2001).

IRS1 also interacts with growth factor receptor bound protein 2 (Grb2) (Skolnik et al. 1993), an adaptor protein, and SHP2, which induce mitogenic processes through Fos and ETS domain containing protein 1 (ELK1) transcription factors. Upstream of this, the IR also interacts with a substrate, SHC, which thereby activating the Ras/MAPK pathway independently of IRS1 interaction (Bevan 2001).

The IR can also be bound by insulin-like growth factor 1 (IGF1), which is a growth factor which is similar in structure to insulin. Usually insulin signals through the IR and IGF through the IGF-R, but each can bind to the other, albeit with lower affinity (Belfiore et al. 2009). Interestingly, heterodimers also exist containing, for example, one IRA and one IRB subunit, and receptors can even form hybrids which incorporate IGF receptor subunits. IRA is expressed particularly in the brain whereas IRB exist mainly in peripheral insulin sensitive tissues such as the liver, adipose tissue, muscle and kidney (Belfiore et al. 2009). Hybrid receptors account for up to 50%

of all insulin responsive receptors, but are expressed at low levels in liver, with higher levels recorded in brain, heart, adipose, kidney and muscle (Belfiore et al. 2009). Hybrids of IRA/B with IGFR have reduced affinity for insulin compared to homodimers (Benyoucef et al. 2007).

1.3.2 Insulin Resistance

Insulin resistance occurs where there is a diminished response to a normal level of insulin. Insulin resistance is invoked by factors such as inflammation, high fat diet and stress, and can be linked to perturbations in insulin signalling. Indeed, mice which lack IRS1 are insulin resistant (Araki et al. 1994) and mice lacking IRS2 are diabetic, with reduced beta cell mass and glucose intolerance (White et al. 1998).

Mechanistically, it has been shown that serine phosphorylation of IRS1 contributes towards insulin resistance (Qiao et al. 1999) by reducing its ability to bind PI3K as a substrate, in contrast to its tyrosine phosphorylation. One key source of insulin resistance during obesity arises through increased levels of ER stress. In *ob/ob* and HFD fed mice, levels of liver and WAT ER stress are increased (Özcan et al. 2004), leading to increased levels of c-JUN N terminal kinase (JNK), which can also be induced by factors such as free fatty acids and stress, contributes towards inflammation and has been shown to induce insulin resistance by phosphorylating IRS1 at serine 307 (Lee et al. 2003).

Activation of mTOR by amino acids or indeed by hyperinsulinemia causes serine phosphorylation of IRS1 by p70 s6 kinase, and mice lacking this enzyme are significantly remain sensitive to insulin (Um et al. 2004), with reduced IRS1 serine phosphorylation.

Inflammation induces insulin resistance, and TNF-α is one of the key pro-inflammatory cytokines involved in this process. It has been shown that TNF-α can also induce serine phosphorylation of IRS1 in mouse adipocytes (Hotamisligil et al. 1996). Another pro-inflammatory protein is

protein kinase C theta (PKCθ). This kinase has been shown to cause serine phosphorylation of IRS1 *in vitro* (Li et al. 2004).

Another proposed mechanism for insulin resistance occurs downstream of IRS1. PI3K is known to itself exist as a heterodimer, consisting of a catalytic unit known as p110 and a regulatory subunit, known as p85. The p85 subunit exists both as a monomer and as a heterodimer, but both compete for the same binding point on IRS1. It has been demonstrated in cultured muscle cells that increased expression of p85 is associated with decreased PI3K activity (Giorgino et al. 1997).

1.4 Glucose

Glucose is a carbohydrate which is of vital importance as the major energy source for cellular respiration. Glucose is converted to and stored in a complex branched form as glycogen, with the largest reserves in the liver. Within the liver, hepatocytes take up glucose from the glucose transporter GLUT2 (Roden & Bernroider 2003). Glucose is then converted to glucose-6-phosphate, utilizing glucokinase, an enzyme which can be inhibited by Glucokinase Regulatory Protein (GKRP). The reverse reaction is catalysed by glucose-6-phosphatase. Glucose-6-phosphate is converted to glucose-1-phosphate, which is converted to UDP-glucose by UDP-glucose pyrophosphorylase. Glycogenin is required for the addition of the first few glucose molecules, which bind to a tyrosine residue within the enzyme's active site. At this point, glycogen synthase (GS) begins to facilitate the addition of glucose monomers to the existing oligomer by creating an α-1,4-glycosidic bond. Glucose can also be produced by gluconeogenesis from non-carbohydrate precursor sources including amino acids and triglycerides.

The reverse occurs during lipogenesis, in which acetyl-coenzyme A is produced from glucose and is converted into fatty acids and subsequently triglycerides (Kersten 2001). This process occurs in liver and adipose tissue and is regulated by numerous hormones, most notably insulin (Kersten 2001), which occurs through upregulation of transcription factors

including sterol regulatory-binding-element-binding-protein c (SREBPc), which can invoke the production of GK and fatty acid synthase (Azzout-Marniche et al. 2000). Skeletal muscle also stores a significant amount of glycogen, and is vital for rapid energy production (Ørtenblad et al. 2013), particularly during exercise .

1.4.1 Glucose Homeostasis

Glucose homeostasis is the maintenance of a normal physiological range of blood glucose, and is tightly regulated process. Insulin is a key determinant of blood glucose. Insulin promotes glucose uptake from the blood, primarily through Glucose Transporter (GLUT) proteins. This family of transporters are facilitative hexose transmembrane proteins, of which there are 14 forms known of in humans (Thorens & Mueckler 2010). All play a role in glucose processing, but the majority of peripheral insulin dependent glucose uptake is through GLUT4 transporters, by increasing the rate of translocation of GLUT4 vesicles to the plasma membrane and by slightly decreasing the amount of receptor internalization, thus increasing the overall quantity of GLUT4 on the plasma membrane, allowing glucose transport into the cell (Saltiel & Kahn 2001). Whilst skeletal muscle is responsible for around 75% of insulin stimulated glucose uptake (Klip & Paquet 1990), the WAT is clearly important, as it has been shown that specific knock out of GLUT4 in the WAT causes insulin resistance, with secondary impacts within both the muscle and liver (Abel et al. 2001). Glucose can be transported through GLUT1 in an insulin independent manner (Ebeling et al. 1998), with GLUT1 playing an important role in maintaining basal glucose uptake (Kraegen et al. 1993).

Conversely, secretion of glucagon from pancreatic alpha cells when low blood glucose is detected stimulates glycogenolysis- breakdown of glycogen back to glucose- to occur. Debranching enzyme and glycogen phosphorylase (GP), convert glycogen back into glucose-1-phosphate. Glucagon achieves this through activating PKA which, in turn, leads to phosphorylation of GP kinase, which can then phosphorylate- thereby activating GP itself (Jiang & Zhang 2003). Glucagon also inhibits

glycogenesis by causing phosphorylation of glycogen synthase, which in this case is an inactivating phosphorylation (Bollen et al. 1998).

Numerous other factors modulate glucose homeostasis. Two examples are the gut incretin peptides such as GIP (Gastric Inhibitory Polypeptide) and GLP-1 (Glucagon like Peptide 1) which both reduce blood glucose by increasing insulin secretion (Andersen et al. 1978; Orskov et al. 1996). Another important peptide is amylin, which is secreted from beta cells and acts by slowing gastric emptying and suppressing glucagon secretion (Aronoff & Berkowitz 2004). Other factors can also raise blood glucose, including adrenaline- which raises glycogenolysis; cortisol, which induces gluconeogenesis; and thyroxine, which also induces glycogenolysis.

1.5 Adipose Tissue

1.5.1 White Adipose Tissue (WAT)

The White Adipose Tissue (WAT) is composed of fat containing adipocytes and a stromal vascular fraction (SVF), which contains microvascular cells, pre adipocytes, and a number of resident immune cells (Lafontan 2014). Indeed, some reports have previously suggested that the SVF contributes to up to 50% of the cells in WAT (Trayhurn & Beattie 2017). For decades, it was assumed that WAT was primarily a tissue whose main role was to store energy in the form of fat, but more recent studies have revealed a much more widespread importance, to the extent that WAT is now considered a highly important, highly metabolically active tissue (Rosen & MacDougald 2006; Trayhurn & Beattie 2001).

1.5.1 Locations and Distribution

Mammalian WAT depots can be roughly divided into 2 major categories- firstly the subcutaneous depots, which arise underneath skin, such as inguinal fat. The second are visceral depots, which are deeper deposits, which often form around organs, such as the peri-renal or epididymal depots (Tchkonia et al. 2013). Some have suggested that the most damaging fat accumulation during obesity is ectopic fat- that is, fat which accumulates around organs where there is normally no fat present.

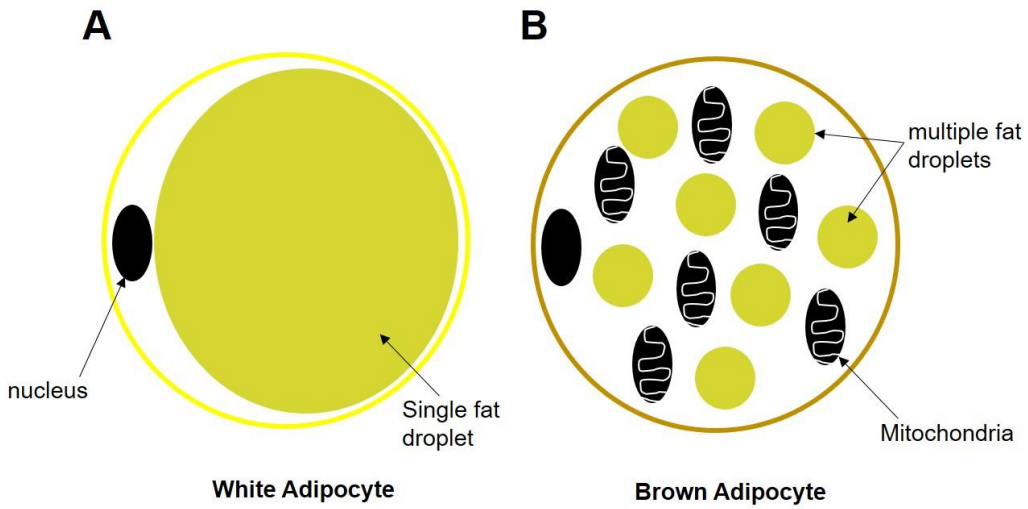

Figure 1.2 Basic morphology of Adipocytes

Structures of an (A) white and (B) brown adipocyte.

1.5.2 Brown Adipose Tissue

Brown adipose tissue (BAT) is a distinct type of adipose tissue found in mammals, which has been given increasing attention over recent years. Morphologically, BAT differs in its structure to WAT. Instead of the single lipid droplet characteristic of WAT, BAT cells contain several smaller droplets (Figure 1.2). The major function of BAT is in non-shivering thermogenesis, the production of heat. BAT contains a large number of mitochondria, and achieves this heat production through the uncoupling of oxidative phosphorylation from ATP synthesis (N & Fain 1968). This process is mediated by uncoupling protein 1 (UCP1) (Nicholls et al. 1978), indeed, BAT is usually recognised as such by expression of this protein (Boudina & Graham 2014).

Rodent studies suggested that BAT activation is associated with a healthier phenotype. Indeed, over 30 years ago, several drugs which activate the sympathetic nervous system were found to reduce fat mass and body weight, with increased metabolic rate in several different rat and mouse models of obesity (Dulloo & Miller 1984). Interestingly, if BAT is transplanted into donor mice, glucose tolerance and insulin sensitivity is improved, with enhanced glucose uptake (Stanford et al. 2013). Activation

of AMPK leads to insulin independent glucose uptake in BAT (Teperino et al. 2012).

For some time, it had been thought that these studies may not be translational, as in humans BAT was mainly present in new-borns, which is then reduced in adulthood. However, recent research has suggested that some healthy, adult individuals possess regions of BAT, as determined through Positron emission tomography–computed tomography (PET-CT) scanning and by UCP1 expression (Cypess et al. 2009; Virtanen et al. 2009). Because of this research, BAT has been suggested to be an "anti-diabetic" tissue in humans. Indeed, one study using a small number of human participants demonstrated that men who possessed BAT had enhanced glucose disposal and energy expenditure following cold exposure, in contrast to men lacking BAT (Chondronikola et al. 2014).

Perhaps more interesting is the potential for WAT to go through a "browning" process, resulting in "beige" or "brite" adipose tissue (Nedergaard & Cannon 2014) by which WAT begins to express uncoupling protein 1 (UCP1) through adrenergic activation, thereby raising the possibility that it may be conceivable to induce non-shivering thermogenesis to burn excess fat. Indeed, in humans, brown fat is more likely to in fact be of this variety rather than BAT *per se*. Beige adipocytes may develop *de novo* in subcutaneous WAT, as demonstrated by Wang and colleagues. Mature adipocytes were labelled with LacZ, and mice then cold-exposed. UCP1 positive cells were found not to express LacZ , showing they had been newly differentiated (Q. A. Wang et al. 2013). Alternatively, it has also been postulated that beige adipocytes are converted from white adipocytes upon stimulation, as UCP1 staining appears to increase without an overall increase in adipocyte number, suggesting conversion rather than synthesis of new cells (Vitali et al. 2012). These adipocytes have enhanced thermogenic potential when stimulated, such as during cold exposure or as a response to adrenergic agonist drugs (Wankhade et al. 2016). Browning of adipocytes occurs predominantly in subcutaneous rather than visceral depots, and appears to be heavily reliant

on the expression of PR domain containing 16 (Prdm16), a transcriptional regulator predominantly expressed in subcutaneous WAT (Seale, Heather M. Conroe, et al. 2011). Indeed, haploinsufficiency of Prdm16 results in reduced browning capacity of subcutaneous WAT in response to beta 3 adrenergic agonist treatment (Seale, Heather M Conroe, et al. 2011).

Many factors have been reported to be involved in inducing browning in response to cold exposure or other stimuli such as adrenergic activation. These factors generally serve to interact with PGC-1α, peroxisome-proliferator- activated receptor gamma (PPARγ) or PGC-1α, which in itself shows increased expression in response to cold exposure (Puigserver et al. 1998). This gives rise to activation of a browning transcriptional programme, incorporating genes such as deiodinase 2 (DIO2), UCP1 and cidea (Lo & Sun 2013).

In the browning process, thermogenesis is started through sympathetic activation, followed by increased cAMP activation leading to PKA activation, which induces lipolysis, causing influx of free fatty acids into mitochondrial membranes. Knock-out of perilipin reduces norepinephrine stimulated thermogenesis (Souza et al. 2007), demonstrating the importance if phosphorylating this protein in adaptive thermogenesis. These fatty acids prevent the inhibition of UCP1, which therefore gives rise to an influx of protons, thus uncoupling phosphorylation. The energy created in this process is then dissipated as heat (Figure 1.3).

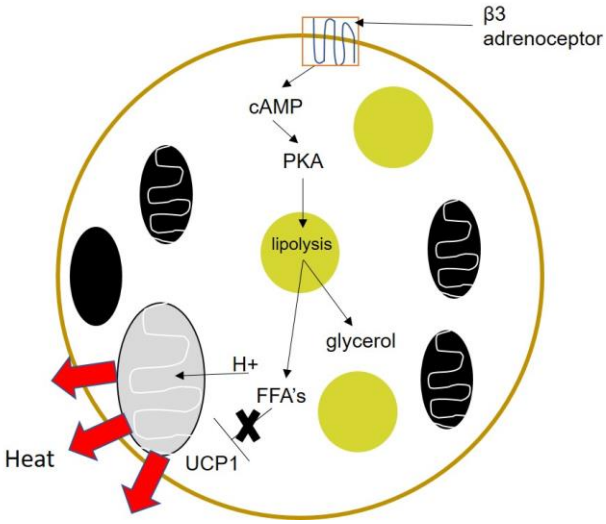

Figure 1.3 Thermogenesis within BAT

Thermogenesis occurs via sympathetic activation, leading to raised cAMP and PKA levels. This induces lipolysis, and the production of FFAs, which prevent inhibition of UCP1, giving rise to the passage of H^+ from the intermembrane space, through the inner mitochondrial membrane and on to the mitochondrial matrix down its electrochemical gradient, creating energy which is dissipated as heat.

Much attention has therefore been focussed on activating this non-shivering thermogenesis, as it allows increased energy expenditure and is seen as a strong pharmacological target for treating obesity. As stated, a large number of varying factors have been reported to enhance thermogenesis in animal models, ranging from micro RNAs to existing drugs such as the cancer drug imatinib and novel new targets such as FGF signalling (Wankhade et al. 2016).

1.5.3 Functions of WAT

One of the primary functions of WAT is, of course, as a long-term store of energy. WAT stores fatty acids, and releases them for use by other tissues at times of energy shortage by lipolysis (Duncan et al. 2007). This process is innervated by the sympathetic nervous system.

It has also become evident that WAT plays an important role in maintaining glucose homeostasis and energy balance in general. Mice without WAT are profoundly diabetic, with significantly raised plasma glucose, insulin and free fatty acids. They also have increased post-natal mortality rates

(Moitra et al. 1998). Much of these effects are due to the release of adipose derived cytokines, variably named as adipokines of adipocytokines, and their paracrine effects as discussed below.

In contrast to obesity, there are rare cases of lipodystrophic syndromes, which is where fat production is limited or even completely ablated. Interestingly, patients with these syndromes often have similar metabolic deficits to obese individuals, with impaired insulin sensitivity and elevated levels of lipid in the blood (dyslipidemia) (Huang-Doran et al. 2010). Loss of fat storage capacity in mice results in fat accumulation in other tissues, causing non-alcoholic fatty acid liver disease (NAFLD), reduced pancreatic islet function and ultimately symptoms very similar to T2DM (Savage 2009). This further emphasises the importance of adipokines and the WAT in general as a metabolic tissue.

1.5.4 Leptin and leptin signalling

Perhaps the best characterised adipokine is leptin. In the 1950s, the *ob/ob*, or obese, mouse was first found through a chance mutation. The *ob/ob* mouse gains weight rapidly throughout its lifespan, and is hyperglycemic and has life-long insulin resistance (Fellmann et al. 2013; Garthwaite et al. 1980). In 1994, leptin was discovered to be responsible for the phenotypic effects of the *ob gene* (Zhang et al. 1994). Leptin is a 16kDa adipose tissue derived hormone, and was discovered to have 'anti-obesity' properties. Leptin has a key role in regulating energy balance in mammals, with plasma levels of the protein being highly correlated with both BMI and body fat percentage (Maffei et al. 1995).

Treatment of lipodystrophic patients with leptin significantly improves glycaemic control (Oral et al. 2002). Central administration of leptin to lean mice was shown to reduce food intake and body weight, which suggested that the primary site of leptin action was the brain. (Halaas et al. 1997) Furthermore, these effects were not replicable in obese mice, suggesting that obese animals are resistant to the effects of increasing levels of leptin.

There are 5 alternatively spliced leptin receptor forms, named Ob-R(a-e). The long form of the receptor, Ob-Rb, is responsible for leptin signaling which occurs primarily in the hypothalamus for the purposes of regulating energy homeostasis (Friedman & Halaas 1998). Db/db mice have a point mutation which prevents leptin signaling through Ob-Rb (Chua et al. 1996; Chen et al. 1996), and these mice also have obese phenotypes similar to the ob/ob mouse. The db/db mouse becomes diabetic within 2 weeks of birth, with elevated plasma insulin and glucose, polyuria and depletion of pancreatic beta cells, which results in premature death if left unresolved.

The leptin receptor binds to Janus Kinase 2 (JAK2), which, when stimulated by leptin is activated and autophophorylated, which then phosphorylates Ob-Rb on three tyrosine residues, namely Tyr985, 1077 and 1138 (Figure 1.4). These phosphorylated residues act as the binding sites for downstream effector proteins, which contain a Src homology 2 (SH2) domain (Zhou & Rui 2013).

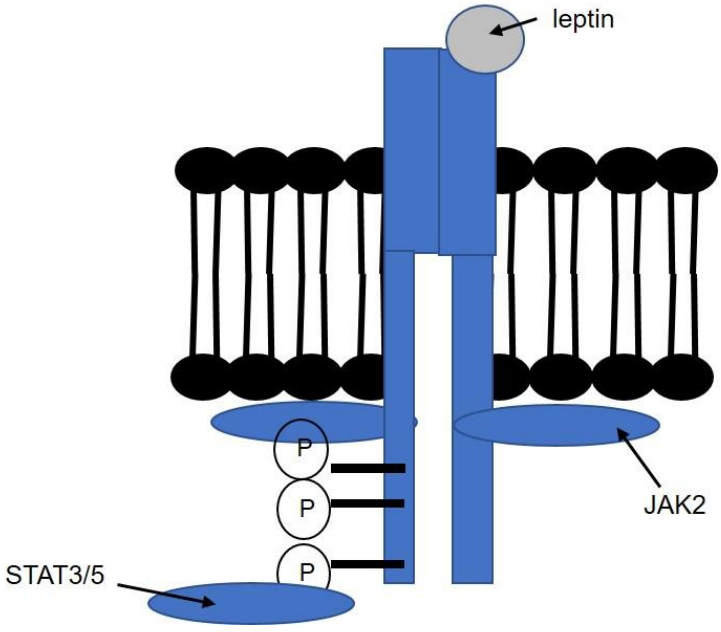

Figure 1.4 Leptin Signalling

Leptin binds to the leptin receptor and causes activation of JAK2. JAK2 induces phosphorylation of tyrosine residues of the leptin receptor. Phosphorylation of tyrosine 1138 induces activation of leptin signaling, primarily via STAT3

Two important downstream proteins are the signal transducer and activation of transcription (STAT) proteins STAT3 and STAT5. Both are phosphorylated and activated by JAK2. When STAT3 is activated, it dimerizes and translocates into the nucleus, where it acts as a transcription factor for several proteins, including Suppressor of Cytokine signalling 3 (SOCS3). Preventing STAT3 activation by mutating the tyrosine site on JAK2, to which it binds, to a serine residue, results in mice with an obese phenotype, which clearly demonstrates the importance of this signalling pathway in energy homeostasis (Bates et al. 2003).

1.5.5 Leptin Resistance

Leptin resistance is a state that arises during obesity. Leptin resistance is defined by an inability of the body to respond to leptin by reducing food intake and appetite. During obesity, high levels of circulating leptin- termed hyperleptinemia- arise. There are a few mechanisms that have been suggested as responsible for the development of leptin resistance. The theory that hyperleptinemia directly causes leptin resistance by activating negative feedback mechanisms is supported by studies which show that SOCS3, which acts as a negative modulator of leptin signaling is itself induced by leptin (Figure 1.5, Bjørbaek et al. 1998). SOCS3 binds phosphorylated tyrosine 985 of the leptin receptor (Bjorbak et al. 2000). Furthermore, SOCS3 reduction in the brain is associated with enhanced leptin sensitivity (Howard et al. 2004). Another negative regulator of leptin signaling is PTP1B, which can act by directly dephosphorylating JAK2, thus preventing further signaling from occurring (Figure 1.5, Zabolotny et al. 2002).

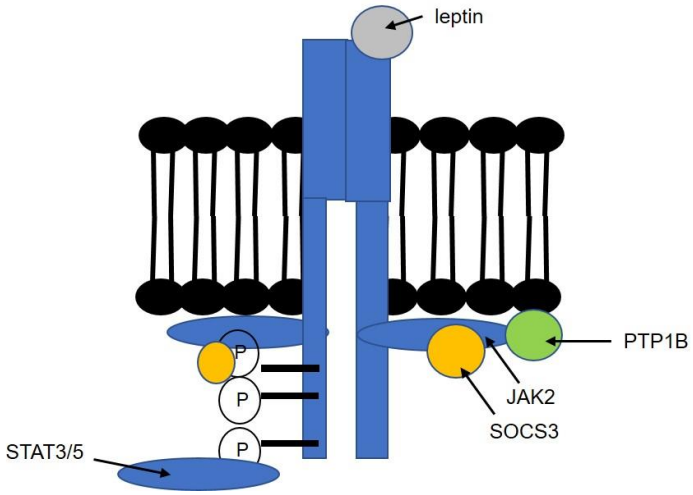

Figure 1.5 Negative regulation of leptin signalling

SOCS3 and PTP1B are the major negative regulators of leptin signaling, targeting and causing dephosphorylation of JAK2 and the leptin receptor itself to prevent leptin signalling

More recently it has also been demonstrated that hyperleptinemia itself is necessary for the onset of leptin resistance (Knight et al. 2010), as clamping leptin levels in obese ob/ob mice on a high fat diet to lean levels retained leptin sensitivity, as measured by reduced food intake in response to an acute dose of leptin, adding further credence to this theory.

Alternatively, it has also been proposed that dietary fats themselves are directly responsible for leptin resistance. Direct central infusion of the fatty acid palmitate can in itself induce leptin insensitivity as measured by reduced phosphorylated STAT3 (Kleinridders et al. 2009). MyD88 is an adapter in fatty acid-TLR4 signalling thought to contribute to peripheral insulin resistance, and removing this in the CNS enhances leptin sensitivity. It is also possible that the consequences of raised fat levels can contribute to leptin resistance through modulating intermediary paths such as endoplasmic reticulum (ER) stress and inflammation. ER stress leads to an accumulation of misfolded proteins within the ER, and induction of ER stress with exogenous factors in SHSY-5Y cells is able to reduce leptin signaling through enhancing PTP1B signaling (Bjørbaek et al. 1998), which is another negative regulator of leptin signaling. Central injection of inducers of ER stress worsen leptin sensitivity and prevents the

anorexigenic effects of leptin in mice (Won et al. 2009)Furthermore, in obese mice, hypothalamic ER stress is raised, and is associated with leptin resistance. Upregulating the unfolded protein response (UPR) enhances leptin sensitivity (Ozcan et al. 2009) and reducing ER stress pharmacologically can enhance ob/ob mouse leptin sensitivity (Ozcan et al. 2009).

Interestingly, both SOCS3 and PTP1B are also associated with insulin signaling and insulin resistance, which suggests that there may be some common mechanisms between the two pathways. SOCS1 and SOCS3 were first revealed as able to degrade IRS1 and 2 (Rui et al. 2002), although later studies have suggested that SOCS1 and SOCS3 reduce insulin signaling via differing paths, as overexpressing SOCS3 reduces phosphorylation of both IRS1 and IRS2 whereas overexpressing SOCS1 in hepatocytes preferentially affected IRS2 (Ueki et al. 2004). Leptin is able to signal via PI3K, another pathway shared within insulin. Initial evidence suggested that leptin stimulated PI3K activity occurs specifically via IRS2 (Kellerer et al. 1997), however the situation now appears to be more complex. The adapter protein SH2B1 appears able to interact with JAK2 and also IRS1, with binding of SH2B1 able to promote JAK2 mediated phosphorylation of IRS1 via its SH2 domain (Li et al. 2007). PTP1B is also heavily involved in insulin signaling, as mice lacking PTP1B are resistant to obesity and have enhanced insulin sensitivity (Elchebly et al. 1999). The PI3K pathway also appears to be important in hypothalamic neurons, as PI3K is stimulated by both leptin and insulin in the anorexigenic POMC neurons (Xu et al. 2005). In the arcuate nucleus, infusing 2 different PI3K inhibitors prevents insulin dependent weight loss (Niswender et al. 2003). Fa/Fa rats, which are susceptible to obesity have improved glucose tolerance when injected with an adenoviral vector expressing the signaling form of the leptin receptor, but this is reversed with PI3K inhibitors (Morton et al. 2005).

Insulin is able to stimulate leptin gene expression in primary murine adipocytes (Lee et al. 2001), and can also stimulate secretion from

adipocytes. This process requires PI3K signaling, as blocking it with wortmannin prevents leptin secretion (Wang et al. 2014). Another potential link between insulin and leptin resistance is the lipid signaling molecule ceramide. Inhibiting ceramide synthesis in the murine myotube C2C12 cell line improves insulin sensitivity by raising phosphorylation of PKB (Chavez et al. 2013). This may be through SOCS3, as inhibition of ceramide synthesis also reduces SOCS3 and reduces leptin mRNA expression in obese mice, while SOCS3 mRNA is raised in 3T3-L1 adipocytes when stimulated with ceramide (Yang et al. 2009).

1.5.6 Adiponectin and Adiponectin Signalling

More recently, adiponectin has been revealed to be another highly important adipokine in energy homeostasis, particularly within peripheral tissues. It was discovered shortly after leptin, and is induced in differentiated 3T3-L1 adipocytes (Scherer et al. 1995). Not long after this the same protein was identified within human plasma (Nihon Seikagakkai. et al. 1996). Unlike a majority of adipokines, plasma adiponectin decreases in obese individuals (Arita et al. 1999).

Use of transgenic mouse models demonstrated that adiponectin plays a key role in insulin sensitivity, as adiponectin knock out mice are insulin resistant and glucose intolerant on a high fat diet background (Kubota et al. 2002; Maeda et al. 2002). Adiponectin circulates as multimers formed by di-sulphide bonds, which can be divided into high molecular weight, medium molecular weight and low molecular weight categories. Recent work has shown that it is the highest molecular weight multimer that appears to be most relevant to insulin sensitivity, with reduced levels of this form correlated with insulin resistance and impaired lipid oxidation (Lara-castro et al. 2006).

Adiponectin production is controlled by a number of means. Adiponectin is increased acutely, as demonstrated using fast-refeed experiments, via CCAAT enhancer binding protein (C/EBP) (Park et al. 2004). There is also a sexual dimorphism, with males producing less adiponectin than females,

suggesting androgens may be important in the negative regulation of adiponectin (Whitehead et al. 2006) . Production can also be reduced by TNF-α, endothelin-1, β-adrenergic agonists, IL-6 and glucocorticoids such as dexamethasone (Whitehead et al. 2006). Another factor which influences adiponectin is fibroblast growth factor 21 (FGF21), which increases adiponectin in adipocytes (Lin et al. 2013).

Adiponectin signals through 2 known receptors, AdiponectinR1 is expressed mostly in skeletal muscle, whereas adiponectinR2 is mostly found in liver (Whitehead et al. 2006). Adaptor protein, phosphotyrosine interacting with PH domain and leucine zipper 1 (APPL2), has been revealed to bind to the receptors, and is necessary for transducing adiponectin signalling (Mao et al. 2006). Through this signalling pathway, adiponectin can act to activate AMPK, PPARα and IRS1/2 (Ruan & Dong 2016). Through these mediators adiponectin mediates its physiological function, to enhance insulin signalling, fatty acid oxidation, energy expenditure and glucose uptake.

Adiponectin has also been shown to induce browning of WAT. Adiponectin KO mice do not undergo the beiging process when cold-exposed, but this is recovered when they are supplemented with exogenous adiponectin (Hui et al. 2015), showing another way in which adiponectin could influence adiposity.

1.5.7 Other Adipokines

Besides leptin and adiponectin, a plethora of novel adipokines have been identified as capable of modulating whole body metabolism. Apelin, which has been shown to enhance insulin sensitivity and decreased fat accumulation (Castan-Laurell et al. 2012). Omentin, which is inversely correlated with obesity (M et al. 2015), and VEGF, which has been shown to prevent metabolic dysfunction through its angiogenic properties (Sung et al. 2013).

1.5.8 Adipose Tissue dysfunction in Obesity

During the development of obesity, a number of different events occur within adipose tissue which can lead to dysfunction and many of the chronic pathologies associated with obesity.

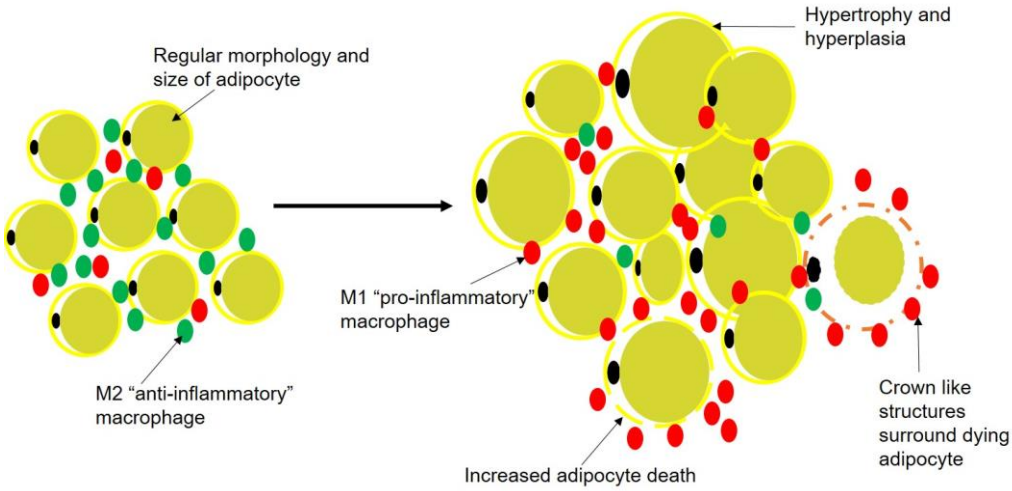

Figure 1.6 Adipose tissue dysfunction during obesity

During obesity the number and size of adipocytes increase, and the inflammatory status of the WAT is pushed towards an M1 pro-inflammatory phenotype, with crown-like structures forming around dead and dying adipocytes.

One issue that arises during chronic obesity is a change in the ability of WAT to expand. During periods of over nutrition adipose tissue expands by increasing the size of the adipocytes (known as hypertrophy), and increasing the number of adipocytes (termed hyperplasia). During obesity, the more important of these is hypertrophy (Jo et al. 2009). In humans the number of adipocytes has been reported to remain almost constant during adulthood, demonstrating the importance of hypertrophy in obesity (Spalding et al. 2008). These processes requires a number of adaptations to occur within WAT (figure 1.6). If these adaptations cannot keep pace with the required expansion, serious metabolic defects such as insulin resistance and fibrosis are likely to occur (King & Newmark 2012). One example is the remodelling of the extracellular matrix (ECM). Collagens are upregulated in diabetic rodent models and removal of collagen VI is associated with improved metabolic health (Khan et al. 2009).

Furthermore, adipose tissue expansion often results in reduced vasculature coverage, making the tissue hypoxic. In humans it has been shown that WAT oxygen levels are reduced in obese individuals, and reduced oxygen levels in the tissues are correlated with increased inflammation (Pasarica et al. 2009), which is discussed in more detail in the following section. There is also evidence that hypoxic adipose tissue has a reduced capacity to secrete the insulin sensitiser adiponectin (Wang et al. 2007).

One study provided evidence that in patients with abdominal obesity there was a reduced capacity to store NEFAs (non-esterified fatty acids) after meals (McQuaid et al. 2011), suggesting that this abnormal lipid metabolism could contribute to the accumulation of ectopic fat. Lipotoxicity is the accumulation of fat in non-adipose tissue regions, predominantly occurring in muscle and liver, and is often as a result of lipid processing intermediates such as diacylglycerols (DAGs) and ceramides. In human muscle, cell lipid concentration is correlated with diminished whole body insulin sensitivity in non-obese individuals (Krssak et al. 1999).

Therefore a key theory in adipocyte biology is the “overspill theory”, whereby WAT appears to have limited expandability, if this storage capacity is breached, or if adipocyte differentiation is prevented, there is significant overspill of fat into other peripheral tissues, leading to insulin resistance and T2DM in a similar way to lipodystrophic syndromes (Danforth 2000). Indeed, impaired differentiation of adipocytes is implicated in obesity, because in the Pima Indian population, who are predisposed to diabetes, consumption of high calorie diet is associate with an increase in weight, but not adipocyte size (Kashiwagi et al. 1985). This was an acute over-feeding study rather than a chronic diet, suggesting differences in adipocyte metabolism in these two scenarios.

1.5.9 Inflammation in WAT

An important aspect of obesity is the emergence of a chronic low-grade inflammatory status, which is now well characterised and is associated with

insulin resistance and T2DM. WAT is particularly implicated in these processes. Some inflammatory molecules are created in adipocytes, and multiple others within the macrophages associated with WAT, within the SVF. WAT can secrete a wide range of such molecules, including TNF-α, IL-6, MCP1, PAI-1 and visfatin (Shoelson et al. 2006), alongside a plethora of others. It is now clear that both upregulation of endogenous inflammatory components and increased chemoattraction of exogenous immune cells contribute to the pathogenesis of insulin resistance and metabolic dysfunction during chronic nutrient excess.

In 2003 Xu and colleagues demonstrated that a number of inflammatory related genes found in macrophages, including MIP-1α and MCP-1, were upregulated in WAT in mice fed a high fat diet, as well as in *ob/ob* and *db/db* mice. Equally, adipocytes were shown to have increased macrophage levels in high fat fed mice (Xu et al. 2003). During obesity, large numbers of macrophages infiltrate the WAT (Ouchi et al. 2011), which differentiate into M1 like (classically activated) macrophages, which possess a pro-inflammatory phenotype (Kwon & Pessin 2013), in contrast to the alternative, more anti-inflammatory M2 (alternatively activated) phenotype. Unlike regular inflammatory responses, where the pro-inflammatory phase is resolved with an anti-inflammatory phase, in obesity there remains a chronic low-grade inflammation response in the WAT. In obesity, there is an increased adipocyte death rate as shown by increased TUNEL staining and increased expression of pro apoptotic factors such as caspase-3. Furthermore this is associated with impaired glucose tolerance (Alkhouri et al. 2009). Macrophages which infiltrate the WAT appear to surround dead or dying adipocytes, forming so called “crown-like structures”, which play a role in scavenging the residual lipid droplets left over (Cinti et al. 2005).

The chemoattractant Monocyte Chemoattractant Protein 1 (MCP-1, also known as CCL2) is considered particularly important, as it induces macrophages to enter the adipose tissue, as well as dendritic cells and memory T-cells. The mRNA levels in WAT and plasma protein levels of

MCP-1 increase in diet induced obese mice, and levels were found to correlate with body weight (Takahashi et al. 2003). Furthermore, overexpression of MCP-1 within the WAT causes a systemic insulin resistance and a hugely increased quantity of macrophages within the WAT (Kamei et al. 2006).

Mechanistically, within adipocytes, high levels of glucose and saturated fatty acids up- regulate IL-6 and TNF-α via TLR and NFκB activity (Ajuwon & Spurlock 2005). This causes an increase in the expression of NFκB- a transcription factor responsible for controlling the expression of many of these pro-inflammatory adipokines. NFκB can further be activated upstream by IKKβ. Indeed, heterozygous deletion of IKKβ improves glucose homeostasis (Yuan et al. 2001).

TNF-α was one of the first inflammatory cytokines found to be released from WAT. In 1993, it was shown that by blocking TNF-α signaling insulin sensitivity was greatly increased (Hotamisligil et al. 1993). TNF-α mRNA is present in the WAT of obese mice, and it was found that stimulating these cells with chronic TNF-α decreased the expression of a number of genes found in adipose, including GLUT4, which indicated a link between release of factors from WAT which could directly influence insulin stimulated glucose uptake (Youssef-Elabd et al. 2012).

Other adipokines can also modulate inflammation. Leptin appears to be strongly pro-inflammatory. TNF-α upregulates leptin receptor expression and also increases the amount found on the cell surface (Gan et al. 2012). Leptin itself is able to increase cytokine production in mouse macrophage cells (Gainsford et al. 1996). Expression of the chemoattractants CCL3, CCL4 and CCL5 are all upregulated in mouse macrophages by the addition of leptin (Kiguchi et al. 2009).

Adiponectin, on the other hand, has been described as anti-inflammatory. Treatment of macrophages with adiponectin promotes expression of the anti-inflammatory cytokine Arg-1 and IL-10, whereas knock out of

adiponectin results in reduced Arg-1 and increased TNF-α (Ohashi et al. 2010). In RAW264 cells adiponectin suppresses NF-κB signalling (Yamaguchi et al. 2005) by preventing the phosphorylation of the kinase I κB, which then prevents the activation of NF-κB.

1.6 Alzheimer's Disease

Alzheimer's Disease (AD) is the most common form of dementia, first described by Alois Alzheimer in the early 20th century. The major symptom is memory loss, caused by the destruction of neurons within both the cortex and the limbic brain areas (Aderinwale et al. 2010). The exact mechanisms behind this destruction remain unclear, but all AD patients upon post-mortem are found to have characteristic neurofibrillary tangles of hyper-phosphorylated tau and plaques of amyloid beta (Aβ) protein (Rafii & Aisen 2009).

1.6.1 APP Processing

Aβ production stems from the cleavage of Amyloid Precursor Protein (APP), a transmembrane receptor protein (LaFerla et al. 2007). APP is cleaved via two major cleavage pathways. In the amyloidogenic pathway, which occurs approximately 5% of the time, Beta site APP Cleaving Enzyme 1 (BACE1) cleaves APP, leaving a 99-amino acid chain, or C-terminal fragment β (CTF β) bound within the membrane and releasing a soluble APPβ fragment known as sAPPβ. A second cleavage by a γ-secretase enzyme complex, consisting of a complex of four separate elements- presenilin, nicastrin, anterior pharynx defective 1 and presenilin enhancer 2 (Edbauer et al. 2003), cleaving C99 to release a fragment of Aβ between 38 and 43 amino acid residues in length, and leaving behind an APP intracellular domain (AICD) fragment.

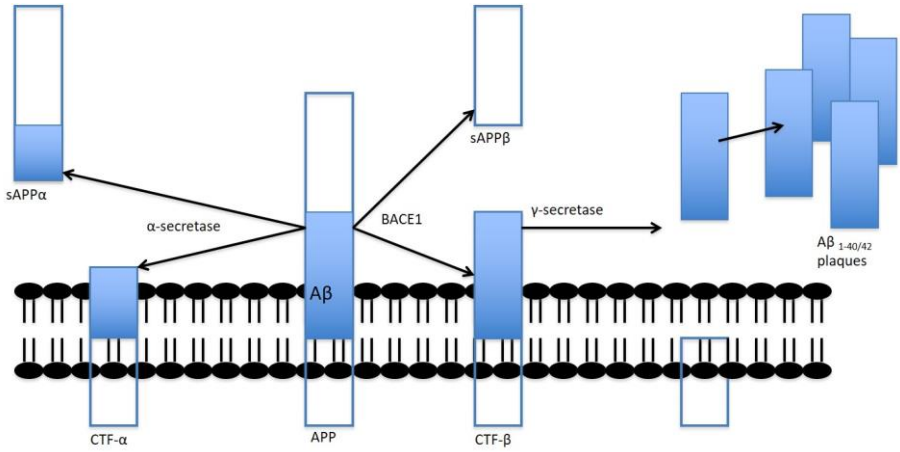

Figure 1.7 APP processing

APP processing occurs via the amyloidogenic (right) and non-amyloidogenic (left) pathways

In the non-amyloidogenic pathway, which occurs most of the time, an α-secretase causes the initial cleavage, but this time within the Aβ domain. This leaves a C terminal fragment (CTFα) and a soluble APPα fragment (sAPPα). Again, this fragment undergoes a second γ-secretase enzyme complex cleavage, leaving an AICD and a soluble N terminal fragment, also known as p3, preventing the formation of amyloidogenic plaques. This process is summarised in figure 1.7.

APP processing may be important for a number of neurological processes. Knock out of APP impairs performance in mice in spatial awareness- as measured through performance in a water maze task. APP KO mice also suffer from impaired long-term potentiation (LTP), which is a measure of synaptic strength often used in studies related to learning and memory, suggesting memory deficits in these mice. Furthermore, these mice display body and brain weight deficits, suggesting APP is important in neuronal developmental processes. All of these phenotypes are rescued by the knock-in of the sAPPα fragment (Ring et al. 2007). As well as this, sAPPα is able to repress BACE1 activity and therefore Aβ production (Obregon et al. 2012) , suggesting a positive feedback mechanism to maintain non amyloidogenic APP processing.

APP processing is pushed more towards the amyloidogenic processing pathway through a number of means, of which high cholesterol or high fat diets are two (Julien et al. 2010; Refolo et al. 2000). Whilst aggregated Aβ is thought to be neuronally toxic, it has been proposed that peptide monomers may have neuroprotective effects. Some evidence for this is the fact that treating hippocampal cells with the first 28 residues of Aβ enhanced survival (Whitson et al. 1989). $A\beta_{1-40}$ is thought to be neurogenic (Chen & Dong 2009), and promotes the entry of neural progenitor cells into S-phase.

1.6.2 Amyloid Aggregation

The major products of the amyloidogenic pathway are amyloid beta (Aβ) peptides 40 or 42 amino acid residues in length, the latter being the most amyloidogenic (Iwatsubo et al. 1994). The amyloid monomers can form dimers, and small oligomers. This is known as a seeding process, and is required for further aggregation. This process is the rate-limiting stage of aggregation, and can be sped up by adding exogenous compound (Harper & Lansbury 1997). From this stage, a seeded growth phase takes place, in which the oligomers aggregate further into proto-fibrils, fibrils and ultimately the plaques found in the brains of AD patients (Finder & Glockshuber 2007). Oligomerisation appears to differ between the $A\beta_{40}$ and $A\beta_{42}$ species, with $A\beta_{40}$ forming monomers, dimers and trimers, compared to $A\beta_{42}$ which form larger paranuclei structures that rapidly form into proto-fibril like structures (Bitan et al. 2003). $A\beta_{42}$ is the more toxic of the two major species, and it forms fibrils at concentrations around 5 times lower than $A\beta_{40}$ (Finder & Glockshuber 2007). There is some debate as to the most toxic structure. Injection of fibrils into rat hippocampi produces effects similar to those seen in AD- particularly impaired neuronal synaptic transmission and working memory tasks (Stéphan et al. 2001), however using a similar protocol, rats injected with oligomeric forms performed much worse in the Morris water maze learning paradigm that those injected with fibrils (He et al. 2012).

1.6.3 The alpha secretase

The α-secretase has the characteristics of a metalloprotease, of which the most likely candidates were members of the a disintegrin and mettaloprotease (ADAM) family. Numerous ADAM family members have been shown to cleave APP *in vitro,* including ADAM9, ADAM10 and ADAM17 (Lichtenthaler 2011). In situ hybridisation studies revealed that ADAM10 in particular co-expressed with APP (Lammich et al. 1999) suggesting that it, rather than ADAM17, may be the most likely candidate as the main α-secretase.

Knockdown of any of these three ADAMs did not result in complete abrogation of α-secretase cleavage of APP, suggesting that all 3 could play a role in APP cleavage, and that compensation may occur where one is not available.

More recent studies have revealed that ADAM10 is likely the most physiologically relevant ADAM from α-secretase. Firstly, α-secretase cleavage of BACE1 is significantly reduced in a brain specific ADAM10 knock out mouse (Jorissen et al. 2010). As well as this, RNAi knockdown of ADAM10 but not ADAM9 or ADAM17 in SHSY-5Y, HEK293 and primary neurons results in abolition of APP cleavage via the α-secretase pathway (Kuhn et al. 2010).

1.6.4 The gamma secretase

Knock-out of the presenilin 1 element of the gamma secretase complex in mice significantly reduced the production of amyloid beta (De Strooper et al. 1998) and is known to contain the catalytic unit of the complex, and so is considered the most important member of the complex. The other components have other roles in the maturation of the enzyme and substrate recognition. Beyond APP, the gamma secretase is also a substrate for other substrates including notch, neuroligin and EphrinA4 (M et al. 2015).

The gamma secretase has been investigated as a potential target for AD, but due to the number of different substrates for gamma secretase, the majority of gamma secretase inhibitors have failed due to significant side effects, including gastrointestinal issues, increases in skin cancer and a worsening in cognitive performance (Henley et al. 2014) which have been in many cases attributed to inhibition of notch signalling.

1.7 Beta Site APP Cleaving Enzyme 1 (BACE1)

1.7.1 Identification and characterisation as the beta-secretase

The rate-limiting step for the amyloidogenic events is BACE1 activity. As such, a lot of work has been done to characterize the protein. BACE1 was first identified as the protein responsible for beta secretase activity by Vasser and colleagues, using an expression cloning strategy. Overexpression was found to increase secretase activity, and mRNA for the protein was found to be expressed predominantly in the brain, particularly in the hippocampus, cortex and cerebellum, but also in several peripheral tissues, most notably in the pancreas (Vassar R, et al. 1999). Subsequent investigation revealed that mRNA in the pancreas was a splice variant missing much of exon 3, which results in an immature protein lacking enzymatic activity (Bodendorf et al. 2001) .

At a similar time, several other groups independently reported on BACE1, under the name asp2, or aspartic protease 2, which exhibited the same properties as BACE1 (Sinha et al.1999; Hussain et al. 1999). BACE1 was found to possess all the properties anticipated of an enzyme which cleaved APP to produce amyloid beta peptides. Firstly, overexpression of BACE1 into HEK293 cells stably expressing APP did not alter APP levels, but did increase the production of both $A\beta_{1-40}$ and $A\beta_{1-42}$ (Vassar et al. 1999) BACE1 possesses two aspartic protease active site motifs, and mutating the aspartic acid residue on either of these 2 sites was shown to prevent enzymatic activity. Finally, it was shown that BACE1 cleaved APP exclusively at the residues that had been previously detected- namely asp1, the residue at which amyloid protein begins.

BACE1 is a highly promiscuous enzyme, with a number putative substrates already identified using proteomic approaches (Hemming et al. 2009). A large number of these targets are type 1 transmembrane proteins, but do not appear to possess a sequence which could be predictive of cleavage by BACE1. A study utilising bioinformatics to search for potential substrates found over 900 examples (Johnson et al. 2013) A large number of potential substrates are involved in cell communication, but there are also wide ranging other roles of the putative substrates. Some of the identified proteins could be relevant to the present studies. For example, BACE1 may target several proteins involved in immune cell regulation, such as the toll-like receptors and T cell receptors, or mitofusin-2 (Johnson et al. 2013), which is important for mitochondrial fusion, and therefore could be relevant to hypothalamic ER stress as discussed earlier.

BACE1 presents a particularly attractive target for AD drugs, as its activity is the rate limiting step in the production of Aβ- thus targeting the enzyme has the potential to prevent the accumulation of neurotoxic Aβ. As a result, much work has been undertaken to understand the role of BACE1 in normal physiology. Knock out mice were generated, and it was found that loss of BACE1 activity prevented the formation of Aβ plaques, and significantly abrogated the levels of Aβ species in the brain, with normal tissue morphology (Luo et al. 2001). Further studies showed that such mice are behaviourally and developmentally normal (Roberds et al. 2001). Even at 14 months of age, no abnormalities or compensatory gene changes are detectable in knock out mice (Luo et al. 2003).

Conversely, some groups have reported certain deficits in knock-out mice. Dominguez and colleagues found increased pup mortality and growth defects, alongside a slightly hyperactive phenotype, shown through increased total movement in open field and elevated zero maze tasks (Dominguez et al. 2005). Our laboratory has also utilised BACE1 KO mice, but have found no evidence of increased seizures, and also have comparable nose to tail body length (Meakin et al. 2012). Myelination also seems to be affected, with hypomyelination detected in the hippocampus

and cerebral cortex of BACE1$^{-/-}$ mice (Willem et al. 2006). In optic nerves, myelin sheath thickness was reduced in knock out mice (Hu et al. 2006). Knock out mice also appear more susceptible to seizures (Hitt et al. 2010) compared to wild-type controls, and hippocampal mossy fibre axon guidance defects (Hitt et al. 2012). These phenotypes indicate that BACE1 has a role in a number of physiologically important functions, and therefore completely abolishing BACE1 activity may not be advantageous. Instead, partial inhibition of BACE1 may prevent any of these possible roles from being impacted too heavily, and a number of drug companies have produced BACE1 inhibitors, which have reached various levels of development, with several in clinical trials between stage I and III (Vassar 2014).

1.7.2 Regulation

BACE1 is an aspartyl protease 501 amino acids in length, which is coded from a region on the long arm of chromosome 11 (Kim & Tanzi 1999). Structurally, the protein consists of a 21 amino acid residue length N-terminal domain, a pro-domain, a catalytic domain, which contains 2 aspartic acid catalytic residues typical of the aspartyl proteases, a transmembrane domain and cytoplasmic tail (Figure 1.8, Rossner et al. 2006). BACE1 is produced in the endoplasmic reticulum, and then localises to the golgi, trans golgi network and endosomes, which is the primary site of Aβ production.

BACE1 can be regulated both at a transcriptional and translational level. The BACE1 promoter contains a number of transcription factor binding sites. Putative binging regions have been discovered for NF-κB, Sp1, and PPARγ (Rossner et al. 2006). NF-κB signalling has been shown to up-regulate BACE1 transcription using a luciferase reporter assay, and levels were up-regulated in AD patients (Chen et al. 2012b). However, the situation may be more complex, as it has also been proposed that whereas NF-κB may act as an activator of BACE1 transcription in the activated astrocytes that are commonplace in AD, in neurons in normal physiological conditions NF-κB instead acts as a repressor (Bourne et al. 2007). As many

inflammatory stressors such as LPS, TNF-α and IL-1β can induce NF-κB signalling, this may be an important way in which BACE1 regulation could contribute towards metabolic dysfunction.

PPARγ is known to repress BACE1 transcription, and several drugs which work as PPARγ agonists such as ibuprofen also repress BACE1 (Sastre et al. 2006). PPARγ is a signalling molecule involved in a multitude of processes related to lipid and glucose metabolism as well as the process of adipogenesis (Wahli et al. 1995).

Another two transcription factors with binding sites on the BACE1 promoter are sp1 and yin yang 1 (YY1). Sp1 upregulates BACE1 (Christensen et al. 2004), whereas YY1 also promotes BACE1 gene expression in primary rat neurons, although there is limited co-localisation between BACE1 and YY1 *in vivo* (Nowak et al. 2006), suggestive of a limited physiological relevance.

HIF-1α, a transcription factor that responds to low cellular oxygen concentrations, has also been suggested as a regulator of BACE1, and it has been shown that over-expression of HIF-1α increases BACE1 levels at both an mRNA and protein level, and that conditional knock-out of HIF-1α in the hippocampus and cortex reduces BACE1 in these brain regions (Zhang et al. 2007). It has also been shown that high glucose, as is seen in T2DM patients, up-regulates BACE1 via HIF-1 α (Lee et al. 2016).

There are also suggestions that BACE1 expression can be regulated by cholinergic signalling. Stimulation of M1 or M3 muscarinic receptors with agonists raises BACE1 protein expression in a dose dependent manner, whereas stimulation of M2 receptors reduces BACE1 protein expression in SHSY-5Y cells (Zuchner et al. 2004). Indeed, for many years it has been known that secretion of sAPP fragments is upregulated by stimulating cells which over-express M1 and M3 muscarinic receptors (Nitsch et al. 1992). Furthermore, AD patients have an upregulation of M1 receptors relative to M2, potentially providing a mechanism for the increased BACE1 activity in the disease. Muscarinic receptors perform a number of roles relating to

glucose homeostasis. M1 receptors are responsible for acetylcholine stimulated glucose uptake in C2C12 cells (Gautam et al. 2006), and mice lacking the M3 receptor in these cells possess impaired glucose homeostasis and insulin release, which is reversed when the receptor is over-expressed (Gautam et al. 2006)

The post translational control of BACE1 is also important in its physiological function (figure 1.8). The bioactive lipid ceramide has been shown to increase the half-life of BACE1, and also regulates APP processing, as inhibitors of ceramide synthesis reduces both α and β CTFs (Puglielli et al. 2003). Ceramide is lipid molecule with a number of biological functions, ranging from cell proliferation to apoptosis (Hannun & Obeid 2008), and is also involved in insulin resistance. Interestingly, lipid induced insulin resistance in muscle has been strongly linked to increased ceramide synthesis. This occurs via TLR4 signalling, specifically with saturated fatty acids (Holland et al. 2011). A precursor to ceramide production, palmitate, has also been shown to upregulate BACE1 at a transcriptional level (Liu et al. 2013). Recently, it has been suggested that palmitic acid induces BACE1 and amyloid production via the PKB pathway (Kim et al. 2017). Therefore, BACE1 may be upregulated by fatty acid metabolism, and these processes may provide a link between BACE1, HFD and insulin resistance.

BACE1 possesses a long 5' untranslated region (UTR), and it is believed that this region may also have a role in BACE1 translation. Presence of the 5' UTR but not the 3' UTR is able to suppress BACE1 protein, but not mRNA levels (Lammich et al. 2004).

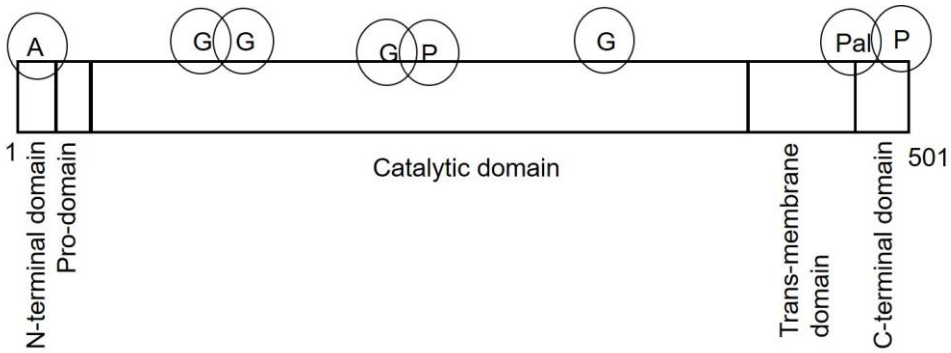

Figure 1.8 Structure and post translational modification of BACE1

BACE1 undergoes a number of post-translational modifications which are important in its function. P= phosphorylation, A=acetylation, G=glycosylation, Pal= palmitoylation

BACE1 trafficking is important for its function. Mature BACE1 is trafficked from the trans-golgi network to the surface of the cell where it undergoes endocytosis to early endosomes, in which the majority of its APP cleavage role is performed (Vassar et al. 2014). From here BACE1 can be recycled between the plasma membrane and endosomes (Huse et al. 2000), for which the cytoplasmic tail is vital, as its removal increases accumulation upon the cell surface. Alternatively, BACE1 can be retrogradely trafficked back to the trans-golgi network, or sorted to late endosomes and later lysosomes for subsequent degradation. Much of these processes are dependent on post translational modification.

The most important BACE1 modification appears to be the N- linked glycosylation of the protein at 4 asparagine residues. Site directed mutagenesis has shown that they are very important for the enzymatic activity of BACE1 (Charlwood et al. 2001) , with mutation of just one site limiting proteolytic activity to just 40% of none mutated protein. Initial glycosylation occurs within the endoplasmic reticulum, before more complex glycosylation takes place to produce mature BACE1 within the golgi (Capell et al. 2000). As well as glycosylation, palmitoylation occurs at 3 cysteine residues in the transmembrane/cytosolic tail region, which have been theorized to have a role in anchoring BACE1 to the plasma membrane (Benjannet et al. 2001). It has been reported that palmitoylation of BACE1 may be important in targeting the protein to lipid rafts (Araki

2016), which are regions of the plasma membrane characterised by high concentrations of cholesterol and glycosphingolipids. The precise relevance of this feature is still unclear, but it has been suggested that APP cleavage by BACE1 occurs within these areas preferentially, as depletion of cholesterol *in vitro* reduces Aβ production (Ehehalt et al. 2003).

BACE1 also possesses a di-leucine motif, which binds to Golgi localised γ ear containing ARF binding protein 3 (GGA3). The binding can be increased through phosphorylation of serine residue 498 on BACE1, and is important in the cycling of proteins between the golgi and endosomes, (Kang et al. 2010). This phosphorylation step occurs only within mature BACE1 (Walter et al. 2001). Equally, BACE1 is ubiquitinated at lysine 501, and GGA's are also able to bind ubiquitin, trafficking BACE1 to lysosomes for subsequent degradation. More evidence for the importance of GGA3 in lysosomal degradation of BACE1 is that inhibition of GGA3 stabilises BACE1 (Tesco et al. 2007).

More recently, an additional BACE1 phosphorylation site has been identified at threonine 252. This phosphorylation is mediated by p25/cdk5. Mutation of the residue reduces BACE1 activity, and, interestingly, levels of phosphorylated BACE1 at this site are also elevated in AD patients (Song et al. 2015), suggesting this may be a good way to target BACE1 in AD.

Finally, transient acetylation of BACE1 by ATases 1 and 2 occurs at 7 lysine residues within the N terminal domain. BACE1 is acetylated within the golgi during maturation. Acetylated protein is required for BACE1 to leave the endoplasmic reticulum, whereas non acetylated protein is retained and degraded within the endoplasmic reticulum (Costantini et al. 2007).

1.7.3 BACE 2

An additional aspartyl protease, BACE2, was discovered very shortly after BACE1. BACE2 is a homolog of BACE1, and some have argued it cleaves

APP at the β site (Farzan et al. 2000). Others, however suggest cleavage is limited at this site and instead acts more like an alternative α- secretase (Yan et al. 2001). Initial studies of the enzyme suggested that, unlike with BACE1, inhibition of BACE2 did not reduce production of amyloid-β in cells (Yan et al. 2001). The mRNA expression levels of BACE2 in the brain are lower than those of BACE1, with BACE2 more highly expressed peripherally, particularly within the colon, kidney and pancreas (Bennett et al. 2000). As a result, BACE2 has not been as widely studied as BACE1 as a target for treating AD. Global knock out of the BACE2 gene in mice gives rise to healthy and viable offspring, and does not result in any abnormal behavioural phenotype (Dominguez et al. 2005).

1.8 Links between Metabolic Disease and Alzheimer's Disease

It is known that having T2DM can lead to cognitive defects and an increased risk of suffering from AD (Biessels et al. 2006). Conversely, AD sufferers have been shown to be more prone to developing T2DM than non-AD control patients (Janson et al. 2004). Therefore, it seems likely that the two are linked by some common factors. Interestingly, the similarities are such that some have suggested Alzheimer's essentially represents a brain specific "type 3 diabetes" (Steen et al. 2005; de la Monte & Wands 2008). Although precise mechanisms are unclear, there are known parallels between the two disease states. Magnetic resonance imaging has shown that in some areas of the brain there is reduced glucose metabolism in AD patients (Cummings 2004). Advanced glycosylation end products (AGEs) form at accelerated rates in diabetics, and have been shown to occur within the plaques and tangles prevalent in AD. RAGE (Receptor for AGE) has been found to also function as cell surface receptors for Aβ (Luchsinger & Gustafson 2009), which suggests they may play a role in the neurodegeneration events of AD. One common symptom of T2DM is hyperinsulinemia- a high level of circulating insulin. Whilst insulin can be produced within the brain, it is also able to cross the blood-brain barrier. There, it has been shown to compete with amyloid beta (Aβ) peptide for the Insulin Degradation Enzyme (IDE), and deletion of the IDE

gene causes increases in endogenous levels of Aβ (Farris et al. 2003). Insulin signalling is also impaired in AD brains through increased levels of TNF-α, which raises stress kinases such as JNK, ultimately deactivating IRS1 (Bedse et al. 2015). Therefore, a key feature of AD is impaired central insulin signalling, in contrast to T2DM, which is traditionally viewed as a disease borne of impaired peripheral insulin signalling.

1.9 Links between BACE1, APP and Metabolic Disease

A number of different metabolic stresses have been shown to up-regulate BACE1 levels, including high fat and cholesterol diets (R. Wang et al. 2013), inflammation (Chen et al. 2012b), and oxidative stress (Mouton-Liger et al. 2012). Generally, this suggests that BACE1 may have an important role to play in sensing cellular stress.

Recently, our lab have demonstrated that when challenged with a high fat diet, BACE1 knock out mice are resistant to weight gains that occur in wild-type mice (Meakin et al. 2012). This manifests as a reduction in the increase in the percentage of body fat compared to wild-type controls. These mice also have increased glucose tolerance and insulin sensitivity. Furthermore, we have found that pharmacological inhibition of BACE1 in C2C12 muscle cells results in enhanced insulin sensitivity. Although the exact mechanisms behind these phenotypes are yet to be elucidated, we have also found that UCP1 protein levels are raised in the BAT of BACE1 knock out mice, alongside an increased resting energy metabolic rate, suggesting increased thermogenesis could be implicated in BACE1 knock out mice. Overexpression of BACE1 in C2C12 cells also decreases glucose uptake. This is accompanied by reduced glucose oxidation and oxygen consumption rate of the cells (Hamilton et al. 2014), indicating that BACE1 can modulate metabolism in skeletal muscle.

Conversely, it has also been shown using a knock in model that over-expressing human BACE1 specifically in the forebrain is sufficient to induce a diabetic phenotype in mice (Plucińska et al. 2016). This effect was

demonstrated by the impaired glucose tolerance, increased adiposity and impaired glycogen synthesis in the liver.

Whilst these data may suggest that central BACE1 is responsible for many of the phenotypes associated with obesity and diabetes, there is also strong evidence that peripherally derived BACE1 activity could also play an important role. In mice a high fat diet is able to increase APP levels in both subcutaneous and visceral WAT, concomitant with increased levels of TNF-α (Puig et al. 2012). Importantly, similar findings are evident in humans, where APP levels within WAT are significantly raised in obese individuals, and is correlated to hyperinsulinemia and levels of chemokines such as MCP1 and MIP-1α (Lee et al. 2008). Although taken from a study with a small sample size, it has been shown that even in healthy adults, plasma levels of Aβ42 are correlated with BMI (Balakrishnan et al. 2005). Preliminary data from the lab has suggested that BACE1 knock-out is associated with reduced WAT inflammation, and healthier adipocyte morphology (unpublished observations).

Raised levels of BACE1 activity promote increased production of Aβ, and this increase may be the mediator of metabolic consequences. Indeed, mice injected peripherally with Aβ display hepatic insulin resistance, which is mediated through the JAK2/STAT3/SOCS-1 signalling pathway (Zhang et al. 2013). Our lab data suggests that raised Aβ may be important in modulating insulin sensitivity centrally, as infusion of a $A\beta_{1-42}$ icv induces a diabetic phenotype in mice, with associated perturbation in hypothalamic leptin sensitivity, without accompanying deficits in hypothalamic inflammation or ER stress (Meakin et al. 2018)

1.10 Project Aims

There is, then, clear evidence that BACE1 activity has the capacity to regulate energy metabolism in mice. It is unclear, however, whether these effects are mediated by signalling from the brain, or whether intrinsic BACE1 in peripheral tissues could play a role in the phenotypes previously observed in BACE1 global knock-out mice.

Additionally, it is currently unclear through which substrate BACE1 works to facilitate its effects. Although APP is by far the most extensively studied substrate, due to its association with amyloid pathology, there are many other putative BACE1 substrates that could be responsible for some of our observations. To test the role of peripheral BACE1 and APP processing in energy metabolism this thesis aimed to investigate the following:

1. To examine the role of BACE1 in adipocyte function, by using cre-loxP recombinase technology to generate an adipocyte specific BACE1 knock out mouse
2. To metabolically phenotype this mouse on the background of a high fat diet (HFD)
3. To use this mouse line to investigate the role of adipocyte BACE1 in the development and maintenance of chronic low-grade inflammation associated with obesity.
4. To investigate whether BACE1 exerts its metabolic phenotypes through peripheral APP processing

The central hypothesis of this project is that peripheral modulation of APP processing will significantly alter whole body energy homeostasis. It is proposed that removal of BACE1 from adipocytes will protect mice from diet induced obesity and reduce the associated chronic low-grade adipocyte inflammation associated with obesity. Conversely, it is hypothesised that peripheral infusion of $A\beta_{1-42}$ will exacerbate weight gain, glucose homeostasis and acute insulin sensitivity.

It is hoped that by achieving these aims will help to establish whether BACE1 could be an attractive therapeutic target to combat the current trend of rising levels of obesity and metabolic disease worldwide.

Chapter 2 - Materials and Methods

2.1 General

2.1.1 Chemicals and Reagents

All chemicals and commonly used lab reagents were purchased from Sigma Aldrich unless otherwise stated. Chloroform, methanol and ethanol were purchased from VWR. Isopropanol was purchased from Fisher Scientific. Cell culture plates were purchased from Nunc (ThermoFisher Scientific). Acrylamide solution was purchased from National Diagnostics.

2.1.2 Statistical Analysis

All data is expressed as mean ± standard error of the mean. Statistical analysis was carried out using GraphPad software (Prism 6). Data was analysed by 1-way ANOVA, linear regression or unpaired two-tailed student's tests were used as appropriate. A p value ≤0.05 was considered statistically significant, with levels of significance defined as p≤0.05=*, p≤0.01=**, p≤0.001=***.

2.2 Animal Studies

2.2.1 Maintenance of Animal Lines

Animal procedures were performed in accordance with Home Office guidelines with project licences PPL 60/4280 (prior to September 2016) and PPL 70/9068 (subsequent to September 2016) held by Prof. Michael Ashford and PIL I281D91D7 held by David Allsop. All procedures were also approved by the local ethics board and the Dundee University Named Veterinary Surgeon. All animals were maintained on a 12-hour light/dark cycle at constant temperature, and provided with ad libitum access to food (normal chow (NC) 7.5% fat, 17.5% protein and 75% carbohydrate by energy) and water. For high fat diet (HFD) studies mice were firstly provided with a mixed diet (50% NC and 50% HFD) for one week before switching to a full HFD ((Special Diet Services; 824053) 45% fat, 20% protein, 35% carbohydrate by energy) regime for the remainder of their study. At the end of studies where tissue was required, mice were sacrificed by either cervical dislocation or CO_2 inhalation. Tissues were excised and dissected as necessary. All tissue for cDNA or protein analysis

was flash frozen in liquid nitrogen, and subsequently stored at -80^{o}C until required. Blood was collected in an EDTA coated tube, and spun at 1500rpm for 15 minutes at 4^{o}C to separate red blood cells from plasma. The plasma supernatant was removed and frozen at 80^{o}C until required. Tissue for staining was placed in formalin solution and stored at room temperature.

2.2.2 Creation of the Adipocyte Specific BACE1 Knock-out Mouse

The adipocyte specific BACE1 AdKO mouse was created using the cre-loxP system. In this system, a "floxed" mouse is generated, which flanks the target gene with loxP sites. A second "cre" mouse is created, which expresses a cre recombinase enzyme under the control of a tissue specific promoter. The two mice strains are cross-bred. The cre recombinase then recombines the loxP sites, allowing excision of the DNA between them. For these studies an adipoQ cre on the C57BL/6 background was mouse was obtained from Jackson Laboratories. The BACE1 floxed mouse was obtained from Merck (Model number: 8263; C57BL/6-Bace1tm1.1mrl)

To generate BACE1 AdKO mice, homozygous BACE1 floxed mice were bred with mice which were homozygous floxed and heterozygous for cre. This generated litters consisting of homozygous floxed mice which were either cre null (used as littermate controls), or heterozygous for cre. Separately, WT mice were bred with mice heterozygous for cre. This generated litters of either WT with heterozygous cre littermates. All mice used as breeders originated from the same stock cre and BACE1 floxed mice.

2.2.3 DNA Extraction

Ear notch samples were collected from mice and placed into a 1.5ml Eppendorf tube. A master mix containing 100µl extraction buffer (Sigma Aldrich; E7526) and 25µl tissue preparation solution (Sigma Aldrich; T3073) for each sample was made, and 125µl added to each Eppendorf. The samples were mixed using a vortex mixer and spun briefly at 13000

rpm in a centrifuge to ensure the notch was at the bottom of each tube. Samples were incubated for 10 minutes at room temperature, before being placed in a dry heat block for 3 minutes at 95°C. 100µl of neutralisation buffer (Sigma Aldrich; N3910) was added to each sample, which was mixed before being placed on ice. Samples were then frozen at -20°C until required for genotyping.

2.2.4 Genotyping the BACE1 Floxed Mouse

A master mix was made according to table 2.1 and mixed gently. 5µl of the extracted DNA mix was added to a PCR tube and 45µl of master mix added. The solution was mixed by vortex and centrifuged to ensure all the solution was at the bottom of the tube. The tubes were then placed in the PCR machine (Veriti 96 well thermal cycler) and the appropriate protocol was run as shown in table 2.5

Component	Volume per reaction (µl)
KOD 10x buffer (Novagen; 71155)	5
25mM $MgSO_4$ (Novagen; 71156)	3
dNTPs (Novagen; 71154)	5
PCR grade water	29.5
KOD Taq (Novagen; 71316)	1
Primer 1775	0.75
Primer 1779	0.75

Table 2.1 Components of the BACE1 floxed mouse PCR reaction

After the PCR, the samples were loaded onto a 1% agarose gel with a 1 in 10000 dilution of SYBER™safe (Invitrogen; S33102) added to allow visualisation of DNA bands under UV light exposure. The gel was loaded with a 100bp DNA ladder (Promega; G210A), and was run at 120V for 45 minutes. The products of this PCR protocol are a WT band at 806bp and a floxed band at 967bp. The presence of both bands indicated a heterozygous mouse (see figure 3.1 for details).

Primer	Sequence (5'-3')
1775	CAGCCATGGCACTCCTGGA
1779	CCCGGTGAGAACATGGTGAAAGG

Table 2.2 Primer sequences for BACE1 floxed mouse PCR

2.2.5 Genotyping the AdipoQ Cre Mouse

A master mix was made according to table 2.3 and mixed gently. 5µl of the extracted DNA mix was added to a PCR tube and 45µl of master mix added. The solution was mixed by vortex and centrifuged to ensure all the solution was at the bottom of the tube. The tubes were then placed in the PCR machine and the appropriate protocol was run, as shown in table 2.5

Component	Volume per reaction (µl)
KOD 10x buffer	5
25mM $MgSO_4$	4
dNTPs	5
PCR grade water	20
KOD Taq	1
Primer LysM (F)	0.75
Primer LysM (R)	0.75
Primer oIMR 7338	1.5
Primer oIMR 7339	1.5

Table 2.3 Components of the AdipoQ Cre mouse PCR reaction

After the PCR, the samples were loaded onto a 1% agarose gel with a 1 in 10000 dilution of SYBER™safe added to allow visualisation of DNA bands under UV light exposure. The gel was run at 120V for 45 minutes. The products of this PCR protocol are a Cre band at 600 base pairs and a control 324 base pairs. The control band appeared in all samples.

Primer	Sequence (5'-3')
LysM Fwd	AAATGGTTTCCCGCAGAACC
LysM Rev	TAGCTGGCTGGTGGCAGATG
oIMR 7338	CTAGGCCACAGAATTGAAAGATCT
oIMR 7339	GTAGGTGGAAATTCTAGCATCATCC

Table 2.4 Primer sequences for AdipoQ Cre mouse PCR. oIMR primers are internal positive controls

	BACE1 floxed mouse		AdipoCre Mouse	
Stage	**Temperature (ºC)**	**Duration**	**Temperature (ºC)**	**Duration**
Activation	95	2 mins	95	2 mins
Denaturation	94	45 secs	95	20 secs
Annealing	65	1 min	62	15 secs
Elongation	72	1 min	70	7 secs
Terminal elongation	72	5 min		
Hold	4	∞	4	∞

Table 2.5 PCR reaction steps for genotyping BACE1 floxed and AdipoQ Cre mice

2.3 Metabolic Studies

2.3.1 EchoMRI Scanning

Mice were weighed then placed in a glass cylinder tube, which was inserted into the MRI analyser (Echo MRI™, Echo Medical Systems). Three separate scans were recorded for each mouse. Each scan provided a lean mass and fat mass value, which were averaged and calculated as a percentage of total body mass.

2.3.2 Glucose Tolerance Test (GTT)

Mice were fasted overnight prior to glucose tolerance testing. Mice were placed in a restraint and blood was extracted via a small nick to the tail vein and glucose concentrations assessed using a glucometer (Contour,

Bayer). Mice were injected i.p. with 1mg/kg D-glucose (dissolved in PBS), with glucose levels assessed basally and 15, 30, 45, 60 and 120 minutes post injection.

2.3.3 Insulin Tolerance Test (ITT)

Mice were fasted for four hours prior to insulin tolerance testing. Mice were placed in a restraint and blood was extracted via a small nick to the tail vein and glucose concentrations assessed using a glucometer (Contour, Bayer). Mice were injected i.p. with 0.75IU/kg insulin (Actrapid) diluted in PBS, with glucose levels assessed basally and 15, 30, 60, 90 and 120 minutes post injection.

2.3.4 Glucose Stimulated Insulin Secretion (GSIS) Test

Mice were fasted overnight prior to the GSIS test. Mice were placed in a restraint and blood was extracted through a small nick to the tail vein. Approximately 10-30μl blood was taken and placed into an EDTA coated tube. A basal glucose reading was also taken with a glucometer. Following this a 2mg/kg dose of D-glucose was injected i.p. Blood was taken as before at 3, 15 and 30 minutes post injection. At the 3 minute time point a second glucose measurement was taken to confirm successful injection. At the end of the procedure, blood was spun as described previously, and plasma stored in Eppendorf tubes at -80^{o}C for running on an insulin ELISA.

2.3.5 CLAMS

The OxyMax CLAMS (Complete Lab Animal Monitoring System; Columbus Instruments) is a piece of equipment which allows a number of metabolic parameters to be measured in live mice, including food and water intake, locomotor activity, oxygen consumption, CO_2 production and respiratory exchange ratio (RER). The machine was calibrated as per the manufacturer's instructions. Mice were individually housed for a period of 72 hours, with the first 24 hours of data discounted to allow for acclimatisation. Energy expenditure was calculated by the device as a function of oxygen consumption, given by the formulae:

Energy expenditure = calorific value * oxygen consumption.
Calorific value= 3.815 + 1.232 X RER

2.3.6 Insulin Stimulations

For studies where mice were stimulated with insulin prior to sacrifice, mice were injected with a 3U/kg dose of insulin or PBS vehicle control before sacrifice by cervical dislocation after 5 minutes. Insulin stimulated tissue was taken in the same order- the largest liver lobe was taken first immediately, before the muscle was taken a further minute later and the peri-gonadal WAT pad a minute later were taken from the same side of the mouse each time and immediately snap frozen in liquid nitrogen.

2.3.7 Mini-pump Surgery

Mice were anaesthetised by a mix of 5% isofluorane and oxygen. A small area of fur was shaved with an electric razor on the back of the mouse to the side of the backbone. The mouse was placed onto a heat mat for the duration of surgery. A subcutaneous analgesic agent was injected into the area before the skin was sterilised with iodine and 70% ethanol. An approximately 2-3cm subcutaneous nick was made in the centre of the shaved area was made. A pocket large enough to fit the osmotic minipump (Alzet) was blunt dissected down the flank of the mouse and the minipump, containing either $A\beta_{1-42}$ or scrambled peptide control (3.36 μg/kg, Bachem) was inserted, before the cut was sutured. Mice were placed in heated incubators to recover for around 30-60 minutes, with access to further analgesia and soft food as required. All surgery was performed alongside Dr. Paul Meakin.

2.3.8 Fluorescence-activated Cell Sorting (FACS)

After mice were sacrificed, tissue was excised and retained in 15ml falcon tubes and placed on ice. For these studies, we used 100μl of whole blood, a whole spleen, approximately 1 fifth of a whole liver and approximately 1 fat pad. Tissue was chopped in a petri dish into very small pieces using scalpels and 2ml FACS medium (RPMI with 1% penicillin/streptomycin and

2.5% FBS) was added into a fresh 15ml falcon tube with a Pasteur pipette. The petri dish was further rinsed with another 2ml medium to ensure all tissue was digested. Next, 1ml of digestion buffer (1mg/ml Type II collagenase and 10U/ml DNAse I) was added to each tube and mixed at room temperature with rotation for 25 minutes for liver and WAT and 15 minutes for spleen. For the final 5 minutes 200µl 0.5M EDTA was added. After digestion, tissue was filtered through a 100µm mesh filter. Any lumps remaining were forced through the mesh using a syringe plunger. Tissue was washed through with 3ml of FACS medium. Samples were then spun at 400xg for 5 minutes. The pellets were resuspended in 2ml red blood cell lysis buffer (0.15M NH_4Cl, 0.01M $KHCO_3$, 0.1mM EDTA at pH7.4) for 3 minutes before being neutralised with 3ml FACS medium. Samples underwent a further spin at 400xg for 5 minutes before the supernatant was resuspended in 400µl FACS buffer (PBS with 2% FBS and 1mM EDTA) for blood and WAT or 1ml FACS buffer for liver and spleen. Cells were pipetted into a 96 well round bottom plate and spun down at 400xg for 3 minutes. The supernatant was removed and the cells were resuspended in 200µl FACS buffer. The supernatant was discarded and the cells resuspended by brief vortex, before 200µl FACS buffer was added with a multi-channel pipette. The plate was spun down again and the supernatant discarded. The cells were again resuspended with gentle vortexing. Next 50µl of the appropriate FACS stain was added to each sample. FACS stains were made in FACS buffer with dilutions of 1:100 for FITC and Fc block stains and 1:200 for all other stains, as detailed in table 2.6. 100µl FACS stain was added to control cells and 50µl to other cells. After mixing by brief vortexing the samples were incubated for 30 minutes at 4°C. Following this, the cells were once more washed in 200µl FACS buffer twice, before being resuspended in 180µl FACS buffer and transferred from the plate to the FACS tubes. Prior to acquiring data 20µl DAPI was added to each tube before being run through the Fortessa machine.

Stain:	A	B	C
Conjugate	**Antibody**		
FITC	B220	CD86	CD44
PE	CD206	CD206	CD25
PerCP	Gr-1	Gr-1	CD4
PE-Cy7	CD4	CD11c	B220
APC	CD11b	CD11b	CD69
APC-Cy7	F4/80	F4/80	CD8a
Fc block	Fc block	Fc block	Fc block

Table 2.6 Conjugates and antibodies for FACS

Stain A was used for blood, whereas stains B and C were both used for liver, WAT and spleen samples. For analysis, cells were gated for live, single cell populations, before being gated for the appropriate antibodies. For cells per gram calculations, the following formula was used:

cells per gram = (cells in gate) * (volume remaining/total volume of cells) * (amount of tissue taken for analysis/total amount of tissue excised) * tissue weight

2.4 Tissue Biochemistry

2.4.1 RNA Extraction

Eppendorf tubes containing tissue were removed from the -80^{o}C freezer before being submerged in liquid nitrogen until required. An appropriate section of tissue was cut from the sample, and placed into a tight-fit glass homogeniser. For muscle samples, tissue was broken down into a powder under liquid nitrogen using a pestle and mortar before being added to the homogeniser. 1ml TRIzol® Reagent (Thermo-Fisher Scientific; 15596018) was added into the homogeniser, and the sample was mixed with the TRIzol® Reagent using the homogeniser's glass handle, until a homogenous solution was created. The solution was removed into a fresh Eppendorf and stored at -80^{o}C until required for further processing.

Prior to RNA extraction, samples were thawed and then spun in a micro-centrifuge at 13000rpm for 15 minutes to remove any remaining solid tissue or fat. Fat floating at the top of the spun solution was removed and the supernatant transferred to a fresh Eppendorf.

200µl chloroform was added to the eppendorf and shaken vigorously for 15 seconds. Samples were allowed to stand at room temperature for 15 minutes before being spun at 12000 x g for 15 minutes. The clear aqueous phase was removed to a fresh tube and mixed with 500µl isopropanol. This was left at room temperature for 10 minutes before undergoing a spin at 12000xg for 10 minutes.

At this stage, a pellet containing the RNA is visible at the bottom of the eppendorf. The supernatant was removed, and the pellet washed with 1ml 75% ethanol solution. The tube was spun at 12000xg for 5 minutes and the supernatant removed. The pellets were then allowed to air dry in a fume hood for 7.5 minutes before 30µl RNAse free water was added to the pellet and heated at 60^{o}C for 15 minutes. The resulting RNA was stored at -20^{O}C until required for cDNA synthesis.

2.4.2 cDNA Synthesis

RNA concentration was assessed using the NanoDrop ND-8000 Spectrophotometer using nuclease free water to blank the machine. Purity was also assessed at this stage, with a 260/280 ratio ≥1.7 required to continue to the cDNA synthesis step. cDNA was produced according to the Invitrogen™ protocol and reagents (Invitrogen; 10864-014) for Superscript™ II reverse transcriptase. Briefly, a mix consisting of 1µl of random primers, 1µl dNTP mix and 1µg RNA made up to a total volume of 13µl with PCR grade water was made in a 1.5ml eppendorf and heated to 65^{o}C for 5 minutes and then quickly chilled on ice. Next, 4µl 5x first strand buffer and 2µl 0.1M DTT was added to the mix and gently mixed and left at room temperature for 2 minutes. 1µl of SuperScript™ II RT was then added and the whole mixture mixed gently by pipetting up and down. The

samples were then left at room temperature for a further 10 minutes before being incubated at 42°C for 50 minutes, after which the reaction was inactivated by heating at 70°C for 15 minutes. The cDNA was then diluted 1 in 10 with 180µl PCR grade water and mixed before being stored at -20°C until needed for TaqMan® analysis.

2.4.3 Quantitative Gene Expression analysis using Real Time PCR

Gene expression can be quantified by using gene expression assays by TaqMan® (Applied Biosystems). In this technology, a primer/probe mix for a specific gene is provided, which uses normal PCR primers, but with addition of a probe molecule, which has a FAM dye label on the 5' end and a quencher on the 3' end which lies in the middle of the cDNA sequence of interest. When the target gene is amplified, the exonuclease activity of the Taq enzyme separates the FAM dye from the quencher, allowing for fluorescence analysis, which correlates with the total amount of amplified product. This information can be used to quantify the level of gene expression.

For TaqMan® analysis, 2.5µl cDNA was loaded into a 96 well plate and mixed with 17.5µl of a pre-made master mix, consisting of 6.5µl PCR grade water, 1µl of the appropriate primer/probe mix (Life Technologies; see table 2.8) and 10µl of TaqMan® 2X mastermix (Applied Biosystems; 4324020) per sample. Samples were loaded in duplicate.

Once filled, the 96 well plate was covered with a film lid and spun in a centrifuge to ensure all the solution was collected at the bottom of the plate. The plate was then placed in a real-time PCR machine (Applied Biosystems, 7900HT) and run according to the protocol in table 2.7. Steps 2 to 4 were repeated for a total of 40 cycles.

Step		Temperature (°C)	Time
1	Initial	95	10 mins
2	Denaturing	95	15 secs
3	Annealing	60	1 min
4	Elongation	60	1 min

Table 2.7 Steps for TaqMan® process

The machine creates a copy number which can be used to quantify gene expression. The mean copy number from the duplicate samples was taken and normalised to the endogenous control, actin.

Probe Name	Species	Code
Actin	Mouse	4352663
adipoQ	Mouse	Mm00456425_mM
AdipoR1	Mouse	Mm01291334_mH
AdipoR2	Mouse	Mm01184032_m1
AgRP	Mouse	Mm00475829_g1
Arg1	Mouse	Mm00475988_m1
adrb3	Mouse	Mm02601819_g1
BACE1	Mouse	Mm00478664_m1
CCL2	Mouse	Mm00441242_m1
CCL3	Mouse	Mm00441259_g1
CCL4	Mouse	Mm00443111_m1
CCL5	Mouse	Mm01302427_m1
Dio2	Mouse	Mm00515664_m1
FGF21	Mouse	Mm00840165_g1
FGFR1	Mouse	Mm00438930_m1
IGFBP2	Mouse	Mm00492632_m1
IL-10	Mouse	Mm00439614_m1
IL-1β	Mouse	Mm00434228_m1
Klb (β-klotho)	Mouse	Mm00473122_m1
lepRb	Mouse	Mm00440181_m1

Leptin	Mouse	Mm00434759_m1
NOS2	Mouse	Mm00440488_m1
Ppargc1 (PGC1α)	Mouse	Mm01208835_m1
POMC	Mouse	Mm00435874_m1
Prdm16	Mouse	Mm00712556_m1
PTP1B	Mouse	Mm00448431_m1
Slc2a1	Mouse	Mm00441480_m1
Slc2a4	Mouse	Mm01245502_m1
SOCS3	Mouse	Mm00545913_s1
TNF-α	Mouse	Mm00443260_g1
UCP1	Mouse	Mm01244861_m1
YM1	Mouse	Mm00657889_mH

Table 2.8 List of TaqMan® probes used

2.4.4 Protein Extraction

Tubes containing tissue were removed from the -80ºC freezer and placed into liquid nitrogen until needed for lysis. An appropriate section of tissue was cut from the sample and placed into a tight-fit glass homogeniser. For muscle samples, tissue was broken down into a powder under liquid nitrogen using a pestle and mortar before being added to the homogeniser. An appropriate volume of lysis buffer (See commonly used lab solutions section for detail), 1-100-200μl for brain samples or 500μl for larger pieces of tissue- was added to the homogeniser and mixed until a homogenous solution was created. The solution was removed into a fresh Eppendorf and stored at -80ºC until required.

Protein concentration was determined by Bradford assay (Bradford 1976). Standard wells of known protein concentration were loaded in triplicate onto a 96 well plate (Nunc) using 2mg/ml BSA (Thermo Scientific; 23209) to create a standard curve. For unknown samples, lysates were mixed by vortexing and 1μl of sample lysate was added to 9μl MilliQ water, and 250μl Bradford reagent (Sigma Aldrich; B6916) was added to each well. The 96 well plate was covered and left to develop for 15 minutes at room

temperature before absorbance at 595nm was recorded using the EnVision® 2104 Multilabel Plate Reader. The standard curve was then created using the mean absorbance of the known concentration values, and using the equation of the line of best fit, the concentrations of unknown sample were interpolated.

Equal amounts of protein were mixed with 4x sample buffer (see table 2.9) and boiled at 95^{o}C for 5 minutes prior to loading on a gel. For membrane proteins, the boiling step was skipped to prevent protein aggregation.

Constituent	Volume
0.5M Tris pH 6.8	4ml
glycerol	3.2ml
20% SDS	3.2ml
β-mercaptoethanol	1.6ml
bromophenol blue	pinch

Table 2.9 Constituent Parts of 4x sample buffer

2.4.5 SDS-PAGE

Sodium Dodecyl Sulphate Polyacrylamide gel electrophoresis (SDS-PAGE) is a widely used technique for separating proteins of different sizes. SDS is an anionic agent, which coats proteins in a negative charge. Using an electrical current, these proteins can be separated on a polyacrylamide gel, with the negatively charged proteins migrating away from the negatively charged electrode. Larger proteins take a greater amount of time to pass through the gel than smaller ones, hence allowing size separation. The percentage of acrylamide in the gel can be altered to allow optimal resolution of the protein. Lower percentage gels have larger pores, allowing better resolution of larger proteins.

Gels were hand poured using BioRad casting equipment. A small glass plate was placed in front of a larger casting glass plate and placed in a casting cassette, which was then clamped shut on a flat surface. The cassette was then clipped into a casting stand, and checked for leaks by

pouring distilled water between the plates. Once checked, the water was poured off, and excess was removed using Whatman blotting paper. An appropriate percentage running gel was mixed as in table 2.10 and poured between the plates. Bubbles were removed by pipetting a small volume of 50:50 mix of butanol and distilled water. Gels were left to set for 15-20 minutes and the butanol poured off the top of the set gel. The top of the gel was washed with distilled water 3 times to ensure complete removal. Excess water was removed with Whatman blotting paper.

	Percentage of gel		
Constituent	**7%**	**10%**	**15%**
ddH_2O	5.45ml	4.15ml	2.3ml
Lower Buffer	3.15ml	3.15ml	3.15ml
30% Acrylamide	2.35ml	3.75ml	5.5ml
10% SDS	110µl	110µl	110µl
TEMED	11µl	11µl	11µl
20% APS	55.35µl	55.35µl	55.35µl

Table 2.10 Components of lower gels for western blotting

The stacking gel was then made according to the recipe in table 2.11 and poured on top of the running gel. Immediately after pouring, combs were inserted into the top of the gel. The gel was allowed to set for 10-15 minutes.

Constituent	**Volume**
ddH_2O	4.15ml
Upper Buffer	3.15ml
30% Acrylamide	3.75ml
10% SDS	110µl
TEMED	11µl
20% APS	55.35µl

Table 2.11 Components of upper gels for western blotting

Once set, the comb was removed and the gels moved into the electrophoresis module, and placed in the electrophoresis tank. 1x running buffer was poured into the tank, and any bubbles in the combs removed by syringe. The gel was then loaded with the appropriate amount of protein, with SeeBlue Pre-Stained Protein Standard (ThermoFisher Scientific; LC5925) added to one well for use as a reference. The gel was then run for approximately 75 minutes at 150V to allow protein separation.

2.4.5 Protein Transfer

Once the gels run sufficiently, it is necessary to undergo a second stage, known as transfer, to transfer the proteins from the gel onto a membrane, which can undergo subsequent immunoblotting. Prior to this, transfer buffer was made up (See commonly used lab solutions section for detail), and 4 pieces of Whatman paper, 2 large black sponges, 2 smaller white sponges and a piece of nitrocellulose membrane (Amersham Biosciences) per gel were pre-soaked in the buffer.

Once soaked, a piece of Whatman paper was placed in a petri dish containing a small amount of transfer buffer. Separately, a transfer cassette was placed into a tub containing transfer buffer, with the clasp of the cassette at the top edge of the tub. The first black sponge was placed on the bottom plate of the transfer cassette. On top of this was the first piece of Whatman paper.

The gel was prised open so that the gel was on the larger plate and the stacking gel removed and discarded using a spatula. The gel was then placed onto a piece of Whatman paper, which was then transferred, still facing upwards, on top of the piece of Whatman paper on top of the transfer cassette. The nitrocellulose membrane was added on top of the gel and rolled gently to remove bubbles but avoid cracking the gel. Two further pieces of Whatman paper were added on top, before the final white, then black, sponge was added. The whole cassette was rolled once more to remove bubbles before being clasped together.

The transfer cassettes were placed in a transfer tank. An ice pack was added to the other side of the tank and the transfer was run for 1 hour at 100V.

2.4.6 Immunoblotting

Membranes were rinsed with Ponceau S solution to ensure even and efficient protein transfer. Ponceau was washed off with TBS-T solution (See commonly used lab solutions section for detail), before the membranes were blocked in a 5% w/v milk solution (made up in TBS-T) for one hour at room temperature with gentle rocking.

Following the blocking step, membranes were rinsed briefly in TBS-T, before 10ml primary antibody as detailed in table 2.12, which were then left to incubate overnight at 4^{o}C with gentle rocking. The following day, the antibody was removed and washed three times for ten minutes with TBS-T. After this, IgG-HRP goat anti-rabbit (Santa Cruz Biotechnology; sc-2004) or IgG-HRP goat anti-mouse (ThermoFisher Scientific; 31450) secondary antibody, as appropriate, was placed on to the membrane and left at room temperature with gentle rocking for one hour. Following this incubation, membranes were washed three times for ten minutes each before being stored at 4^{o}C until required for visualisation. Membranes were visualised using Pierce™ ECL Western Blotting Substrate (ThermoFisher Scientific; 32106), and exposed to X ray film. Films were labelled and scanned, and quantification was performed using Licor (Image Studio Lite 4) software.

2.4.7 Non-reducing, partially denaturing immunoblotting

For separation of adiponectin multimers, 1μl plasma was diluted in 49μl 1x non-reducing partially denaturing sample buffer (3% SDS, 50mM Tris-HCl, pH 6.8, 10% glycerol, 0.05% bromophenol blue) and left at room temperature for 20 minutes. 15μl was loaded onto a gradient gel (Invitrogen Novex Midi Bis-Tris gel; NP0323). Samples were run at 150v in MOPS running buffer (See commonly used lab solutions section

below). Following this, gels were transferred onto a PVDF membrane (Millipore; IPVH00010), which was soaked in methanol for 1 minute prior to use. The protein was transferred at 100V for 1 hour in non-reducing, partially denaturing transfer buffer (see commonly used lab solutions section below), and then immunoblotting proceeded as normal.

Antibody	**Species**	**Dilution**	**Source**	**Code**
Actin	Rabbit	1:5000	Sigma Aldrich	A2066
adiponectin	Rabbit	1:2000	Sigma Aldrich	A6354
BACE1	Rabbit	1:1000	Sigma Aldrich	B0681
BACE1	Rabbit	1:1000	Cell Signalling	5606s
Cd68 (used for light microscopy)	Rat	1:100	AbD Serotec	MCA1957
F4/80 (used for light microscopy)	Rat	1:100	AbD Serotec	MCA497
FGFR1	Rabbit	1:1000	Abcam	Ab137781
perilipin	Rabbit	1:1000	Cell Signalling	9349s
Phospho PKB (ser 473)	Rabbit	1:1000	Cell Signalling	9271s
Total PKB	Rabbit	1:1000	Cell Signalling	9272s
STAT3	Mouse	1:1000	Cell Signalling	9139s

Phospho STAT3 (Tyr705)	Rabbit	1:1000	Cell Signalling	9131s

Table 2.12 List of primary antibodies used

2.4.8 Insulin ELISA

Insulin from serum samples were run on an Ultra Sensitive Rat Insulin ELISA kit (Crystal Chem Inc.; 90060) as per the manufacturer's instruction. Briefly, 95μl sample diluent was added to each well of a 96 well plate, with 5μl of sample or appropriate standard solution (loaded in duplicate) then added. The plate was covered and incubated for 2 hours at 4°C. Well contents were then removed and the plate washed five times with 300μl of wash buffer per well, ensuring the plate was fully dry after each wash. 100μl insulin conjugate was then added to each well, and the plate incubated for a further 30 minutes at room temperature. The well contents were again removed, and washed using 300μl wash buffer seven times. 100μl per well of enzyme substrate solution was added, and the plate incubated for 40 minutes at room temperature, protected from light. After this incubation, 100μl enzyme reaction stop solution was added to each well, and the well absorbance values read at 450nm and 630nm wavelengths using the EnVision 2104 Multilabel Plate Reader. A standard curve was then created and sample values interpolated from the resulting graph.

2.4.9 Leptin ELISA

Leptin from serum samples were run on a Quantikine ELISA mouse/rat leptin immunoassay (R&D systems; M0B00) as per the manufacturer's instructions. Briefly, samples were diluted 1 in 20 with the provided diluent. 50μl sample diluent was added to each well, before 50ul of standard or sample was added, in duplicate, as appropriate. The plate was tapped for a minute to mix thoroughly, and left to incubate at room temperature with gentle rocking for 2 hours. Well contents were then removed and the plate washed five times with 300μl of wash buffer per well, ensuring the plate was fully dry after each wash. Next, 100μl mouse/rat leptin conjugate was

added to each well, and left to incubate for a further 2 hours at room temperature with gentle rocking. The wash step was repeated, before 100μl substrate solution was added to each well. The plate was incubated for 30 minutes at room temperature for 30 minutes and protected from light, before 100μl stop solution was added to each well. The plate was gently tapped to ensure mixing, and the optical densities at 450nm and 540nm were read. A standard curve was then created and sample values interpolated from the resulting graph.

2.4.10 Adipokine Array

A proteome profiler adipokine array kit was purchased (R&D Systems; ARY013) and was used to quantify levels of adipokines within WAT samples. The procedure was performed as per the manufacturer's instructions. Briefly, samples were homogenised in PBS with 10μg/ml aprotinin, 10μg/ml leupeptin and 10μg/ml pepstatin (Sigma Aldrich; P4265). After homogenisation, triton X-100 was added to a final concentration of 1% v/v. After freezing, samples were spun at 10000 rpm for 5 minutes to remove debris, before protein concentration was determined by Bradford assay as previously described. For the assay, 2ml of array buffer 6 was added to each well of a multi-dish. Pre-made membranes coated with capture antibodies were added and left to block for one hour at room temperature. Meanwhile, 500μl of array buffer 4 was added to 275μg of protein lysate, which was topped up to a final volume of 1.5ml with array buffer 4. 15μl of reconstituted mouse adipokine detection antibody cocktail was added to each sample tube, which was mixed and incubated at room temperature for an hour. Following the incubation step, the array buffer 6 was removed from the multi-well dish. And the antibody/sample mix was added, and left to rock overnight at 4°C. Following this, each membrane was moved to an individual dish and washed with 20ml 1X wash buffer three times for 10 minutes each. Meanwhile the multi-dish was washed with deionised water and dried. The membranes were returned to the multi dish, having had excess wash buffer blotted off using tissue, and 2ml of diluted streptavidin-HRP was added to

each membrane. The membranes were incubated for 30 minutes at room temperature with gentle rocking. The wash steps were repeated, before the membranes were placed on the bottom sheet of a plastic sheet protector. 1ml chemi reagent mix was added to each membrane, and covered with the top sheet of the plastic protector. The membranes were smoothed out and bubbles removed to ensure the chemi reagent was in full contact with the whole membrane. Paper towels were placed around the edges of the membranes to remove excess reagent. Membranes were then placed in an autoradiography fil cassette and exposed to x ray film for varying exposure periods (between 1 and 30 minutes) to gain results. Quantification was performed using Licor (Image Studio Lite 4) software as with immunoblotting.

2.4.11 Immunohistochemistry

All immunohistochemistry was performed by Tayside Tissue Bank. Tissue segments were paraffin embedded and sliced onto glass sides. Antibodies were used as described in table 2.12. Images were obtained using a light microscope (Leica AF600), and taken at 10x magnification using a dry-objective lens.

2.4.12 Light Microscopy Analysis

Images were analysed using ImageJ software (ImageJ 1.49p). Adipocyte size calculations were performed using the Adiposoft plug-in (Adiposoft 1.0). Diameter and area were averaged for each slide analysed. For assessing hepatic steatosis a colour threshold was created to identify regions of steatosis, which was then measured in pixels and expressed as a percentage of total pixels in the image.

2.5 Cell Culture

2.5.1 3T3-L1 Cell Maintenance

3T3-L1 cells are a murine fibroblast cell line, which can be differentiated into adipocyte like cells (Green & Kehinde 1974), and as such are used commonly as a cell line for the study of mammalian adipose tissue function.

3T3-L1 cells were grown in maintenance media (Life Technologies; DMEM 41966 with sodium pyruvate) supplemented with 10% v/v BCS (Sigma Aldrich; 1213CC), 2% v/v 1M HEPES solution at pH 7.4 (Sigma Aldrich; H0887), 1% v/v l-glutamine (Gibco by Life Technologies; 25030-024) and 1% penicillin/streptomycin solution (Gibco by Life Technologies; 15070-063). Transfected cells (see below) were further supplemented with a 1% v/v G418 (Sigma Aldrich; G8168) for selection of transfected cells. Cells were grown in T75 plates until they reached around 75% confluency at which point they were split. Old media was poured off the plates, which were then washed with 5ml PBS. 2ml pre-warmed Trypsin solution (Gibco by Life Technologies; 25300-254) was added per plate to detach cells. The plate was returned to the incubator for up to 5 minutes to allow the cells to detach from the plate surface. After this, cells were diluted with maintenance media and re-plated at the desired density.

2.5.2 Differentiation

Cells were seeded in 6 well plates at a density of 100 000 cells per well in a total volume 2.5ml maintenance media. The cells were allowed to grow for 2 days after reaching confluence, before the differentiation media with 10% v/v FBS (Seralab; EU000F), 2% v/v 1M HEPES solution at pH 7.4, 1% v/v l-glutamine and 1% penicillin/streptomycin antibiotic, supplemented with 167nM insulin, 0.115mg/ml IBMX (Sigma Aldrich; I5879), 10mM dexamethasone (Sigma Aldrich D4902) and 2μM rosiglitazone (Sigma Aldrich; R2408) and grown for a further 48 hours. After this, the media was replaced, with the IBMX and dexamethasone removed. After a further 2-3 days the media was changed to differentiation media without any of the added supplements. Cells were assessed visually for successful differentiation before subsequent lysis. Cells were lysed by first washing each well twice with 1ml PBS, before 100μl lysis buffer or 1ml TRIzol reagent was added and cells scraped to detach from the surface.

2.5.3 Stable Transfections

Undifferentiated cells were seeded in 6 well plates, at a density of 300 000 cells per well. After 4 hours, or upon surface adherence, cells were transfected. For transfecting, 2μl pcDNA3.1 (at a concentration of 0.5μg/μl) was mixed with 296μl opti-MEM per well in an eppendorf (tube A). For a positive control, eGFP was used. For a negative control, nuclease free water was used in place of DNA. In a second eppendorf (tube B), 4μl lipofectamine 2000 was mixed with 296μl opti-MEM. Tube A was pre-incubated for 5 minutes at room temperature before being mixed with the contents of tube B, and left for a further 30 minutes of incubation at room temperature. The seeded cells were washed with 1ml PBS twice, and after the 30 minute incubation, 500μl of the tube mix was added to each well for transfection and returned to the incubator. After 24 hours, the positive control cells were assessed for transfection using a light microscope equipped with the appropriate filter. Following successful transfection, the opti-MEM media was removed and replaced with normal media for 24 hours. Following this, the media was again changed to maintenance media + 2% v/v G418 selection agent, which was then changed every 48 hours. Once the negative control cells had all died, colonies of transfected cells appeared. The transfected cells were expanded and characterized for BACE1 gene and protein expression.

2.6 Commonly used Lab Solutions

Transfer Buffer (for 2L)

Constituent	Quantity
methanol	400ml
Tris-HCl	11.62g
Glycine	5.86g
dH_2O	Up to total 2L

TBST (for 2L)

Constituent	Volume
1M Tris-HCl solution (pH 7.4)	40ml
4M NaCl solution	74ml
Tween 20	1ml
dH_2O	Up to total 2L

1x Stock Lysis Buffer

Constituent	Quantity
1M Tris-Hcl solution (pH7.4)	12.5ml
750mM NaF solution	33.5ml
4M NaCl solution	12.5ml
500mM EDTA solution	10ml
200mM EGTA solution	12.5ml
Triton x-100	5ml
500mM NaPPi solution	10ml
dH_2O	400ml

Lysis buffer (immediately prior to use):

Constituent	Quantity	Notes
Sucrose	92mg per ml lysis buffer used	
β-mercaptoethanol	1µl per ml lysis buffer	
1mM Na_3VO_4	2µl per ml lysis buffer	Heat activate for 5 minutes at $95^{O}C$ prior to use
1mM benzamidine	1µl per ml lysis buffer	
0.1nM PMSF	1µl per ml lysis buffer	Add last, decays quickly

MOPS SDS-PAGE running buffer (1L, x5):

Constituent	Quantity
MOPS	52.31g
Tris Base	30g
EDTA	6.51g
SDS	17.5g

Non-reducing, partially denaturing transfer buffer (1L, x10)

Constituent	Quantity
Tris Base	30.25g
Glycine	142.63g
SDS	0.5g

*note, make up to 1x using 100ml transfer buffer, 200ml methanol and 700ml milliQ water

Chapter 3 - The role of adipocyte BACE1 in metabolic function

3.1 Introduction

BACE1 is most associated with AD, as it is the key enzyme in the rate-limiting step for production of the amyloid plaques that are typically found in the brains of AD patients, and is thought to be a major contributor towards the pathogenesis of the disease. There are a number of both genetic and lifestyle risk factors for the development of AD. Middle age overweight and obesity is associated with an increased risk (Xu et al. 2011), as are both type 1 and type 2 diabetes (Biessels et al. 2006). The risk of developing AD increases greatly in obese or diabetic individuals. Recently, evidence that BACE1 be involved in the pathogenesis of obesity and T2DM and could therefore represent a key protein linking the conditions has emerged. Pima Indians possess a genetic mutation in the 11q23 region, where the BACE1 gene is located, and are more susceptible to excessive weight gain and development of T2DM (Baier et al. 2002). Furthermore, there is a suggestion that BACE1 could directly influence insulin gene expression or secretion, with BACE1 siRNA treated mice expressing less insulin mRNA, and BACE1$^{-/-}$ mice possessing reduced levels of plasma insulin concentrations (Hoffmeister et al. 2013).

A number of BACE1 inhibitors are currently undergoing clinical trials (Vassar 2014), with a primary purpose of being used to treat AD. However, given some of the potential side effects associated with reducing levels of BACE1, such as hypomyelination of nerves and increased propensity for seizures (Dominguez et al. 2005), it is important to consider the mechanisms through which BACE1 might function, particulary in peripheral tissues, as the vast majority of previous research has focussed on BACE1's role in the brain.

Previous work from our laboratory has shown that BACE1 plays an important role in modulating energy metabolism and metabolic health. Global removal of BACE1 from mice protects against excessive weight gain and impaired glucose and insulin sensitivity, even in the context of a HFD (Meakin et al. 2012). More recently, we have shown that infusion of at least 2 differently structured BACE1 inhibitor compounds are able to

reduce body weight and improve glucose homeostasis in DIO mice. These effects, are observed whether the drugs are administered centrally, through i.c.v injection, or peripherally, via constant infusion of drug via a subcutaneous minipump (Meakin et al. 2018), or via oral gavage. Therefore, although it is clear that BACE1 could be a useful target for preventing the development of obesity, it is at present unclear as to the mechanisms that provide for this outcome, or whether the effects of BACE1 activity reduction are mediated centrally or peripherally.

We, and others, have also previously examined the periphery to establish the tissues in which BACE1 is expressed. We have found that it is expressed in multiple tissues, in particular the insulin sensitive tissues- liver, muscle and WAT (Meakin et al. 2012). Furthermore we and others have found that BACE1 levels increase in response to metabolic stress or HFD in a variety of tissues (Oliverio et al. 2016; Meakin et al. 2012; Velliquette et al. 2006). Within several human adipose depots- both subcutaneous and visceral- it has been shown that APP, BACE1's major substrate in the brain, is upregulated in obese individuals, as is production of its Aβ cleavage products (Y.-H. Lee et al. 2009; Lee et al. 2008), suggesting increased BACE1 activity in these tissues during obesity.

There is evidence that BACE1 could play a role in modulating energy homeostasis in other peripheral tissues. In C2C12 muscle cells, inhibiting BACE1 enhances glucose uptake and GLUT4 transporter translocation to the surface of the cell. Conversely, over-expression of BACE1, but not a protease dead mutant form, results in impaired glucose uptake and decreased glucose oxidation (Hamilton et al. 2014). Furthermore, in neuronal SH-SY5Y cells, glucose oxidation is reduced by over-expression of BACE1 (Findlay et al. 2015).

Data from previous studies performed in the lab demonstrates that global removal of BACE1 alters adipocyte function. Firstly, histological staining of adipocytes has shown that on a HFD, BACE1 knock-out mice have smaller adipocytes compared to WT mice (Ashford lab, personal communication).

Adipocytes are also of a more regular “healthy” structure with reduced evidence of crown like structures and associated adipose tissue inflammation.

Leptin levels usually correlate directly with fat mass. In BACE1 KO mice the relationship between leptin content and overall fat mass is significantly altered. This suggests that global removal of BACE1 causes adipocytes to produce comparatively less leptin than expected for their fat mass (Ashford lab, personal communication).

Therefore, to try and establish whether adipose tissue BACE1 expression and activity was involved in modulating energy metabolism, a conditional BACE1 knock-out model (BACE1 AdKO) was generated to remove BACE1 specifically from adipocytes and characterised their response to a 22 week HFD protocol, assessing multiple parameters relating to body mass and composition, glucose homeostasis and metabolic process, with tissues retained after sacrifice for subsequent biochemical analysis. Further to this, a complimentary *in vitro* model was created, using differentiated 3T3-L1 adipocyte cells transfected to over-express BACE1 to more closely examine any important signalling pathways identified using the *in vivo* model. The hypothesis was that removing BACE1 solely from adipocytes would be sufficient to protect mice against diet induced obesity and glucose intolerance associated with obesity.

3.2 Results

WT, BACE1 floxed, AdipoQ Cre and BACE1 AdKO (BACE1 AdKO) mice were placed on a 45% by energy HFD for 22 weeks. No normal chow diet control was included as the key aim of the study was to investigate the role of adipocyte BACE1 in the context of obesity. Body weight was assessed weekly, and body composition analyses using the EchoMRI machine were performed in weeks 1, 10 and 20 of the study. At 10 and 19 weeks GTTs were performed, and at 11 and 20 insulin tolerance was measured with ITTs. Insulin secretion was assessed using a GSIS in week 21 of the study. To examine food intake, physical activity and other metabolic parameters

such as oxygen consumption, respiratory exchange ratio (RER) and energy expenditure mice were placed in the CLAMS device for a 72-hour period in week 22 of the study, before mice were culled the following week. This is summarised below in figure 3.1.

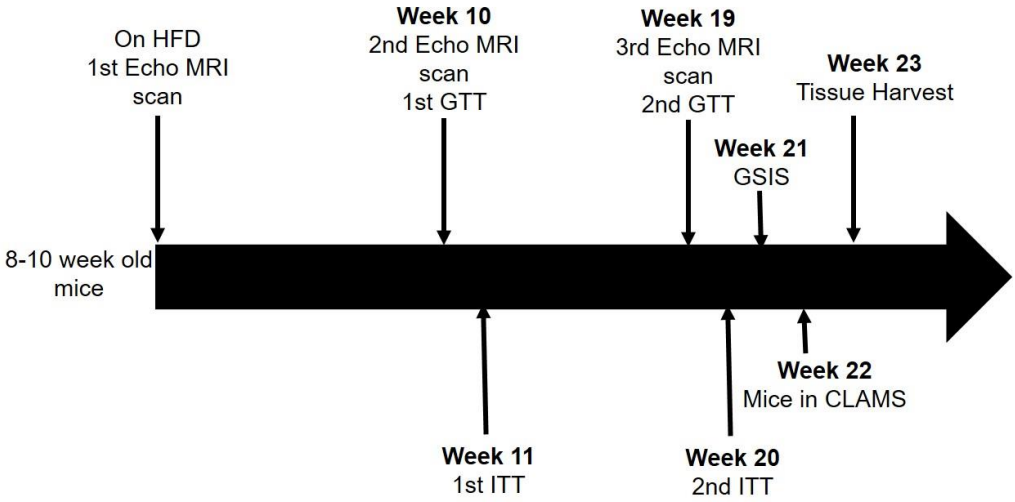

Figure 3.1 Protocol for the 22 week adipocyte BACE1 knock-out HFD study

The raw weights of a number of peripheral tissues (spleen, liver, heart, BAT, inguinal WAT (iWAT), epididymal WAT (eWAT)) and whole brain were measured and tissues then stored for subsequent biochemical analysis. Sections of liver, muscle and eWAT were preserved in formalin for histological analysis.

3.2.1 Conditional Knock-out of BACE1 in adipocytes is confirmed at a gene and protein level

Approximately 2 weeks before mice were assigned to the study a small ear biopsy was taken with which genotyping could be performed. For each mouse two separate PCR reactions were run. Firstly, the floxing of the BACE1 gene was assessed using appropriate primers (Figure 3.2A). The presence or absence of AdipoQ Cre was checked with cre primers (Figure 3.2B). For this reaction 3 different cre primer sets were tested, which gave highly comparable results.

To confirm excision of BACE1 from adipose tissue, protein levels of BACE1 were examined in the mice using western blotting. As shown in figure 3.3A, no BACE1 band was detected in BACE1 AdKO mice in either eWAT (Figure 3.3A) or iWAT (Figure 3.3B), indicating an efficient conditional knock out. No BACE1 was detected in BAT in all genotypes, even in mice on a HFD (Figure 3.3C) Importantly, BACE1 was still present in other tissues examined including muscle (Figure 3.4A), liver (Figure 3.4B) and hippocampus (Figure 3.4C). Taken together, these analyses suggest that the conditional knock-out model produces a mouse in which BACE1 is efficiently removed from adipocytes but retained in other tissues.

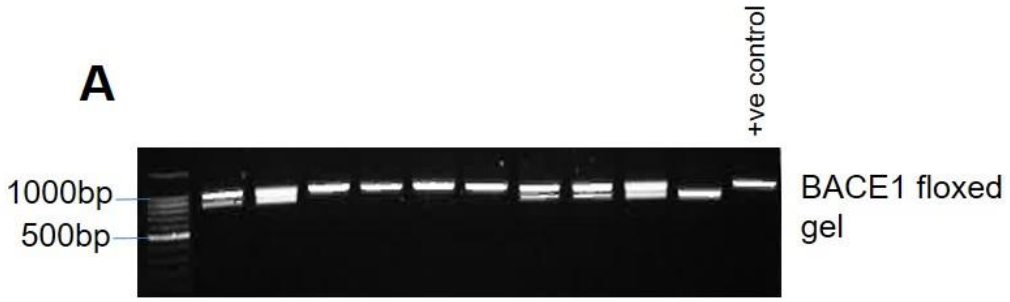

Band size present (bp)	Genotype
806	WT
967	BACE1 floxed
806 and 967	Heterozygote

Band size present (bp)	Genotype
324 and 600	Cre positive
324 (internal control only)	Cre negative

Figure 3.2 Genotyping of BACE1 adipose specific conditional knockout mice

An ear biopsy was taken from each mouse and DNA extracted. PCR gels run using **(A)** BACE1 floxed primers and **(B)** cre primers were used to determine the genotype of individual mice using positive and negative controls.

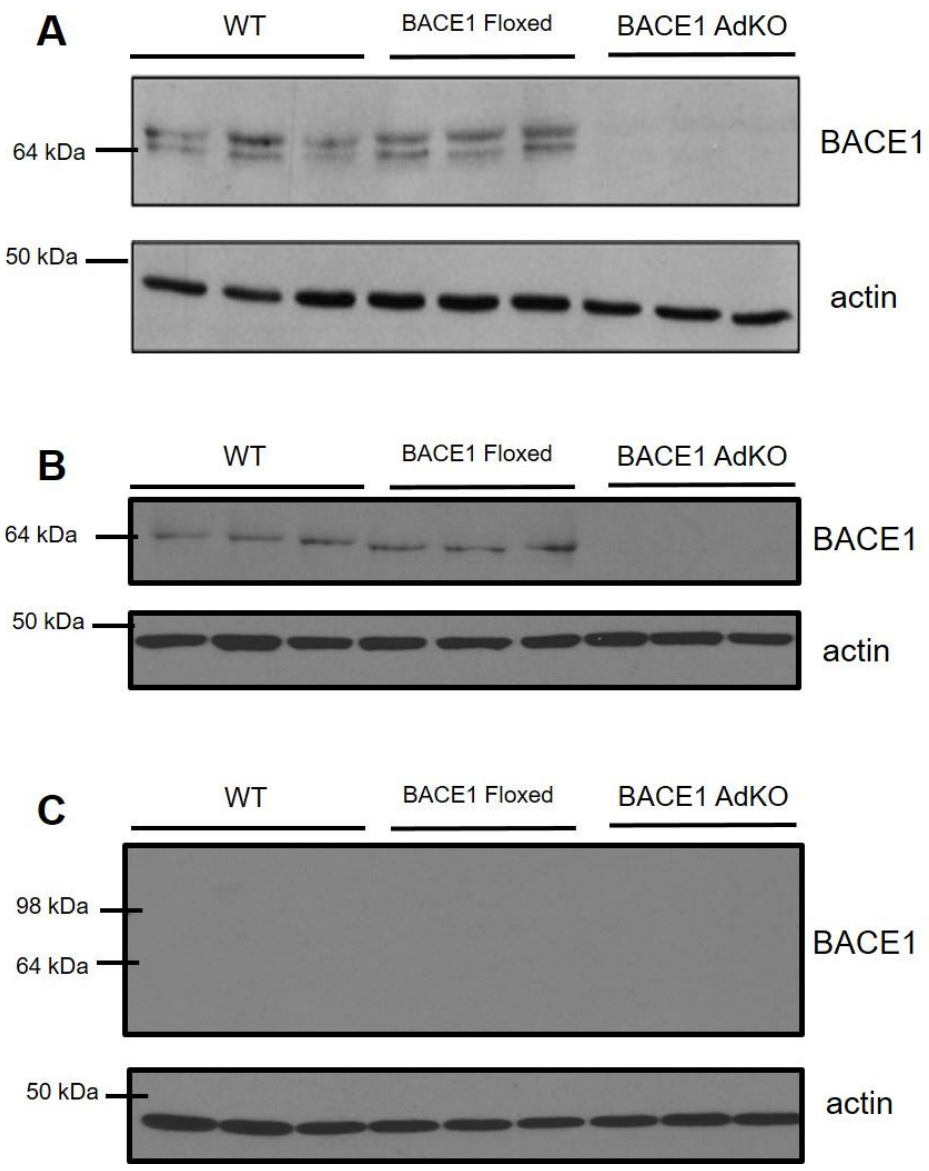

Figure 3.3 Conditional removal of BACE1 is confirmed by protein expression in eWAT, and iWAT, but BACE1 is not present in BAT

Fat pads were excised from mice and protein extracted. 20µg protein was loaded onto gels and separated by SDS-PAGE **(A)** BACE1 protein expression in eWAT, **(B)** iWAT and **(C)** BAT

n=3-6

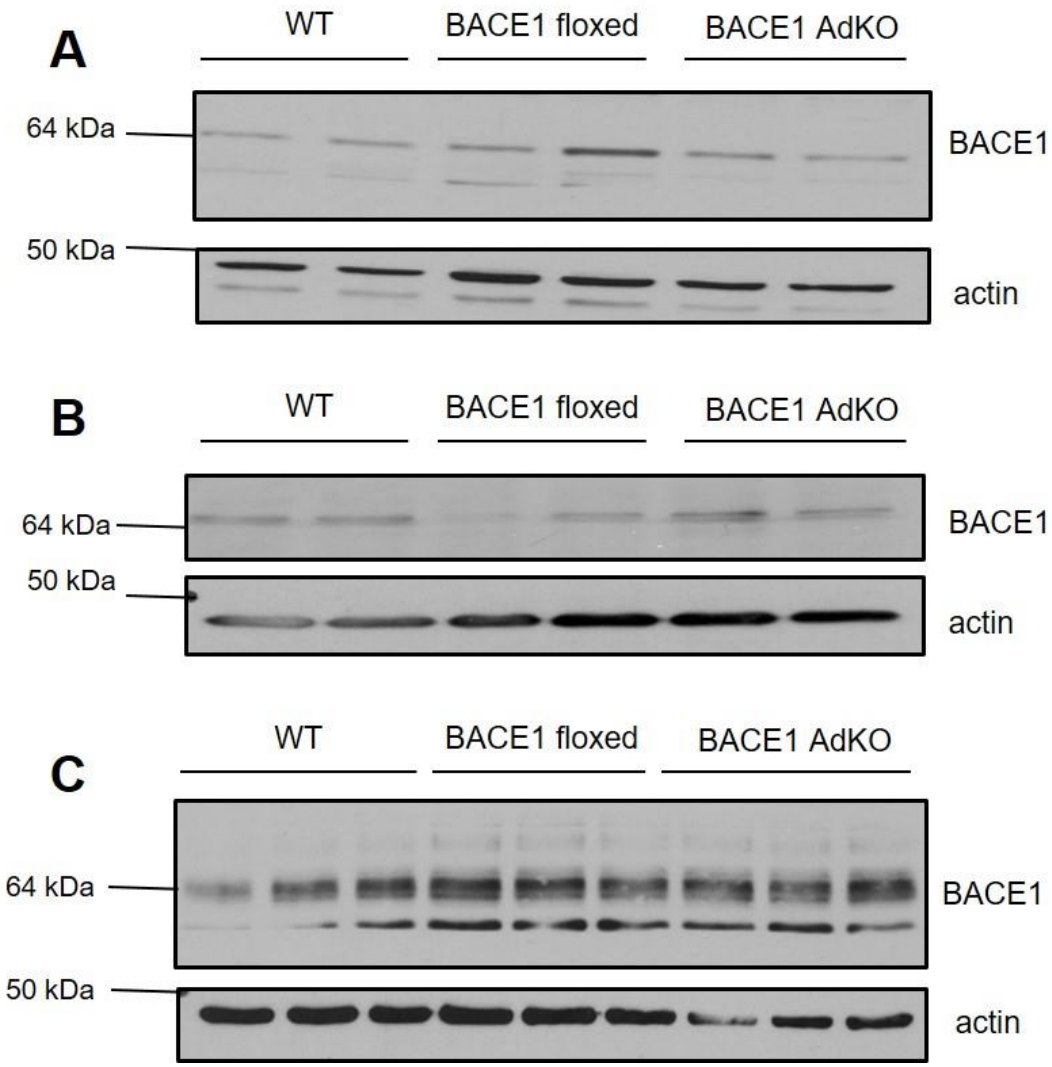

Figure 3.4 BACE1 is retained in other peripheral and brain tissues in the BACE1 AdKO model

Tissue was excised from mice and protein extracted. 20µg protein was loaded onto gels and separated by SDS-PAGE **(A)** BACE1 expression in liver **(B)** muscle, and **(C)** hippocampus

n=3-4

3.2.2 Conditional Knock-out of BACE1 in adipocytes reduces weight gain through reduced fat mass

The body weight of the mice was monitored for a period of 22 weeks, but weight gain is only reported up to week 19 due to weight loss associated with the number of different tests the animals underwent in the final 3 weeks of the study. During the 19 week period BACE1 AdKO mice gained significantly less weight compared to the other 3 groups (Figure 3.5A). Compared to WT mice BACE1 AdKO gained significantly less weight (Figure 3.5B- WT 19.96g ± 1.28 v BACE1 AdKO 11.87 ± 1.20g, n=10-14; p=0.0001), and this was also true when compared to AdipoQCre mice (AdipoQCre 21.19g ± 1.07, n=11; p=0.0001) and BACE1 floxed mice (BACE1 floxed 17.44g ± 0.86, n=29; p=0.0013). This was also the case when expressed as a percentage gain of body weight gain compared to starting weight (Figure 3.5C- WT 75.66 ± 4.82% v BACE1 AdKO 49.01 ± 4.43%, n=10-14; p=0.0005), and compared to AdipoQCre (AdipoQCre 81.41 ± 5.44%, n=11; p<0.0002), and BACE1 floxed mice (BACE1 floxed 69.70 ± 3.41%, n=29; p=0.0014).

EchoMRI scans were performed throughout the study to test body composition. At the start, before being placed on the HFD there was a significantly raised fat mass in the AdipoQ Cre mice compared to WT (Figure 3.6A- WT 6.18 ± 0.66% v AdipoQ Cre 9.46 ± 0.98%, n=10-12; p=<0.01). This effect was not observed after 10 and 20 weeks of study. After 10 weeks of the study BACE1 AdKO mice had significantly reduced fat mass compared to WT mice (Figure 3.6B- BACE1 AdKO 12.71 ± 2.36%, n=11; p=<0.0001). This was associated with a concomitant increase in lean mass (WT 67.35 ± 1.56% v BACE1 AdKO 80.85 ± 2.19, n=11-14; p=<0.0001) The effect was retained after 20 weeks with fat mass still reduced (Figure 3.6C- WT 36.31 ± 1.11% v AdipoQ Cre 38.34 ± 1.88 v BACE1 Floxed 31.03 ± 1.17 BACE1 AdKO 19.21 ± 3.18, n=10-29; p=<0.0001 for all comparisons), and lean mass still increased (WT 59.73 ± 1.10% v AdipoQ Cre 57.64 ± 1.73 v BACE1 Floxed 63.88 ± 1.10 BACE1 AdKO 75.10 ± 3.24, n=10-29; p=<0.0001 for all comparisons). The study

was performed alongside a further 2 conditional knock-out models. As a result, BACE1 floxed mice were pooled from the other 2 studies as it was unclear as to whether BACE1 floxed mice may have a confounding body weight and fat mass phenotype. All BACE1 floxed mice nevertheless originated from the same stock mice for all studies. For subsequent biochemical studies, floxed mice from all 3 studies were used in equal numbers to represent the BACE1 floxed control group.

To confirm this, the weights of the eWAT (a representative visceral fat depot), iWAT (a representative subcutaneous depot) and interscapular BAT fat depots were analysed, both as raw wet mass, and as a percentage of total body mass. There was no difference in the size of the BAT (Figures 3.7A and B) or eWAT (Figures 3.7C and D). However, the iWAT was significantly smaller in BACE1 AdKO mice compared to WT as raw weight (Figure 3.7E- WT 1.54 ± 0.14g v BACE1 AdKO 0.73 ± 0.17; n=9-11, $p<0.05$). Adipo Q Cre mice had a higher iWAT fat pad size compared to BACE1 floxed mice (AdipoQ Cre 2.03 ± 0.13g v BACE1 Floxed 1.24 ± 0.35; n=8-11, $p<0.05$). The reduction in fat pad mass was also significant in BACE1 AdKO mice versus AdipoQ Cre mice ($p<0.001$).

The weights of the non-adipose tissues were also measured. There was no significant difference in spleen weight (Figure 3.8A and B). The BACE1 AdKO mice had a significantly smaller raw brain weight (Figure 3.8B- BACE1 floxed 0.49 ± 0.008g v BACE1 AdKO 0.41 ± 0.03, n=9-10; $p<0.05$). As a percentage of total mass the brain weight was raised in BACE1 AdKO mice compared to AdipoQ cre mice (Figure 3.8D- AdipoQ Cre 1.39 ± 0.07% v BACE1 AdKO 1.43, n-=9-10; $p<0.05$). The heart weight was unchanged as raw mass (Figure 3.8E) but increased in BACE1 AdKO mice, versus AdipoQ Cre mice when expressed as a percentage of total weight (Figure 3.8F- AdipoQ Cre 0.42 ± 0.04% v BACE1 AdKO 0.61 ± 0.07, n=9; $p<0.05$). The livers of AdipoQ Cre mice were larger in AdipoQ cre mice compared to BACE1 AdKO mice (Figure 3.8G- AdipoQ Cre 1.09 ± 0.18g v BACE1 AdKO 0.97 ± 0.97, n=9-10; $p<0.05$). There was no difference in liver weight when analysed as a percentage of total mass (Figure 3.8H).

Taken together, this data indicates that BACE1 AdKO mice have a reduced fat mass compared to control groups, which can be attributed mainly to a reduction in subcutaneous iWAT fat pad size.

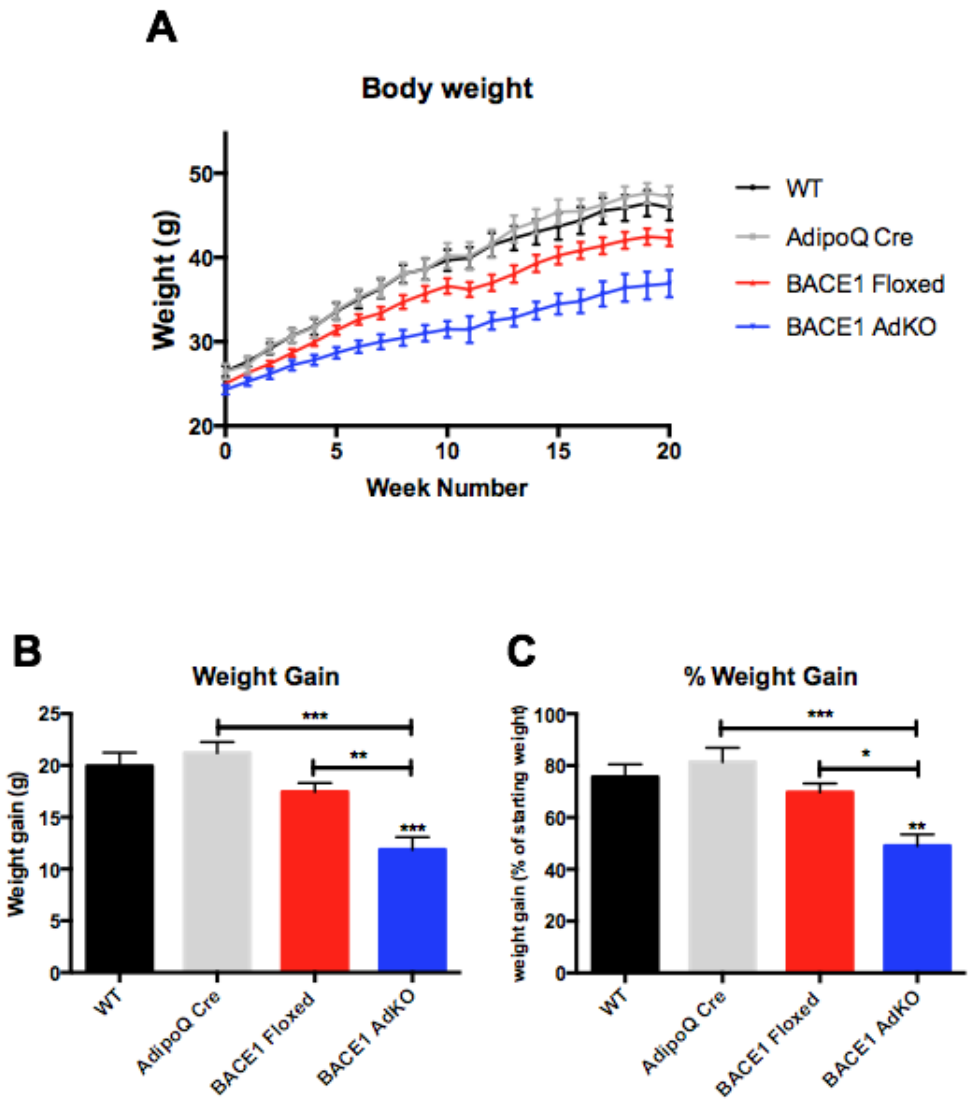

Figure 3.5 Conditional removal of BACE1 from adipocytes reduces body weight and weight gain on a HFD background

Mice were fed a HFD for 22 weeks **(A)** Average weight of the mice over the course of the first 20 weeks HFD study. **(B)** Net weight gain over the course of the study. BACE1 AdKO mice gained significantly less weight than WT and AdipoQ cre mice and BACE1 floxed mice. **(C)** Percentage weight gain over the course of the study. BACE1 AdKO mice gained significantly less weight than WT, AdipoQ cre, and BACE1 floxed mice and BACE1 floxed mice.

n=11-29; *p<0.05, **p<0.01, ***p<0.001

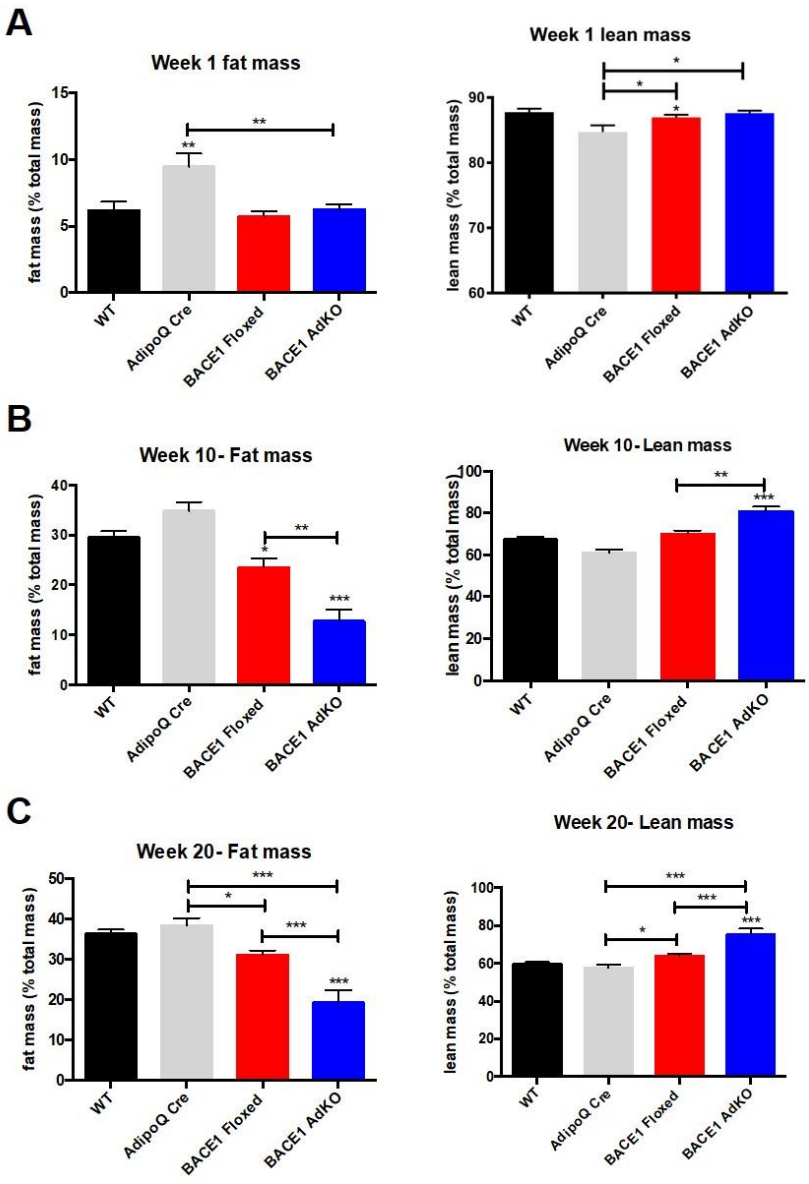

Figure 3.6 Conditional removal of BACE1 from adipocytes reduces fat mass

Body composition was assessed by EchoMRI scan prior to starting the HFD, and then at the mid-point and end-point of the study **(A)** Prior to starting on the HFD, AdipoQ Cre mice had a higher percentage fat mass compared to WT (n=10-29) with an associated decrease in lean mass. **(B)** After 10 weeks, AdKO mice had significantly reduced fat mass and associated lean mass compared to both floxed and WT (n=11-29) mice. **(C)** After 20 weeks this phenotype is retained- AdKO mice had significantly reduced fat mass and associated lean mass compared to both floxed (p=<0.01) and WT (n=11-29) mice.

*p<0.05, **p<0.01, ***p<0.001

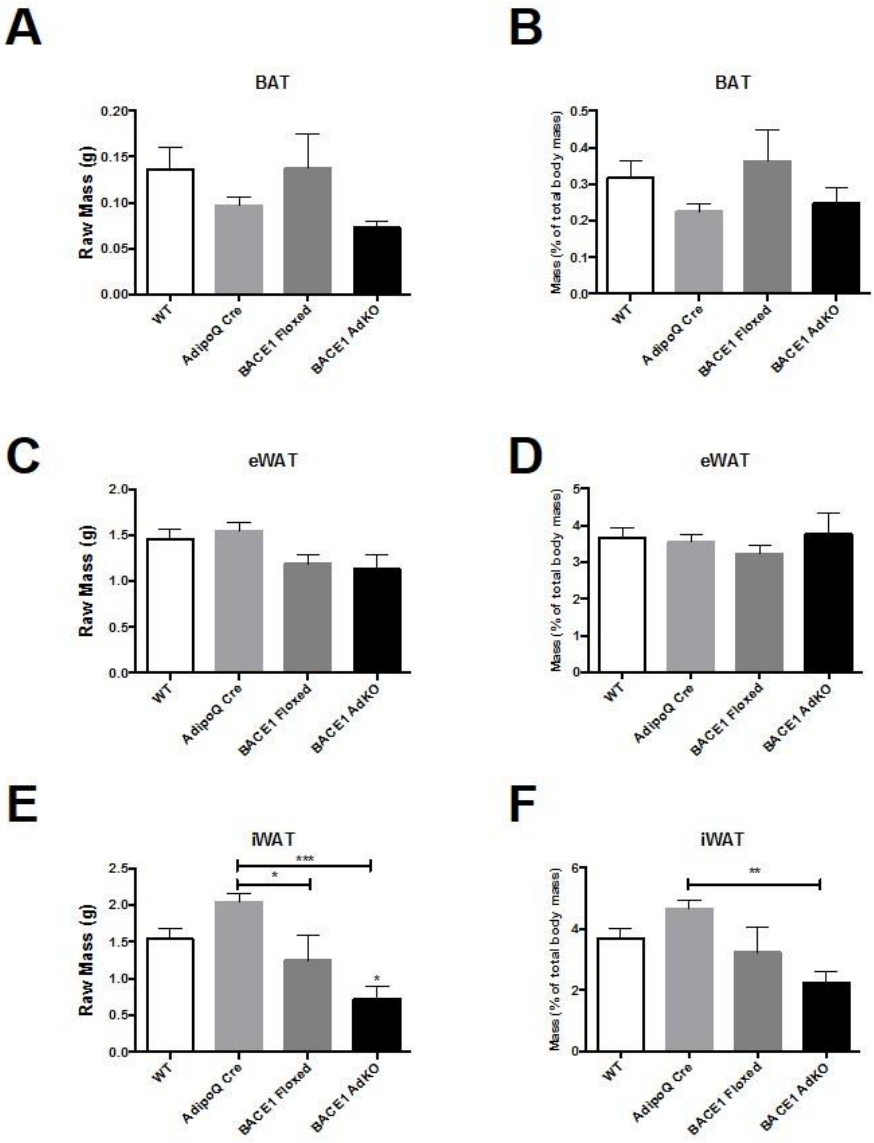

Figure 3.7 Conditional removal of BACE1 from adipocytes reduces iWAT fat pad weight

Mice were fed a HFD for 22 weeks, after which tissue weights were assessed **(A)** Average raw wet mass of the BAT and **(B)** Average BAT weight as a percentage of total body mass are unchanged between groups. **(C)** Average raw wet mass of the eWAT and **(D)** Average eWAT weight as a percentage of total body mass are unchanged between groups. **(E)** Average raw wet mass of the iWAT is significantly reduced in BACE1 AdKO mice compared to WT and AdipoQ Cre mice. iWAT fat pad weight is also reduced in BACE1 floxed mice compared to Adipo Cre mice and **(F)** average iWAT weight as a percentage of total body mass is reduced in BACE1 AdKO mice compared to AdpoQ Cre mice

n=7-12; *p<0.05***p<0.001

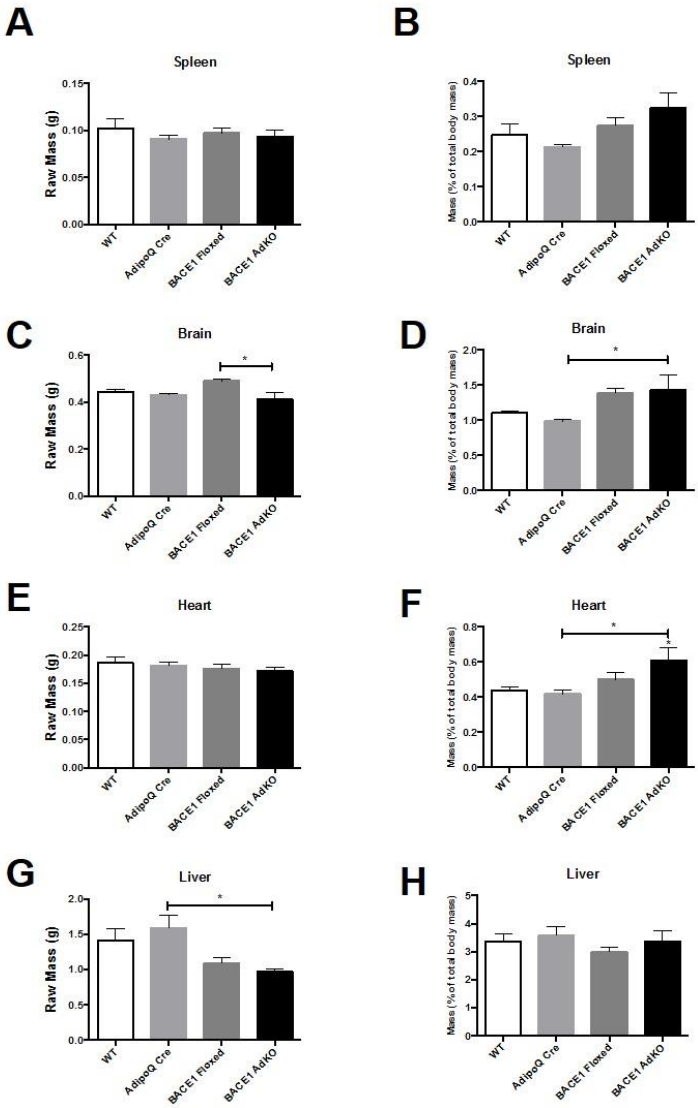

Figure 3.8 Conditional removal of BACE1 from adipocytes slightly alters weights of other tissues

Mice were fed a HFD for 22 weeks, after which tissue weights were assessed **(A)** Average raw wet mass of the spleen and **(B)** Average spleen weight as a percentage of total body mass are unchanged between groups. **(C)** Average raw wet mass of the brain is reduced in BACE1 AdKO mice compared to BACE1 floxed mice. **(D)** Average brain size as a percentage of total body mass is raised in BACE1 AdKO mice compared to AdipoQ Cre mice. **(E)** Average raw wet mass of the heart is unchanged between groups **(F)** **a**verage heart weight as a percentage of total body mass is raised in BACE1 AdKO mice compared to AdipoQ Cre mice. **(G)** Average raw wet mass of the liver is decreased in BACE1 AdKO mice compared to AdipoQ Cre mice. **(H)** Average liver size as a percentage of total body mass are unchanged between groups.

n=7-12; *p<0.05***p<0.001,

3.2.3 Conditional Knock-out of BACE1 in adipocytes enhances glucose disposal but not insulin sensitivity or secretion

Glucose tolerance was first assessed after 10 weeks of HFD. There was no significant difference in fasting blood glucose between groups (Figure 3.9A). Glucose disposal was assessed by examining the area under the curve (AUC). Reduced AUC is associated with improved glucose disposal. Indeed, glucose disposal was improved in BACE1 AdKO mice compared to all groups (Figure 3.9B- WT 1590 ± 106.1 v AdipoQ Cre 2003 ± 122.6 v BACE1 floxed 1448 ± 60.58 v BACE1 AdKO 1093 ± 58.66, n=11-29; $p<0.01$ v WT, $p<0.05$ v BACE1 floxed and $p<0.001$ v AdipoQ cre). Interestingly, the AdipoQ Cre mice exhibited significantly poorer glucose tolerance compared to WT mice ($p<0.05$).

This phenotype was retained after 19 weeks of HFD. There was no difference in fasting blood glucose between genotypes (Figure 3.9C). When the GTT results were quantified, BACE1 AdKO mice still had improved glucose disposal (Figure 3.9D- WT 1242 ± 123.4 v AdipoQ Cre 1667 ± 122.4 v BACE1 floxed 1042 ± 65.13 v BACE1 AdKO 792.8 ± 81.04, n=11-29; $p<0.01$ v WT, $p<0.05$ v BACE1 floxed and $p<0.001$ v AdipoQ cre). Once again, the AdipoQ Cre mice had impaired glucose disposal compared to WT mice ($p<0.05$).

Improved glucose disposal is often associated with improved insulin sensitivity. To examine this an i.p. ITT was performed. However, after 11 weeks HFD there was no difference in insulin sensitivity (Figure 3.10A) between the 4 studied groups. There was also no significant difference in the final ITT after 20 weeks of HFD (Figure 3.10B).

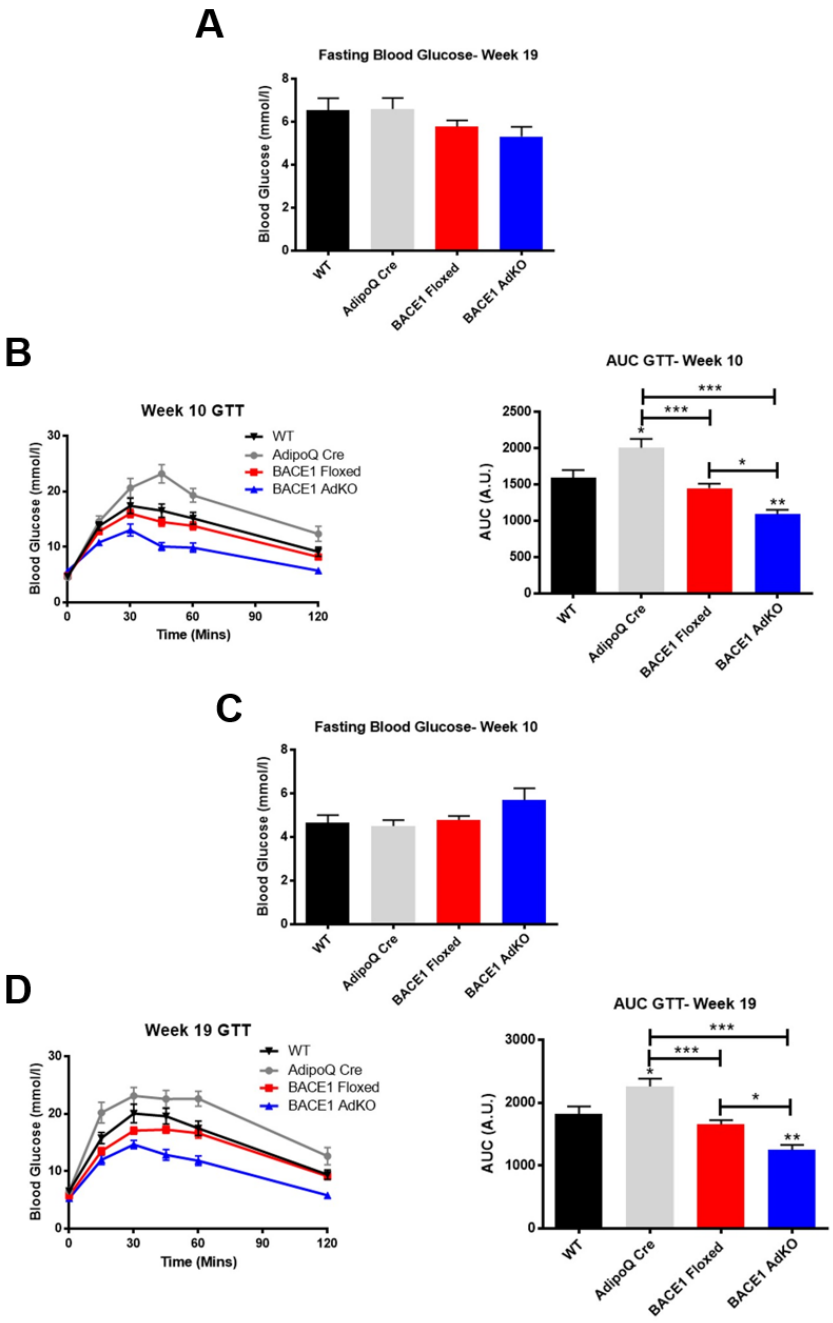

Figure 3.9 Conditional removal of BACE1 from adipocytes improves glucose disposal after 10 and 19 weeks of HFD

GTTs were performed by injecting 1mg/kg D-glucose intra-peritoneally after 10 and 19 weeks of HFD **(A)** Fasting blood glucose after 10 weeks HFD is unaltered by removal of adipocyte BACE1. **(B)** Glucose tolerance test, quantified by AUC shows glucose disposal is improved in BACE1 AdKO mice compared to all other groups **(C)** Fasting blood glucose after 19 weeks HFD is unaltered by removal of adipocyte BACE1 **(D)** Glucose tolerance test, quantified by AUC shows glucose disposal is improved in BACE1 AdKO mice compared to all other groups

n=11-29; *p<0.05, **p<0.01, ***p<0.001

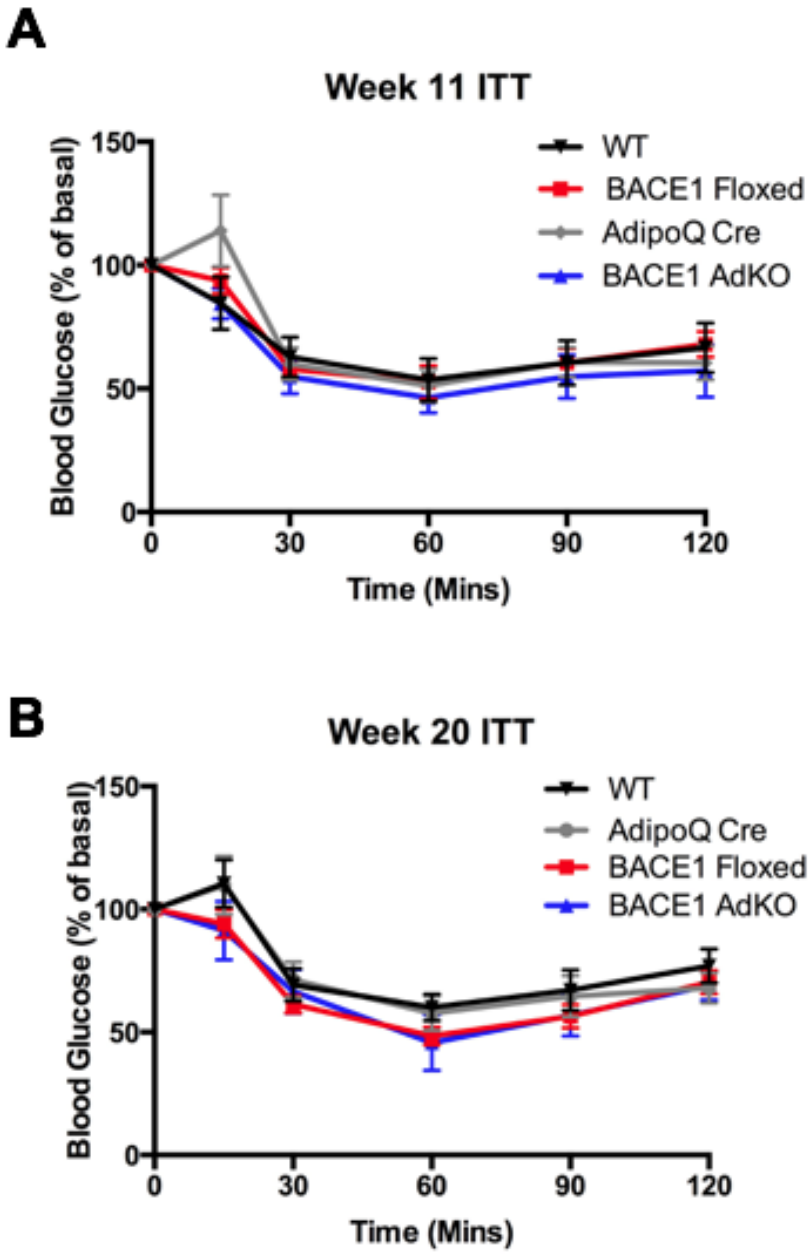

Figure 3.10 Conditional removal of BACE1 from adipocytes does not alter insulin sensitivity after 11 or 20 weeks HFD

ITTs were performed by injecting 0.75U/Kg insulin intra-peritoneally after 11 and 20 weeks of HFD **(A)** Insulin tolerance test after 11 weeks HFD was unaltered (n=11-17) **(B)** Insulin tolerance test after 20 weeks HFD was also unchanged between all genotypes (n=6-26)

Although there was no change in sensitivity to insulin, there remained the possibility that there was, instead, altered insulin secretion to explain the enhanced glucose disposal. There was a decrease in levels of fasting insulin with BACE1 AdKO mice having decreased levels compared to WT (Figure 3.11A- WT1.46 ± 0.25ng/ml v BACE1 AdKO 0.58 ± 0.12, n-7-8; p=0.01). However, when a GSIS test at the end of the study was undertaken no differences were ascertained in insulin secretion in response to a dose glucose (Figure 3.11B). Enhanced glucose uptake can occur through insulin independent mechanisms, and in the WAT this is often via GLUT1 transporters (Kraegen et al. 1993), in contrast to GLUT4 mediated insulin dependent glucose uptake, which occurs through insulin acting to promote translocation of GLUT4 to the cell surface and fusion to the membrane via PI3-kinase (Saltiel & Kahn 2001) and SNARE proteins, which is disrupted in obese and insulin resistant individuals (Huang & Czech 2007). To see if there was any potential role of insulin independent glucose uptake gene expression of GLUT1 and the insulin dependent transporter GLUT4 was examined in the eWAT and iWAT. In eWAT, GLUT1 gene levels were unaltered (Figure 3.12A). GLUT4 was significantly decreased in floxed mice compared to WT mice (Figure 3.12B- WT 1.00 ± 0.19 v BACE1 fFloxed 0.67 ± 0.11, n=7-8; p=0.02), but there was no significant alteration in the BACE1 AdKO group (Figure 3.12B). GLUT1 was significantly increased in BACE1 AdKO mice compared to WT mice in iWAT (Figure 3.12C- WT 1.00 ± 0.06 v BACE1 AdKO 2.09 ± 0.35, n=8; p=0.02) and compared to BACE1 floxed mice (1.03 ± 0.10, n=6; p=0.02), whereas GLUT4 levels were unchanged (Figure 3.12D). These data, taken as a whole, indicate that BACE1 AdKO mice have enhanced glucose disposal, which is potentially mediated through increased insulin independent glucose uptake in WAT, rather than through altering insulin sensitivity or secretion.

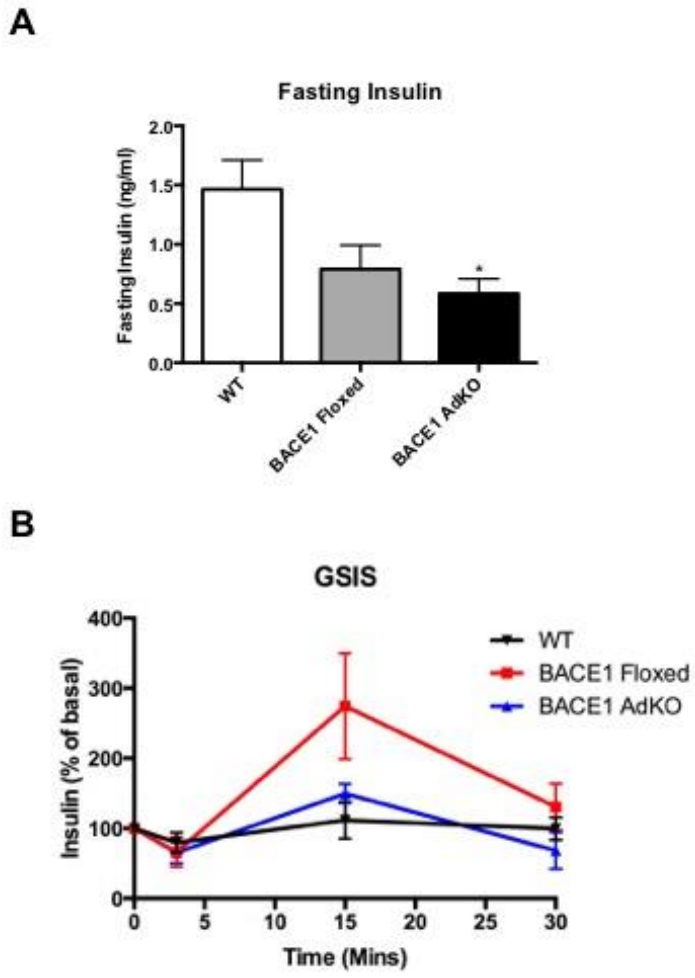

Figure 3.11 Conditional removal of BACE1 from adipocytes does not alter insulin secretion

To assess insulin secretion, a GSIS test was performed after 21 weeks HFD. Mice were injected i.p. with 2mg/kg glucose, and the blood samples taken run on an insulin ELISA plate **(A)** There was a significant reduction in fasting insulin levels in BACE1 AdKO mice compared to WT mice **(B)** insulin secretion was also not significantly altered

n=7-8; *p<0.05

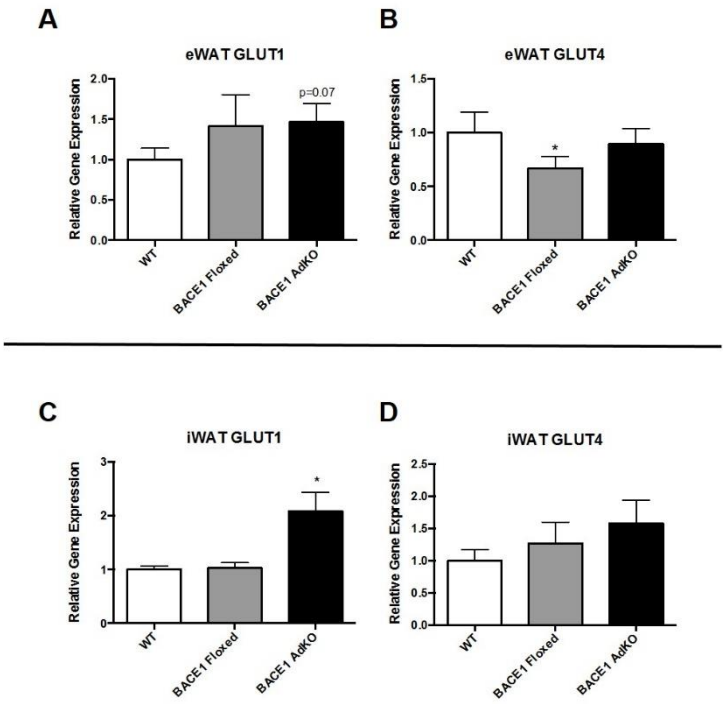

Figure 3.12 Conditional removal of BACE1 from adipocytes enhances GLUT1 expression in iWAT

Following the 22 week HFD protocol, WAT from the epididymal and inguinal fat pads were excised. RNA was extracted and cDNA synthesised, to examine gene expression **(A)** Levels of GLUT1 expression are unchanged in eWAT (n=7-9) **(B)** GLUT4 is reduced in BACE1 floxed mice ($p<0.05$, n=7-9) but unaltered in BACE1 AdKO mice **(C)** GLUT1 is significantly upregulated in AdKO mice (n=6-8) compared to WT mice, whereas **(D)** GLUT4 remains unaltered (n=6-8)

*$p<0.05$

3.2.4 Conditional Knock-out of BACE1 in adipocytes alters energy expenditure and oxygen consumption

To try and ascertain what was responsible for the resistance to obesity phenotype a number of metabolic parameters were assessed using the CLAMS device. We did not detect any changes in physical activity or average daily food intake (Figure 3.13A and B). There was also no change in RER (Figure 3.13C), indicating that there was no switch in fuel utilisation between groups. RER was just over 0.80, indicating no preference for fat or glucose oxidation (Speakman 2013). Absolute oxygen consumption was decreased in BACE1 floxed mice compared to WT mice over a 48 hour time period (Figure 3.14A- WT 2.25 ± 0.11 ml/min v BACE1 floxed 1.98 ± 0.06, n=7-12; $p<0.05$), but increased in BACE1 AdKO mice compared to BACE1 floxed, but not WT mice (BACE1 AdKO 2.25ml/min ± 0.05, n=7; $p<0.05$). This difference was shown to be primarily through increased oxygen consumption in the light cycle, where oxygen consumption was decreased in BACE1 floxed mice compared to WT (Figure 3.14B- WT 2.10 ± 0.09ml/min v BACE1 floxed 1.83 ± 0.05, n=8-12; $p<0.05$). The oxygen consumption was raised in BACE1 AdKO compared to BACE1 floxed mice (Figure 3.14B- BACE1 AdKO 2.12 ± 0.06, n=7; $p<0.05$). There was no difference in oxygen consumption during the dark cycle (Figure 3.14C). When plotted against body mass (Figure 3.14D), there was a striking difference between groups, with a significant difference in the linear regression slopes. Whereas in WT mice there is a relatively linear relationship between weight and oxygen consumption, this is disrupted in BACE1 AdKO mice.

Energy expenditure measured over a 48 hour time period decreased in BACE1 floxed mice compared to WT mice (Figure 3.15A- WT 0.66 ± 0.02 kcal/hr v BACE1 floxed 0.57 ± 0.02, n=4-12; $p<0.05$), and increased in BACE1 AdKO mice compared to BACE1 floxed, but not WT, mice (BACE1 AdKO 5.65 kcal/hr ± 0.02, n=7; $p<0.05$). As with oxygen consumption, this effect was observed to be within the light cycle. BACE1 floxed mice had reduced energy expenditure compared to WT mice (Figure 3.15B- WT 0.61

± 0.02 kcal/hr v BACE1 floxed 0.53 ± 0.02, n=10-12; $p<0.05$). Energy expenditure was raised in BACE1 AdKO mice compared to floxed mice in the light cycle (Figure 3.15B- BACE1 floxed 0.64 kcal/hr ± 0.04 v BACE1 AdKO 0.61 ± 0.02, n=7-12; $p<0.01$). There was no difference in energy expenditure in the dark cycle (Figure 3.15C).

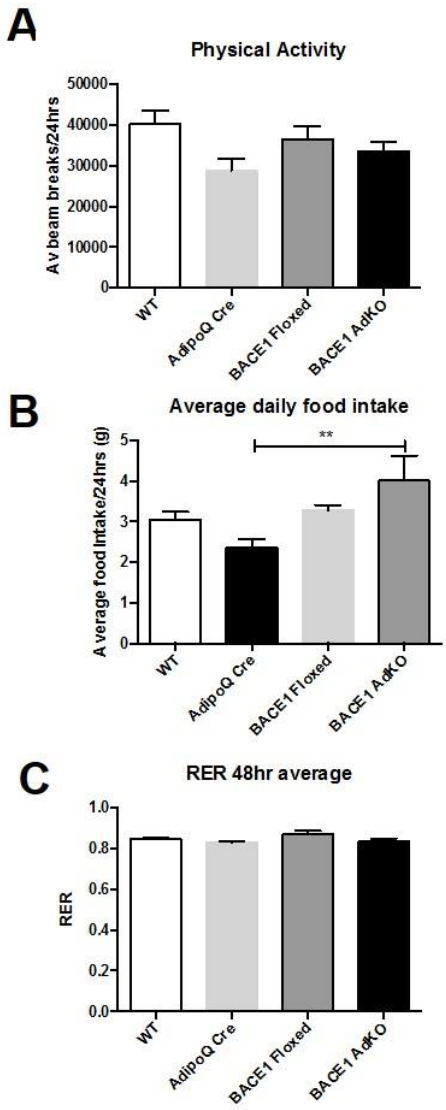

Figure 3.13 Conditional removal of BACE1 from adipocytes has no impact on physical activity or food intake

In the final week of the HFD study, mice were placed in the CLAMS device for 72 hours to assess a number of metabolic parameters. The data from the first 24 hours was excluded from analysis to allow for acclimatisation to the cage **(A)** Average daily physical activity over a 48 hour recorded period shows no significant difference between groups **(B)** Average daily food intake is raised in BACE1 AdKO mice compared to AdipoQ Cre mice **(C)** RER is unchanged between groups

n=7-12, **p<0.01

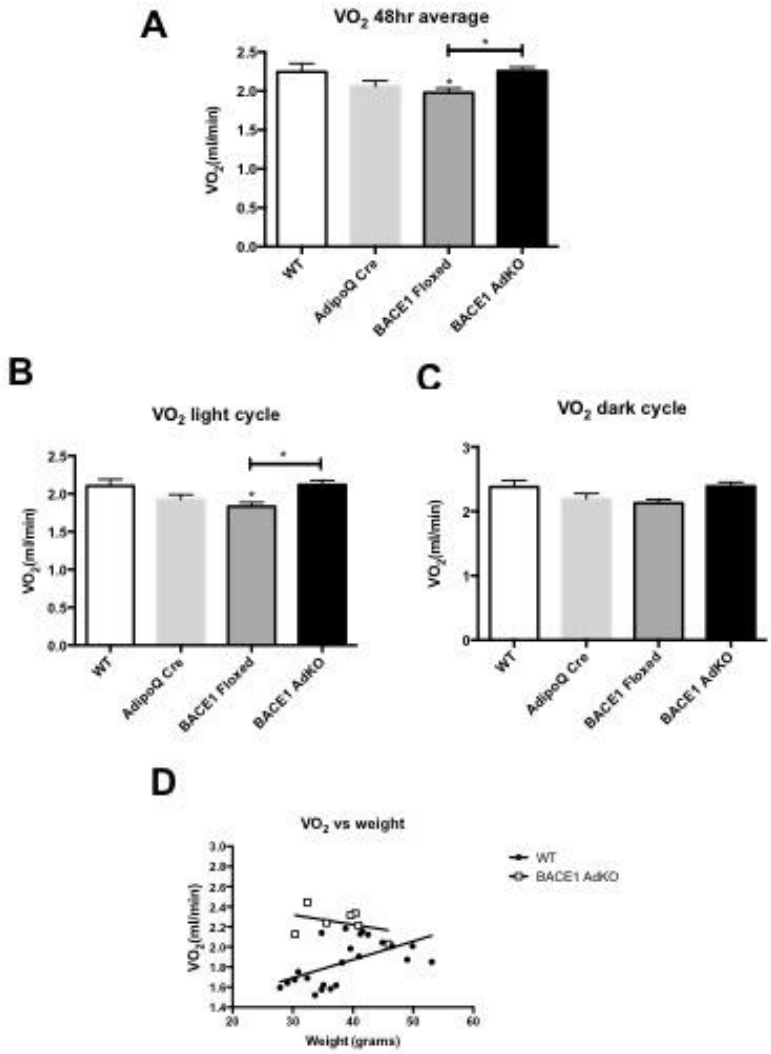

Figure 3.14 Conditional removal of BACE1 from adipocytes alters oxygen consumption

In the final week of the HFD study, mice were placed in the CLAMS device for 72 hours to assess a number of metabolic parameters. The data from the first 24 hours was excluded from analysis to allow for acclimatisation to the cage **(A)** Oxygen consumption is raised in BACE1 AdKO mice compared to BACE1 floxed mice. Oxygen consumption is decreased in BACE1 floxed mice compared to WT mice **(B)** This alteration is due to changes during the light cycle. Oxygen consumption in the light cycle is raised in BACE1 AdKO mice compared to BACE1 floxed mice. Oxygen consumption is decreased in BACE1 floxed mice compared to WT mice **(C)** There was no difference of oxygen consumption within the dark cycle **(D)** Weight plotted against oxygen consumption in a scatter plot. For this graph additional data, produced previously by Dr. Paul Meakin was used from normal chow fed WT mice, to demonstrate the linear relationship between VO_2 and body weight (WT n=23)

n=7-12 unless stated, *p<0.05, **p<0.01

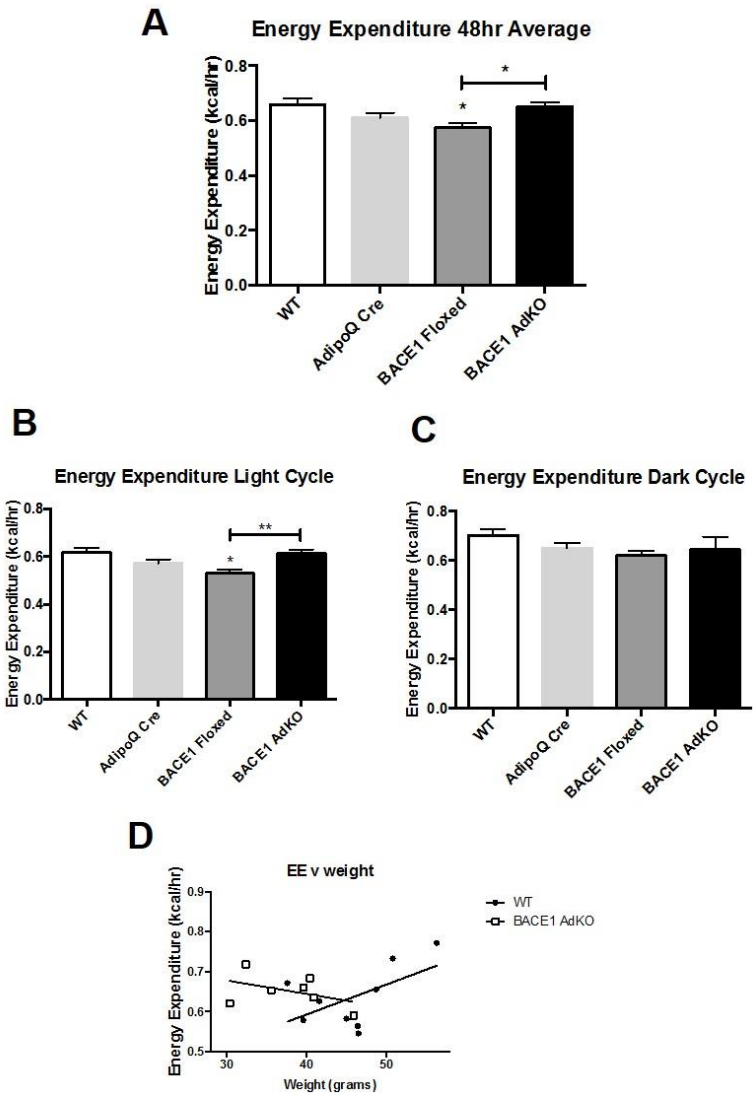

Figure 3.15 Conditional removal of BACE1 from adipocytes increases energy expenditure, particularly within the light cycle

In the final week of the HFD study, mice were placed in the CLAMS device for 72 hours to assess a number of metabolic parameters. The data from the first 24 hours was excluded from analysis to allow for acclimatisation to the cage **(A)** Energy expenditure is raised in BACE1 AdKO mice compared to BACE1 floxed mice Energy expenditure is decreased in BACE1 floxed mice compared to WT mice **(B)** This alteration is due to changes during the light cycle. Energy expenditure in the light cycle is raised in BACE1 AdKO mice compared to BACE1 floxed mice Energy expenditure is decreased in BACE1 floxed mice compared to WT mice **(C)** There was no difference of energy expenditure within the dark cycle **(D)** Weight plotted against energy expenditure in a scatter plot

n=7-12; *p<0.05 **p<0.01

3.2.5 Conditional Knock-out of BACE1 in adipocytes reduces circulating leptin

Fasting leptin levels were measured in the plasma of the mice by ELISA. In BACE1 AdKO mice circulating leptin was significantly reduced compared to WT mice (Figure 3.16A- WT 43113 pg/ml ± 4003 v BACE1 AdKO 9433pg/ml ± 6214, n=8; $p<0.01$) and compared to BACE1 floxed mice (BACE1 floxed 35227pg/ml ± 6214, n=8; $p<0.01$). We also wanted to examine WAT leptin content, so examined eWAT by ELISA.

Leptin content was reduced in the BACE1 AdKO mice (Figure 3.16B- WT 6983pg/ml ± 163 v BACE1 AdKO 3419 ± 603.6, n=8; $p<0.01$). BACE1 floxed mice also had reduced leptin content compared to WT mice (BACE1 floxed 4307 ± 818.3, n=8; $p<0.05$), but there was no significant difference between BACE1 floxed and BACE1 AdKO mice. This may simply be due to the reduction in fat mass, so we next associated leptin content of the mice with the final known fat mass. We found that there was no difference in the slopes between the 3 groups (Figure 3.16C), which suggests that leptin secretion, but not production, in adipocytes is altered by removal of BACE1 from adipocytes.

Next the expression levels of leptin and the leptin receptor gene were checked in the fat pads. Within eWAT there were no significant differences between groups (Figure 3.17A). In iWAT there was again no significant difference in leptin receptor expression, but leptin mRNA was reduced in BACE1 AdKO mice compared to BACE1 floxed mice (Figure 3.17B- WT 1.00 ± 0.16 v BACE1 AdKO 0.44 ± 0.18, n=7; $p=0.02$). The difference between BACE1 floxed and BACE1 AdKO mice was almost significant (BACE1 floxed 1.025 ± 0.21, n=8; $p=0.05$). The majority of leptin's actions on energy homeostasis are mediated in the hypothalamus, so we also looked at the expression of leptin and leptin receptor in this region. There was no significant difference between genotypes (Figure 3.18A and B), and there was also no difference in expression in negative regulators of leptin signalling SOCS3 (Figure 3.18C) or PTP1B (Figure 3.18D) across the

genotypes. Leptin signalling is often analysed by examining the phosphorylation status of STAT3 at tyrosine residue 705. When this was examined, basal levels of phosphorylation were reduced in BACE1 floxed mice compared to WT (Figure 3.18E- WT 1.00 ± 0.10 v BACE1 floxed 0.57 ± 0.15, n=8-1; p=0.02)

Two neuropeptides, POMC and AgRP, which are involved in modulating food intake were also analysed. The orexigenic peptide AgRP was increased in BACE1 floxed mice compared to WT mice. There was no difference in POMC expression (Figure 3.19B), and no significant difference in the ratio between the two genes were found. (Figure 3.19C)

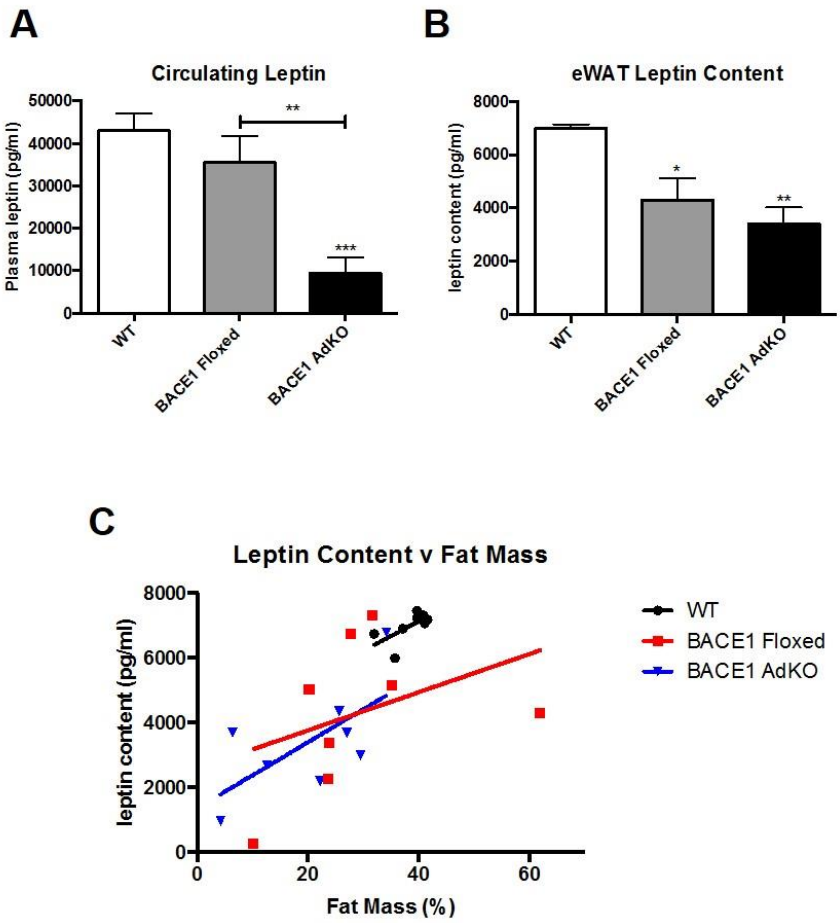

Figure 3.16 Conditional removal of BACE1 from adipocytes reduces levels of leptin in the serum and eWAT

Serum taken at the conclusion of the study and eWAT were excised from mice, and run on a leptin ELISA plate **(A)** Leptin levels in BACE1 AdKO mice are decreased compared to WT mice and BACE1 floxed mice **(B)** Leptin levels in the eWAT were reduced in BACE1 floxed mice compared to WT mice an in BACE1 AdKO mice compared to WT mice. **(C)** Leptin content was associated with fat mass

n=8, *p<0.05 **p<0.01 ***p<0.001

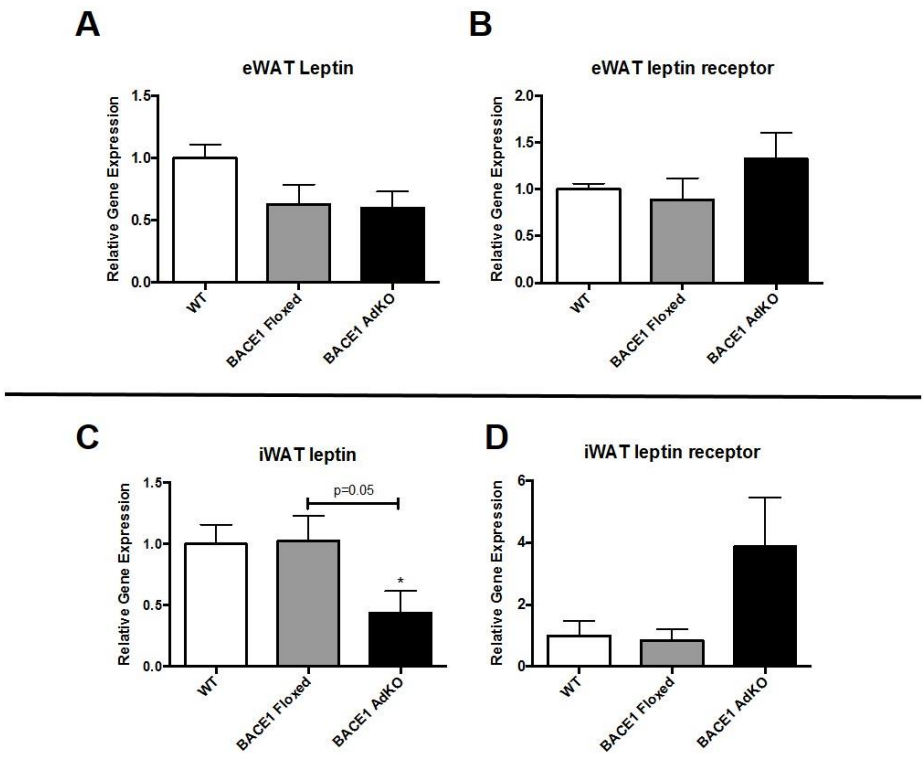

Figure 3.17 Conditional removal of BACE1 does not alter expression of leptin or leptin receptor in eWAT but reduces leptin in iWAT

eWAT and iWAT were excised and processed for gene expression analysis. 12.5ng cDNA was loaded onto a TaqMan® plate **(A**) Leptin and **(B)** leptin receptor gene expression is unaltered in BACE1 floxed on BACE1 AdKO mice in eWAT (n=8-10). **(C)** Leptin expression is reduced in iWAT of AdKO mice compared to WT mice (n=7-8) **(D)** Leptin receptor expression is unaltered in iWAT (n=7-8)

*p<0.05

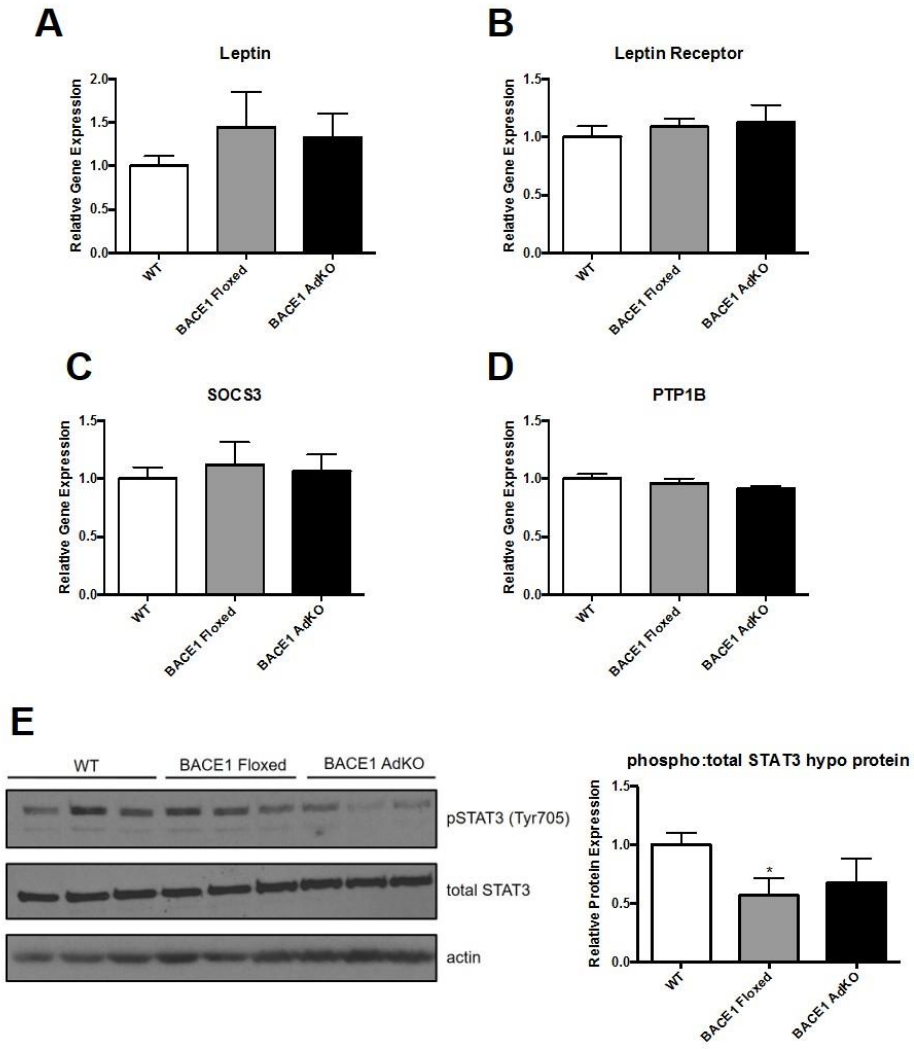

Figure 3.18 Conditional removal of BACE1 from adipocytes does not impact on hypothalamic expression of leptin signalling associated genes

After 22 weeks HFD, hypothalamus was excised from each mouse. Half was taken for gene analysis and the other half for protein quantification **(A)**Gene expression of leptin **(B)** leptin receptor **(C)** SOCS3 and **(D)** PTP1B in the hypothalamus are all unaltered by removal of BACE1 from adipocytes **(E)** Protein analysis shows reduced phosphorylation of STAT3 in BACE1 floxed mice compared to WT controls

n=8, *P<0.05

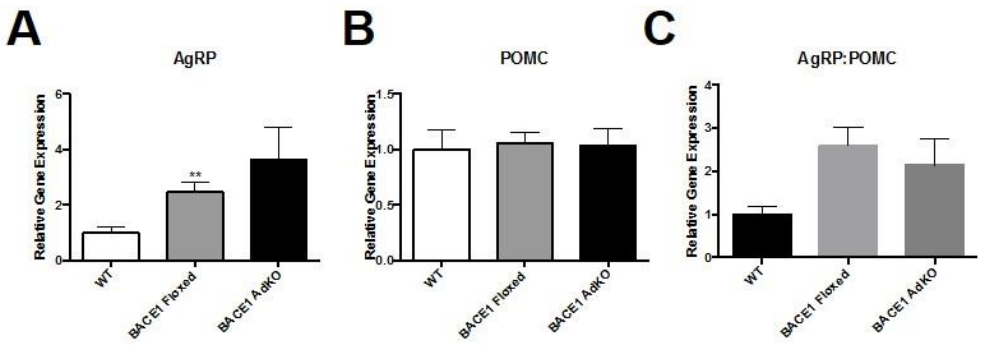

Figure 3.19 Conditional removal of BACE1 from adipocytes does not impact on hypothalamic neuropeptide expression

After 22 weeks HFD, the hypothalamus was excised and half was processed for gene expression analysis. 12.5ng cDNA was loaded onto a TaqMan® plate **(A)** Expression of AgRP was raised in BACE1 floxed mice compared to WT but not significantly in BACE1 ADKO **(B)** POMC expression was unaltered between groups. **(C)** The ratio of AgRP:POMC was not significantly changed between groups

n=8, **P<0.01

3.2.6 Conditional Knock-out of BACE1 in adipocytes may alter thermogenic programming in iWAT

Increased energy expenditure is often associated with increased non-shivering thermogenesis and browning of WAT. To look at this as a possible explanation for our phenotype the gene expression levels of a series of thermogenic markers were checked in both eWAT and iWAT. In eWAT UCP1 (Figure 3.20A), PGC-1α (Figure 3.20B), DIO2 (Figure 3.20C) and PRDM16 (Figure 3.20D) were all unaltered. In iWAT UCP1 was generally increased, but with a high degree of variability (Figure 3.20E). PGC-1α was raised to levels trending towards significance in BACE1 AdKO mice compared to WT (Figure 3.20F WT 1.00 $\pm$ 0.18 v BACE1 AdKO 3.21 $\pm$ 0.97, n=7-9; p=0.052). There were no significant differences between groups for DIO2 (Figure 3.20G) or PRDM16 (Figure 3.20H). Browning can be induced by activation of the sympathetic nervous system, and in particular through the beta3 adrenergic signalling in WAT. To see if there was enhanced activation of this pathway we looked at the expression level of beta 3 adrenergic receptor in the iWAT. We found that the gene expression of this receptor was greatly enhanced in BACE1 AdKO (Figure 3.20I- WT 1.00 $\pm$ 0.19 v BACE1 AdKO 15.32 $\pm$ 4.65, n=8; p=0.017). Taken together, these data imply that iWAT, but not eWAT has increased browning in high fat fed mice housed at 23^{o}C.

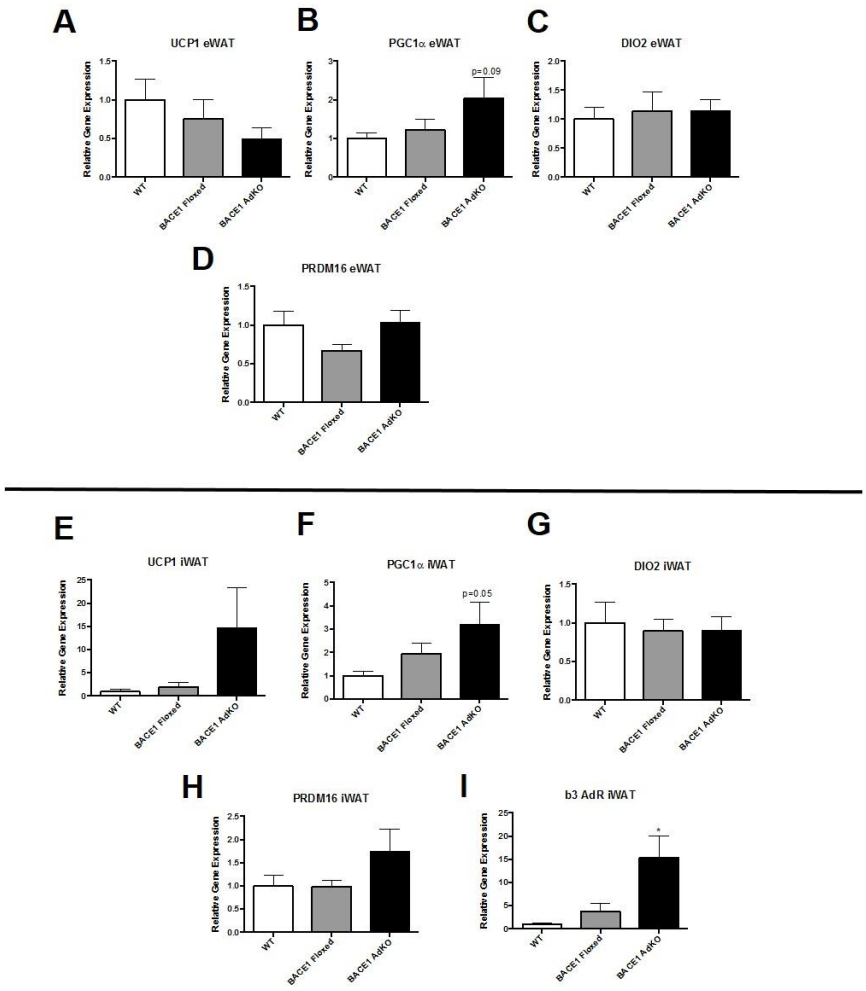

Figure 3.20 Thermogenic markers are subtly altered in eWAT and iWAT of BACE1 AdKO mice

Following the 22 week HFD protocol, WAT from the epididymal and inguinal fat pads were excised. 12.5ng cDNA was loaded onto a TaqMan® plate **(A)** Levels of UCP1, **(B)** PGC1α, **(C)** DIO2 and **(D)** PRDM16 are unaltered in eWAT. **(E)** Within iWAT UCP1 is increased, albeit not significantly (n=5-7). **(F)** PGC1α, **(G)** DIO2, **(H)** PRDM16 are unchanged. **(I)** beta 3 adrenergic receptor is upregulated in BACE1 AdKO mice compared to WT mice

n=7-9 unless stated; *p<0.05

3.2.7 Conditional Knock-out of BACE1 in adipocytes reduces hepatic steatosis and alters adipocyte number

After tissue was harvested liver, muscle and eWAT samples were retained for histological analysis. H and E staining was carried out to look at overall morphology of these tissues. The adipocyte area, diameter and number were assessed. WT and Cre mice were of a comparable size and number so analyses from both these genotypes were grouped into a single control group. Compared to this group, BACE1 AdKO mice trended towards having a smaller area (Figure 3.21B). Adipocyte diameter was unaltered (Figure 3.21C). The number of adipocytes in each field view was greater in BACE1 AdKO mice compared to controls, suggesting a higher rate of adipogenesis (Figure 3.21D- WT/AdipoQ Cre 133 $\pm$ 19 v BACE1 AdKO 208 $\pm$ 20, n=9; p=0.02).

During obesity, there is often an associated “lipid spillover”, leading to an accumulation of fat in liver and muscle. We first examined the muscle, but could see no evidence of fat accumulation or changes in overall morphology (Figure 3.22). We next examined the liver and quantified the level of steatosis in each tissue. The level of steatosis was quite variable in WT and BACE1 floxed mice, but we found minimal evidence of steatosis in BACE1 AdKO mice (Figure 3.23A), which was significantly reduced compared to WT mice when steatosis (see method section) was calculated as a percentage of total pixels in the image (Figure 3.23B- WT 42.36 $\pm$ 14.72 v BACE1 AdKO 0.98 $\pm$ 0.24 n=6; $p<0.05$).

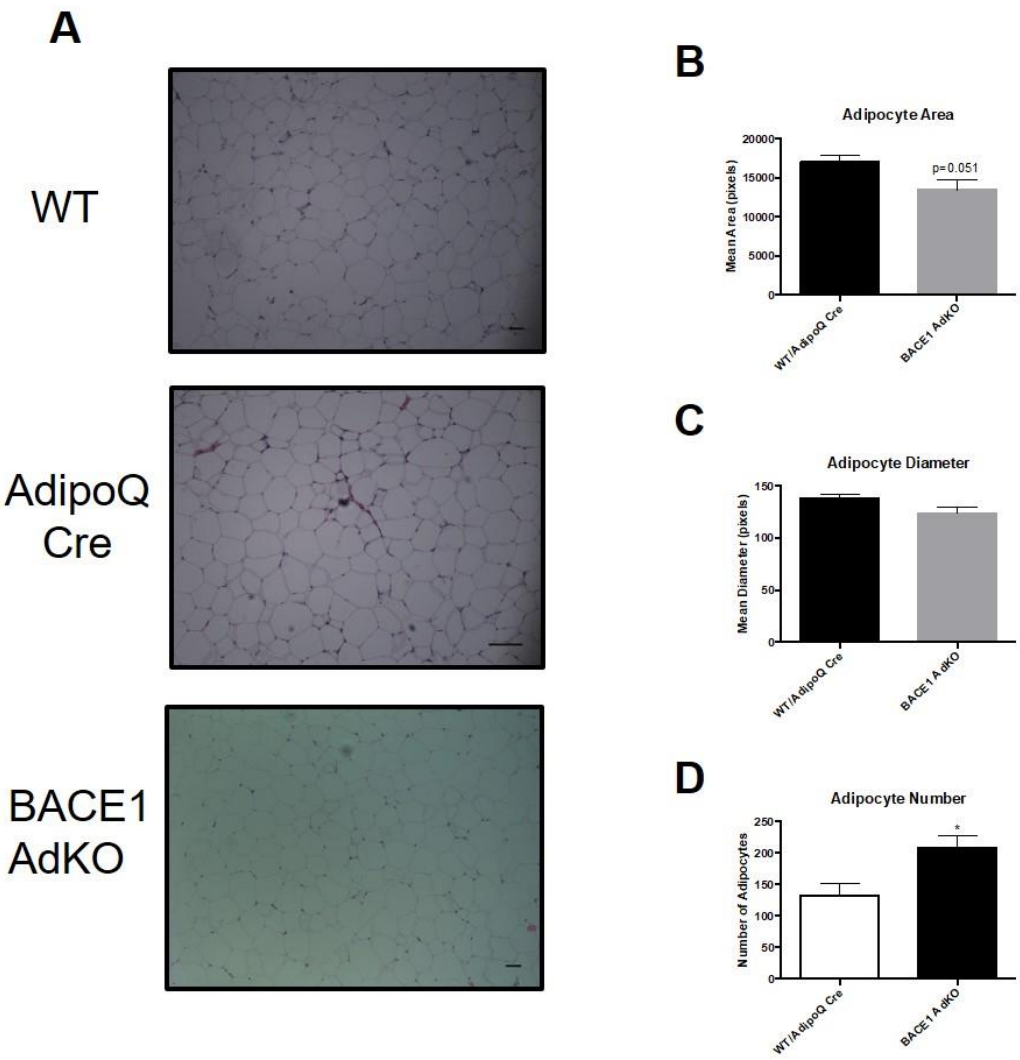

Figure 3.21 The number of adipocytes are increased in BACE1 AdKO mice

Following the 22 week HFD protocol, a section of eWAT was excised and preserved in formalin. Tissue was then embedded with paraffin, sliced and stained for H + E **(A)** H + E stain of WT, AdipoQCre and BACE1 AdKO mice, magnification x10, scale bars- 100μm **(B)** Quantification of adipocyte area shows no significant difference between groups **(C)** Adipocyte diameter is also unchanged. **(D)** Adipocyte number is raised in BACE1 AdKO mice compared to a pooled set of WT and AdipoQ Cre mice

n=3-6; *P<0.05

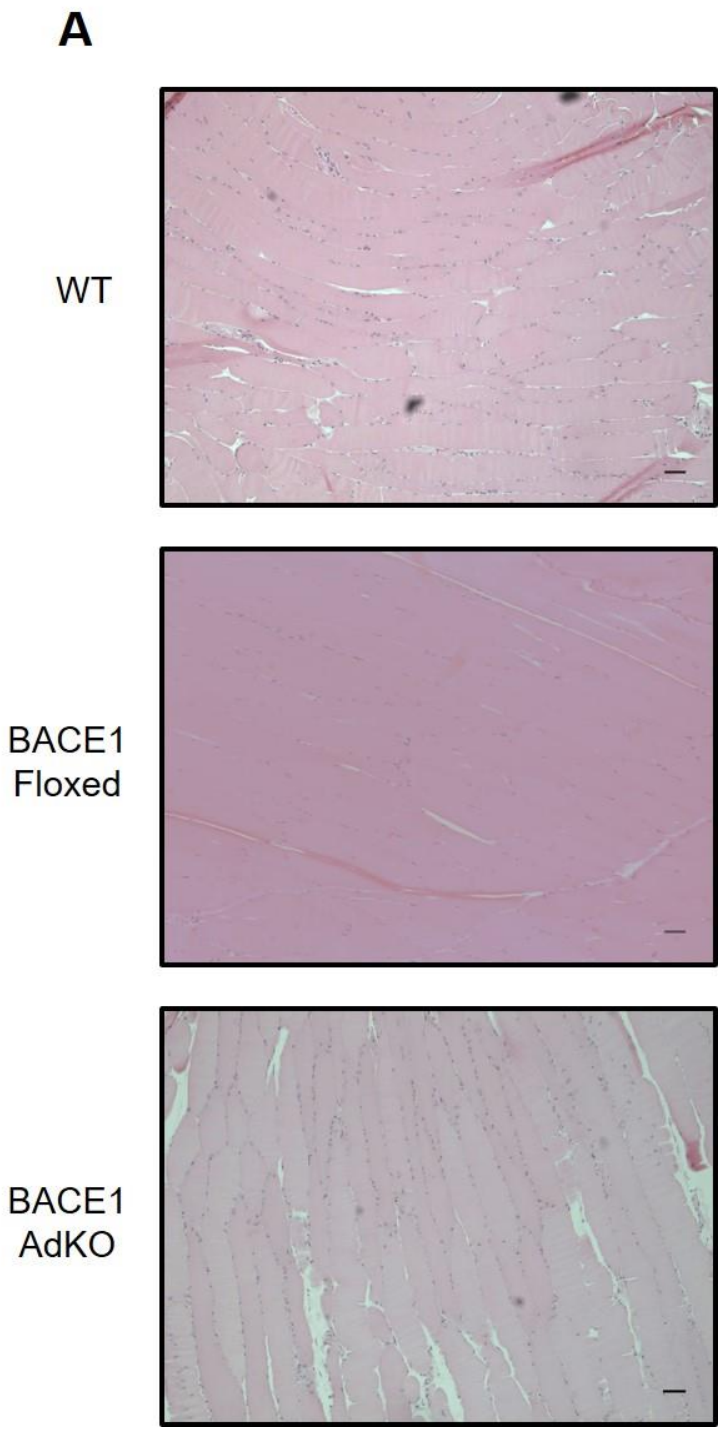

Figure 3.22 Conditional removal of BACE1 from adipocytes does not alter muscle morphology

Following the 22 week HFD protocol, a section of muscle was excised and preserved in formalin. Tissue was then embedded with paraffin, sliced and stained for H + E **(A)** H+E stains of muscle from WT, BACE1 floxed and BACE1 AdKO mice. Magnification x10, scale bar- 100μm

n=6

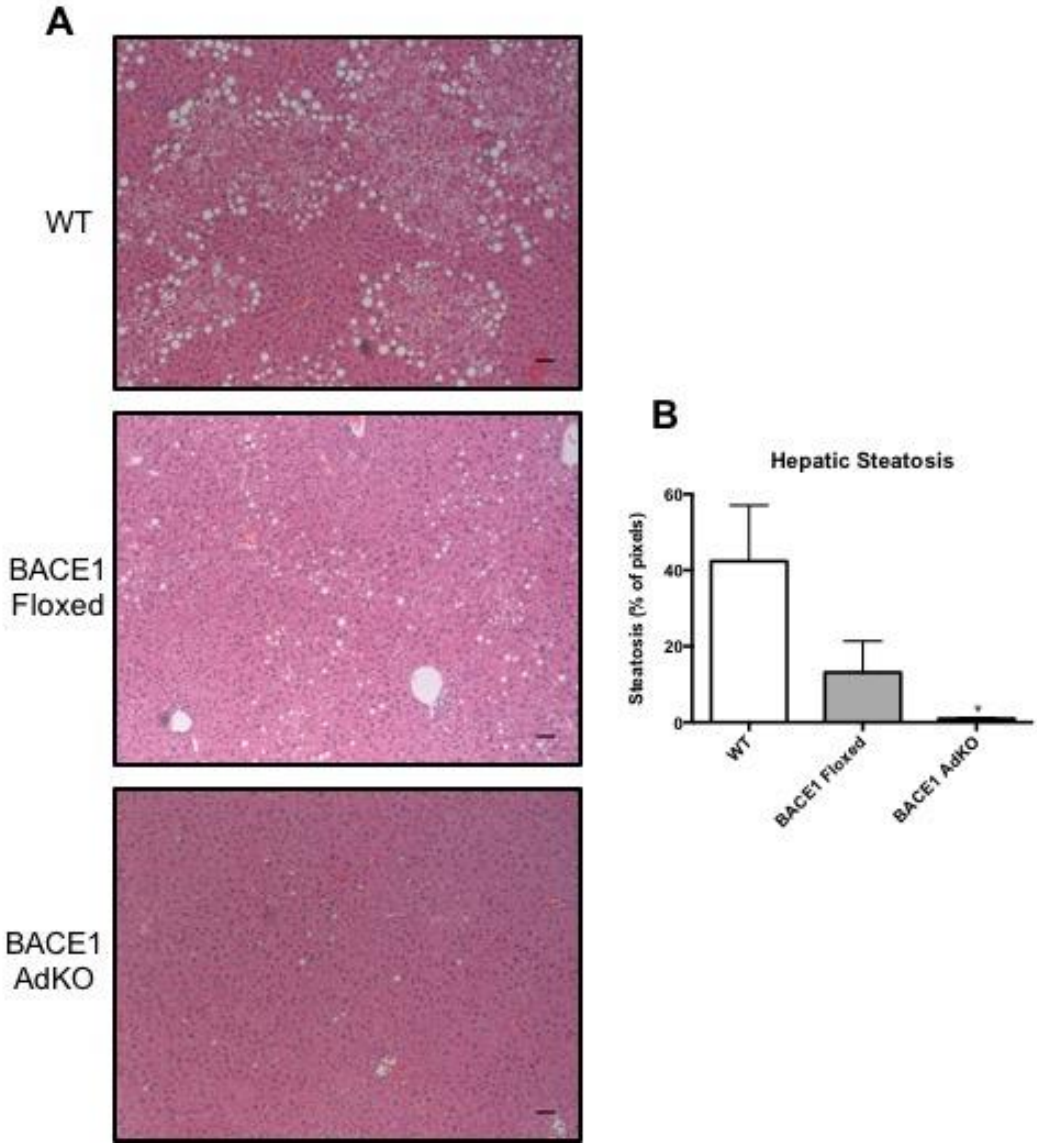

Figure 3.23 Conditional removal of BACE1 from adipocytes reduces hepatic steatosis

Following the 22 week HFD protocol, a section of liver was excised and preserved in formalin. Tissue was then embedded with paraffin, sliced and stained for H + E **(A)** H+E stains of livers of WT, BACE1 floxed and BACE1 AdKO mice. Magnification x10, scale bar=100μm **(B)** Quantification of percentage steatosis was performed by creating a colour threshold on ImageJ (ImageJ 1.49p), which allows quantification of coloured versus non-coloured pixels shows a significant decrease in steatosis in BACE1 AdKO mice.

n=6; $p<0.05$

3.2.8 The phenotype of conditional BACE1 Knock out mice may be due to enhanced Fibroblast Growth Factor 21 (FGF-21) Signalling

The next aim was to try and establish a molecular mechanism to explain the observed phenotype. First, a wide-ranging approach was attempted to test levels of various adipokines in the eWAT using an adipokine array. The array analyses the protein levels of 38 different adipokines and obesity associated molecules simultaneously (R&D Systems 2018). Adipokine levels in 2 WT mice were compared to 2 BACE1 AdKO mice. Only one protein- IGFBP2 appeared to be noticeably altered in BACE1 AdKO mice (Figure 3.24A), raised approximately 2-fold. To try to confirm this finding in a greater number of mice gene transcription levels were assessed, but there was difference in expression (Figure 3.24B), and It was not possible to gain a western blot to assess protein levels due to technical problems with the antibody.

It has previously been demonstrated that increased FGF-21 signalling can result in increased energy expenditure, browning of WAT and improved glucose homeostasis in other rodent models. Furthermore, FGF-21 has been shown to induce expression of the GLUT1 glucose transporter and increase glucose uptake within adipocytes (Ge et al. 2011). Initially, the expression of FGF21, its major receptor in the WAT FGFR1, and the co-receptor which is required for functional FGF-21 signalling, β-klotho, were assessed in the iWAT and eWAT. Within eWAT FGF21 was unaltered between any groups. The FGF receptor 1 gene was upregulated in BACE1 AdKO mice compared to WT (Figure 3.25B- 1.00 ± 0.11 v BACE1 AdKO 1.59 ± 0.19, n=8; p=0.02) and BACE1 floxed mice (BACE1 floxed 0.94 ± 0.14, n=7; p=0.02). The co-receptor β-klotho had the same expression pattern (Figure 3.25C- WT 1.00 ± 0.23 v BACE1 AdKO 3.58 ± 0.79, n=8; p=0.01) and, again, BACE1 floxed mice were significantly different to BACE1 AdKO (BACE1 floxed 1.34 ± 0.51, n=7; p=0.03). Within iWAT FGF-21 itself was increased at a gene level in AdKO mice compared to WT mice (Figure 3.25D- WT 1.00 ± 0.27 v BACE1 AdKO 3.55 ± 1.06, n=6-8; p=0.047). BACE1 floxed mice also had higher levels of FGF-21 compared

to WT mice (BACE1 floxed 1.83 ± 0.27, n=8; p=0.02). There was no significant difference between BACE1 floxed and BACE1 AdKO mice. The FGF receptor 1 was raised in BACE1 AdKO mice compared to WT mice (Figure 3.25E- WT 1.00 ± 0.20 v BACE1 AdKO 2.00 ± 0.39, n=7-9; p=0.03), but not compared to BACE1 floxed mice. The co-receptor β-klotho was also raised in BACE1 AdKO mice compared to WT mice (Figure 3.25F- WT 1.00 ± 0.22 v BACE1 AdKO 3.76 ± 0.90, n=7-9; p=0.02).

Immunoblotting was performed to see if these gene expression changes were reflected at a protein level in eWAT and iWAT. There was no difference in eWAT (Figures 3.26A and B). There was a suggestion of increased FGFR1 protein in iWAT (Figure 3.26 C and D), however this was not statistically significant. Increased FGF-21 signalling is associated with increases in adiponectin signalling. We therefore examined the gene expression levels of adiponectin and its 2 main receptors adipoR1 and adipoR2 in iWAT. We found that adiponectin was raised in BACE1 AdKO mice compared to WT mice (Figure 3.27A- WT 1.00 ± 0.16 v BACE1 AdKO 2.06 ± 0.39, n=8; p=0.03), but not compared to BACE1 floxed mice. AdipoR1 was also raised in BACE1 AdKO mice compared to WT mice (Figure 3.27B- WT 1.00 ± 0.12 v BACE1 AdKO 2.08 ± 0.35, n=8; p=0.02). AdipoR2 followed this pattern as well, with BACE1 AdKO significantly increased over WT mice (Figure 3.27C- WT 1.00 ± 0.16 v BACE1 AdKO 2.74 ± 0.45, n=8; p=0.007). BACE1 AdKO mice also expressed significantly more AdipoR2 than BACE1 floxed (BACE1 floxed 1.52 ± 0.30, n=7; p=0.047).

Adiponectin can exist as differently sized multimers, with high molecular weight (HMW) adiponectin considered most important in mediating its insulin sensitising effects compared to medium molecular weight (MMW) and low molecular weight (LMW) forms. To examine this, plasma was taken from the mice and the amounts of the HMW and total adiponectin forms were determined. Total adiponectin was reduced in BACE1 AdKO mice compared to WT mice (Figure 3.28C- WT 1.00 ± 0.20 v BACE1 AdKO

0.66 ± 0.11, n=8; p=0.015), but the ratio of HMW to total adiponectin was unaltered (Figure 3.28D).

Taken together, this section of work suggests that removal of BACE1 may be involved in upregulating FGF-21 signalling, which may play an important role in modulating the increased energy expenditure, browning and improved metabolism- which may stem from increased signalling through the insulin sensitiser adiponectin.

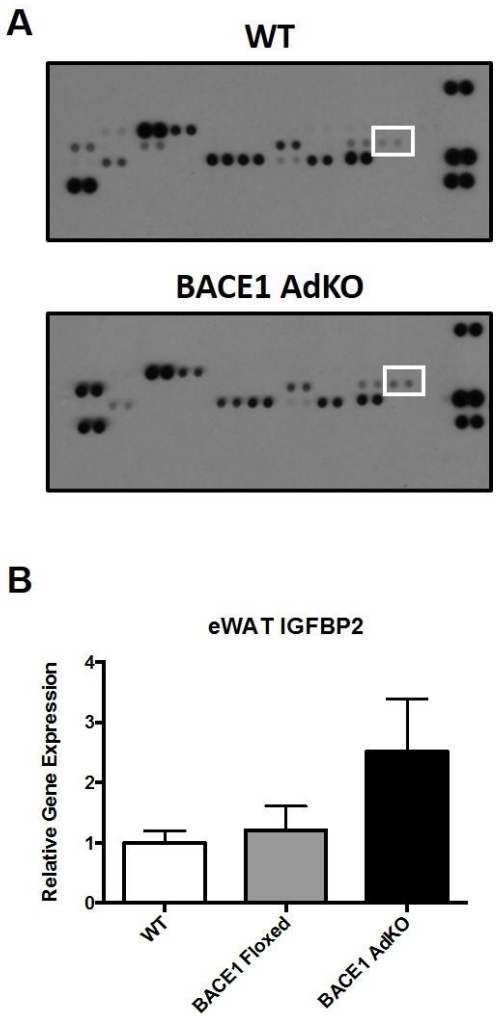

Figure 3.24 Adipokine array of plasma samples from WT and BACE1 AdKO mice

After 22 weeks HFD a section of eWAT was excised and processed for protein and gene analysis. 275µg protein was loaded into an adipokine array **(A)** Example adipokine array, with the only significantly altered protein (lGFBP2) highlighted (white boxes) (n=2) **(B)** Gene expression of the protein shows no significant differences in a larger cohort (n=4-6)

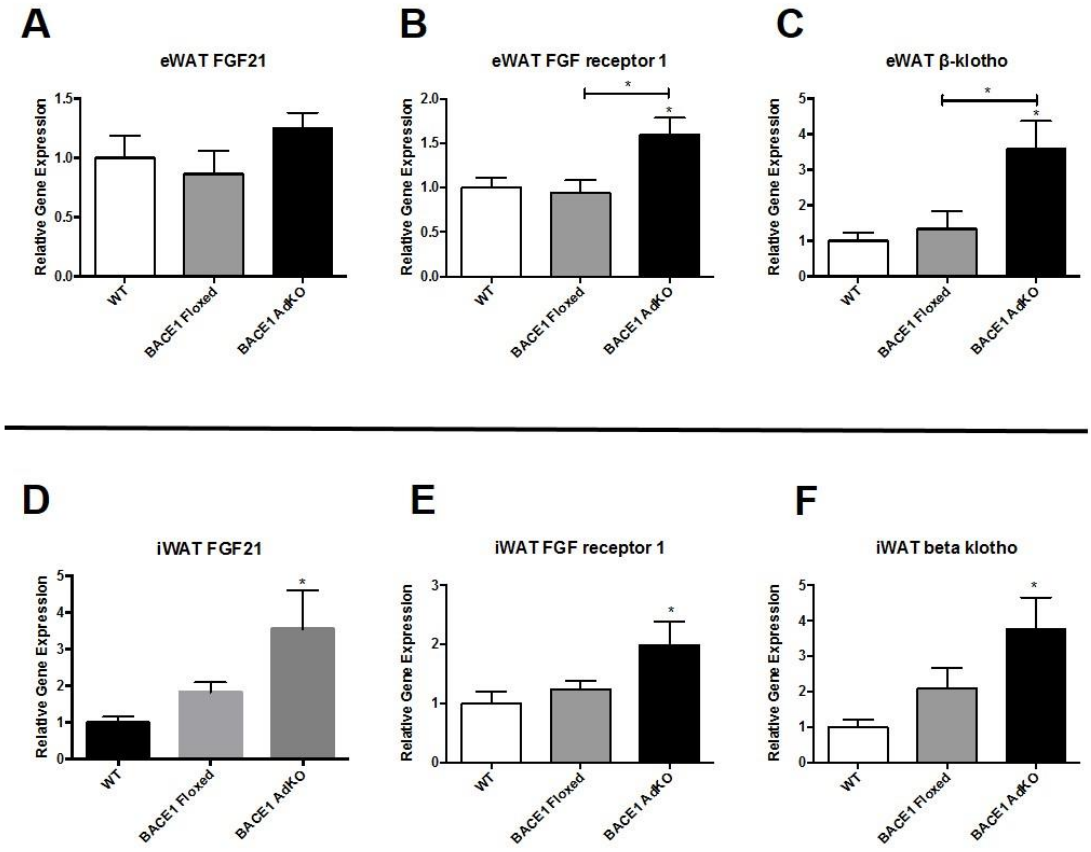

Figure 3.25 Conditional removal of BACE1 from adipocytes increases levels of genes associated with FGF-21 signalling

Following the 22 week HFD protocol, WAT from the epididymal and inguinal fat pads were excised. 12.5ng cDNA was loaded onto a TaqMan® plate **(A)** Gene expression of FGF-21 in eWAT is unchanged, whereas **(B)** FGF receptor 1 is upregulated compared to WT and BACE1 floxed mice **(C)** Expression of β-klotho is also increased in BACE1 AdKO mice compared to both WT and BACE1 floxed mice **(D)** Within the iWAT gene expression of FGF21 is upregulated compared to WT mice **(E)** Expression of FGF receptor 1 is also upregulated compared to WT mice **(F)** Expression of β-klotho is increased in BACE1 AdKO mice compared to WT mice

n=6-8; *P<0.05

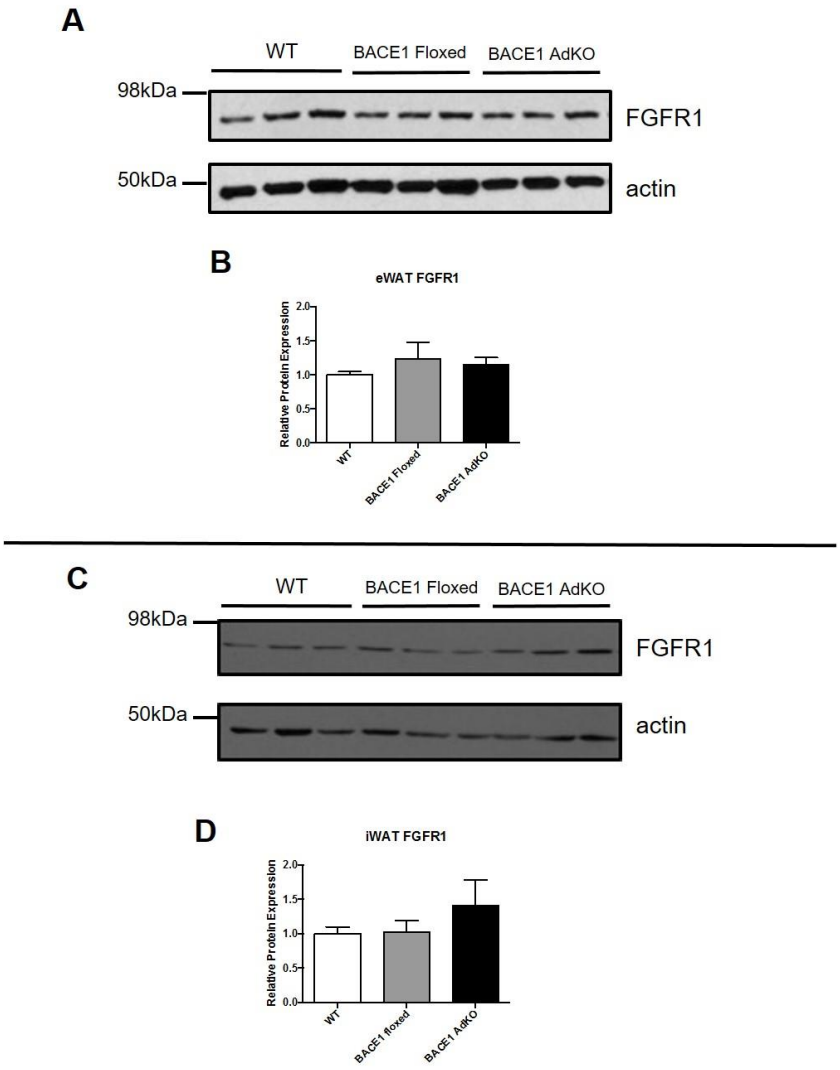

Figure 3.26 Conditional removal of BACE1 from adipocytes increases FGFR1 protein in iWAT but not eWAT

eWAT and iWAT was excised and processed for protein analysis. 20µg protein was loaded onto a gel and proteins separated by SDS PAGE **(A)** Western blot showing FGFR1 protein in eWAT (**B)** Quantification shows no significant difference between groups (n-8-10). **(C)** Western blot showing FGFR1 protein in iWAT. **(D)** Quantification of C shows a trend towards raised in FGFR1 protein level in BACE1 AdKO mice (n-6-8)

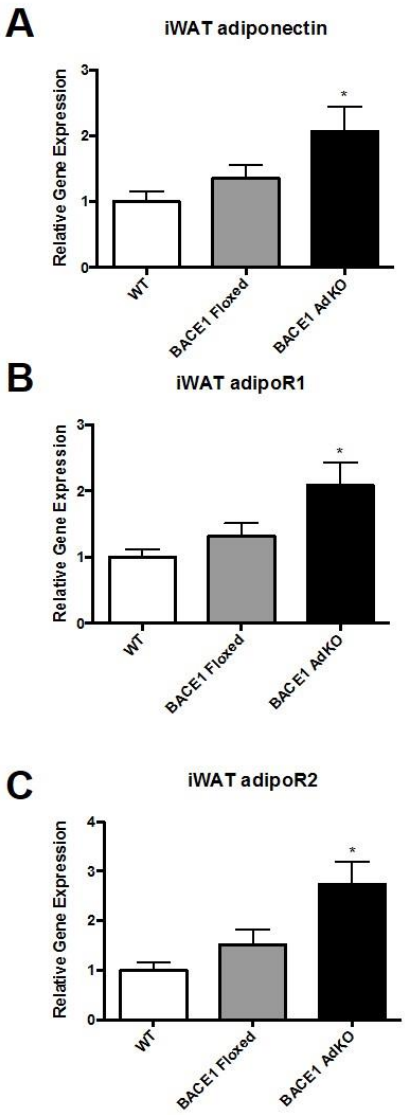

Figure 3.27 Conditional removal of BACE1 from adipocytes increases levels of genes associated with adiponectin signalling

Following the 22 week HFD protocol, iWAT was excised. 12.5ng cDNA was loaded onto a TaqMan® plate **(A)** Levels of adiponectin gene are raised in BACE1 AdKO mice compared to WT mice (p=<0.05, n=7-8). **(B)** Levels of adiponectin receptor 1 gene are raised in BACE1 AdKO mice compared to WT mice (p=<0.05, n=7-8). **(C)** Levels of adiponectin receptor 2 gene are raised in BACE1 AdKO mice compared to WT mice.

n=7-8; *p<0.05

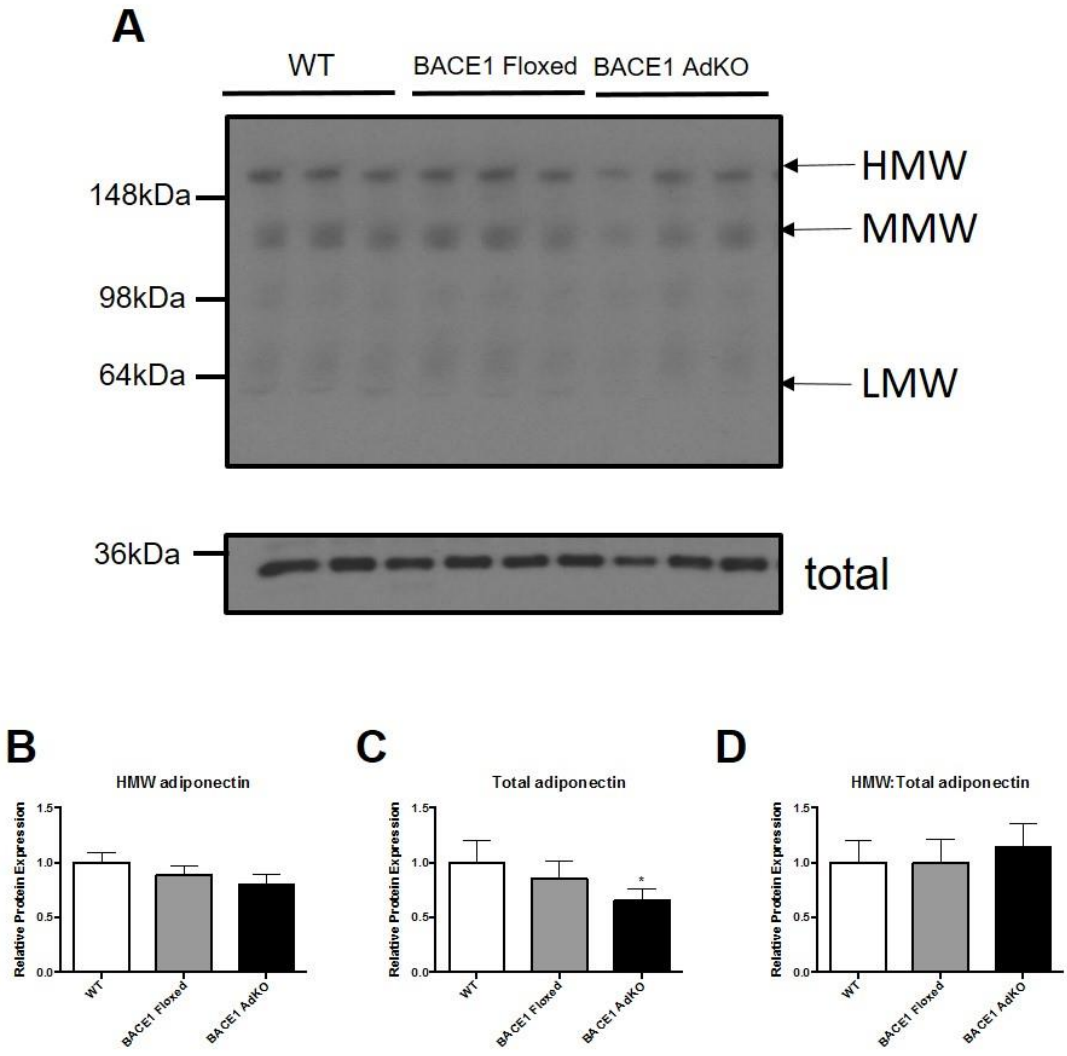

Figure 3.28 Adiponectin multimers in the plasma of WT, BACE1 floxed and BACE1 AdKO mice

After 22 weeks HFD, a 50-fold dilution of plasma was made in sample buffer. Multimeric forms of adiponectin were separated on a gradient gel in non-reducing conditions, and total adiponectin was run in reducing conditions **(A)** Multimeric and total adiponectin gels. **(B)** Quantification of HMW adiponectin shows no difference between groups. **(C)** Quantification of total adiponectin shows a decrease in BACE1 AdKO mice compared to WT mice. **(D)** Quantification of HMW:total adiponectin ratio shows no difference between groups

n=8; *P<0.05

3.2.9 Overexpression of BACE1 in 3T3-L1 cells appears to have reverse effects on FGF-21 signalling

As there were striking phenotypes associated with reduction of BACE1 in adipocytes, it stands to reason that in a model of adipocytes with high levels of BACE1 we should expect to see the opposite effects if indeed the phenotypes are due to the direct effects of BACE1. To try and produce such a model, we used 3T3-L1 cells, which is a murine fibroblast cell line that can be differentiated into adipocytes using a common and well-established protocol. The cells were transfected to either over express BACE1 (BACE1 o/e) or to express an empty vector (EV) and the cells differentiated before examining the pathways we found altered in the *in vivo* model.

Three independent sets of cells were transfected and validated by examining expression of BACE1 by western blotting. A transfection of the cells featuring a protease dead form of BACE1 (BACE1mut) was also attempted, but unfortunately this transfection did not work efficiently in any of the 3 lines examined. Two of the transfected cell lines did over-express BACE1 (Figure 3.29A), however, and the 1st line was taken forward as it produced the greatest amount of BACE1. To check differentiation was not impaired, expression levels of PPARγ were examined, with no significant difference being detected (Figure 3.29B).

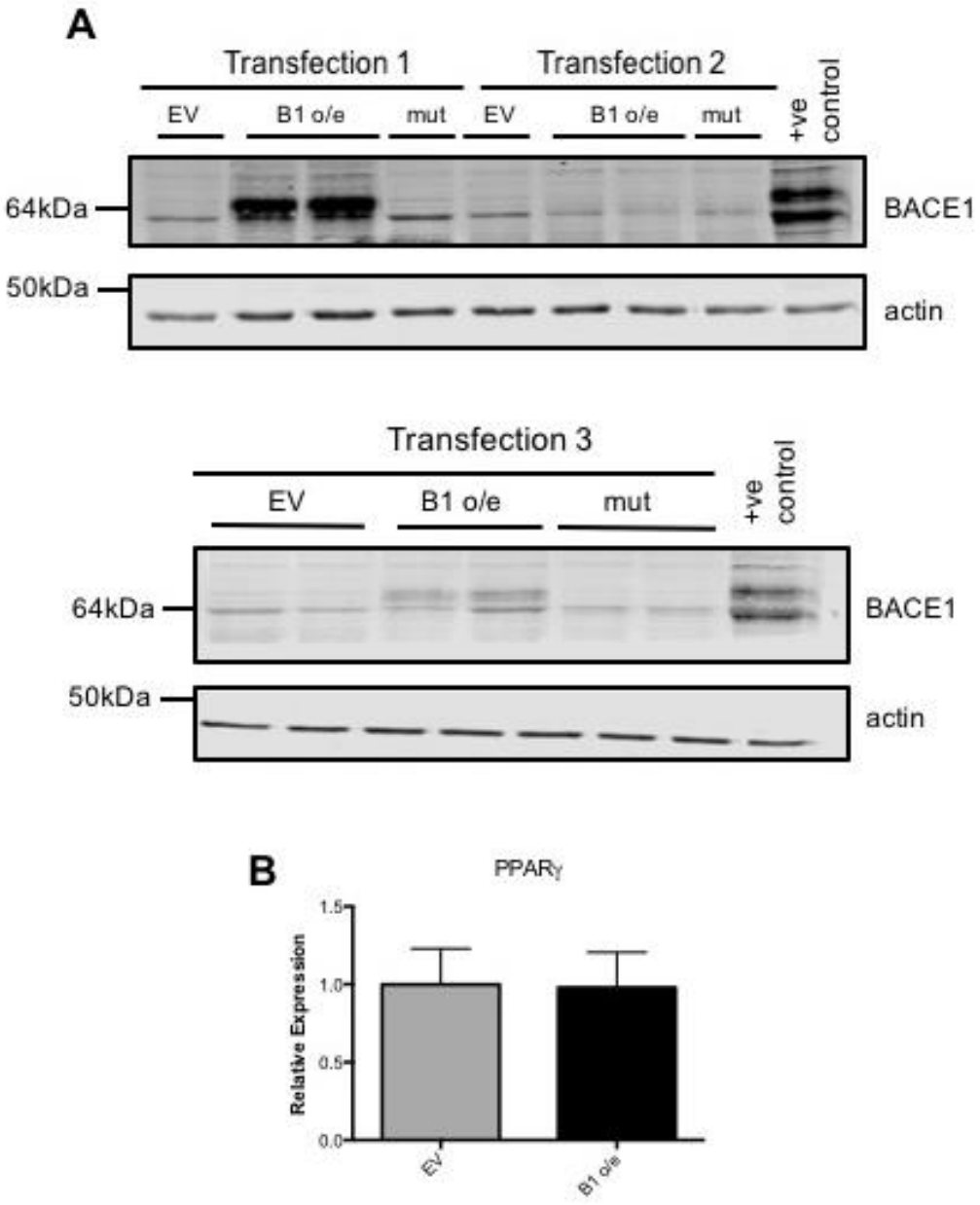

Figure 3.29 Transfection of 3T3-L1 cells to over-express BACE1

Three separate transfections of 3T3-L1 cells with EV, B1, or mutant BACE1 were attempted. **(A)** Transfection 1 provided the most robust overexpression. **(B)** Gene expression of PPARγ in differentiated 3T3-L1 cells shows no significant difference (n=3)

EV= empty vector, B1o/e= BACE1 over-expressing, mut= BACE1 protease-dead mutant.

Gene levels of FGFR1 and β-klotho, which were both increased in the conditional knock-out mouse model were checked in the cell line. In differentiated 3T3-L1 cells over-expressing BACE1, FGFR1 was raised in EV cells compared to WT cells (Figure 3.30A- WT 1.00 ± 0.10 v EV 2.08 ± 0.45, n=4; p=0.048). Crucially, however, in B1 o/e cells FGFR1 expression was significantly reduced compared to EV cells (B1o/e 0.87 ± 0.13, n=4; p=0.03). Likewise, β-klotho was reduced in B1 cells compared to EV cells (Figure 3.30B- EV 2.45 ± 0.62 v B1o/e 0.29 ± 0.05, n=4; p=0.02). B1 o/e cells had very highly significantly reduced β-klotho compared to WT cells (Figure 3.30B- WT 1.00 ± 0.05, n=4; p<0.0001). There was no significant difference between WT and EV cells.

Finally, FGFR1 was examined at a protein level. EV cells contained greater levels of protein compared to WT (Figure 3.31B- WT 1.00 ± 0.14 v EV 1.42 ± 0.08, n=3; p<0.05) There was no significant difference between EV and B1 o/e cells.

Taken together, the *in vitro* data complemented the *in vivo* data, suggesting that raising BACE1 can impair FGF signalling. The data from this chapter overall demonstrates that adipocyte BACE1 plays an important role in whole body energy homeostasis.

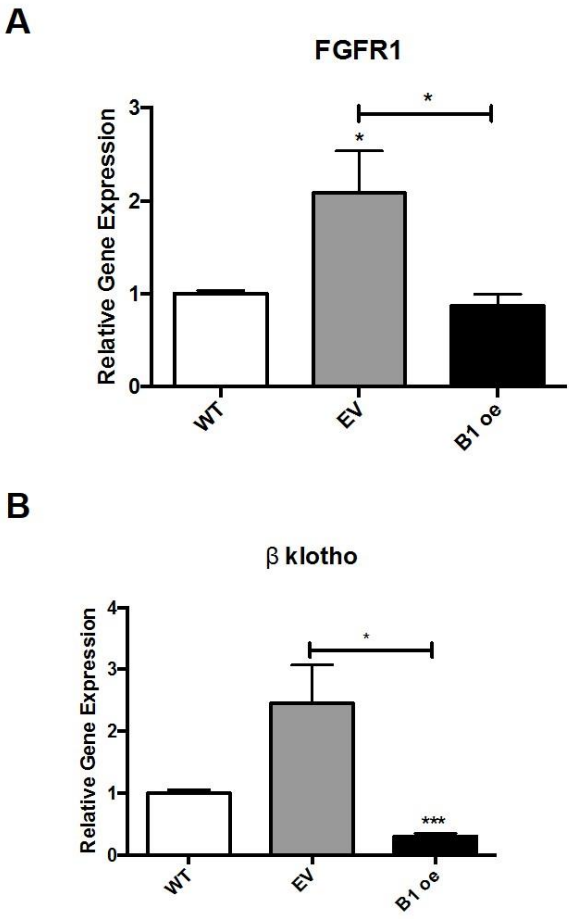

Figure 3.30 Over-expression of BACE1 in differentiated 3T3-L1 cells reduces expression of FGFR1 and β-klotho

3T3-L1 cells were differentiated for 7 days and cells lysed and processed for gene analysis. 12.5ng cDNA was loaded onto a TaqMan® plate **(A)** Expression of FGF-R1is reduced in BACE1 o/e cells compared to EV cells (p=<0.05, n=3). **(B)** Expression of β-kltoho is also reduced in BACE1 o/e cells compared to EV cells.

EV= empty vector, B1o/e= BACE1 over-expressing. n=4; *P<0.05, ***P<0.001

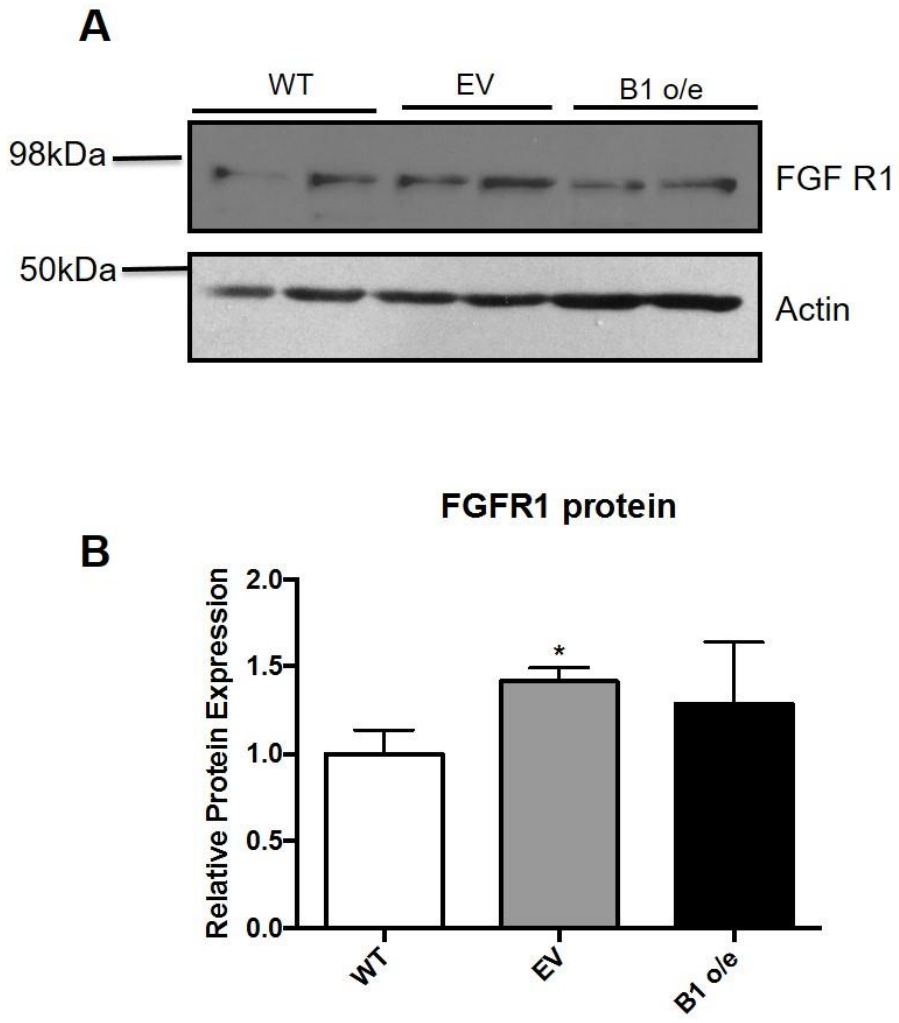

Figure 3.31 Over-expression of BACE1 in differentiated 3T3-L1 cells does not alter protein expression of FGFR1

3T3-L1 cells were differentiated for 7 days and cells lysed and processed for protein analysis **(A)** Western blot shows a reduction in FGFR1 expression in differentiated 3T3-L1 cells. **(B)** Quantification of western blotting data shows significant reduction in FGFR1 protein compared to EV cells

EV= empty vector, B1o/e= BACE1 over-expressing. n=3; *P<0.05

3.3 Discussion

3.3.1 Conditional removal of BACE1 using the AdipoQ Promoter

The first aim of this study was to successfully generate an adipocyte specific conditional knock-out mouse. To do this we used adiponectin (AdipoQ) as the gene promoter. The most common alternative promoter that others have used to create adipocyte KO mice is aP2 (adipocyte protein 2, also known as FABP4). Adiponectin was chosen, however, because the cre recombination appears to be more specific, with reports that aP2 cre mice can present with recombination in certain heart and skeletal muscle cells (K. Y. Lee et al. 2013), where we have previously shown BACE1 to be present.

Other studies using the same driver have shown that recombination occurs in all fat pads, including epididymal WAT, subcutaneous WAT and BAT (Polak et al. 2008). We confirmed BACE1 KO in eWAT, and it would be useful to confirm these findings in iWAT. We did examine BAT, but could not detect BACE1, including within WT and BACE1 floxed mice. Others have demonstrated BACE1 is present in BAT (Oliverio et al. 2016), with relatively low expression in normal chow fed mice, which rises in HFD fed mice. For this reason, in the present study, HFD BAT was examined, with no BACE1 protein expression identified. This is likely due to the development of BAT, which stems from muscle cell like progenitors (Harms & Seale 2013), which, as shown in this study, have relatively low levels of BACE1 protein as well.

3.3.2 Conditional knock-out of BACE1 improves a diabetic and obese phenotype

Within this chapter, we have demonstrated that removal of BACE1 from adipocytes prevents the excessive weight gain associated with HFD, with a concomitant reduction in fat mass, and improvement in glucose homeostasis and in particular glucose disposal following a glucose load. This phenotype bears a striking resemblance to the phenotype of the global BACE1 KO mouse (Meakin et al. 2012), which strongly suggests that a significant contributor to the improved obese and diabetic phenotype

observed is due to loss of adipocyte BACE1. The reduction in fat mass was primarily from a reduction in iWAT mass. When weighed the reduced iWAT size was about 1g between WT and BACE1 AdKO mice. This is much smaller than the approximately 8g difference in whole body weight. This apparent discrepancy could be for multiple reasons. Firstly, only one subcutaneous and visceral depot was measured. Further, the mice were fasted prior to sacrifice, which will account for some loss in fat mass. Finally, the tissue harvest is performed after numerous procedures such as GTT and ITT tests, and metabolic measurement in the CLAMS device. These procedures did cause a reduction in body weight, as explained in section 3.2. Loss of fat mass may be higher in control groups as these mice had greater fat mass and therefore greater capacity for weight loss.

The reduction in fat mass could be explained by either an inability for adipocyte differentiation, or a limited ability of existing adipocytes to expand. The data showed an increase in adipocyte number in a given area. Adipocyte area is almost significantly decreased, which is consistent with a greater number of cells within the cross-section. Overall, this is supportive of reduced hypertrophy in BACE1 AdKO mice, however needs to be investigated in more depth to confirm this. Additional mice should be added to the analysis, and additional cross-sections would need to be analysed and mean values calculated for each mouse to confirm this finding. Furthermore, more detailed analysis could be performed. For example, although average adipocyte area is unaltered, the distribution may be altered- for example with greater numbers of smaller area adipocytes and reduced numbers of adipocytes with the largest areas. WT mice exhibited evidence of hepatic steatosis which was lower in BACE1 floxed mice. No evidence of liver steatosis was found in BACE1 AdKO mice despite having been placed on the same HFD for a chronic period of 22 weeks as controls- which indicates the absence of “overspill” of fat into other tissues. The lack of difference in adipocyte size suggests an increase in fat utilization, which is discussed further below in section 3.3.3.

The one major difference between these two mouse models is the absence of any improvement in insulin sensitivity in the BACE1 AdKO mice which was a prominent feature of the BACE1$^{-/-}$ mice. The ITT results compare to WT mice fed a HFD (Meakin et al. 2012), suggesting the mice all had diminished insulin sensitivity due to the diet. A lack of alteration in insulin sensitivity despite improvements in glucose disposal is an unusual finding, and could have been due to an alteration in insulin secretion, but this possibility was discounted by performing a GSIS test. To fully discount the possibility of any change in insulin sensitivity it would be best to perform a hyperinsulinemic euglycemic clamp, which is considered the gold standard techniques for investigating such phenotypes. This would also allow for the direct insulin-dependent and basal measurement of glucose uptake into tissues.

The other explanation for the lack of change in insulin sensitivity would be the presence of enhanced insulin independent glucose uptake. In adipocytes, the GLUT1 transporter uptakes glucose into cells in this manner (Ebeling et al. 1998), and as this transporter is upregulated at the transcriptional level in the iWAT of BACE1 AdKO mice, this could help to explain the phenotype. However, this explanation makes a number of assumptions. Firstly, it depends on GLUT1 transporter protein also being upregulated, and translocated to the cell membrane to allow glucose transport to take place. This could be confirmed by confocal microscopy. Secondly, it would mean that the large improvement of glucose homeostasis is due entirely due to increased adipocyte uptake, despite the overall reduction in fat mass in this model and despite WAT only contributing to approximately 10% of normal glucose uptake (Rosen & Spiegelman 2006). It is clear that, although small, there is a significant role of adipose tissue in glucose uptake, as removal of GLUT4 specifically from adipocytes causes a large perturbation of glucose disposal (Kotani et al. 2004), whereas overexpression of GLUT4 in adipocytes improves glucose homeostasis (Shepherd et al. 1993). However, these phenotypes are not solely due to adipose tissue function. Interestingly, overexpressing GLUT4 in adipocytes is sufficient to restore glucose homeostasis in mice which

lack GLUT4 in muscle (Carvalho et al. 2005), indicating the importance of adipose tissue to these processes. This mouse model, however was slightly obese, in contrast to our model which is lean. There is little work that has examined GLUT1 in these circumstances. WAT produces a large number of adipokines, including adiponectin, which may contribute to enhancing glucose uptake in other insulin sensitive tissues such as the liver or muscle. Therefore, to truly assess whether glucose uptake through insulin independent means is occurring it will be necessary to fully assess the secretion of such adipokines, and examine any compensatory mechanisms at play in the liver or muscle. As our lab has previously shown that muscle glucose uptake is enhanced by removal of BACE1 with enhanced GLUT1 protein levels (Hamilton et al. 2014), it is possible that this could be the case. Increased thermogenesis could also increase glucose uptake, as discussed below.

An important consideration in this study is the presence of a phenotype in the BACE1 floxed mice and AdipoQ Cre mice. The BACE1 floxed mice showed a small, albeit not significant reduction in weight gain and fat mass compared to WT mice, and subtle differences in parameters such as WAT leptin content. It is difficult to assess the reasons for these small differences. The BACE1 floxed mouse is newly created and thus there are no other studies that have reported on their phenotype. The likely explanation is that the BACE1 floxed mouse creates a hypomorph with either reduced levels of BACE1 expression or activity in tissues other than adipocytes. We have looked at protein levels in numerous tissues but didn't find any noticeable decrease in BACE1 expression. It would be useful to analyse BACE1 protease activity, for example by looking at sAPPβ levels using an ELISA kit.

The AdipoQ Cre mouse exhibited significantly increased fat mass and impaired glucose disposal compared to WT mice. Again, this is difficult to explain as numerous studies using the same cre mouse have been published without mention of such a phenotype. It is possible that the specific mouse line used to generate the cre mice could be responsible for

the phenotype, as different mouse lines can have substantially differing energy metabolism phenotypes (Champy et al. 2008). A number of metabolic alterations, including in insulin sensitivity and body composition have been reported in a number of cre models in the central nervous system (Harno et al. 2013). Importantly, as the AdipoQ Cre mouse had a worsened obese/diabetic phenotype, the overall effect of removal of BACE1 from adipocytes could in fact be even more profound once the effect of the cre mouse is removed. The differences in BACE1 floxed and AdipoQ cre mice need to to be studied in much greater detail. It would be interesting to perform this experiment again using these control mice, perhaps from different sources to establish the significance of these differences in control groups

3.3.3 Increased metabolism in BACE1 AdKO mice

The reduced body weight of BACE1 AdKO mice compared to controls could be explained by the mice taking in less energy or expending more- either through increased excretion or through increased energy expenditure. The data from the CLAMS machine provides significant evidence that the latter of these is more likely to explain the phenotype. Oxygen consumption is increased in BACE1 AdKO mice compared to BACE1 floxed mice, which is indicative of greater energy expenditure (Speakman 2013). Energy expenditure is not directly measured, but derived from calorific value and oxygen consumption, and is also raised in BACE1 AdKO mice compared to BACE1 floxed mice. This is expected as energy expenditure is largely a function of oxygen consumption. However, it should be noted that calorific value is itself calculated from RER (see section 2.3.5), therefore if RER were altered, raised oxygen consumption may not necessarily lead to raised energy expenditure. The data could be analysed in more detail, for example by plotting a line graph showing changes in VO_2 and energy expenditure as in real time rather than split simply into light and dark cycles. This could pick up on subtle differences not revealed in the data presented here. The raised energy expenditure is particularly interesting given the relative leanness of the BACE1 AdKO mice, and also matches with the phenotype of both BACE1$^{-/-}$ mice (Meakin

et al. 2012). As the mice consume the same amount of food despite weighing less, we can hypothesise that BACE1 AdKO mice are hyperphagic and energy inefficient relative to their control counterparts. This is in agreement with the slightly raised expression levels of the orexigenic AgRP neuropeptide in comparison to the unaltered expression of POMC in the hypothalamus (Sohn 2015). In BACE1$^{-/-}$ mice, and in DIO mice treated with a BACE1 inhibitor, AgRP and NPY levels are also raised, with lower levels of POMC (Meakin et al. 2018). It would therefore be useful to investigate neuropeptide levels in the hypothalamus of BACE1 AdKO mice further. It would also be interesting to assess the loss of extra energy through faeces, which could be measured using bomb calorimetry. It may not be anticipated that any extra energy is lost in this way, as faecal lipid content is in fact significantly reduced in BACE1$^{-/-}$ mice (Meakin et al. 2012).

Other than physical activity, which is unaltered in BACE1 AdKO mice, the major likely driver for increased energy expenditure is increased thermogenesis, which can be mediated through BAT and the browning of WAT. We have shown in this chapter that this is likely to be the case in BACE1 AdKO mice, too. Although many of the gene markers- PGC-1α, PRDM16, and DIO2 were either unchanged or only subtly increased in eWAT, there was a non-significant increase in the key thermogenic gene UCP1 in iWAT (Nedergaard & Cannon 2014). This lack of significance is likely due to the high variation between individual mice, and further quantification of protein levels of UCP1 is necessary. This is in keeping with other studies that suggest the majority of browning occurs in subcutaneous rather than visceral fat depots, mediated through the higher level or PRDM16, in these depots compared to visceral (Seale, Heather M. Conroe, et al. 2011). Thermogenesis is often induced by activation of the sympathetic nervous system, and specifically through the beta 3 adrenergic receptor (b3adr)- indeed treatment of mice (Yoshida et al. 1994) and rats (Ghorbani & Himms-Hagen 1997) with specific beta 3 adrenergic agonists capable of inducing thermogenesis and reducing a diabetic phenotype. We found significant upregulation of this receptor in the iWAT

of BACE1 AdKO mice. Activation of the sympathetic nervous system is associated with control of lipolysis (Bartness et al. 2014). It has been shown that iWAT and eWAT are differently innervated (Nguyen et al. 2014). In Siberian hamsters treated with MT-II, an agonist of the melanocortin 3 and 4 receptors, increases in phosphorylated hormone sensitive lipase (pHSL) and perilipin A (pPerilipin A) were detected within the iWAT (Shrestha et al. 2010), indicating upregulated lipolysis in this depot. In the present study, iWAT raw weight was reduced but eWAT was unchanged. This could be indicative of increased lipolysis, and measurement of pHSL and pPeriplipin A in iWAT and eWAT for comparison would be a good approach to testing this hypothesis.

Browning of white adipose tissue results in increased glucose utilisation, and therefore increased uptake from the plasma. Recently it has been shown that “brite” adipocytes in iWAT have enhanced glucose uptake (Mössenböck et al. 2014), and this is independent of insulin stimulation. Furthermore this change is accompanied by raised levels of GLUT1 (Mössenböck et al. 2014), similar to that seen in the BACE1 AdKO mouse. Measuring glucose uptake *ex vivo* within the iWAT of the BACE1 AdKO mice could be achieved by treating primary adipocytes excised from mice with tritiated 2 deoxy-glucose, and measuring subsequent uptake into the cells, compared to WT mice.

A possible explanation for the lack of significant increases other than the beta 3 adrenergic receptor expression is the fact that these mice were unstimulated. Cold exposure or stimulation with a β3 adrenergic agonist such as CL 216,343 would produce more clear evidence of any increased propensity for browning of the WAT. The temperature of the studied animals is an important consideration. In mice, true thermoneutrality is between 25 and 30^{o}C, thus implying that the mice being modelled are already under thermal challenge (Cannon & Nedergaard 2010). This has been countered, though, by others who have suggested that as mice are usually group housed with additional bedding, and have argued that because humans are usually in environments slightly below

thermoneutrality, that current practice is physiologically relevant (Speakman & Keijer 2012). Given there is limited fat mass expansion in the BACE1 AdKO mice, it is feasible that the insulation capabilities of the remaining WAT are limited, meaning any browning is a normal physiological response to mild thermal challenge.

Adaptive thermogenesis can be induced centrally via the hypothalamic neurocircuitry (Yang & Ruan 2015). To assess the contribution of central components compared to direct effects within WAT, it may be necessary to perform a sympathectomy experiment to prevent sympathetic signalling to the fat depots and assess whether adaptive thermogenesis still takes place. Another approach could be to perform a chemical sympathectomy, using 6- hydroxydopamine to deplete sympathetic neurons (Kostrzewa & Jacobowitz 1974).

The alternative to browning of WAT is the reduction in “whitening” of BAT, which was not investigated in this study. Whitening refers to the decreased vascularisation and hypoxic state of BAT in obesity. This is associated with decreased expression of genes including UCP1 (Shimizu et al. 2014). BACE1 has been linked to BAT function previously. Raised expression of BACE1 in BAT during obesity is thought to occur by reduced expression of a micro RNA (miR328), which itself usually represses BACE1 (Oliverio et al. 2016). BACE1 inhibitor treated mice had increased expression of brown adipocyte markers, in subcutaneous WAT and BAT (Oliverio et al. 2016), and also exhibited small, but significant improvements in glucose homeostasis and reduction of body weight in agreement with our studies.

Therefore, it will be important to directly assess BAT function in the AdKO mice to assess its role in the increased energy expenditure associated with the model. BAT function can be assessed in a number of ways including temperature probing, BAT lipid content and gene markers including UCP1, PGC1α/β, DIO2 and Elovl3, which is induced rapidly by cold exposure (Virtue & Vidal-Puig 2013). Examining whitening in BAT by assessing lipid content to see if this occurs in response to a HFD in WT

mice is another approach- it would be hypothesised that this effect would be absent in BACE1 AdKO mice.

3.3.4 The potential role of FGF signalling in BACE1 AdKO mice

Of the large number of potential drivers of browning of WAT, we have focussed in this chapter on FGF21, as many of the reported effects associated with enhanced FGF21 signalling are similar to those observed in BACE1 AdKO mice. FGF21 has gained much attention recently because of its purported role in obesity. FGF21 is produced in the liver but has numerous effects within adipocytes. Treatment of obese mice with FGF21 has been shown by multiple groups to reduce body weight and fat mass, without changes in food intake. This accompanied by improved glucose homeostasis and insulin sensitivity, mediated through increased energy expenditure (Xu et al. 2009; Coskun et al. 2008). This evidence suggests that FGF21 may be a useful therapeutic target. Furthermore, in adipocytes FGF21 treatment has been shown to increase glucose uptake via upregulation of the GLUT1 but not GLUT4 transporters both *in vitro* in 3T3-L1 cells and *in vivo* in ob/ob mice (Kharitonenkov et al. 2005). Paradoxically circulating levels of FGF21 are raised in obese mice and humans. Thus, similarly to leptin, it has been argued that chronic obesity represents an FGF21 resistant state (Fisher et al. 2010).

FGF21 signals through its major receptor in adipocytes FGFR1, and also requires its co-receptor β-klotho in order for proper function (Ogawa et al. 2007). FGF21 signalling activates MAPK and FGF receptor substrate 2a (FRS2a) in adipocytes (Kharitonenkov et al. 2005), and also induces the expression of adiponectin, which is clearly important in mediating FGF-21 function, as many of the beneficial phenotypes associated with FGF21 administration are abrogated in adiponectin knock-out mice (Lin et al. 2013). However, it should be noted that a more recent study has countered this theory, arguing that FGF21 mediated improvements in insulin sensitivity and raised energy expenditure do not require adiponectin (BonDurant et al. 2017). The transcription factor PPARγ is important in this process , which has been shown previously to be involved in mediating

adiponectin gene transcription (Iwaki et al. 2003). In terms of energy expenditure, FGF21 appears to work via increasing AMPK activity, which ultimately drives increased expression of PGC-1α, which contributes to increasing mitochondrial oxygen consumption (Chau et al. 2010). Adiponectin can also activate AMPK, so could be the key factor in modulating adipocyte dependent effects in energy metabolism. This would be in keeping with the present study, in which adiponectin, adiponectin receptors and PGC-1α were all raised in BACE1 AdKO mice. However, there is some debate as to how important AMPK activation is, however, as a more recent study using adipocyte specific AMPK double β1/β2 subunit knock-out mice, which completely ablated AMPK activity, showed that FGF21 could still enhance glucose disposal and energy expenditure in the absence of intact AMPK signalling (Mottillo et al. 2017), suggesting instead that UCP independent thermogenic mechanisms could explain the phenotypes.

The co-receptor for FGF21 signalling is β-klotho, which is a member of the klotho gene family. These genes are known to be involved in fibroblast growth factor signalling, with klotho seemingly important in mediating signalling of FGF23, and β-klotho for FGF19 and FGF21 (Kurosu & Kuro-o 2009). Of particular interest is the evidence that klotho can be cleaved by BACE1 (Bloch et al. 2009). There is around 40% homology between klotho and β-klotho, meaning it is quite possible that BACE1 may also be able to cleave β-klotho. It will be important in future to establish whether BACE1 cleaves β-klotho, and the exact cleavage site used if this is the case. One recent study demonstrated that over-expressing β-klotho in adipocytes was not sufficient to prevent FGF21 resistance associated with obesity, as downstream phosphorylation of ERK1/2 and FRS2 was similar in mice overexpressing β-klotho and WT controls in mice on a HFD background (Markan et al. 2017). This data suggests that FGF21 resistance occurs downstream of β-klotho. Conversely, adipocyte β-klotho conditional knock-out mice have impaired insulin and glucose sensitivity in mice treated with FGF21 compared with heterozygous controls, with these mice also losing less weight in response to FGF21 (Ding et al. 2012),

suggesting β-klotho is vital in modulating the effects of FGF21. Therefore, it is unclear whether β-klotho itself is directly important in modulating FGF21 resistance. It may be, however, that overexpressing β-klotho has limited effect as without also changing levels of the FGFR1 receptor it cannot functionally increase FGF21 signalling.

Therefore, because BACE1 levels appear to correlate well with β-klotho and FGFR1 levels in two differing models- both *in vitro* and *in vivo*, it is proposed that removal of BACE1 in adipocytes decreases the shedding of β-klotho. This would then enable more FGF21 signalling to occur and then go on to produce the physiological benefits described within this chapter, as summarised in figure 3.32. Raised FGF21 signalling could then in turn increase GLUT1, as it has previously been shown that FGF21 can raise GLUT1 at the transcriptional level via the phosphorylation and subsequent activation of ERK1/2, which in turn causes the transcription factor Serum Related Factor (SRF) and transcriptional activator Elk-1 to associate with the GLUT1 promoter (Ge et al. 2011), activation transcription Through separate mechanisms, FGF21 could increase adiponectin signalling as discussed above. One issue which still needs to be resolved in the *in vitro* model utilised herein is the role of PPARγ. During the differentiation of 3T3-L1 cells, a number of PPARγ agonists are used. Given the potential interactions of BACE1 and PPARγ as discussed earlier, it will be important to check firstly that PPARγ agonists do not work to down-regulate BACE1 during the differentiation process, or that conversely the high levels of BACE1 do not limit the levels of differentiation of the cells to lower levels that the controls used. Initial evidence shows no change in PPARγ expression, but this can be confirmed further, by checking protein levels and performing oil-red-O staining to compare the ability of the cells to differentiate.

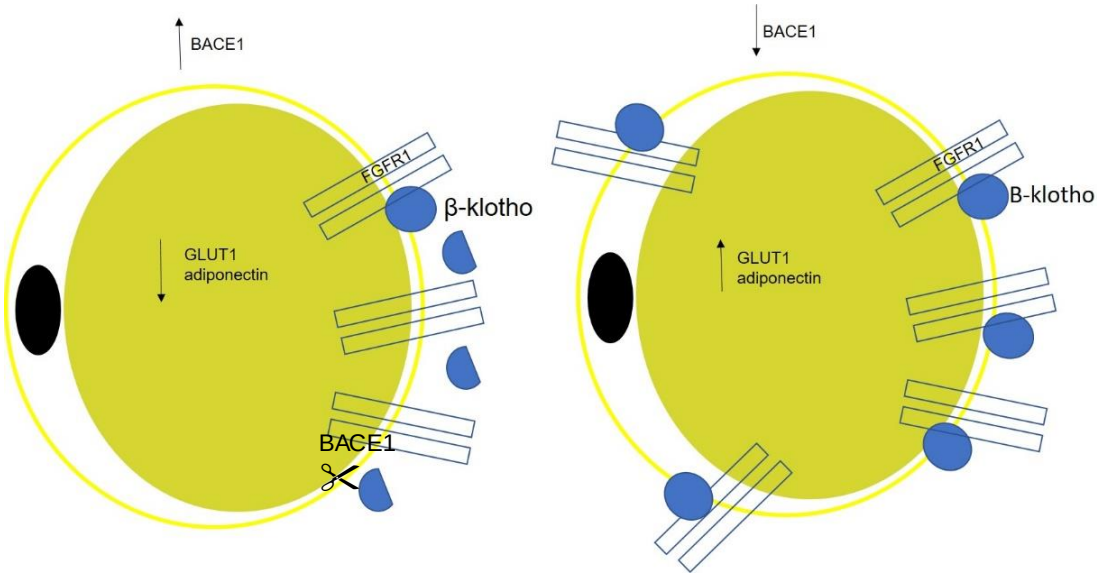

Figure 3.32 Proposed model of potential interaction between BACE1 and FGF21 signalling in adipocytes

FGF21 signalling requires intact β-klotho. BACE1 may shed β-klotho to prevent FGF21 signalling. Removal of BACE1 may increase FGF21 signalling

To firmly assess the potential role of FGF21 signalling in BACE1AdKO mice further experimentation is required. It is possibly to block FGF21 signalling through FGFR1 antagonists. One experiment could be to feed mice a HFD for 5 weeks, by which point BACE1 AdKO mice already start to exhibit reduced body weight compared to controls, then treating them with an FGFR1 antagonist or vehicle to see if blocking FGF21 signalling reverses the benefit of removing BACE1 from adipocytes. As well as this, it would be interesting to see if BACE1 AdKO mice were more sensitive to FGF-21 by infusing FGF21 over several days in a sub-cutaneous osmotic minipump, and measuring energy expenditure in CLAMS. After an acute dose of FGF21, activation of downstream pathways such as the MAPK pathway could be assessed by immunoblot.

3.3.5 The potential role of other adipokines

In this discussion, much focus has been placed on adiponectin, but as discussed in chapter 1 of this thesis, there are a huge number of different adipokines which are in some way implicated in metabolic health. In this

chapter characterisation of levels of most of these adipokines was not completed. A very small sample of 2 was used to examine adipokine content within adipocytes, but in future studies it would be advantageous to examine these with increased n numbers, as well as looking at total circulating levels, as many adipokines exert their effects in a paracrine manner in tissues beyond the WAT.

In this chapter leptin levels were recorded. Indeed, leptin secretion was significantly decreased down to levels that would be normally associated with NC fed WT mice (unpublished observations). This shows that removal of BACE1 from adipocytes prevents the hyperleptinemia associated with obesity. Although the leptin levels were shown to correlate with fat mass as would be expected, this is still an interesting finding, as reducing hyperleptinemia suggests there could be an improvement in hypothalamic leptin sensitivity.

In the present study, basal phosphorylation levels of STAT3 were assessed within the hypothalamus. Although not reaching significance in the BACE1 AdKO group, there was a trend towards a decrease in basal phosphorylation. Performing a leptin sensitivity test by injecting mice i.p. with a bolus of leptin prior to sacrifice, and then measuring hypothalamic pSTAT3 levels would be a useful experiment to perform on BACE1 AdKO mice. It would be anticipated that phosphorylation levels would significantly increase upon leptin stimulation. Thus, leptin sensitivity could be said to be improved in BACE1 AdKO mice as the change in amplitude from basal, unstimulated tissue to stimulated tissue would be larger than in control groups. Indeed, leptin sensitivity is increased in global BACE1$^{-/-}$ mice and in obese mice treated with a BACE1 inhibitor (Meakin et al. 2018). It would also be interesting to see if hypothalamic inflammation or ER stress are reduced in the mice, as these would also indicate reductions in leptin resistance and provide evidence that removal of BACE1 from adipocytes can have wider reaching impact, and potentially play a role in modulating energy metabolism via central as well as peripheral mechanisms. Finally,

the protein levels of the negative regulators of leptin signalling, SOCS3 and PTP1B could be measured to gain further insights.

3.3.6 Summary

Within this chapter, we have demonstrated that removal of BACE1 from adipocytes is sufficient to induce many features of phenotypes observed in BACE1$^{-/-}$ mice, as well as in models which have had BACE1 pharmacologically inhibited. This suggests that adipocyte BACE1 is hugely important in energy homeostasis. Furthermore, initial evidence is presented that changes in β-klotho could be responsible for this phenotype. Therefore, targeting reduction of BACE1 in adipocytes could be a novel potential therapeutic target in limiting the progression of obesity and other dangerous related pathologies by modulating FGF21 signalling. Many BACE1 inhibitors are already undergoing clinical trials for the treatment of AD. Furthermore, it raises the possibility that compounds that inhibit BACE1, but cannot cross the BBB may still have a useful function, and indeed could be preferable to the current BACE1 inhibitors, as some reported side-effects from inhibiting BACE1 in the brain, such as increased propensity for seizures, could be avoided.

Chapter 4 - The Role of Adipocyte BACE1 in modulating Inflammatory response to High Fat Diet

4.1 Introduction

Inflammation is a normal physiological response to an injury or tissue stress. Many inflammatory events are acute, meaning an initial state of inflammation in response to a stimulus, which is then resolved, returning tissue to a normal physiological state. A key factor in the development of obesity is the presence of a chronic, low grade level of inflammation (Olefsky & Glass 2010), which persists over months or years. This inflammation is thought to be key in the progression of insulin resistance and further metabolic dysfunction.

Within WAT, a large amount of this inflammation is thought to stem from the infiltration of macrophages into the fat pads, which is associated with HFD (Weisberg et al. 2003; Lafontan 2014). There is a population of resident adipose tissue macrophages, which have been reported to have important functions. Firstly, resident macrophages appear to contribute towards maintaining insulin sensitivity, as knock-out of macrophage PPARγ prevents alternative macrophage activation, and diminishes glucose homeostasis (Odegaard et al. 2007). Resident macrophages had also been reported to be involved in thermogenesis, and indeed have been shown to secrete catecholamines upon cold exposure (Nguyen et al. 2011), but this has since been contradicted by more recent studies demonstrating thermogenic genes are not induced by activation of bone marrow derived macrophages (Fischer et al. 2017).

Increased inflammation in adipocytes is associated with cell death, hypoxia, impaired glucose homeostasis and hypertrophy. It has been argued that during nutrient excess, as in obesity, adipocyte hypertrophy is followed by adipocyte hypoxia and death prior to infiltration of macrophages, which then go on to recruit pre adipocytes and support adipogenesis (Hill 2015). The alternative to this is that adipocyte hypertrophy in obesity is followed by an adipocyte “whitening” effect, in which mitochondrial biogenesis is decreased, with concomitant increased lipid content, preventing adipose tissue from being able to provide enough energy for normal function, resulting in cell death, followed by macrophage

infiltration as a result. This then results in hypoxia, which stimulates adipogenesis in an attempt to resolve the situation (Hill 2015). WAT shows signs of hypertrophy, but not macrophage infiltration after 6 weeks of HFD in mice (Cummins et al. 2014), despite glucose homeostasis impairment, suggesting inflammation doesn't drive metabolic dysfunction.

Other studies, however, demonstrate that increases in macrophage number in obese adipose tissue correlate strongly with markers of insulin resistance, and importantly appears to occur prior to rises in circulating insulin levels in obese mice (Xu et al. 2003), suggesting the process may be a key driver of obesity associated insulin resistance. A significant cause of the increase in macrophage population is the increase in chemoattractant cytokines such as CCL2, also sometimes referred to as MCP1, which are significantly raised in obese mice (Kanda et al. 2006). Furthermore genetic depletion of either CCL2 (Kanda et al. 2006), or its receptor CCR2 (Weisberg et al. 2006), reduces macrophage infiltration, and improves insulin sensitivity in the WAT of obese mice.

While the overall number of macrophages infiltrating WAT during obesity increases, the nature of the macrophages themselves also shifts, with a greater polarisation towards an M1, or classically activated state. These macrophages secrete pro-inflammatory cytokines such as TNF-α, and iNOS (Lumeng et al. 2007). This is in contrast to tissue from lean mice, which contain a greater proportion of M2, or alternatively activated macrophages, and secrete chemokines considered anti-inflammatory, such as IL10 and YM1 (Lumeng et al. 2007)

Whilst much of the focus surrounding obesity associated inflammation within the adipose tissue has been on macrophages, there is mounting evidence that other immune cell types could also play important roles in modulating inflammation in adipose tissue during obesity. For example, whilst neutrophils play a role in recruiting macrophages, they also secrete proteins such as neutrophil elastase. Treatment of hepatocytes with exogenous neutrophil elastase generates insulin resistance, and mice with

neutrophil elastase knocked out have improved glucose homeostasis and insulin sensitivity (Talukdar et al. 2012). B cells are also important links between metabolic disease and adipose inflammation, as preventing B cell maturation causes improved glucose tolerance and reduced pro-inflammatory cytokines (Winer et al. 2011). B cells are able to induce both CD4+ and CD8+ T cells, indeed, activation of CD8+ T cells are thought to be a primary event initiating macrophage infiltration into WAT in response to obesity (Nishimura et al. 2009) in certain depots. Depletion of CD8+ T cells with a neutralising antibody decreases the ratio of M1 to M2 macrophages and reduces pro-inflammatory cytokine levels in fat pads (Nishimura et al. 2009).

Previous evidence from our lab has demonstrated a link between BACE1 and inflammatory status. Both global BACE1 knock-out mice and mice treated with a pharmacological inhibitor show an overall reduction in pro-inflammatory cytokines such as TNF-α alongside increased levels of anti-inflammatory cytokines such as IL10. Interestingly, in mice infused peripherally with a BACE1 inhibitor, a shift towards an anti-inflammatory phenotype occurs prior to a subsequent weight loss, which raises the possibility that changes in inflammatory status may well be the driver of the subsequent improvements in metabolic health. Furthermore, when given centrally, the same BACE1 inhibitor produces similar effects, with reduced hypothalamic NLRP3 inflammasome activation, which suggested that the reduction in inflammation associated with reduced BACE1 activity may be mediated via central mechanisms.

In global BACE1 knock-out mice, there is also a substantial reduction in macrophage, B cell and T cell number, with associated hypertrophy within the WAT also reduced. Therefore, given the clear importance of adipose tissue inflammation in metabolic disease, this chapter focusses on the potential role of adipocyte BACE1 in controlling the inflammatory status of WAT, and other peripheral tissues, in terms of the overall level of inflammation and the composition of the resident immune cells of the tissue itself. To achieve this aim, BACE1 AdKO and controls (WT, AdipoQ Cre

and BACE1 floxed mice) were placed on a HFD for 22 weeks. Following this, FACS analysis was performed to examine the immune cell population of epididymal WAT, as well as the blood, liver and spleen for comparison. Gene expression studies were also performed to more precisely assess the overall inflammatory status of both eWAT and iWAT. Our hypothesis was that BACE1 AdKO mice would have lower pro-inflammatory gene levels with concomitant increases in anti-inflammatory genes, likely mediated through a reduced infiltration of macrophages into the WAT.

4.2 Results

4.2.1 Removal of BACE1 from adipocytes does not alter immune cell population in peripheral tissues

Following 22 weeks HFD, mice were sacrificed and tissue was dissected. Some spleen, blood, eWAT and liver was used for FACS. A variety of different immune cell populations, both myeloid and lymphoid, were quantified in each tissue. Two different ways of analysing the data were employed- firstly by measuring the various populations as a percentage of total live, single cells as run through the FACS machine, and secondly as cells per gram of starting tissue.

First, eWAT was considered. There was no significant difference in the relative number of neutrophils present when expressed as a percentage of live cells (Figure 4.1A). There was also no difference in the macrophage population (Figure 4.1B). When assessed as cells per gram of tissue there was also no change in neutrophil (Figure 4.1C) or macrophage population (Figure 4.1D).

The lymphoid lineage cell types were also assessed. There was a significant increase in B cell population in BACE1 AdKO mice compared to AdipoQ Cre mice as a percentage of total live cells (Figure 4.2A- AdipoQ Cre 7.92% $\pm$ 1.15 v BACE1 AdKO 25.38 $\pm$ 4.85, n=8-10; $p<0.01$), but there were no other differences between groups. There was no significant difference between groups for either CD4 T cells (Figure 4.2B) or CD8 T

cells (Figure 4.2C). When examined as cells per gram, there were no significant changes in B cell (Figure 2.2E), CD4 T Cells (Figure 2.2F) or CD8 T Cells (Figure 2.2G).

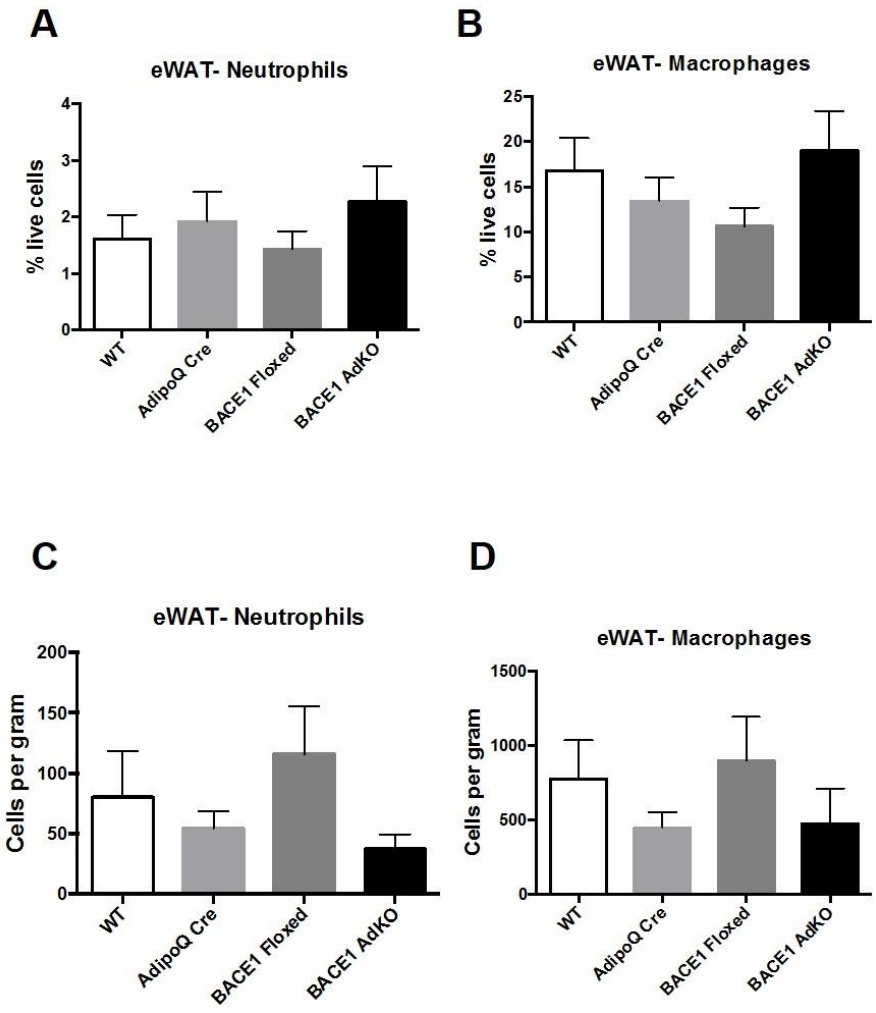

Figure 4.1 Conditional removal of BACE1 from adipocytes does not alter myeloid cell population in eWAT

Following 22 weeks HFD, one whole epididymal fat pad was excised and processed for FACS analysis. When expressed as %age total live cells **(A)** neutrophil and **(B)** macrophage population was unchanged between groups. When analysed as cells per gram of tissue **(C)** Neutrophil and **(D)** macrophage population was unchanged. **All FACS work was carried out in collaboration with Daniella Cavellini (Ashford lab PhD student)**

n=7-10 for all groups

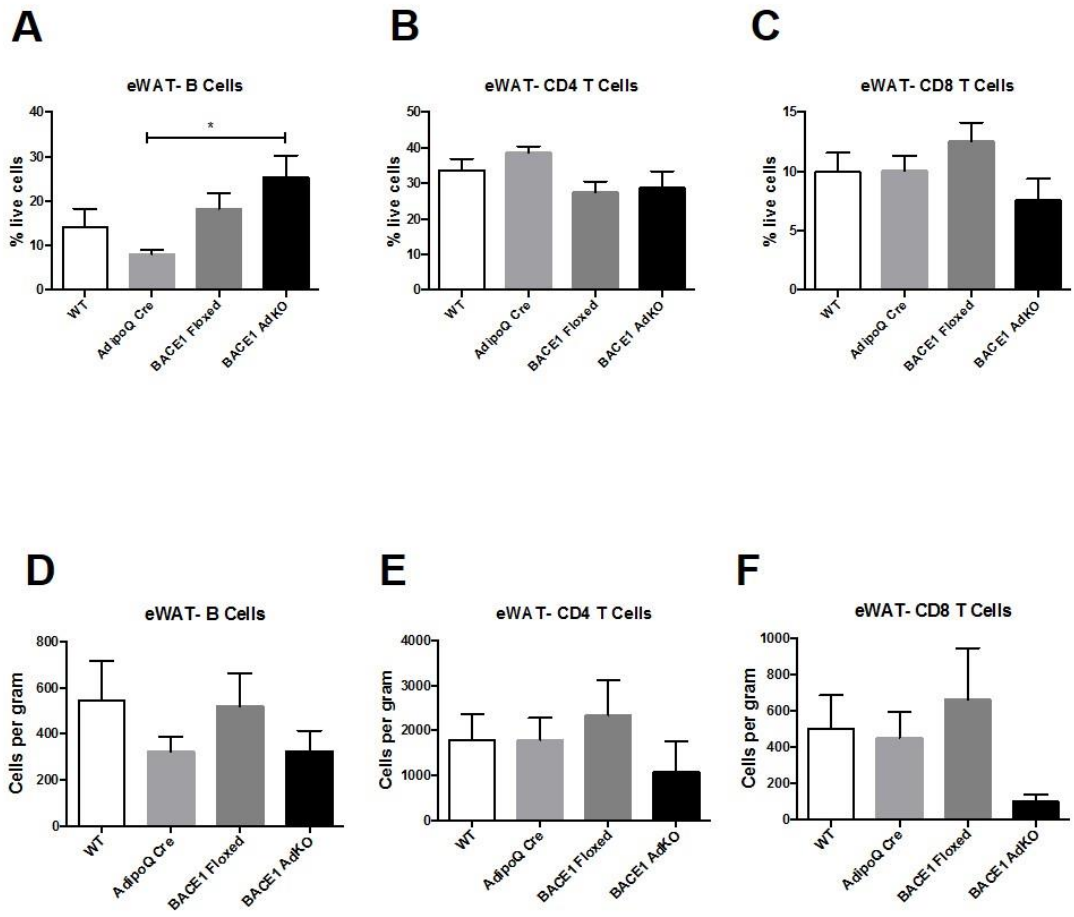

Figure 4.2 Conditional removal of BACE1 from adipocytes does not alter lymphoid cell population in eWAT

Following 22 weeks HFD, one whole epididymal fat pad was excised and processed for FACS analysis. When expressed as %age total live cells **(A)** B Cells were raised in BACE1 AdKO mice compared to AdipoQ Cre mice **(B)** CD4 T cells and **(C)** CD8 T cells were unchanged When analysed as cells per gram of tissue **(D)** B cell, (E) CD4 T cell and **(F)** CD8 T cell population was unchanged between all groups. **All FACS work was carried out in collaboration with Daniella Cavellini (Ashford lab PhD student)**

n=8-10 for all groups; *p<0.05

Next, the liver was examined. There was no significant difference in myeloid immune cell populations- with both neutrophils (Figure 4.3A) and macrophage (Figure 4.3B) levels unaltered in any group. When examined using the alternative method, as cells per gram of tissue there was a significant increase in neutrophil numbers in BACE1 floxed mice compared to WT (Figure 4.3C- WT 15068 cells per gram ± 10090 v BACE1 floxed 66111 ± 14299; $p<0.05$, n=9-10). Neutrophil numbers were also increased in BACE1 AdKO mice compared to WT (BACE1 AdKO 72520 ± 12333; $p<0.05$, n=10)

When analysed as a percentage of live cells there was no difference in B Cell population (Figure 4.4A). There was a significant decrease in CD4 T cells between AdipoQ Cre and BACE1 floxed mice (Figure 4.4B- AdipoQ Cre 31.30 ± 1.59 v BACE1 Floxed 21.65 ± 1.59, n= 8-10; p=<0.01). There was no other significant change in CD4 T cell population, or indeed in CD8 T Cell population (Figure 4.4C). Once again, there were subtle differences when the data was analysed as cells per gram, with B cells raised in BACE1 AdKO mice compared to AdipoQ Cre mice (Figure 4.4D- AdipoQ Cre 1212 ± 227 v BACE1 AdKO 4770 ± 865; n=8-10, $p<0.01$). There was no difference in CD4 T Cell population (Figure 4.4E). In CD8 T Cells there was a significant increase in BACE1 floxed mice compared to AdipoQ Cre mice (Figure 4.4F- BACE1 floxed 218 cell per gram ± 38 v AdipoQ Cre 1153 ± 283; n=8-10, $p<0.01$).

The spleen was also assessed for immune cell population. In myeloid cells, when calculated as percentage of live cells there was a decrease in neutrophils in BACE1 floxed mice compared to AdipoQ Cre mice (Figure 4.5A- BACE1 Floxed 0.73% ± 0.06 v AdipoQ Cre 0.50 ± 0.05; n=8-10, $p=0.009$) as well as in BACE1 AdKO mice compared to AdipoQ Cre mice (BACE1 AdKO 0.50 ± 0.04; n=10, $p<0.01$). There was no difference in macrophage population (Figure 4.5B). When calculated as cells per gram of tissue there were no changes in neutrophil population (Figure 4.5C).

Equally, there were no differences in splenic lymphoid cell populations when calculated as a percentage of live cells- with B Cells (Figure 4.6A), CD4 T cells (Figure 4.6B), or CD8 T cells (Figure 4.6C) all unaltered between groups. However, when analysed as cells per gram of tissue there were some significant differences. In BACE1 AdKO mice there were significantly more B cells compared to AdipoQ Cre mice (Figure 4.6D- AdipoQ Cre- 73336 cells per gram = 6969 v BACE1 AdKO 52301 ± 11832; $p<0.05$, n=8-10) There were significantly more CD4 T cells in BACE1 AdKO mice compared to WT (Figure 4.6E- WT 21745 cells per gram ± 2168 v BACE1 AdKO 40491 + 5037; $p<0.01$ n=9-10, and the difference between AdipoQ cre mice and BACE1 AdKO mice was also significant (AdipoQ Cre 18587 ± 2041; $p<0.01$, n=8). There were also significantly greater numbers of CD8 T cells when expressed as cells per gram in BACE1 AdKO mice compared to WT (Figure 4.6F- WT 11708 cells per gram ± 1142 v BACE1 AdKO 22458 ± 2421; $p<0.001$, $p<0.01$ n=8-10). BACE1 floxed mice also had significantly more of this cell type than WT mice (BACE1 Floxed 20189 cells per gram ± 1920; $p<0.05$, n=9). Both BACE1 floxed and BACE1 AdKO mice possessed greater numbers of CD8 T cells compared to AdipoQ Cre mice (AdipoQ Cre 10274 cells per gram ± 1446; $p<0.01$ n=8).

Finally, the population of circulating immune cells in the blood was investigated. However, once again the immune cell population of Neutrophils (Figure 4.7A), macrophages (Figure 4.7B), B cells (Figure 4.7C) and CD4 T cells (Figure 4.7D) not different between any of the mouse lines investigated.

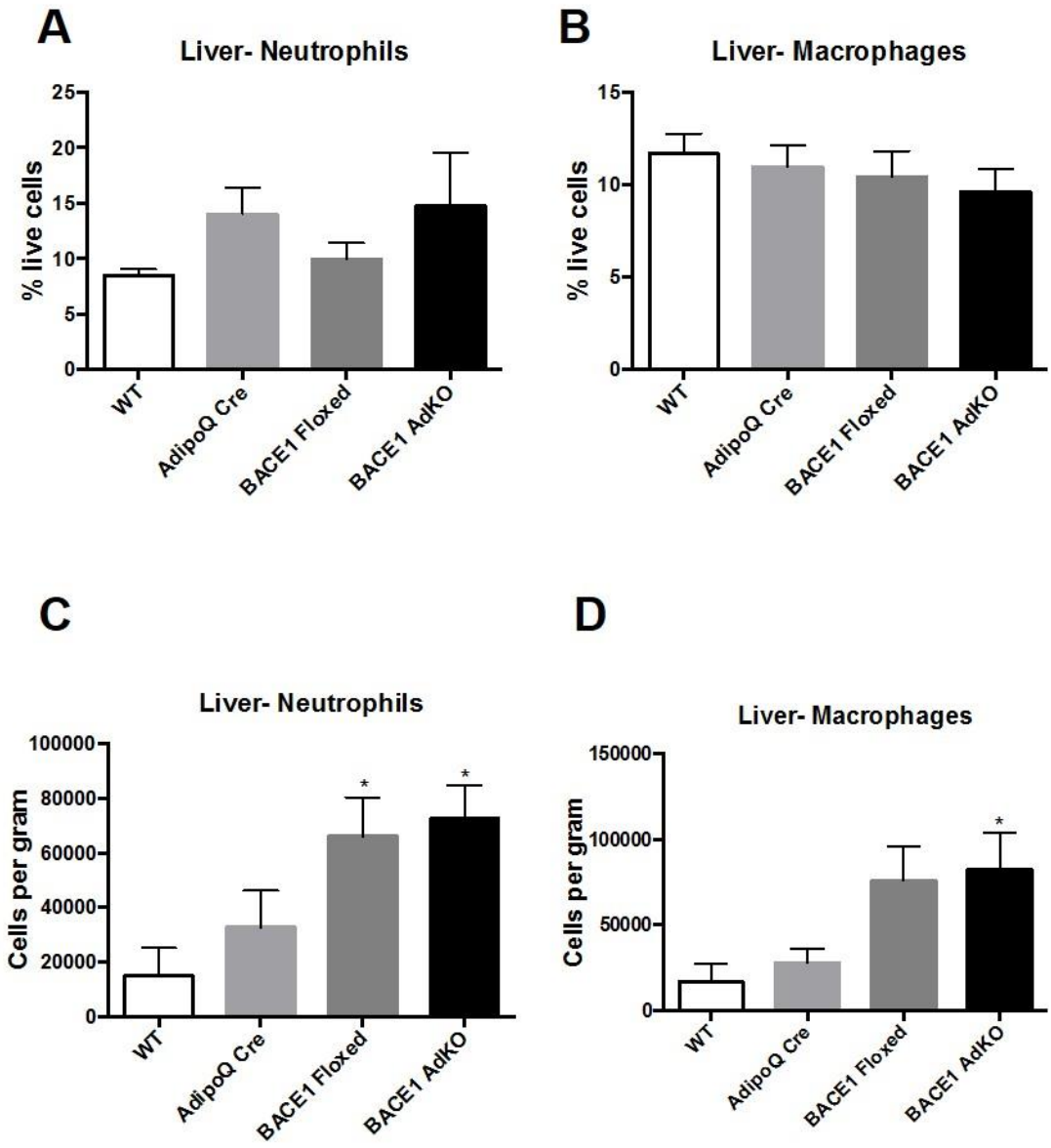

Figure 4.3 Conditional removal of BACE1 from adipocytes may alter myeloid cell population in liver

Following 22 weeks HFD, whole spleen was excised and processed for FACS analysis. When expressed as %age total live cells **(A)** neutrophils were largely unchanged, although BACE1 floxed and BACE1 AdKO mice had reduced numbers compared to AdipoQCre mice **(B)** Macrophages were unchanged **(C)** When analysed as cells per gram of tissue **(C)** neutrophil population was raised in BACE1 floxed and BACE1 AdKO mice compared to WT mice and **(D)** macrophage population was raised in BACE1 AdKO mice compared to WT. **All FACS work was carried out in collaboration with Daniella Cavellini (Ashford lab PhD student)**

n=8-10 for all groups; *$p<0.05$

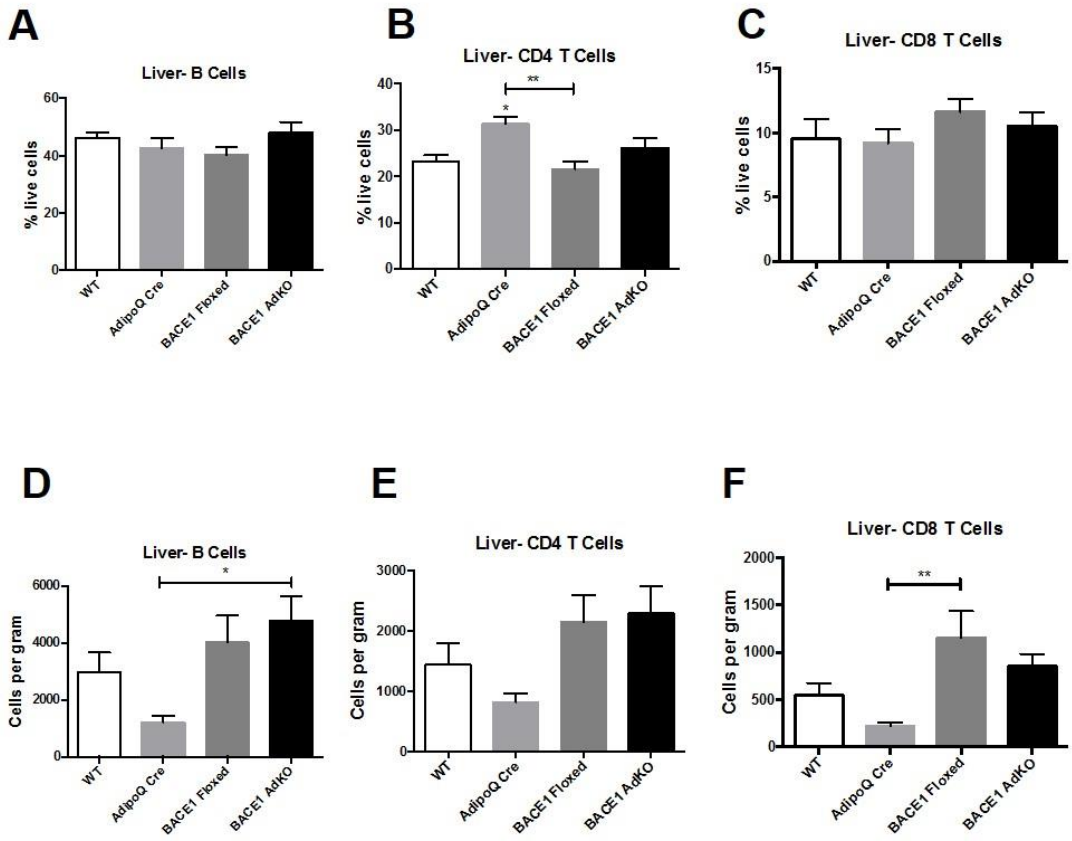

Figure 4.4 Conditional removal of BACE1 from adipocytes may alter lymphoid cell population in liver

Following 22 weeks HFD, approximately one fifth of the liver was excised and processed for FACS analysis. When expressed as %age total live cells **(A)** B cell population was unaltered **(B)** CD4 T Cell population was raised in adipoQ cre mice and decreased in BACE1 floxed mice compared to AdipoQ cre mice **(C)** CD8 T Cell expression was unchanged between groups. When analysed as cells per gram of tissue **(D)** B cell population was raised in BACE1 AdKO mice compared to AdipoQ Cre mice. **(E)** CD4 T Cells were raised compared to WT and AdipoQ Cre mice. **(F)** CD8 T cells were raised in BACE1 floxed mice compared to AdipoQ Cre mice. **All FACS work was carried out in collaboration with Daniella Cavellini (Ashford lab PhD student)**

n=8-10 for all groups; *p<0.05, **p<0.01

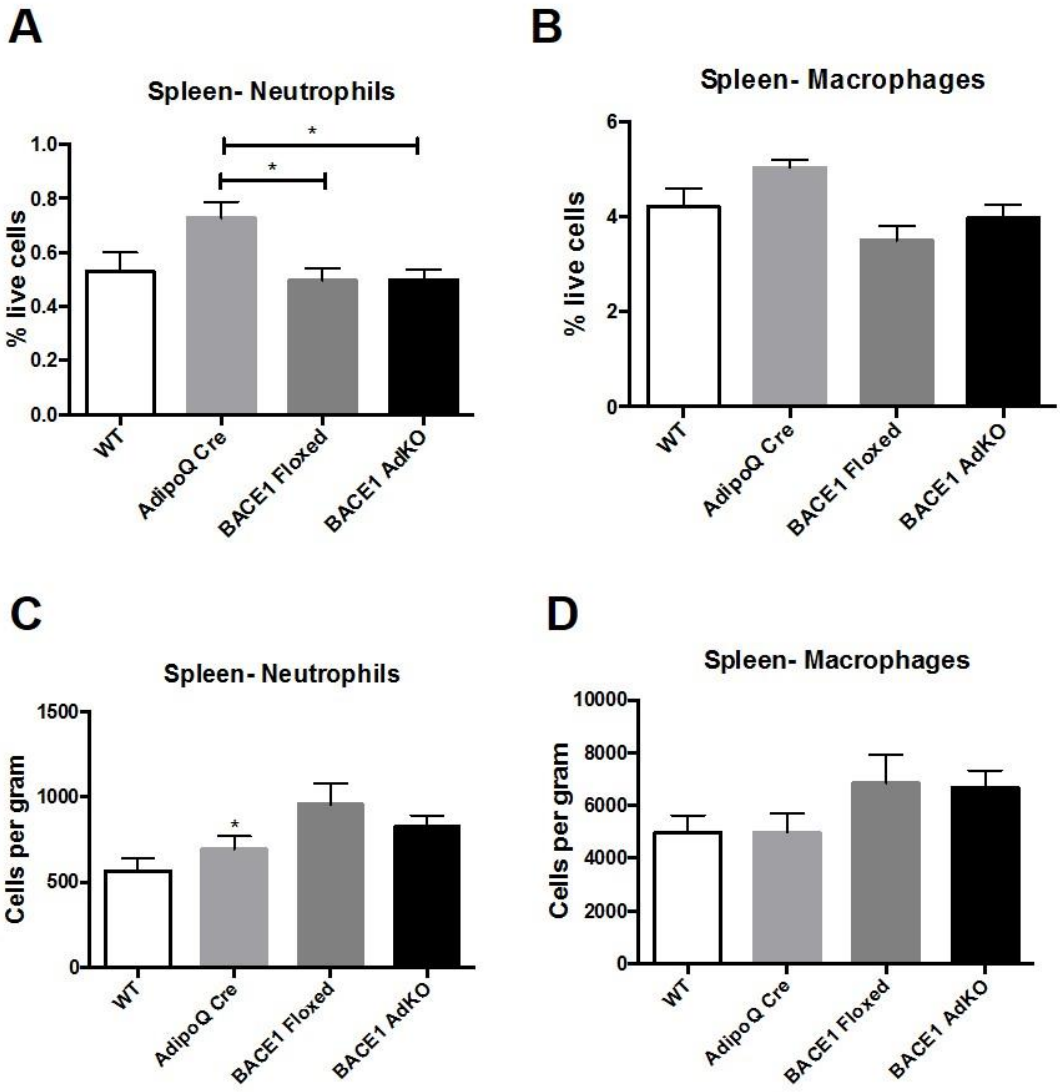

Figure 4.5 Conditional removal of BACE1 from adipocytes does not alter myeloid cell population in spleen

Following 22 weeks HFD, whole spleen was excised and processed for FACS analysis. When expressed as %age total live cells **(A)** neutrophils were largely unchanged, although BACE1 floxed and BACE1 AdKO mice had reduced numbers compared to AdipoQ Cre mice **(B)** Macrophages were unchanged **(C)** When analysed as cells per gram of tissue **(C)** neutrophil population was raised in AdipoQ cre mice compared to control, but **(D)** macrophage population was unchanged between groups. **All FACS work was carried out in collaboration with Daniella Cavellini (Ashford lab PhD student**

n=8-10 for all groups; *p<0.05

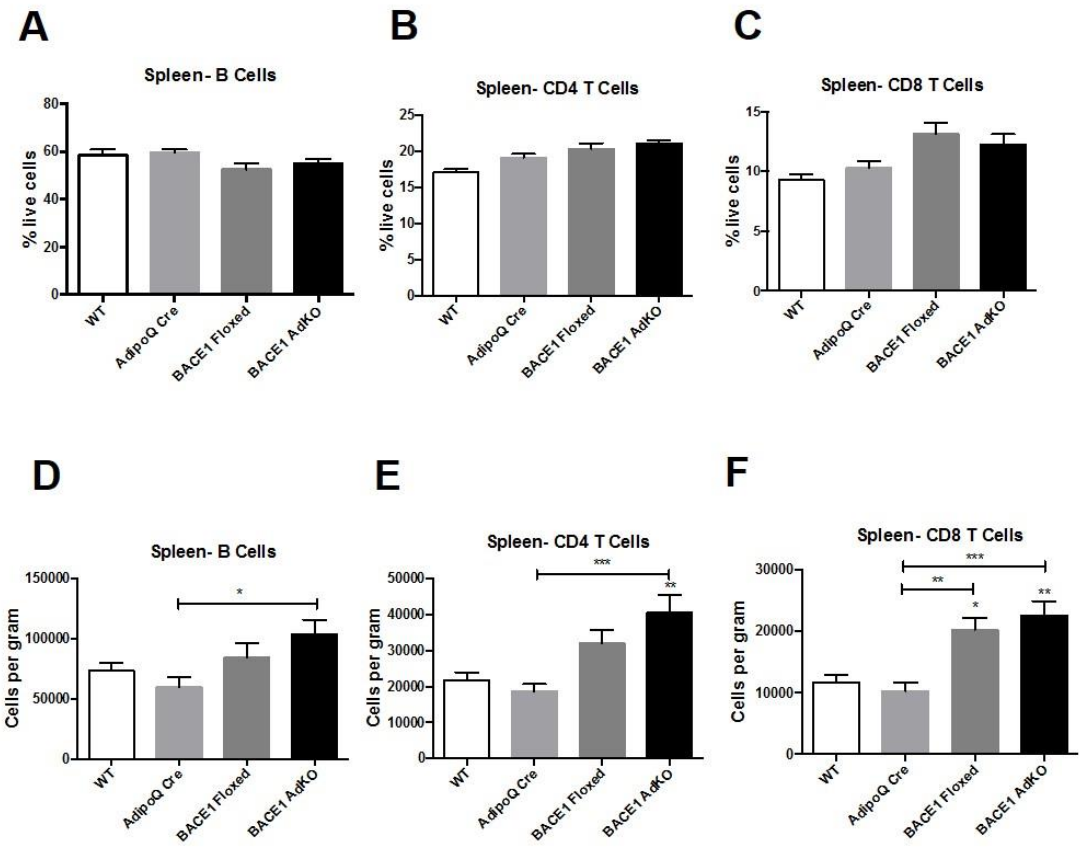

Figure 4.6 Conditional removal of BACE1 from adipocytes may alter spleen lymphoid cell populations

Following 22 weeks HFD, whole spleen was excised and processed for FACS analysis. When expressed as %age total live cells **(A)** B cell, **(B)** CD4 T Cell and **(C)** CD8 T Cell expression was unchanged between groups. When analysed as cells per gram of tissue **(D)** B cell population was raised in BACE1 AdKO mice compared to AdipoQ Cre mice. **(E)** CD4 T Cells were raised compared to WT and AdipoQ Cre mice. **(F)** CD8 T cells were raised in BACE1 AdKO mice compared to WT and AdipoQ Cre mice. BACE1 floxed mice also had raised CD8 cell number compared to WT and AdipoQ Cre controls. **All FACS work was carried out in collaboration with Daniella Cavellini (Ashford lab PhD student)**

n=8-10 for all groups; *p<0.05, **p<0.01, ***p<0.001

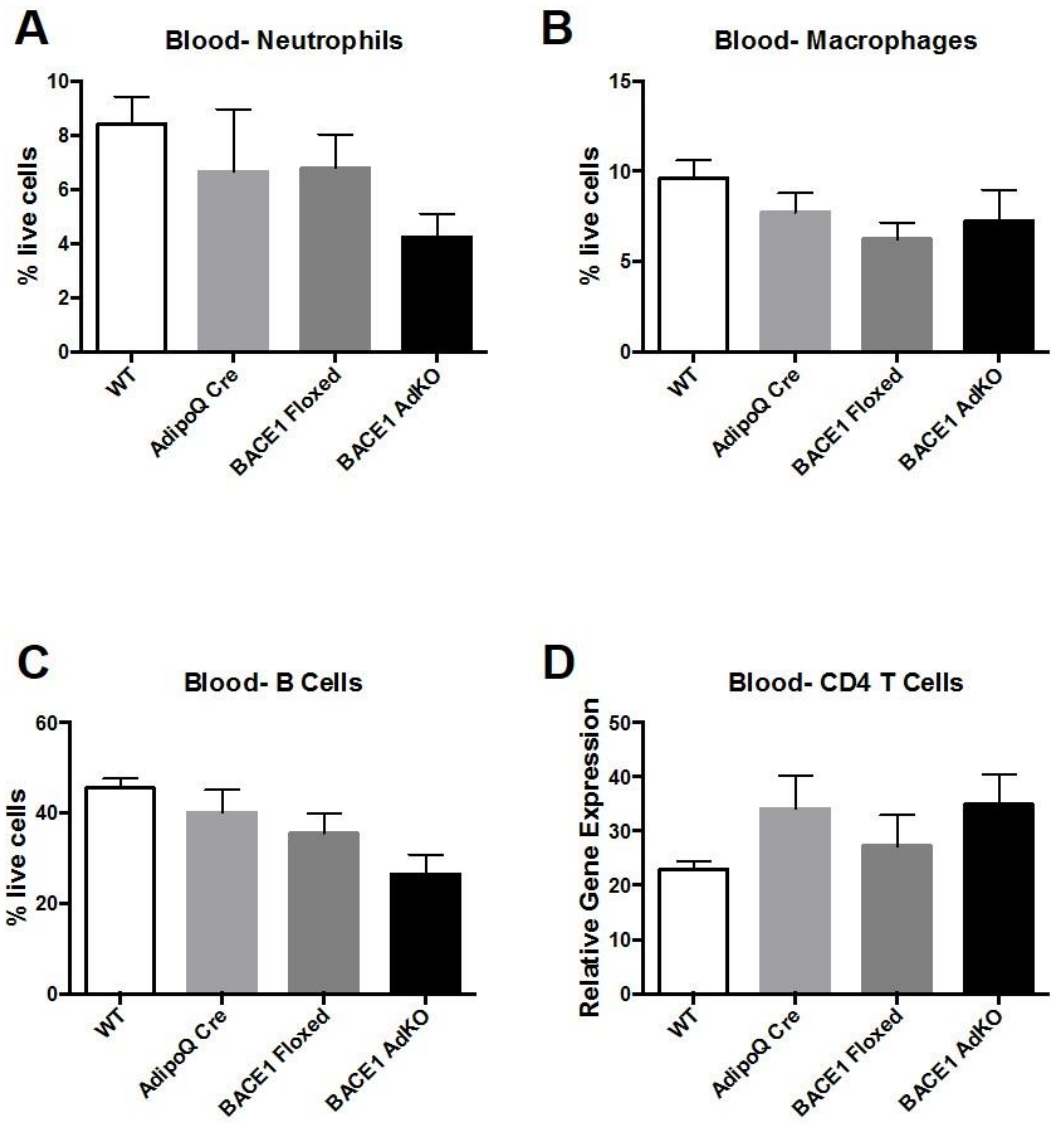

Figure 4.7 Conditional removal of BACE1 from adipocytes does not alter immune cell population in blood

Following 22 weeks HFD, 100µl blood was taken and processed for FACS analysis. When expressed as %age total live cells **(A)** neutrophil **(B)** macrophage **(C)** B cell and **(D)** CD4 T cell population was unchanged between all groups. **All FACS work was carried out in collaboration with Daniella Cavellini (Ashford lab PhD student)**

n=8-10 for all groups

As our labs previous work, particularly with global BACE1 KO mice has previously suggested a reduction of macrophage infiltration, another method was used to confirm the findings from the FACS analysis. Cd68 is a pan-macrophage marker, with F4/80 being another commonly used mouse macrophage marker. These markers were examined in eWAT, with no obvious changes in CD68 (Figure 4.8A) or F4/80 (Figure 4.8B), for example increased staining around adipocytes, which would be indicative of the presence of crown-like structures which form around dead or dying adipocytes. Likewise, there were no noticeable difference in liver tissue in cd68 (Figure 4.9A) or F4/80 staining (Figure 4.9B).

Taken together, this data suggests that removal of BACE1 from adipocytes does not significantly impact the overall immune cell population of peripheral tissues or blood, although the high variation, and lack of data from normal chow fed mice, means firm conclusions are difficult to draw.

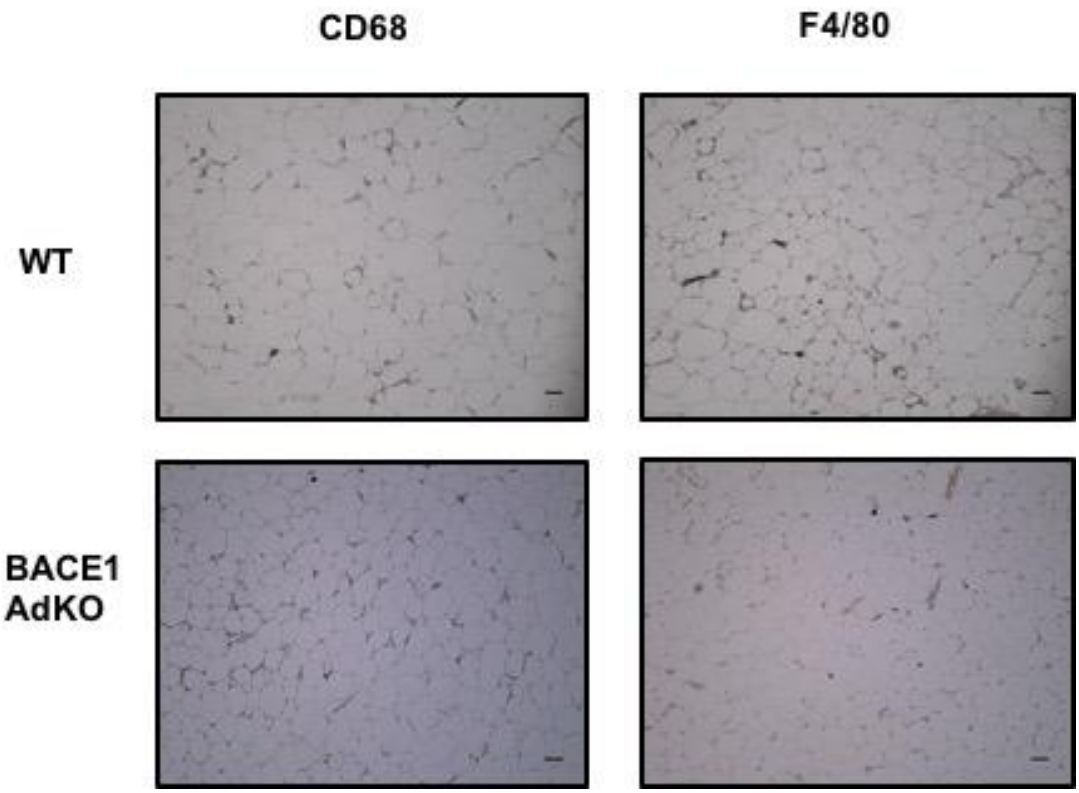

Figure 4.8 Conditional removal of BACE1 from adipocytes does not alter levels of macrophages in eWAT

After 22 weeks HFD, a small portion of eWAT tissue was excised and preserved in formalin, paraffin embedded, cut and stained **(A)** CD68 macrophage marker in WT and BACE1 AdKO mice. **(B)** F4/80 macrophage marker in WT and BACE1 AdKO mice. Magnification x10, scale bars=100μM

n=6

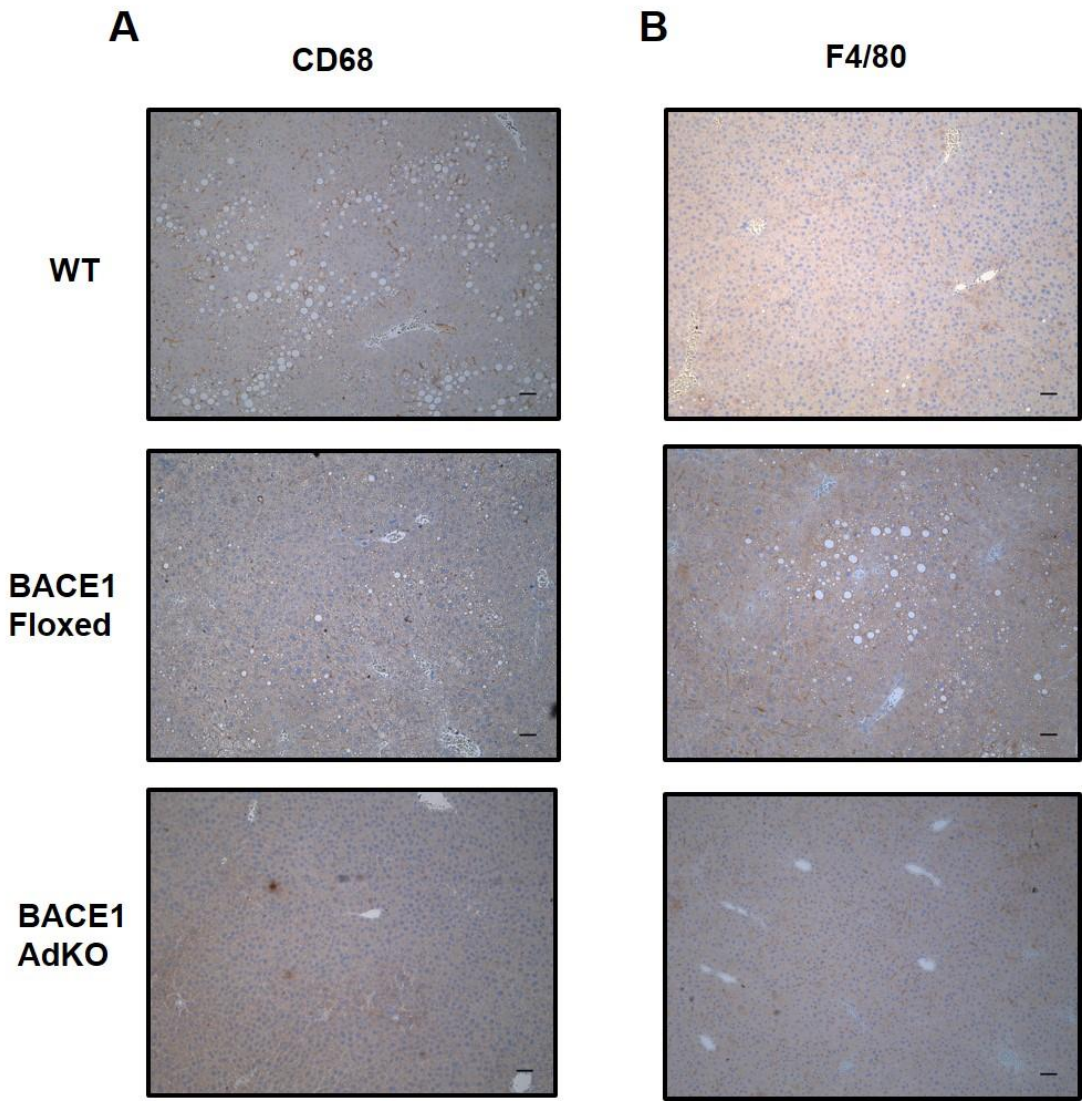

Figure 4.9 Conditional removal of BACE1 from adipocytes does not alter levels of macrophages in liver

After 22 weeks HFD, a small portion of liver tissue was excised and preserved in formalin, paraffin embedded, cut and stained for macrophage markers **(A)** CD68 macrophage marker in WT, BACE1 floxed and BACE1 AdKO mice. **(B)** F4/80 macrophage marker in WT, BACE1 floxed and BACE1 AdKO mice. Magnification x10, scale bars=100μM

n=6 for all groups

4.2.2 Removal of BACE1 from adipocytes does not alter cytokine levels in either eWAT or iWAT

Although there was no overall change in the quantity of immune cells resident in the tissues studied, there was still the possibility that the character of the cells present could be altered, particularly in the adipose tissue. To examine this possibility more closely, the relative number of pro-inflammatory classically activated “M1 type” macrophages was compared to the anti-inflammatory alternatively activated “M2 type” macrophages in eWAT. When expressed as a percentage of total macrophages, M1 type macrophages were significantly raised in BACE1 AdKO mice compared to WT mice (WT 10.33% ± 1.74 v BACE1 AdKO 25.65% ± 4.34, n=9-10; $p<0.01$). This was also significantly higher compared to AdipoQ Cre mice (8.55% ± 0.96, n=7; $p<0.05$) and BACE1 floxed mice (13.25% ± 2.62, n=10; $p<0.05$). There was no difference in the overall M2 macrophage population (Figure 4.10B).

To confirm this finding, eWAT and iWAT were taken and checked for gene expression of a number of pro and anti-inflammatory cytokines, as well as chemokines.

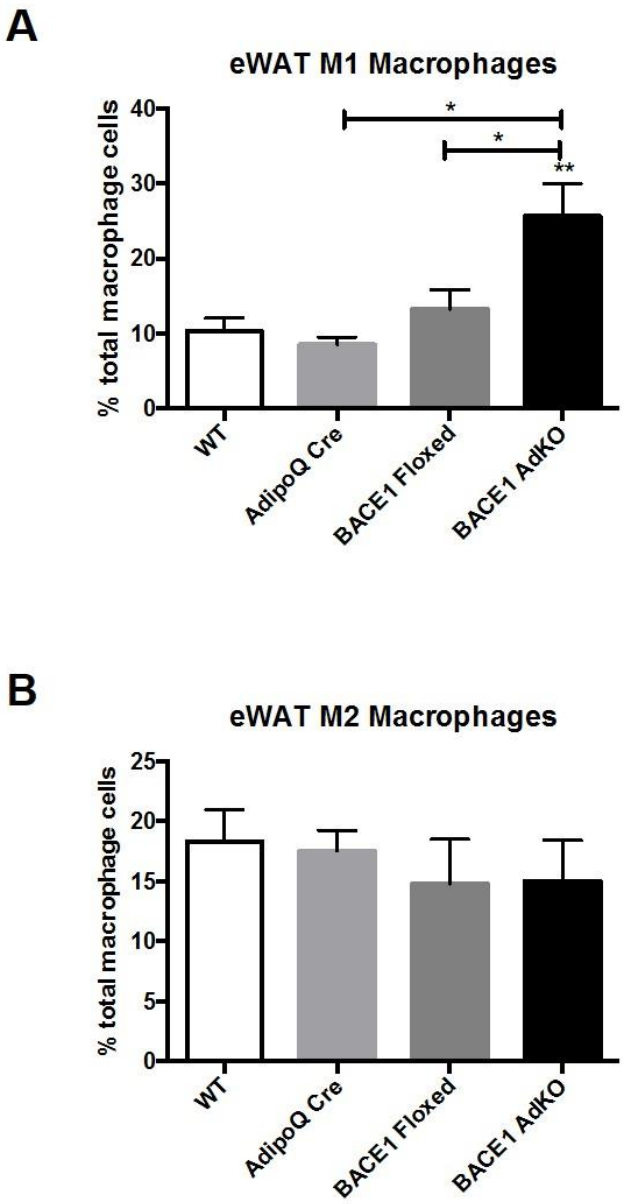

Figure 4.10 Conditional removal of BACE1 from adipocytes may alter the polarisation of macrophages in eWAT

Following 22 weeks HFD, one whole epididymal fat pad was excised and processed for FACS analysis. When expressed as %age of total macrophages **(A)** M1 macrophages were raised in BACE1 AdKO mice compared to WT, AdipoQ Cre and BACE1 floxed mice **(B)** There was no difference in the quantity of M2 macrophages
All FACS work was carried out in collaboration with Daniella Cavellini (Ashford lab PhD student)

n=8-10 for all groups; *p<0.05, **p<0.01

Within eWAT, there was a decrease in gene expression of the pro-inflammatory cytokine TNF-α in BACE1 AdKO mice when expressed as relative levels compared to WT (Figure 4.11A- WT 1.00 ± 0.10 v BACE1 AdKO 0.60 ± 0.12, n=8; p=0.01). There was no difference in the expression of NOS2 (Figure 4.10B) or IL-1β (Figure 4.10C). Conversely, there was no significant difference in TNF-α (Figure 4.10D) or NOS2 (Figure 4.10E) in iWAT.

The anti-inflammatory marker IL10 was significantly decreased in BACE1 AdKO mice compared to WT (Figure 4.12A- WT 1.00 ± 0.17 v BACE1 AdKO 0.33 ± 0.12). There was a significant decrease in BACE1 floxed mice compared to WT (WT1.00 ± 0.50 v BACE1 floxed 0.28 ± 0.08, n=7-8; p<0.0001), and an increase in Arg1 gene expression in BACE1 AdKO mice compared to BACE1 floxed (BACE1 AdKO 1.29 ± 0.40, n=7-8; p=0.04), but not WT mice. There was no difference in the expression of YM1 between groups (Figure 4.12C). There were no significant differences between groups in iWAT, with IL10 (Figure 4.11D), Arg1 (Figure 4.11E), and YM1 (Figure 4.11F) unchanged.

Chemokines can influence the infiltration of immune cells from other tissues, so these were assessed in the eWAT, but CCL2 (Figure 4.12A), CCL3 (Figure 4.12B), CCL4 (Figure 4.12C) and CCL5 (Figure 4.12D) were all unaltered. Taken together, these data indicate that, in contrast to the available FACS data, there may be a small change in the overall inflammatory profile of eWAT, but not iWAT, of BACE1 AdKO mice compared to controls.

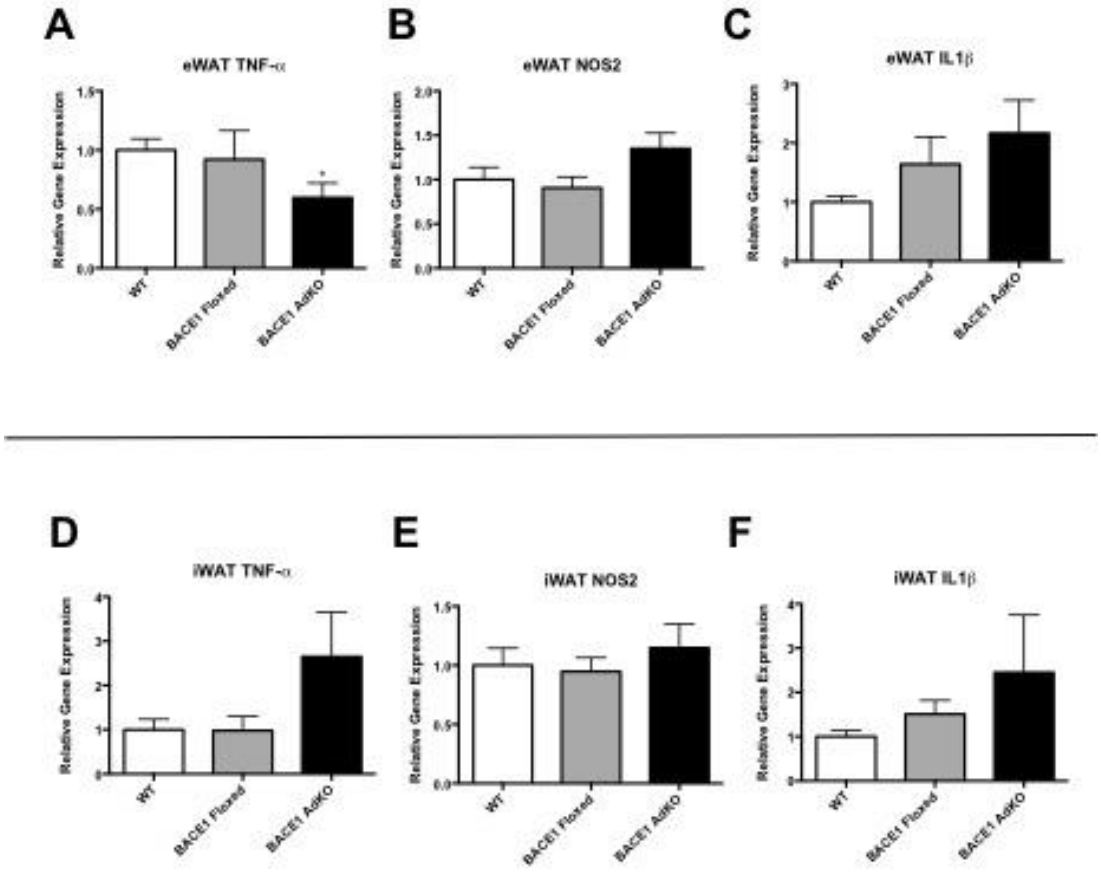

Figure 4.11 Conditional removal of BACE1 from adipocytes plays a limited role in the production of pro-inflammatory cytokines in adipose tissue

After 22 weeks HFD, a small portion of eWAT and iWAT was excised and snap frozen in liquid nitrogen. Gene expression analysis was performed on pro-inflammatory cytokines, and data normalised to WT mice. In eWAT **(A)** TNF-α expression was reduced in BACE1 AdKO mice compared to WT mice (n=8), whereas **(B)** NOS2 (n=8) and **(C)** IL-1β (n=8) expression were unchanged. Within iWAT **(D)** TNF-α (n=7-8), **(E)** NOS2 (n=7-9) and **(F)** IL-1β (n=7-8) were all unchanged

*p<0.05

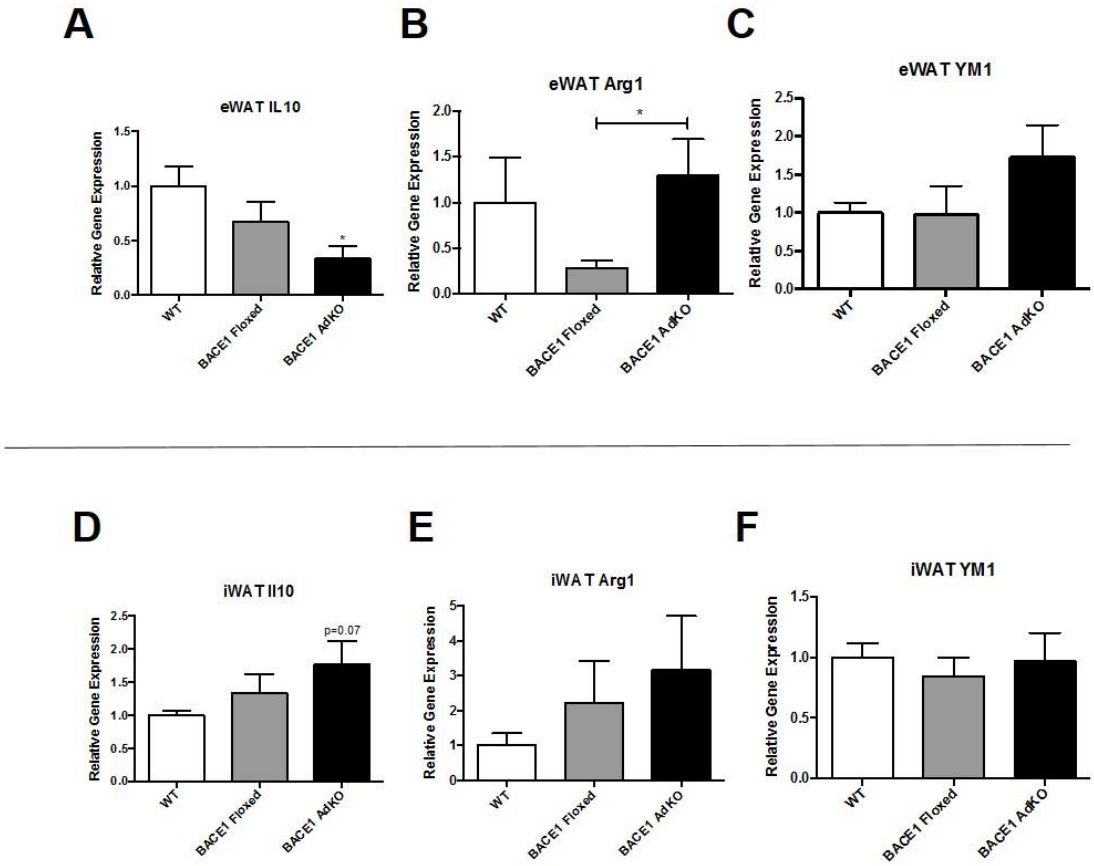

Figure 4.12 Conditional removal of BACE1 from adipocytes may have a limited role in upregulating anti-inflammatory cytokines in adipose tissue

After 22 weeks HFD, a small portion of eWAT and iWAT was excised and snap frozen in liquid nitrogen. Gene expression analysis was performed on anti-inflammatory cytokines, and data normalised to WT mice. In eWAT **(A)** IL10 was reduced in BACE1 AdKO mice (n=7-8) and (B) Arg1 was raised in BACE1 AdKO mice compared to BACE1 floxed mice (n=7-8), whereas YM1 (n=7-8) was unchanged. Within iWAT **(D)** IL10 (n=7-9), **(E)** Arg1 (n=7-8) and **(F)** YM1 (n=7-9) expression were all unchanged between groups

*p<0.05

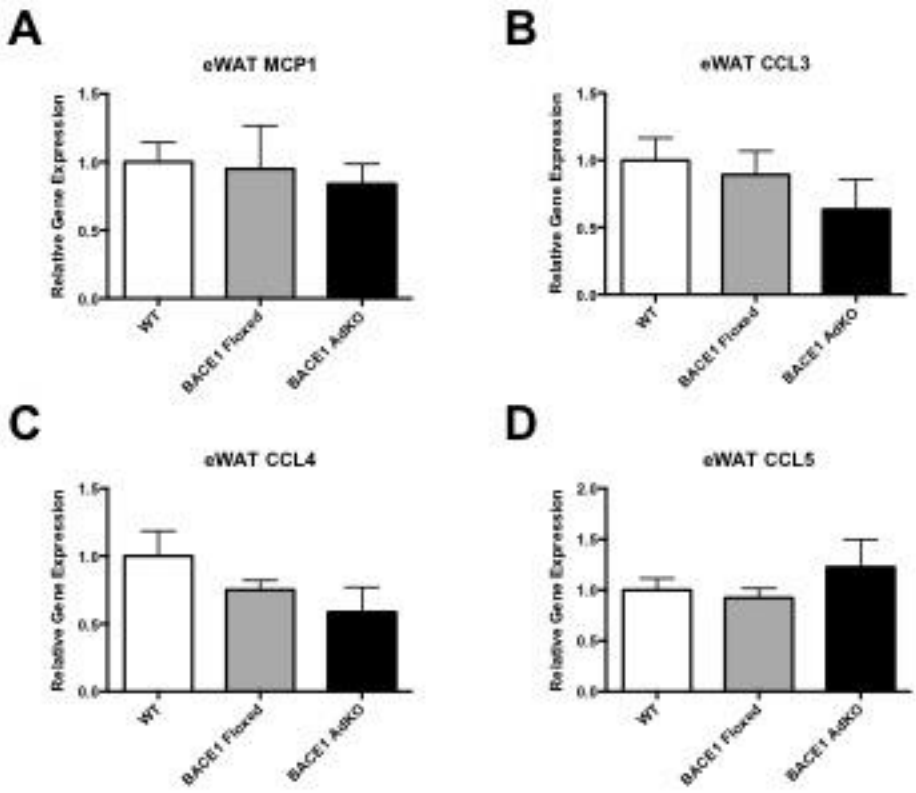

Figure 4.13 Conditional removal of BACE1 from adipocytes plays no role chemokine production in eWAT

After 22 weeks HFD, a small portion of eWAT was excised and snap frozen in liquid nitrogen. Gene expression analysis was performed, and data normalised to WT mice **(A**) CCL2 (n=7-8), **(B)** CCL3 (n=7-8), **(C)** CCL4 (n=7-8) and **(D)** CCL5 (n=8) were all unchanged between groups

4.3 Discussion

4.3.1 Variability in Immune Status between batches

One of the major features of the FACS data presented herein is the high variability of the data, with significant and often opposing data between batches. Inflammatory responses are dependent on a huge number of different factors in mice, including physical injury and biological factors such as infection, stress or HFD. Due to the large number of mice necessary to perform these experiments, mice were placed onto the 22 week HFD as they reached the appropriate age in batches ranging in size from 6 to 12 mice. Many factors could have varied between batches. The early batches of mice completed their time on the HFD study over a year before the last ones. All mice were housed in cages open to the environment, and therefore exposed to potential pathogens which could lead to an inflammatory response. Given the long-term nature of the studies and the large amount of time between the early and latter batches of animals tested, it is possible that the environment the mice were held in could change considerably and impact on inflammation. Furthermore, due to the pattern of breeding, the WT and AdipoQ Cre mice were generally run later in the overall study than the BACE1 floxed and BACE1 AdKO group. One possible measure to remove this variable would be to house mice in individually ventilated cages, which have been shown to significantly reduce exposure to pathogens compared to open-air cages (Clough, Wallace, Gamble, Merryweather, & Bailey, 1995). Alternatively, it would be preferable to complete all FACS data from a single batch to account to ensure the environmental conditions remained constant in each mouse. In one of the batches, mice had to be separated and singly housed part way through the study due to excessive fighting behaviour, and this increased isolation is known to be stressful to mice, which are naturally social animals. This kind of chronic stress could theoretically contribute towards inflammation and mask any genotype effect. An ideal approach may be to use BACE1 AdKO mice and a single control group only, whilst at the same time comparing them to NC fed controls.

This study used two methods to examine the FACS data, and interestingly, in some cases they gave differing interpretations. The percentage live cell measurement could be argued to be the more relevant as it takes into account only the cells which are live and have passed through the machine. However, it does not consider the starting tissue mass taken, which varies between each individual mouse, or the total amount of tissue which was passed through the machine, which is the major advantage of the cells per gram method. This method has drawbacks as well, though, as it makes the assumption that all of the tissue that was initially excised from the mouse was processed without any loss of sample during any of the steps, which includes a number of transfers between tubes, and filtration, which are both likely to lead to some level of discrepancy between starting and ending weights. However, given the experiments were performed by the same individuals it is likely to be a consistent error, which may give this method of analysis an advantage. Many significant differences appeared to be between control groups rather than in the BACE1 AdKO mouse and ultimately, there were very few differences that appeared significant across both methods of analysis, which makes forming any firm conclusions difficult. Given the variability in the data, likely both in the mice and the subsequent analytical techniques used, it is clear that more mice are required to ascertain the true inflammatory status of BACE1 AdKO mice. Importantly, though, within the eWAT, which was the major focus of this chapter, there were no differences between groups, no matter which analysis was used, which would suggest that lack of BACE1 in adipocytes does not prevent the onset of inflammation in high fat fed mice.

An interesting finding in the present study suggested that there was a greater proportion of M1 macrophages, which exhibit a pro-inflammatory phenotype, present in the adipose tissue compared to the more anti-inflammatory M2 macrophages. However, this did not appear to match the subsequent gene expression profiling. Recently, there has been debate as to the usefulness of the M1 v M2 polarisation standard, with arguments that these two wide-ranging definitions should be further sub-divided depending on factors such as the interaction of macrophages with other immune cells

and the way in which macrophages respond to and resolve inflammation (Martinez & Gordon 2014). Furthermore, it has been reported that some genes, such as Arg-1, which are highly upregulated in M2 like macrophages are also upregulated in M1 macrophages (Jablonski et al. 2015). Therefore, the arbitrary staining used to differentiate between the M1 and M2 macrophages in the FACS presented herein may be not be the best way of assessing macrophage polarisation. Some groups have suggested better markers- such as CD38 and Fpr2 for M1 macrophages and Egr2 for M2 macrophages (Martinez & Gordon 2014). Alternatively, it has been postulated that a better measurement is by looking at the ratio of arginase to iNOS, which both use L-arginine as a substrate (Chang et al. 1998), but are associated with different inflammatory outcomes.

In the previous chapter, the AdipoQ cre mouse was shown to have increased fat mass and impaired glucose homeostasis compared to other groups. In the present analyses, many of the significant differences were between the AdipoQ Cre mouse and the BACE1 AdKO mouse, but were often opposite to what would be hypothesised. In an obese mouse, it would be expected that there would be much greater immune cell presence in the WAT than in a leaner mouse, which is the case with the BACE1 AdKO mice compared to the AdipoQ Cre mice. However, this did not appear to be the case. Unfortunately, due to time constraints, no measurement of any of the inflammatory genes was carried out in the AdipoQ Cre mouse, so it would be interesting to perform these studies in the future to compare them to the levels already found in the other three experimental groups.

In the present study FACS was carried out in the visceral epidydimal fat pad. The main reason for this is because visceral fat depots are known to be much more relevant in the study of inflammation during obesity compared to subcutaneous depots (M.-J. Lee et al. 2013). As a comparison, both depots were examined for gene expression.

Importantly, in this study all FACS and gene expression analyses have been completed in mice on a HFD. The assumption is that inflammation is

present in these mice and is simply not diminished by removal of BACE1 from adipocytes. If this was the case the data in this chapter would therefore suggest that the lean BACE1 AdKO mice still have the chronic low-grade inflammation related to HFD, but without any of the metabolic deficits that are usually present. However, to confirm this, similar experiments will need to be performed on mice with the same genotypes as in this study, but fed a NC diet to ascertain the basal levels of inflammation present, and to confirm that this is exacerbated by HFD in control mouse groups. Another potential confounding factor in the study could be from a reduction in body weight in the mice prior to the flow cytometry studies. As explained in chapter 3, in the final weeks of the study the mice underwent a number of different procedures, with the unintended effect of weight loss, particularly in the WT and AdipoQ Cre groups. This may reduce inflammation in these groups and mask any significant difference between the controls and BACE1 AdKO mice. Indeed, weight loss is known to reduce both liver and adipose tissue inflammation, including reduction of crown like structures, indicating reduced macrophage numbers (Wang et al. 2011).

Further to this, more detailed work should be performed on characterising the relative cytokine levels at a protein level using ELISA plates, as all the work performed so far has been focussed on gene expression.

4.3.2 Alternative possibilities for the role of BACE1 in Inflammation

The lack of change in any inflammatory component in this study is in contrast to some of the data previously reported in global BACE1$^{-/-}$ mice, which has suggested that the chronic low-grade inflammation associated with obesity is significantly ameliorated in BACE1 KO mice. In the BACE1 global knock-out study there are reductions in pro-inflammatory markers and increases in anti-inflammatory cytokines, with a significant reduction in macrophages in WAT. Intriguingly, treatment of diet induced obese mice (20 weeks HFD) with a BACE1 inhibitor, infused peripherally, also reduces inflammation in WAT prior to body weight loss (Meakin et al. 2018). Central inhibition of BACE1 causes reduction in hypothalamic inflammation as well

as a reduction in inflammasome markers. Therefore, overall data from our lab appears to indicate that reducing central BACE1 activity can diminish inflammation, and from the data presented in this chapter, it can be concluded that loss of BACE1 from adipocytes does not influence inflammation driven by chronic HFD feeding, despite the fact that adipose tissue inflammation is a key feature of obesity.

Other groups have examined inflammation in BACE1$^{-/-}$ mice and found differing results. In the hippocampus of BACE1$^{-/-}$ mice, a number of genes are up-regulated compared to WT controls, in particular related to IL9 and NFκB signalling (Stertz et al. 2016). Other cellular stresses may also be involved in inflammatory response in BACE1$^{-/-}$ mice, too, as all our studies have been performed in HFD mice, which would, *per se* be expected to activate inflammation- whereas the study looking in the hippocampus was performed in normal chow mice without this added stressor. Age may also be a confounding factor. In the present study, mice are around 7 months old at the time of analysis, and age is known to increase chronic low-grade inflammation (Cevenini et al. 2010). It could be argued that in our previous studies, mice with reduced BACE1 display reduced inflammation as an effect of being leaner rather than being directly influenced by BACE1 activity, but this would contrast with our existing data suggesting that reducing BACE1 activity with pharmacological inhibitors in already obese mice can reduce inflammation before reducing body weight and the present study where BACE1 AdKO mice are leaner but do not appear to have a different inflammatory status.

Taken together, the current available data is unclear, but suggests a complex involvement of BACE1 in both inflammatory and immunoregulatory processes, which may be region or tissue specific, and highly sensitive to other variables.

Rather than adipocyte BACE1 being responsible for modulating adipocyte inflammation, it could be argued that BACE1 within the immune cells known to be resident within the SVF of adipose tissue (Lafontan 2014) is

key in modulating immune responses to HFD. To test this, the lab used the lysozyme 2 (LysM) gene to remove BACE1 specifically from myeloid cells. However, no immune phenotype was present in these mice, which also did not display any metabolic improvement compared to control groups when subjected to the same protocols as outlined in chapter 3 of this thesis (unpublished data). These data, therefore, suggest that BACE1, or BACE1 activity may impact in inflammation in another, as yet undefined way.

Recently, there has been some evidence that Aβ may enable the innate immune system, by functioning as a Damage-associated Molecular Pattern (DAMP) to activate microglia via the CD36 receptor (Heneka et al. 2014) to modulate increased inflammation in AD. This is thought to be via activation of the NLRP3 inflammasome, which induces IL-1β expression. Reduced BACE1 activity, and therefore reduced $A\beta_{1-42}$ production could reduce inflammation overall, but given the relatively low level of BACE1 mediated APP cleavage in murine adipocytes, as demonstrated by the very low levels of sAPPβ present in adipocytes (unpublished observations), it would not be surprising that removing BACE1 solely from adipocytes would not create a significant inflammatory response if this theory was correct.

In contrast to this theory, data from our laboratory found that central infusion of $A\beta_{1-42}$ did not increase hypothalamic, liver or WAT inflammation despite worsening an obese/diabetic phenotype (unpublished observations). Instead, BACE1 removal may lower inflammation by pushing APP processing down the non-amyloidogenic pathway. There is some evidence that this could be possible because anti-inflammatory drugs have been shown to increase secretion of sAPPα within SHSY 5Y neuronal cells (Avramovich et al. 2002).

Other groups have shown, however, that APP expression is fairly high in adipose tissue, and mice with mutant APP have higher levels of macrophage infiltration into adipose tissue when on a HFD (Freeman et al. 2012). Data from human tissue has shown that adipose tissue APP expression increases in obesity, and is correlated with levels of pro-

inflammatory cytokines including CCL2 and IL6 (Lee et al. 2008). It is important to note the significant differences between human and murine inflammatory pathways when considering these studies (Mestas & Hughes 2004). Of particular relevance to these studies, production of NO is induced by different factors in mouse and human macrophages (Mestas & Hughes 2004). It would be interesting to examine BACE1 expression in human adipose tissue and relate levels to obesity, macrophage population and cytokine and chemokine levels. It would also be useful to take *ex vivo* human adipocytes and treat them with a BACE1 inhibitor, which would elucidate adipose specific effects of reducing BACE1 activity in the context of inflammation. An alternative approach would be to take a human adipocyte *in vitro*, such as the hMADS cell line and over-express BACE1 to measure the inflammatory profile of these cells under various cellular stresses.

4.3.3 Links between BACE1, adipokine and Inflammation

Several adipokines have been associated with inflammation. For example, adiponectin is considered anti-inflammatory, whereas leptin and resistin have been reported to have pro-inflammatory effects (Ouchi et al. 2011). Adiponectin knock out mice have increased levels of TNF-α and CCL2 , whereas treating isolated peritoneal macrophages with exogenous adiponectin results in increased expression of IL10 and reduced TNF-α and CCL2 (Ohashi et al. 2010). The previous chapter demonstrated potential increases in adiponectin gene expression, which could contribute towards an anti-inflammatory phenotype. Adiponectin is secreted and has numerous effects in other tissues including skeletal muscle and the cardiovascular system (Dadson et al. 2011), which have not been examined in this thesis. Conversely, leptin is considered a pro-inflammatory (Ikuni et al. 2008), and vice versa, Il-1β and TNF-α appear able to increase leptin expression, creating a loop whereby inflammation can be up-regulated greatly in response to leptin. In the previous chapter, we demonstrated a significant reduction in circulating leptin, without an overall change in adipocyte leptin when associated with adipocyte size.

Therefore, any reduction in pro-inflammatory effects mediated from leptin may also arise out-with adipose tissue.

Of the pro-inflammatory genes analysed, TNF-α was the one which was most clearly changed, which is consistent with a number of the other studies we have performed previously, that have shown reducing BACE1 or BACE1 activity decreases gene expression (unpublished observations). TNF- α induces the NFκB transcription factor, and is itself known to up-regulate BACE1 expression (Chen et al. 2012a). NFκB regulates a huge number of inflammatory response cytokines and chemokines, and similarly to the method described above for leptin, it may be possible that increased BACE1 may in turn increase TNF-α, and reducing BACE1 could have opposing effects. In ex vivo human adipose tissue, inhibiting NFκB significantly reduces TNF-α secretion (Harte et al. 2013). Therefore, it may be interesting to examine NFκB signalling in the adipose tissue of the BACE1 AdKO mice. NFκB signalling is highly pleiotropic, and can have both pro and anti-inflammatory effects (Lawrence 2009), and can be activated via a canonical pathway (in the case of TNF-α), or an alternative pathway by other factors. The canonical pathway leads to the phosphorylation and subsequent activation of the RelA subunit, which may be the best protein to examine downstream of NFκB.

Given there was also a significant increase in the anti-inflammatory IL10 in the eWAT of BACE1 AdKO mice, but no change in any chemoattractant markers, it does appear that any BACE1 role in adipocyte inflammation may be a localised effect, and this could explain why there were smaller changes observed in this mouse compared to the BACE1$^{-/-}$ mouse. Isolating adipocytes cytokine levels- particularly TNF-α and IL10 may be able to more fully establish this, and the potential mechanisms involved.

There is, then, a disparity between global BACE1$^{-/-}$ mice, which are protected from excessive inflammation in HFD models and BACE1 AdKO mice, or mice with BACE1 removed from myeloid cells, which are not. A potential explanation for this discrepancy could be that the BACE1

inflammatory phenotypes are centrally driven. Both the sympathetic and parasympathetic nervous system are involved in modulating inflammatory response (Chobanyan-Jürgens & Jordan 2015). One recent study has demonstrated a central mechanism which is important in modulating TNF-α resident macrophages in adipose tissue. Injection of AgRP, which suppresses sympathetic nervous activity, into the neurons of mice raises TNF-α mRNA levels in eWAT of lean mice, and this effect is lost in mice lacking β-adrenoreceptors (Tang et al. 2015). Furthermore, mice lacking the melanocortin 3 receptor, which are inhibited by AgRP, exhibit reduced TNF-α and MCP1 when fed a HFD compared to WT controls (Ellacott et al. 2007). Recent work from our lab has demonstrated a significant amount of BACE1 is present in NPY positive neurons in the hindbrain, and in close apposition to NPY neurons in the hypothalamus (Jalicy 2015), which co-localises with AgRP (Broberger et al. 1998). Thus, central, and particularly the hypothalamic and hindbrain neurocircuitry could be important in adipocyte immune cell function. It would be interesting to examine the inflammatory profile of mice with BACE1 conditionally removed from hypothalamic cells.

4.3.4 Summary

In conclusion, the data presented in this chapter demonstrates that removal of BACE1 from adipocytes is unlikely to significantly reduce the infiltration of macrophages, or other immune cells into WAT. However, there does appear to be a potential local effect in eWAT, with slight reductions in pro inflammatory cytokines and slight increases in anti-inflammatory cytokines. Therefore, it seems likely that targeting BACE1 centrally or peripherally may still be capable of reducing inflammation, but the mechanism behind any such phenotype does not stem entirely from the adipocytes. Consequently, further work is required to properly establish the role BACE1 has to play in modulating inflammation.

Chapter 5 - The role of Peripheral infusion of $A\beta_{1-42}$ in Energy Homeostasis and Insulin Sensitivity

5.1 Introduction

In the previous chapters, we have demonstrated that peripheral BACE1, and, in particular, adipocyte BACE1, may play an important role in modulating both energy metabolism and inflammation, particularly within the context of a HFD. Despite this, mechanisms surrounding these phenotypes are not clear, although the links between metabolic function and AD suggest that at least some of these mechanisms may be common to both diseases. Indeed, insulin resistance is known to be a significant risk factor for the development of AD.

By far the best studied substrate of BACE1 is APP, which is cleaved by BACE1 and ultimately results in the formation of Aβ fragments, which can oligomerize and eventually form Aβ plaques. One theory that has been put forward is that Aβ plaques themselves may also play a role in the development of metabolic dysfunction and insulin resistance. Indeed, neuronal plaques have been associated with a number of measures of insulin sensitivity, including raised fasting insulin and HOMA-IR in human AD brains (Matsuzaki et al. 2010). It has been postulated that Aβ oligomers may be responsible for impaired insulin sensitivity. Indeed, injection of just 10pM Aβ oligomers into the hypothalamus of mice induces muscle insulin resistance and increased hypothalamic and WAT inflammation (Julia R Clarke et al. 2015), suggesting they may be able to modulate both central and peripheral insulin resistance.

APP is expressed not only in the brain but also in numerous peripheral tissues, which raises the possibility that APP processing and Aβ production in peripheral tissues may still be responsible for the phenotypes we have observed. There is evidence that APP increases in adipose tissue in obesity in both mice (Puig et al. 2012) and humans (Lee et al. 2008). Furthermore, our lab, and others (Maesako et al. 2015), have shown that HFD drives increased BACE1 activity and increased Aβ, particularly the $A\beta_{1-42}$ species, both within the brain, within peripheral tissues and within the circulating plasma. In subcutaneous WAT, APP levels and isoform levels are raised in mice fed a HFD, and may result in

increased Aβ deposition (Min et al. 2017). Hyperglycaemia has been shown to raise Aβ levels in the hippocampus (Macauley et al. 2015) and in human endothelial cells (Chao et al. 2016), and it has been suggested that this may contribute towards increased barrier permeability as seen in diabetes. Finally, in human adipocytes, both glucose and insulin lead to raised secretion of Aβ, alongside reduced phosphorylation of the insulin signalling molecules IRS2 and phosphorylated PKB (Tharp et al. 2016).

However, BACE1 is a highly promiscuous enzyme, with a large number of substrates identified (Hemming et al. 2009). The majority of substrates are type I transmembrane proteins, with a large number expressed within the brain. Some peripheral BACE1 substrates have been identified though, for example the highly expressed in liver tissue alpha 2,6-sialyltransferase (Kitazume et al. 2005). This provides evidence that not all peripheral BACE1 activity is dependent on the availability of APP as a substrate, and thus demonstrates that APP processing, and therefore Aβ may not necessarily be the key component in modulating energy metabolism peripherally.

Insulin signalling is, of course, a key component in energy homeostasis, but is also associated with AD, and has been proposed to be an important link between T2DM and AD. Indeed, T2DM and insulin resistance are risk factors for the development of AD. AD is associated with impaired insulin signalling in the brain (Liu et al. 2011). Levels of IRS1 and IRS2 are reduced in AD patients compared to control (Moloney et al. 2010), suggesting increased insulin resistance in AD brains. Aβ species themselves may compete with insulin to bind to the insulin receptor, as it has been demonstrated that Aβ treatment limits autophosphorylation of the insulin receptor in response to insulin stimulation (Xie et al. 2002). Furthermore, Aβ treatment prevents the association of PDK1 with PKB, thus impairing insulin signalling, in three separate cells lines- C2C12 myotubes, SHSY5Y neuronal cells and HEK293 cells (H.-K. Lee et al. 2009). Insulin signalling usually plays a role in de-activating GSK3. Dysregulated GSK-3 has been implicated in T2DM and AD.

Overexpression of GSK3 not only limits insulin-dependent glucose uptake (Henriksen & Dokken 2006), and in AD over-expression of GSK3 in neurons results in increased levels of hyper-phosphorylated tau, which is associated with neuronal degeneration (Lucas et al. 2001). Finally, it has been shown that IDE also degrades Aβ species, with over-expression of IDE resulting in decreased levels of Aβ in mammalian cells (Vekrellis et al. 2000). Reducing IDE activity results in hyperinsulinemia and Aβ accumulation (Farris et al. 2003). Therefore, insulin and Aβ compete for IDE, which can lead to high levels of both in AD patients.

Insulin is also linked to cognitive decline, which is the main symptom in AD, as depletion of insulin with streptozotocin impairs rat performance in water maze tasks, with decreases hippocampal LTP (Biessels et al. 1998). Streptozotocin also destroys pancreatic beta cells, and is commonly used as a type 1 diabetes model. If administered centrally, streptozotocin induces AD-like symptoms, with impaired brain insulin sensitivity and sporadic Aβ plaque formation (Kamat 2015).

APP/PS1 mice, which overexpress human APP and produce $A\beta_{1-42}$ preferentially over the less toxic forms such as $A\beta_{1-40}$ have impaired glucose and insulin tolerance (Macklin et al. 2017) in an age dependent manner, before the appearance of amyloid plaques. We have previously shown that central infusion of $A\beta_{1-42}$ is able to exacerbate HFD induced weight gain (Meakin et al. 2018), and is also associated with impaired glucose disposal and reduced insulin sensitivity, measured peripherally (unpublished observations; see figure 5.1A-C). This effect appears to mainly stem from hypothalamic Aβ action, as the perturbations of energy homeostasis are also accompanied with diminished hypothalamic leptin sensitivity, however, we also detected raised levels of circulating $A\beta_{1-42}$ in the plasma of mice centrally infused with $A\beta_{1-42}$ (Figure 5.1D). This means we cannot discount the possibility that it is instead peripheral $A\beta_{1-42}$ that is responsible for some of these observations.

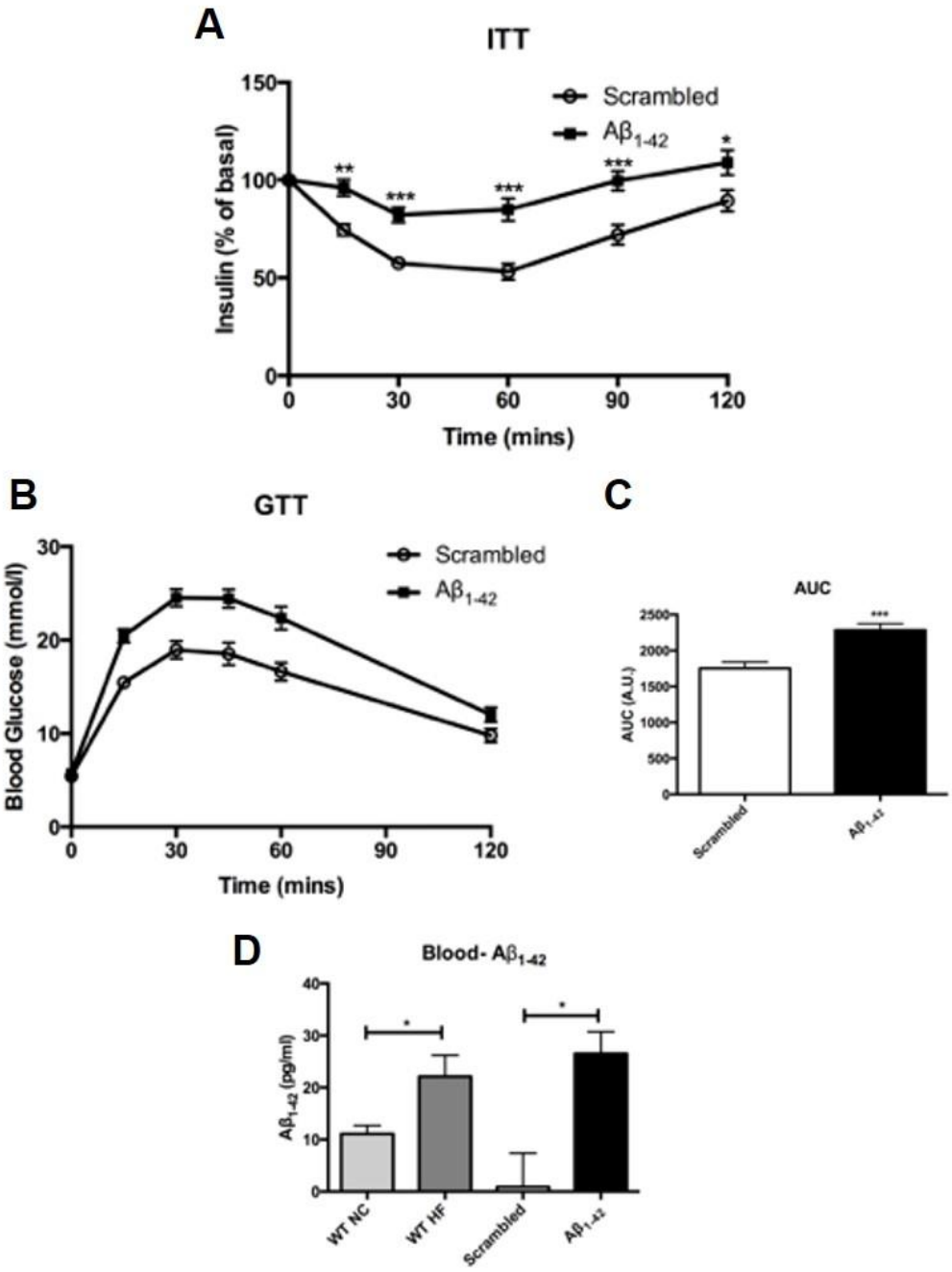

Figure 5.1 Central infusion of $A\beta_{1-42}$ increases body weight, and worsens glucose homeostasis

Mice were fed a HFD and centrally infused with $A\beta_{1-42}$ or scrambled peptide for 6 weeks **(A)** After 5 weeks of infusion, insulin sensitivity was significantly impaired in $A\beta_{1-42}$, (n=15-17) as was **(B)** glucose disposal, as quantified by measuring **(C)** AUC (n=16-17) **(D)** However, circulating levels of $A\beta_{1-42}$ were raised in the blood, to levels similar to those seen in WT mice fed a HFD (n=8-10)

*p<0.05, **p<0.01, ***p<0.001

All data presented were collected and analysed by Dr. Paul Meakin and Dr. Susan Jalicy

Aβ is produced by many peripheral tissues. Platelets are thought to contribute the majority of plasma Aβ (Chen et al. 1995), although some of the plasma Aβ pool arises from Aβ produced in other tissues, perhaps most notably the insulin sensitive liver and muscle (Alex E. Roher et al. 2009).

Therefore, in this chapter, results from experiments are presented in which we peripherally infused WT c57/bl6 mice on a HFD background with either $A\beta_{1-42}$ or scrambled peptide as a control and assessed body weight and composition, glucose and insulin homeostasis and food intake. Further to this, we stimulated mice prior to sacrifice with insulin or a PBS vehicle control to establish the response of peripheral insulin sensitive tissues- muscle, liver, eWAT and iWAT. Through this, we aimed to assess the hypothesis that peripheral APP processing, and subsequently raised peripheral $A\beta_{1-42}$ is important in modulating energy homeostasis in mice. We theorised that infusion of $A\beta_{1-42}$ would exacerbate high fat feeding induced body weight gain and further impair insulin and glucose tolerance, with a reduction in insulin signalling in response to an acute dose of insulin.

5.2 Results

WT mice were placed onto a HFD (40% by energy) for 4 weeks prior to surgery. On the day before undergoing surgery body composition was assessed. An osmotic minipump was inserted to infuse either amyloid β_{1-42} ($A\beta_{1-42}$) or scrambled peptide control (Scr.) for a period of 7 weeks (49 days), during which mice were retained on the HFD. After surgery body weight and food intake was recorded daily, and insulin and glucose tolerance 28 and 35 days post- surgery respectively. Prior to sacrifice body composition was again determined. This protocol is summarised in figure 5.2 below.

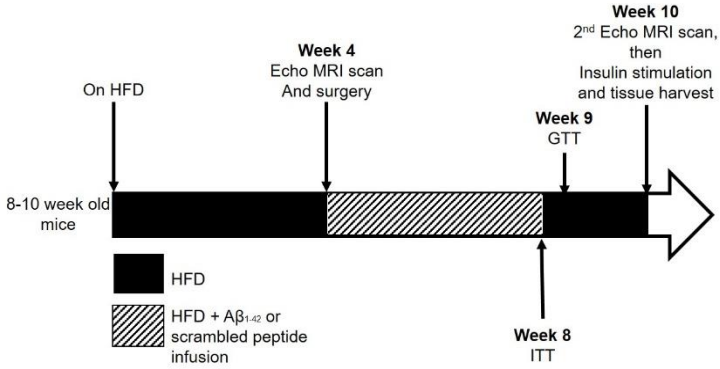

Figure 5.2 Protocol for the peripheral $A\beta_{1-42}$ infusion study

$A\beta_{1-42}$ was implanted after 4 weeks HFD, which was then continuously infused for 4 weeks for technical reasons. Following this no further $A\beta_{1-42}$ was infused, but remained in the circulation

5.2.1 Peripheral Infusion of $A\beta_{1-42}$ increases body weight but does not alter overall body composition

Firstly, the body weight and weight gain of mice infused with $A\beta_{1-42}$ was assessed compared to scrambled infused controls. We matched starting body weights between the 2 groups (Figure 5.3A- Scr. 33.00 $\pm$ 1.16g vs $A\beta_{1-42}$ 33.03 $\pm$ 0.95g, n=9-10; p=0.98) to prevent any potential for bias. Over the course of the experiment, when expressed as a percentage of starting body weight, $A\beta_{1-42}$ mice gained significantly more weight than scrambled control (figure 5.3B- Scr. 9.44 $\pm$ 1.91% vs $A\beta_{1-42}$ 17.27 $\pm$ 1.78%, n=9; p=0.009). To see if this could have been due to an increase in food intake, data from the first 2 weeks of the study was removed to ensure the mice had sufficient time to recover from surgery. Nevertheless, the average daily food intake over the experimental period was unchanged (Figure 5.4B- Scr. 2.87 $\pm$ 0.09g vs $A\beta_{1-42}$ 2.85 $\pm$ 0.15g, n=9; p=0.90).

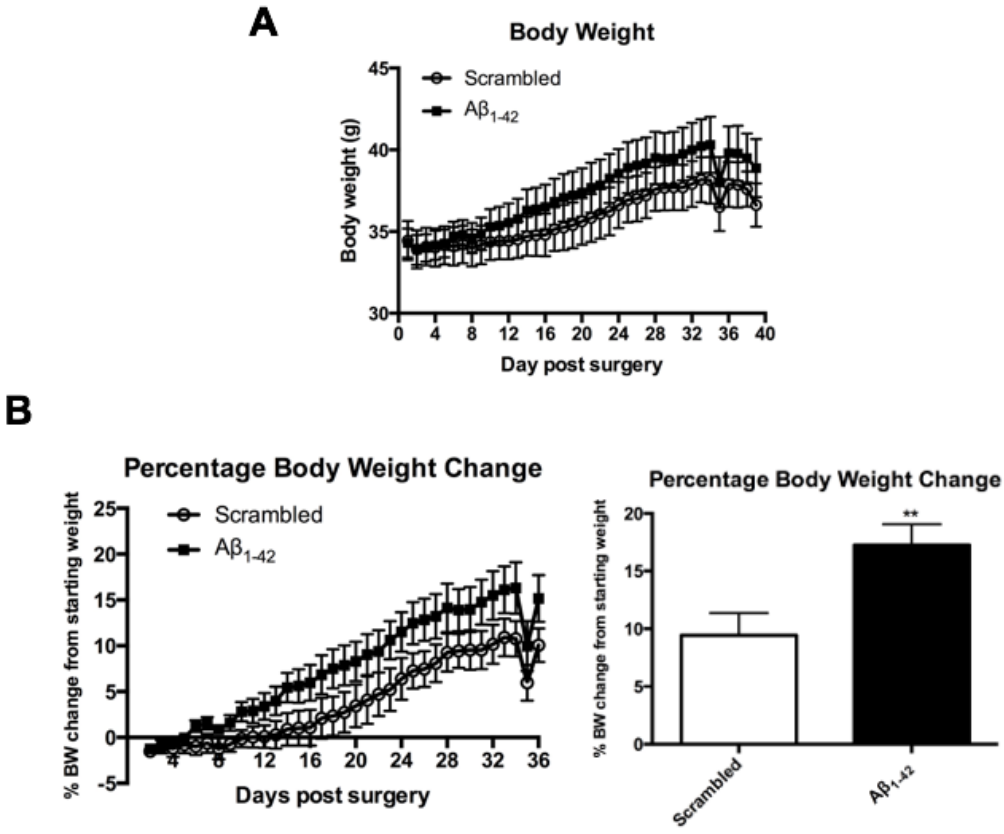

Figure 5.3 Peripheral infusion of $A\beta_{1-42}$ increases body weight

Mice were fed a HFD for 4 weeks prior to surgery, where a subcutaneous minipump was inserted and either $A\beta_{1-42}$ or scrambled peptide was infused for 6 weeks, with body weight measured daily. **(A)** Raw body weight of mice fed HFD post-surgery **(B)** Body weight change assessed as a percentage weight change was significantly higher in mice infused with $A\beta_{1-42}$ vs scrambled peptide.
n=9-10; **P<0.01

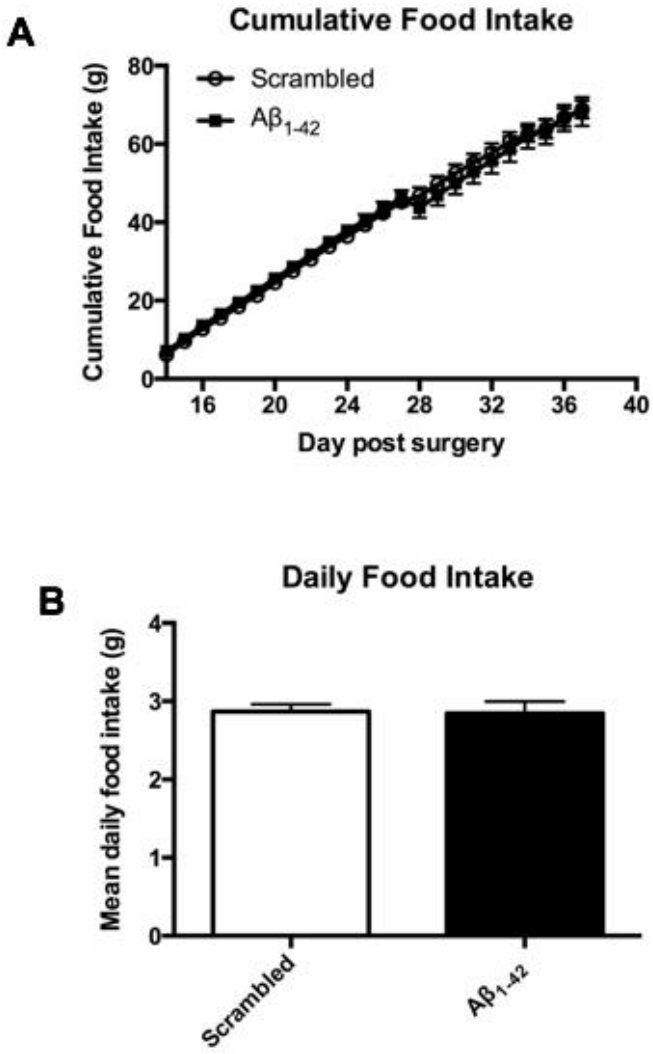

Figure 5.4 Peripheral infusion of $A\beta_{1-42}$ does not alter food intake

Mice were fed a HFD for 4 weeks prior to surgery, where a subcutaneous minipump was inserted and either $A\beta_{1-42}$ or scrambled peptide was infused for 6 weeks, with food intake measured daily. **(A)** Cumulative food intake of mice from 14 days post-surgery onwards and **(B)** Mean daily food intake of mice from 14 days post-surgery onwards show no significant differences between groups

n=9

The EchoMRI machine was utilised to assess body composition. Prior to surgery, as expected, there were no significant differences in fat mass when calculated as a percentage of total body mass. Equally, there was no significant increase in fat mass in either group after 6 weeks of infusion (Figure 5.5A). Likewise, there was no significant alteration in lean mass (Figure 5.5B). As leptin is secreted from adipocytes and is highly associated with changes in energy metabolism we assessed the level of circulating leptin in the plasma of the mice. Although there was a trend towards an increase in plasma leptin in $A\beta_{1-42}$ mice this was not significant (Figure 5.5C- Scr. 14.51 $\pm$ 3.17nM vs $A\beta_{1-42}$ 20.20 $\pm$ 5.00nM n=9-10; p=0.36). Overall, these data suggest that peripheral infusion of $A\beta_{1-42}$ induces a similar weight gain in mice fed a HFD in comparison to mice centrally infused with the peptide, but does not alter body composition.

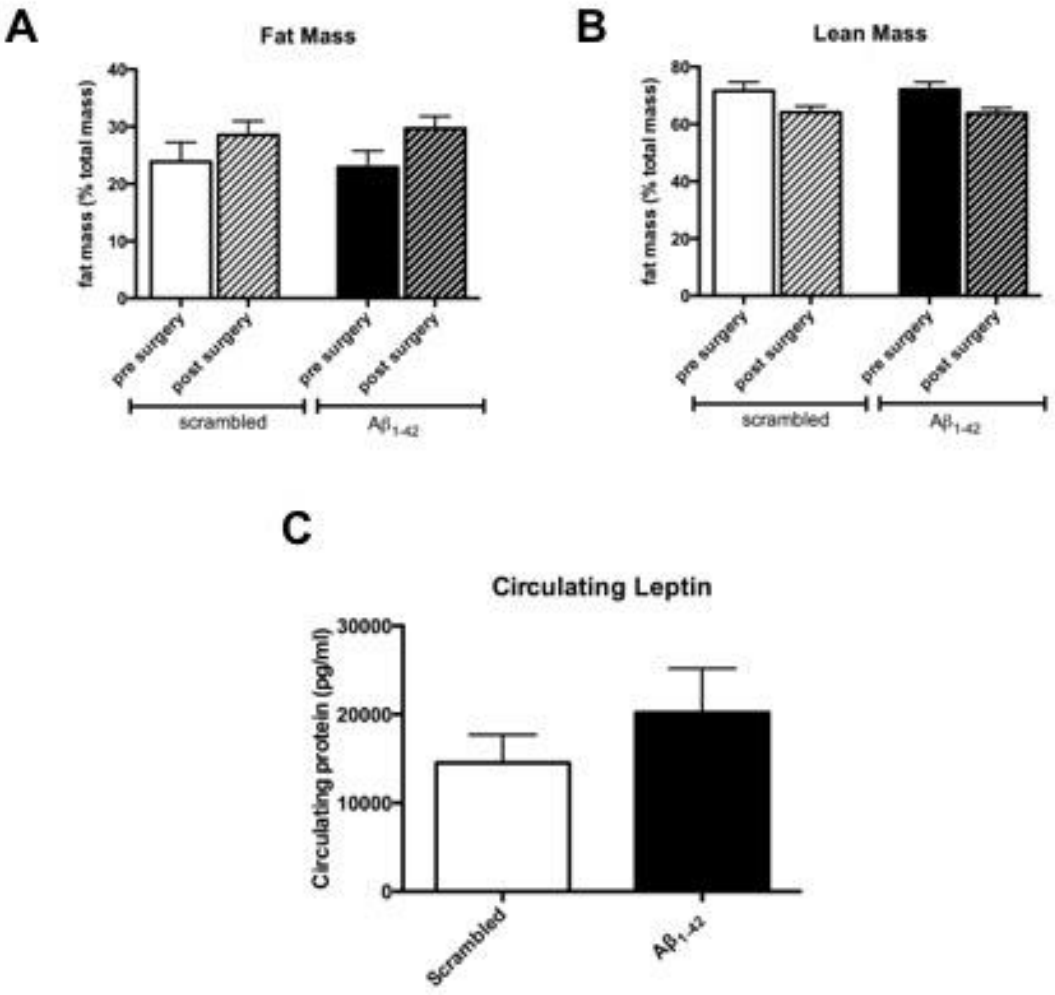

Figure 5.5 Peripheral infusion of $A\beta_{1-42}$ does not affect body composition or levels of circulating leptin

Mice were placed in the EchoMRI machine to assess body composition before surgery and at the end of the study **(A)** Fat mass and **(B)** lean mass were both unchanged between groups, both before and after surgery was performed (n=9-10). **(C)** Levels of serum leptin were measured at the conclusion of the study, and are unaltered by infusion of $A\beta_{1-42}$ (n=8)

5.2.2 Peripheral Infusion of $A\beta_{1-42}$ does not influence glucose or insulin sensitivity

As there was an increase in body weight, the next aim was to assess whether glucose disposal/homeostasis or insulin sensitivity were altered by peripheral infusion of $A\beta_{1-42}$, as our lab data has previously demonstrated was the case in centrally infused mice. Following an overnight fast (around 16 hours), there was no overall change in glucose disposal in response to an acute dose of glucose (Figure 5.6A) as quantified by AUC. Likewise, fasting blood glucose remained unchanged (Figure 5.6B).

There was also no change in insulin sensitivity, as assessed by an insulin tolerance test following a four hour fast (Figure 5.6C). Taken together, these results indicate that, at least in the initial experiments performed herein, peripheral infusion of $A\beta_{1-42}$ is not sufficient to induce metabolic deficits, even on a HFD background, in contrast to the outcomes observed with centrally infused $A\beta_{1-42}$.

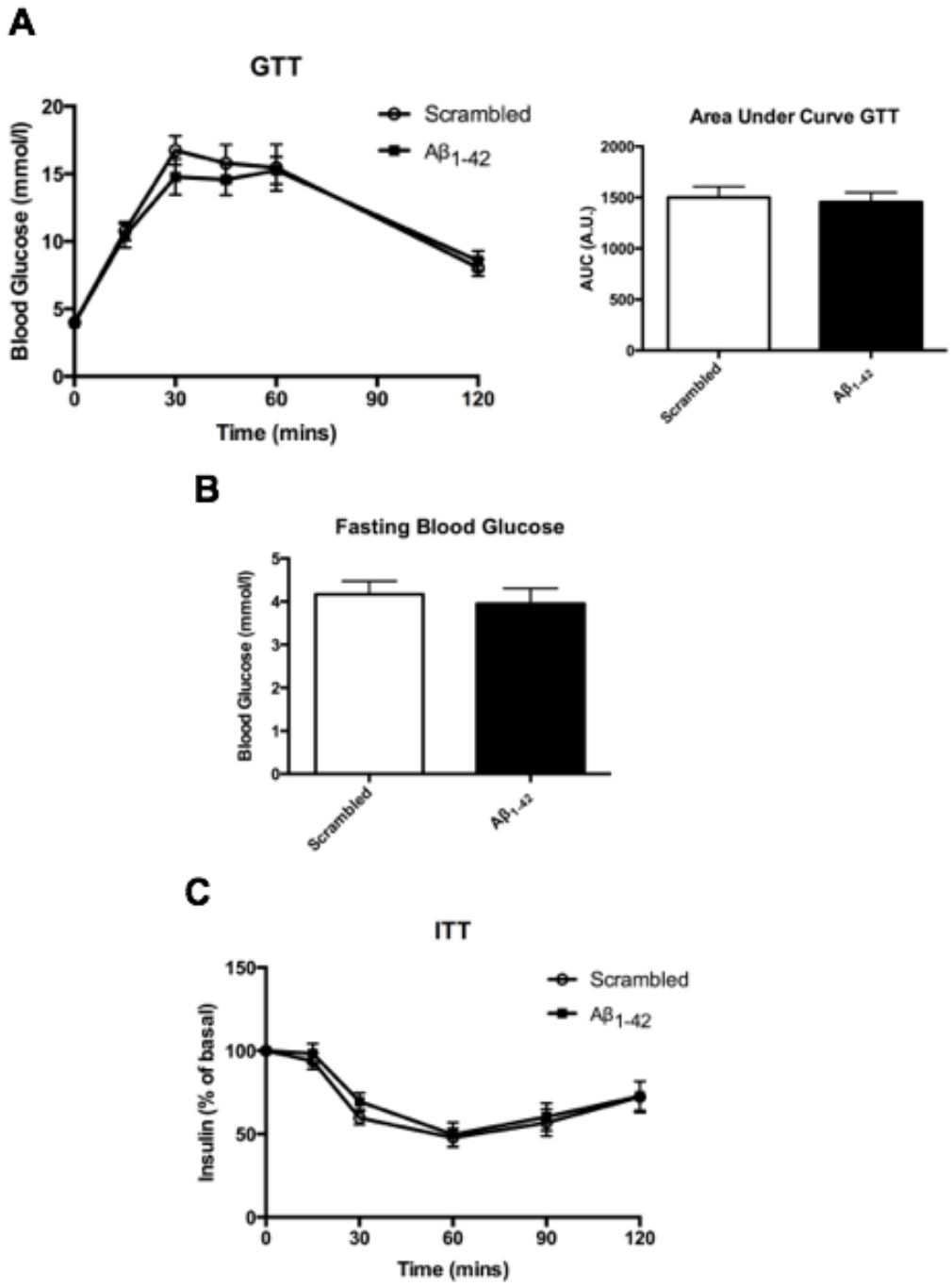

Figure 5.6 Peripheral infusion of $A\beta_{1-42}$ does not alter glucose tolerance or insulin sensitivity

An ITT and GTT was performed 5 and 6 weeks after surgery respectively to assess glucose homeostasis **(A)** Glucose tolerance test quantified by area under the curve revealed no change in glucose disposal or **(B)** fasting glucose levels. **(C)** Insulin sensitivity was also unchanged by infusion of $A\beta_{1-42}$

n=9-10

5.2.3 Peripheral Infusion of $A\beta_{1-42}$ does not influence acute insulin signalling

Although the tolerance test data suggested that overall insulin sensitivity was not altered by the infusion, it was possible that an acute pharmacological dose of insulin would affect insulin signalling. To investigate this, mice were injected with either insulin (3U/kg in PBS) or vehicle (PBS) i.p. for 5 minutes prior to sacrifice. Levels of phosphorylated PKB relative to total protein were assessed, as a read-out of insulin sensitivity in the key tissues- muscle, liver, subcutaneous inguinal WAT (iWAT) and visceral epididymal WAT (eWAT).

Within muscle, insulin increased levels of phosphorylation as expected in insulin stimulated mice, whilst levels of total PKB were unchanged (Figure 5.7A). The ratio of phosphorylated PKB to total PKB was, again, as expected, raised in insulin stimulated mice compared to PBS in both scrambled (Figure 5.7B- PBS 1.00 $\pm$ 0.31 vs Ins 6.00 $\pm$ 0.59, n=4-6; p=0.003) and $A\beta_{1-42}$ (PBS 0.46 $\pm$ 0.10 vs Ins 7.51 $\pm$ 1.00, n=4-6; p=0.003). Interestingly, $A\beta_{1-42}$ mice stimulated with vehicle had significantly reduced ratio of phosphorylated to total PKB compared to scrambled treated mice (Scr PBS 1.00 $\pm$ 0.31 vs Scr Ins 0.46 $\pm$ 0.10, n=4-6; p=0.01), which suggests that basal insulin signalling may be attenuated by $A\beta_{1-42}$ infusion. There was no significant difference in phosphorylation levels between scrambled and $A\beta_{1-42}$ infused mice when infused with insulin.

Similarly, in the liver tissue analysed, insulin increased levels of phosphorylation in insulin stimulated mice (Figure 5.8A), whilst levels of total PKB were unchanged (Figure 5.8A). The ratio of phosphorylated PKB to total PKB was, again, as expected, raised in insulin stimulated mice compared to PBS in both scrambled (Figure 5.8B- PBS 1.00 $\pm$ 0.32 vs Ins 4.50 $\pm$ 0.38, n=4-6; p=0.003) and $A\beta_{1-42}$ (PBS 0.71 $\pm$ 0.24 vs Ins 5.13 $\pm$ 0.14, n=4-5; p=<0.0001). There was no significant difference in phosphorylation levels between scrambled and $A\beta_{1-42}$ infused mice when infused with insulin, or in basal levels of p-PKB.

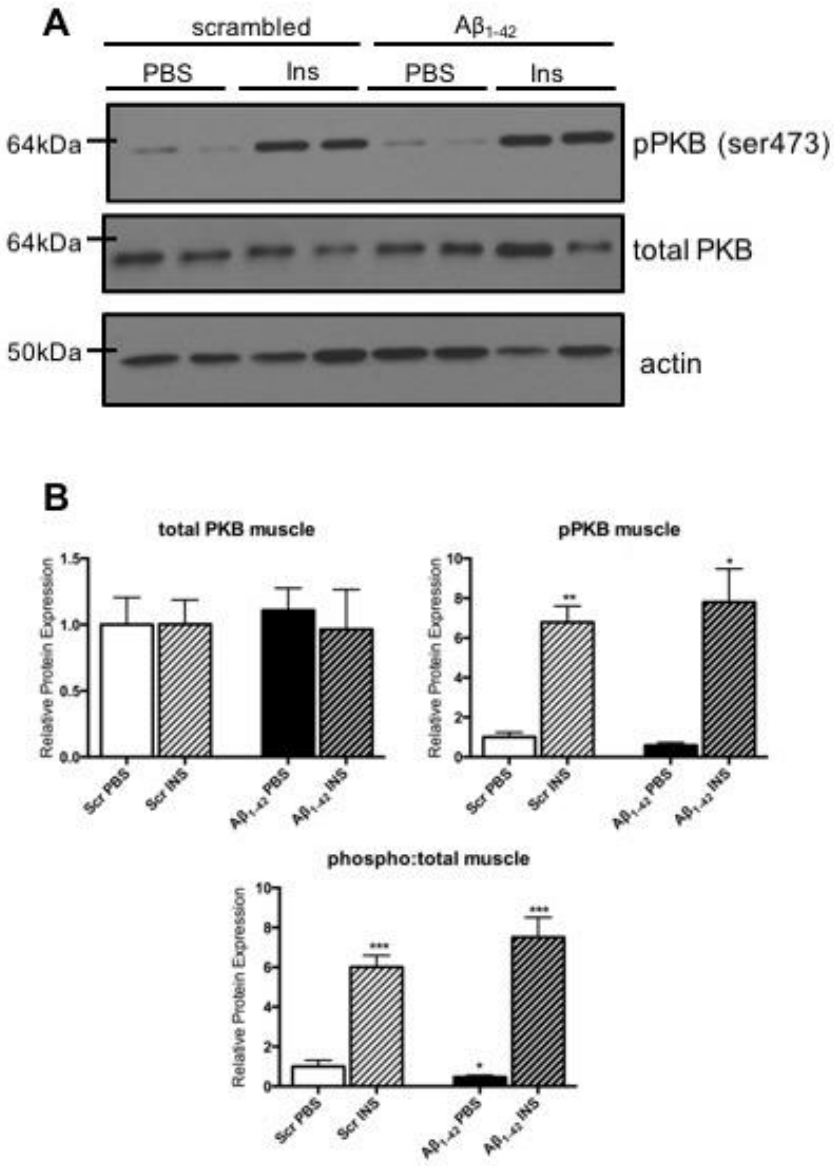

Figure 5.7 Peripheral infusion of Aβ1-42 does not alter phosphorylation levels of PKB within the muscle

Following 6 weeks of infusion with either scrambled peptide or $A\beta_{1-42}$, mice were stimulated with either 3U/kg insulin or PBS, and the gastrocnemius muscle excised after 5 minutes **(A)** Western blot images of phosphorylated and total PKB with actin as a loading control**. (B)** Quantification of the blots show no significant change in the ratio of phosphorylated to total PKB between scrambled and $A\beta_{1-42}$ treated mice (n=4-6)

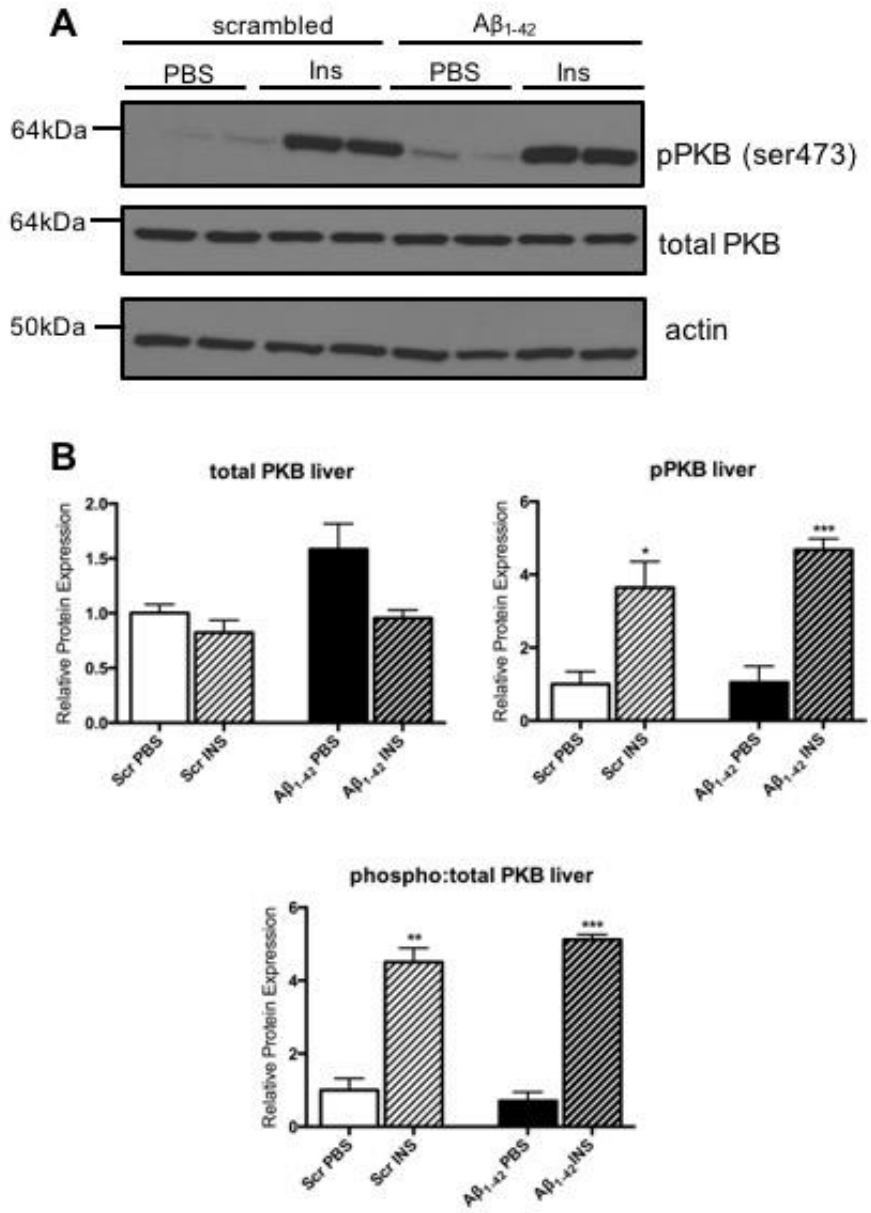

Figure 5.8 Peripheral infusion of Aβ1-42 does not alter phosphorylation levels of PKB within the liver

Following 6 weeks of infusion with either scrambled peptide or $A\beta_{1-42}$, mice were stimulated with either 3U/kg insulin or PBS, and the largest liver lobe excised after 5 minutes **(A)** Western blot images of phosphorylated and total PKB with actin as a loading control. **(B)** Quantification of the blots show no significant change in the ratio of phosphorylated to total PKB between scrambled and $A\beta_{1-42}$ treated mice (n=4-6)

Both subcutaneous and visceral fat depots were examined, as recent studies have suggested that both pads can contribute towards insulin resistance. We firstly examined eWAT, and once more found that insulin increased levels of phosphorylation in insulin stimulated mice, whilst levels of total PKB were unchanged (Figure 5.9A). The ratio of phosphorylated PKB to total PKB was, again, as expected, raised in insulin stimulated mice compared to PBS in both scrambled (Figure 5.9B- PBS 1.00 ± 0.30 vs Ins 7.84 ± 0.42, n=4-6; p=0.0005) and $A\beta_{1-42}$ (PBS1.29 ± 0.25 vs Ins 7.26 ± 0.52, n=4; p=0.001) There was no significant difference in phosphorylation levels between scrambled and $A\beta_{1-42}$ infused mice when infused with insulin.

Within iWAT the ratio of phosphorylated PKB to total PKB was, again, as expected, raised in insulin stimulated mice compared to PBS (Figure 5.10A) in both scrambled (Figure 5.10B- PBS 1.00 ± 0.30 vs Ins 4.80 ± 0.66, n=3-5; p=0.03) and $A\beta_{1-42}$ (PBS 0.97 ± 0.41 vs Ins 3.82 ± 0.07, n=4-5; p=<0.0001). There was no significant difference in phosphorylation levels between scrambled and $A\beta_{1-42}$ infused mice when infused with insulin.

These data indicate that peripheral infusion of $A\beta_{1-42}$ does not impact upon acute insulin stimulated PKB signalling.

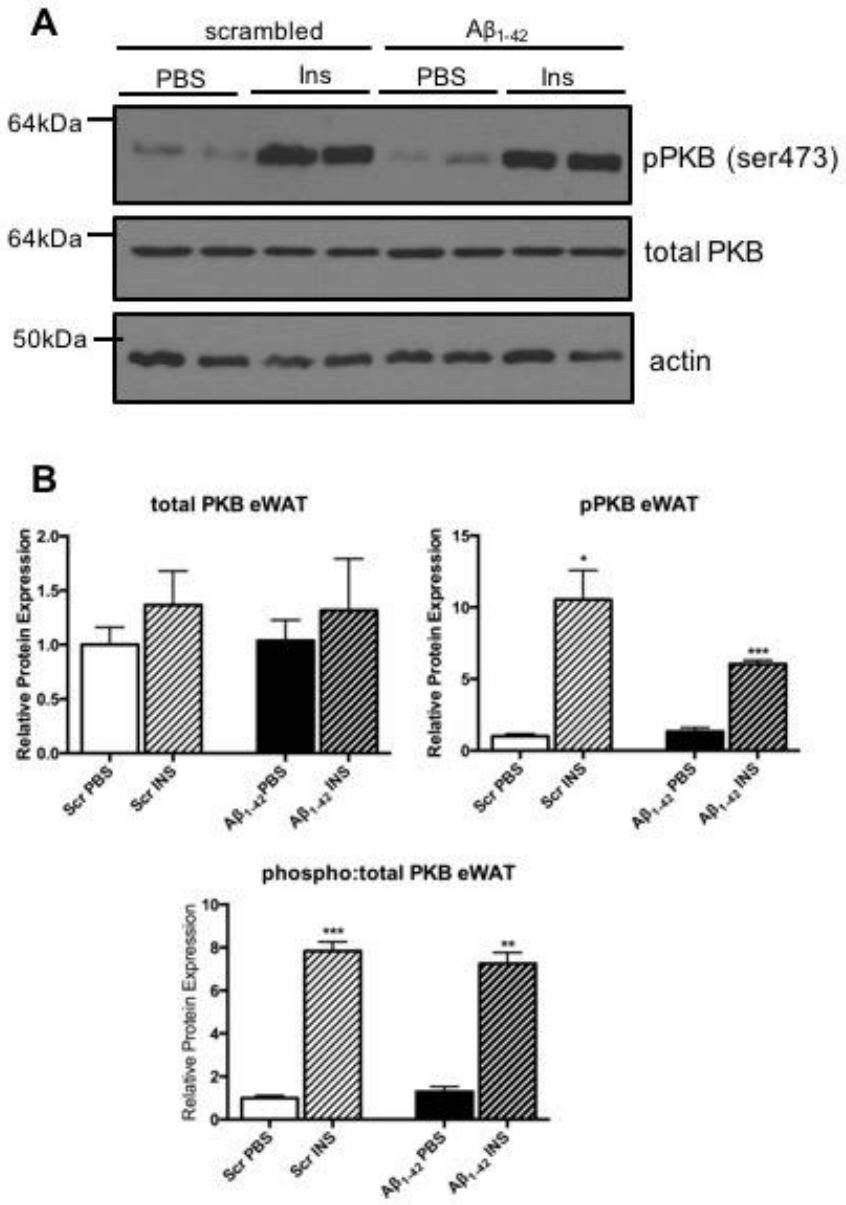

Figure 5.9 Peripheral infusion of Aβ$_{1-42}$ does not alter phosphorylation levels of PKB within the eWAT

Following 6 weeks of infusion with either scrambled peptide or Aβ$_{1-42}$, mice were stimulated with either 3U/kg insulin or PBS, and a epididymal WAT fat pad excised after 5 minutes **(A)** Western blot images of phosphorylated and total PKB with actin as a loading control**. (B)** Quantification of the blots show no significant change in the ratio of phosphorylated to total PKB between scrambled and Aβ$_{1-42}$ treated mice (n=4-6)

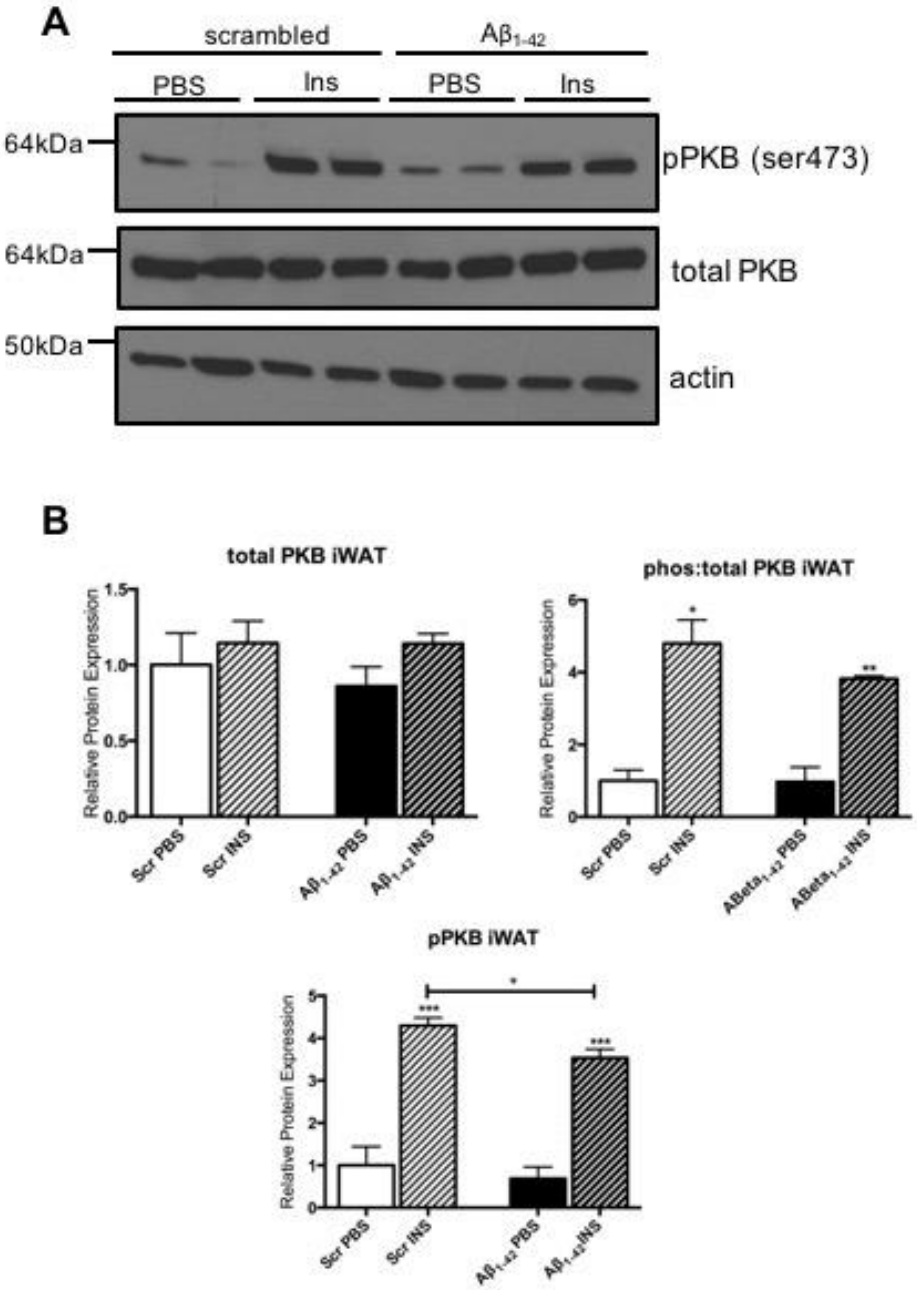

Figure 5.10 Peripheral infusion of Aβ$_{1-42}$ does not alter phosphorylation levels of PKB within the iWAT

Following 6 weeks of infusion with either scrambled peptide or Aβ$_{1-42}$, mice were stimulated with either 3U/kg insulin or PBS, and a single inguinal fat pad excised after 5 minutes **(A)** Western blot images of phosphorylated and total PKB with actin as a loading control. **(B)** Quantification of the blots show no significant change in the ratio of phosphorylated to total PKB between scrambled and Aβ$_{1-42}$ treated mice (n=3-5)

5.3 Discussion

5.3.1 The Role of $A\beta_{1-42}$ in modulating Glucose Homeostasis in Mice

In this chapter, we sought to assess the role of $A\beta_{1-42}$ in whole body energy metabolism. We have previously demonstrated that removal of BACE1 globally can reduce diet induced obesity in HFD fed mice, alongside improved glucose tolerance and insulin sensitivity. The best characterised BACE1 substrate is APP. Processing of APP gives rise to Aβ peptides, and there has been some evidence that $A\beta_{1-42}$ may be able to directly influence insulin sensitivity. Our lab have previously shown central infusion of $A\beta_{1-42}$, but not a scrambled version of this peptide can indeed worsen a diabetic phenotype in HFD fed mice (unpublished data), increase weight gain and diminish glucose disposal and peripheral insulin sensitivity, and that global KO of BACE1 reduces $A\beta_{1-42}$ centrally and peripherally, whilst being protective against the effects of a HFD (Meakin et al. 2012). These data therefore suggested that central infusion of $A\beta_{1-42}$, and central BACE1 activity, could be responsible for the energy homeostasis phenotypes observed in these two models. However, subsequent analysis of the $A\beta_{1-42}$ infused mice revealed increased $A\beta_{1-42}$ in the periphery, which suggested some leakage through the blood brain barrier (BBB), thereby giving rise to the potential that peripheral $A\beta_{1-42}$ could also be responsible for some of the phenotype. We therefore hypothesised that peripheral infusion of $A\beta_{1-42}$ would result in a worsened diabetic phenotype in mice fed a HFD compared to those infused with a scrambled peptide. However, we found that this was not the case, with no worsening of body composition, glucose or insulin tolerance, albeit with a significant increase in body weight.

Both groups of mice studied responded to the HFD as we have previously reported, although the $A\beta_{1-42}$ gained significantly more weight over the course of the 6 week study. Interestingly, this weight gain was similar to the weight gain of centrally infused mice. The most likely explanation for this phenotype would be that these mice ate more, however we did not find this to be the case. This is in keeping with other lab data, which has shown that reduction of BACE1 activity (Meakin, Harper, Hamilton, Gallagher, McNeilly, L. a Burgess, et al. 2012) and central infusion of $A\beta_{1-42}$ (Meakin

et al. 2018) also fails to impact upon food intake. This would suggest that there is instead a reduction of energy expenditure causing the difference in weight. It would be possible to measure physical activity, heat loss and energy expenditure using the CLAMs device discussed in previous chapters to see if this is the case, and this would be a useful addition to any future study. There was no significant alteration in fat mass between scrambled control and $A\beta_{1-42}$ mice. This might be because the 2nd Echo MRI scan was performed after a number of procedures had been performed, causing weight loss which may mask any differences in fat mass between groups. It may have been more representative to perform the post-surgery scan at an earlier time-point, after $A\beta_{1-42}$ had been allowed to infuse but prior to any other procedures. The fact that the body weight increase was similar to the centrally infused mice could also be indicative of leakage of the Aβ peptide through the blood brain barrier. Indeed, HFD is known to weaken the integrity of the BBB (Takechi et al. 2013). However, given there was no change in glucose homeostasis, which appears be a centrally mediated effect given the results of the labs previous study, this may not be the case. An alternative to this could be that leakage into the brain is limited to the hypothalamus, and other brain regions could be responsible for changes in glucose or insulin sensitivity Instead, the weight gain observed could be due to $A\beta_{1-42}$ altering a peripheral factor which influences weight gain. Leptin was the only such factor measured herein, but a plethora of other potential mediators could be responsible, such as gut hormones or other adipokines which are known to have brain specific functions (Fasshauer & Blüher 2015).

There were no observed differences in glucose or insulin tolerance, which suggests $A\beta_{1-42}$ is not an element that gives rise to impaired energy homeostasis in peripheral tissues. There are a number of possible explanations for this.

Firstly, it is possible that $A\beta_{1-42}$ dependent deficits in energy homeostasis are mediated through brain specific pathways. This is supported by the evidence discussed above which suggests central infusion of $A\beta_{1-42}$ can

indeed result in diminished insulin sensitivity and glucose disposal (unpublished observations). Furthermore, in mice which over-express BACE1 specifically in the forebrain- which also raises brain $A\beta_{1-42}$ levels (Plucińska et al. 2014), similar deficits are observed, with impaired glucose homeostasis and systemic diabetes alongside increased levels of the insulin receptor and PTP1B (Plucińska et al. 2016), indicative of an insulin resistant state- although this is not necessarily mediated through Aβ. The Tg2576 AD model mouse, which possesses a mutant form of APP known as the Swedish mutation, generates Aβ from approximately 6 months of age has been studied in this context previously. When fed a HFD, this mouse model gains body weight and has impaired peripheral insulin sensitivity after approximately 16 weeks of age (Kohjima et al. 2010), which is associated with increased $A\beta_{1-42}$ levels. Conversely, $hAPP_{swe}$ mice, which is a different mouse model that possesses the same mutation, do not appear to have diminished glucose or insulin sensitivity (Jalicy 2015) , albeit in this experiment the tests were performed at an earlier time point. This is an important consideration in the current study, too, as the mice were only on the HFD for 4 weeks prior to surgery, after which the peptide was infused for a further 6 weeks. It may be that deficits in glucose homeostasis would only occur after either longer on the HFD, or longer infusion of the peptide. Unfortunately, due to technical constraints with the minipump used in this experiment, it was not possible to infuse the peptides for longer periods of time.

Another study involving Tg2576 mice also found that Aβ correlated with reduced IR phosphorylation and decreased IDE activity (Ho et al. 2004), suggesting that Aβ may have been raised due to reduced clearance by IDE. Similarly, Clarke and colleagues recently demonstrated that icv injection of 10pM Aβ oligomers was able to induce peripheral metabolic deficits, with increased adipose tissue inflammation and reduced GLUT4 protein in the muscle, indicative of impaired insulin stimulated glucose uptake (J. R. Clarke et al. 2015). This group also showed that Aβ binds directly to neurons in the hypothalamus, and induced hypothalamic inflammation prior to the onset of metabolic dysfunction and thus

suggested that this inflammation goes on to drive the altered peripheral glucose homeostasis.

The second possibility is that, although peripheral APP processing can alter energy metabolism, it is not Aβ but another by-product upstream of Aβ that could cause this such as sAPPα or sAPPβ, or indeed the balance between these two which may be important. sAPPα is known to possess neuroprotective properties, and has been shown to protect synaptosomes from Aβ induced glucose uptake impairment (Mattson & Krauski 1998). Lab data has also shown that sAPPα can act as an insulin sensitiser peripherally in C2C12 muscle cells, promoting glucose uptake in these cells in a dose dependent manner, and increasing phosphorylation of PKB whereas sAPPβ had no effect on these processes (Hamilton et al. 2014). Specific inhibition of the α-secretase with batimastat significantly reduces glucose uptake (Hamilton et al. 2014). Given the structures of sAPPα and sAPPβ differ, with sAPPβ not suggested to have as many beneficial properties as sAPPα. sAPPα features an additional 16 amino acids, and has a crystal structure similar to some growth factors (Parker et al. 1999). Therefore, it is reasonable to conclude that it is downregulation of the non-amyloidogenic processing of APP rather than the upregulation of the amyloidogenic pathway, and thus raised Aβ that is the more relevant in promoting metabolic dysfunction. In agreement with this, central inhibition of ADAM10 worsens glucose homeostasis and insulin sensitivity *in vivo* (Jalicy 2015), although it remains to be established as to whether peripheral inhibition of ADAM10 could replicate this phenotype.

The final possibility is that although BACE1 is involved in modulating peripheral insulin sensitivity and glucose homeostasis, it is through processes other than APP processing that this occurs. As previously mentioned a number of alternative substrates have been identified and some could be involved in insulin signalling. Two groups have separately identified IGF2R (IGF receptor 2) as a BACE1 substrate (Hemming et al. 2009; Stützer et al. 2013). The main roles of this receptor revolve around transport of glycoproteins to lysosomes, but it has also been reported that

insulin exocytosis can be stimulated by IGF II binding to this receptor (Zhang et al. 1997). There may be a feedback process in which raised BACE1 limits this process by increasing the cleavage of IGF2R, which in itself is known to reduce the activity of IGF II (Zaina & Squire 1998).

Recently, we have shown in hepatocytes that BACE1, but not a mutated form of the substrate without enzymatic activity, is able to directly cleave the IR, thus preventing insulin signalling (Meakin et al, under review). This novel BACE1 substrate could represent a clear way in which BACE1 could alter insulin sensitivity in peripheral tissues. Within the brain, the IRA subunit isoform is more highly expressed than IRB, whereas IRB is more highly expressed in the periphery in tissues such as the muscle (Belfiore et al. 2009). This may be key, as we have also found that BACE1 more readily cleaves IRA over IRB containing receptors (Meakin et al, unpublished). As the mice infused with $A\beta_{1-42}$ were also placed on a HFD, which in itself will drive increased levels of BACE1 as well $A\beta_{1-42,}$ it will be necessary to replicate the studies in NC mice, or $BACE1^{-/-}$ mice to remove this as a potential confounding factor.

One potential driver of insulin resistance besides weight gain is increased inflammation, which is well established as a known inducer of metabolic dysfunction (Johnson & Olefsky 2013; Shoelson et al. 2006; Hotamisligil 2006). There is strong evidence that Aβ is capable of inducing inflammation itself. Aβ can cause human monocytes to differentiate into macrophages (Fiala et al. 1998) and increases the production of cytokines such as IL-6, IL-12 and TNF-α in a dose dependant manner. In cultured THP-1 cells, which are a human monocytic model, treatment with 10μM fibrillar Aβ was sufficient to increase both TNF-α and IL-1β at a gene and protein level (Yates et al. 2000), although as discussed in the following section, this concentration is likely to be significantly supraphysiological. Furthermore, in AD, significant toxicity is caused by inflammation arising from the microglia, which are brain resident macrophages, which is worsened by the higher Aβ loads in later stage disease (Hickman et al. 2008), so it may be

possible that artificially raising peripheral Aβ could increase pro-inflammatory processes and consequently go on to impair glucose homeostasis. As a result, it would be interesting to assess peripheral and hypothalamic inflammation in the mice studied here, although it has been reported that longer periods of high fat feeding may be necessary to induce inflammation (Cummins et al. 2014).

5.3.2 Potential role of $A\beta_{1-42}$ in Insulin Signalling

Previous studies have suggested a potential role of $A\beta_{1-42}$ in peripheral insulin signalling. In 2012, Zhang and colleagues showed that phosphorylation of the insulin receptor and the PKB was diminished in a time dependent manner by treating primary hepatocytes with $A\beta_{1-42,}$ which was shown to be through a JAK2/STAT3/SOCS1 signalling pathway (Zhang et al. 2012). This data was followed up not long later by the same group, who showed a similar effect in vivo by injecting $A\beta_{1-42}$ into mice twice daily. There was an observed diminishment of phosphorylated insulin receptor and PKB in response to a dose of insulin, alongside diminished insulin sensitivity (Zhang et al. 2013). We did not see similar results in the liver, or indeed any other insulin sensitive tissue, of our insulin injected mice. One possible explanation for this could be the relatively high doses of $A\beta_{1-42}$ used in the earlier studies. In the hepatocyte studies, cells were incubated with 10μM $A\beta_{1-42}$ and the mice in the latter paper were injected with 5μg/μl $A\beta_{1-42.}$ Other groups have previously shown that levels of $A\beta_{1-42}$ in the periphery in humans are on average 124pg/ml (Alex E Roher et al. 2009), and although these do increase in obese individuals, and indeed appear to correlate with BMI (Y.-H. Lee et al. 2009), they do not reach such high concentrations, which suggests that the changes observed may not be physiologically representative. Our infusions used a much lower dose in an attempt to artificially raise $A\beta_{1-42}$ levels to a concentration similar to those seen during chronic HFD at an earlier age. In contrast to this, as discussed earlier, our laboratory (Meakin et al. 2018) and others (J. R. Clarke et al. 2015) have demonstrated much lower doses can induced systemic phenotypes of impaired glucose homeostasis via the brain, which demonstrates that the brain is much more sensitive to Aβ than peripheral

tissues. If this is via the IR, then it may be due to the higher number of IRA containing receptors compared to the periphery or the presence of hybrids with IGFRs. Alternatively, it may be that other pathways such as the leptin signalling pathway are more important in modulating Aβ's effects. Existing data from the lab indicates impaired phosphorylation of STAT3 in the hypothalamus of centrally infused Aβ mice (Meakin et al. 2018), but the full molecular mechanism for this effect is yet to be elucidated. Many signalling pathways are shared between insulin and leptin, as discussed in chapter 1, thus further investigation into the interaction of Aβ with these pathways, for example by examining SOCS3 or PTP1B levels in the hypothalamus, is required.

It would be interesting to measure levels of $A\beta_{1-42}$ in the plasma and brain of the treated mice. As we found that $A\beta_{1-42}$ leaked through the BBB into the periphery in centrally infused mice it is important to check whether the converse is true of the peripherally infused mice. It may be that a small amount of leakage into the brain, and specifically the hypothalamus, may be responsible for the increased body weight observed in these experiments, for example. $A\beta_{1-42}$ is cleared across the BBB through the RAGE receptor (Deane et al. 2003), therefore to confirm that there is no leakage into the brain, it may be necessary to block this receptor pharmacologically at the same time as infusing $A\beta_{1-42,}$ to prevent this process from occurring and ensuring $A\beta_{1-42}$ is raised solely in the periphery, for example using the FPS-ZM1 compound (Yang et al. 2015).

Due to time constraints, in these experiments we have only analysed phosphorylation levels of PKB. As stated previously there are a large number of other sites which can be altered during insulin resistance. Although unlikely, as there are no obvious changes in whole body insulin sensitivity, it would be interesting to see if insulin signalling may be being effected either upstream or downstream of PKB, for example by measuring phosphorylation status of the IR itself.

In this study, we did not see a significant increase in circulating leptin, although levels on average were raised in the $A\beta_{1-42}$ group. It would be interesting to see if leptin sensitivity was altered, as recent lab data shows that central $A\beta_{1-42}$ treatment raises basal phosphorylation of STAT3, and reduced signal amplitude in response to acute doses of leptin independent of any increase in inflammation or ER stress, and indicative of leptin resistance. This was associated with raised levels of plasma leptin, and increased $A\beta_{1-42}$ in the periphery, so it is possible that there may be direct effects of peripheral $A\beta_{1-42}$ to raise leptin and subsequently promote leptin resistance in the hypothalamus. Indeed, treating cultured human adipocytes with a high dose of a short form of Aβ ($A\beta_{25-35}$) induces leptin secretion (Wan et al. 2015). It has been reported that leptin down regulates $A\beta_{1-42}$ in mouse neuroblastoma Neuro2a cells (Fewlass et al. 2004), This process appears to be dependent on BACE1 activity, as BACE1 activity appears reduced, specifically in lipid rafts, upon treatment with leptin (Fewlass et al. 2004). Interestingly, this group also reported that adipocytes from Tg2576 mice had a diminished capacity to express leptin in response to insulin, despite raised levels of APP (Fewlass et al. 2004), countering the data produced by Wan and colleagues as discussed earlier. It is therefore difficult to establish whether raised peripheral $A\beta_{1-42}$ influences leptin secretion by adipocytes or leptin resistance centrally. It may be beneficial to look more closely at leptin production and secretion by adipocytes treated with $A\beta_{1-42}$ compared to controls in future studies.

5.3.3 Summary

The data presented in this chapter strongly suggest that increased peripheral $A\beta_{1-42}$ is not capable of worsening an obese or diabetic phenotype in the context of a HFD in mice. There was no alteration in glucose or insulin sensitivity associated with peripheral infusion of $A\beta_{1-42}$, with a relatively minor increase in body weight. Putting this data together with previous data from our lab, and others, the most likely explanation is that $A\beta_{1-42}$ can drive metabolic dysfunction through altering hypothalamic insulin signalling, but has no direct effect on peripheral tissues, although it cannot be ruled out that longer term infusions may promote metabolic

dysfunction. As a result, reducing $A\beta_{1-42}$ levels in the periphery may not in itself be sufficient for preventing the onset of obesity and diabetes.

Chapter 6 - Final Discussion

6.0 Final Discussion

6.1 The role of BACE1 and APP processing in metabolic health

The UK population is an ageing one, and rates of dementia, and, in particular, AD are rising. In 2025, it is estimated that 1 million people in the UK will be living with dementia, which is predicted to double to 2 million by 2051 (Prince, M, Knapp, M et al. 2014). Similarly, rates of obesity and T2DM are rising alarmingly within the population, almost doubling in prevalence worldwide in the last 25 to 30 years (WHO 2014). T2DM is known to be a risk factor for the development of AD, and therefore particular emphasis has been placed in recent years on identifying potential common factors between the two diseases.

Attention has been paid to BACE1 as one potential link. BACE1 is the enzyme involved in the rate limiting step in the production of Aβ, which forms oligomers and plaques, and is thought to be causative in AD progression as part of the amyloid cascade hypothesis of AD (Hardy & Higgins 1992). BACE1 is upregulated by a number of cellular stresses, and in particular by HFD (Meakin, Harper, Hamilton, Gallagher, McNeilly, L. a Burgess, et al. 2012), hyperglycemia (Macauley et al. 2015) and fatty acids such as palmitate (Kim et al. 2017), which are all associated with T2DM and also drive increased production of Aβ.

Our lab generated BACE1$^{-/-}$ mice and found that they were protected against weight gain and perturbations in glucose homeostasis compared to WT mice, which in part appeared to be due to increased energy expenditure and increased expression of the thermogenic gene UCP1 (Meakin et al. 2012). Pharmacological inhibition of BACE1 activity replicates a number of these phenotypes (Jalicy 2015), and this effect occurs whether the drug is infused centrally or peripherally. Secreted levels of the adipokine leptin were reduced in these treated mice compared to WT mice on a HFD or mice injected with a control rather than the inhibitor.

Further to these findings, additional work within the lab has also demonstrated a role for centrally infused Aβ in diminishing hypothalamic

leptin sensitivity and worsening a diabetic phenotype (Meakin et al. 2018). These data all point towards a critical role for BACE1 and Aβ in modulating energy homeostasis. However, the mechanisms by which altered BACE1 activity and/or raised Aβ levels modify the metabolic phenotype of mice remained unclear, with the BACE1 inhibitor capable of accessing the brain even when administered peripherally, and Aβ peptide able to enter the blood when injected centrally.

The study presented here therefore aimed to further establish the role of BACE1 and Aβ, in modulating energy homeostasis, particularly focussing on mechanisms by which peripheral modulation of these factors may mediate an effect.

6.2 The Role of BACE1 in Adipocyte Function

The first approach in answering these questions was to remove BACE1 from adipocytes only. The data presented herein demonstrate that whole animal resistance to diet induced obesity and improved glucose homeostasis is associated with BACE1 protein reduction in both the iWAT and eWAT. In this study, due to the conditional mouse line used BACE1 is removed from adipocytes from birth. Given HFD drives increased BACE1 expression it is possible that metabolic defects associated with HFD are partly a consequence of increased BACE1 activity, and that therefore the present study merely prevents this from occurring rather than significantly improving metabolic health. To more precisely address this possibility, it would be necessary to use an alternative model. The best option would be to use a tamoxifen-inducible knock out model, in which BACE1 could be removed specifically from adipocytes upon injection of tamoxifen. This could be performed after 6 weeks of HFD, by which stage body weight is likely to have increased, with accompanying worsening of glucose homeostasis. It would be interesting to see if delayed removal of BACE1 from adipocytes could reduce body weight and improve glucose homeostasis, even if the HFD was maintained.

An important consideration in interpreting the results of the present studies are the differences between the two fat pads examined. Multiple studies have demonstrated key differences in the way visceral and subcutaneous fat pads respond to metabolic stress. Metabolic deficits are most associated with expansion of visceral over subcutaneous fat, with abdominal adiposity strongly associated with the development of T2DM in humans (Wang et al. 2005). Transplantation of subcutaneous fat to replace visceral fat improves glucose homeostasis and glucose uptake in obese mice (Tran et al. 2008). Further to this, subcutaneous and visceral depots have differences in their gene expression profiles, and a strong example of this is the increased level of PRDM16 in subcutaneous adipose tissue, which gives rise to the preferential beiging effect observed in subcutaneous fat over visceral fat (Ye et al. 2013). Conversely, the chronic inflammation and macrophage infiltration associated with obesity is particularly associated with visceral fat (Bruun et al. 2005; Fontana et al. 2007).

These observations are consistent with the idea that many of the outcomes associated with the BACE1 AdKO mouse could stem from the subcutaneous iWAT. There is little evidence for any reduction in macrophage infiltration in the eWAT, but browning is increased and fat pad size reduced in the iWAT, as discussed in chapter 3. One concern that this may lead to is that although leaner than their control counter-parts, the HF-fed BACE1 AdKO mice may be at least as metabolically unhealthy as the HF-fed control groups- a so called “unhealthy lean” state. This must be further tested for measures of adipocyte health, for example, direct measures of ER stress and apoptosis- such as caspase 8, bcl and bax (Alkhouri et al. 2009). Adipocyte vascularisation, and markers of adipose tissue expandability, such as the differentiation marker PPARγ in the eWAT of the BACE1 AdKO mouse could also be measured. Although adipocyte inflammation was not substantially altered by removal of adipocyte BACE1, systemic inflammation was not examined, and this could also be an informative step to take.

Another crucial element that differs depending on fat pad is sympathetic outflow. Siberian hamsters subjected to 16 hours of food deprivation raises norepinephrine turnover rate (NETO) in iWAT at a much greater rate than in mesenteric fat (Nguyen et al. 2014), which was used as the visceral fat pad in this study, indicative of a preferential increase in sympathetic drive to this tissue. The same group demonstrated fairly divergent sympathetic outputs to the visceral and subcutaneous fat pads using a viral tract tracer (Nguyen et al. 2014). Over a longer period of caloric restriction, Sipe and colleagues have recently shown switches between sympathetic outputs to the different fat pads to be a highly dynamic process. In the initial stages of weight loss, sympathetic drive to visceral adipose tissue is preferentially raised, but as time goes on, this declines and ultimately subcutaneous sympathetic drive is raised, which also drives lipolysis (Sipe et al. 2017). It would therefore be interesting to examine how NETO is changed in the iWAT and eWAT of BACE1 AdKO mice over time compared to control groups to see how sympathetic drive is altered, if at all, by removal of BACE1 from adipocytes. Other ways to measure this would include sympathectomy experiments by either physically cutting the nerves innervating the adipose depots or using a chemical approach to degrade sympathetic neurons- for example with 6-hydroxydopamine.

It is not clear how sympathetic drive is altered in a HFD scenario over significant time periods, but given the BACE1 AdKO mice eat the same amount of food as their heavier control counterparts and have increased energy expenditure, they could be described as exhibiting relative hyperphagia compared to controls. This would point towards neuronal circuitry changes being important in the mechanisms behind the phenotype.

6.3 Integrating Peripheral and Central Mechanisms

A key question which remains to be answered is how reduction of BACE1 in the adipocyte could have such a profound influence on whole body energy homeostasis. The study has provided some evidence that there may be localised adipocyte consequences when BACE1 is removed from

WAT, such as an increase in FGF21 signalling to promote raised GLUT1 mRNA and enhanced glucose uptake, and potentially the induction of a "beiging" effect, particularly of iWAT. However, there is also evidence of significant alteration in central signalling. The most obvious example is the highly upregulated β3 adrenergic receptor in the iWAT, which is indicative of increased activation of the sympathetic nervous system.

There is good evidence that adipokines can mediate energy homeostasis via central mechanisms. For example it has long been known that leptin acts via leptin receptors in the hypothalamus to influence energy homeostasis by activating POMC neurons and causing the release of α-MSH, an agonist of melanocortin receptors (Friedman & Halaas 1998). This activation increases energy expenditure. Separately leptin also inhibits the release of neuropeptide Y (NPY) and agouti related peptide (AgRP), which leads to a decrease in food intake (Friedman & Halaas 1998). This demonstrates the importance of linking peripheral to central mechanisms.

Both adiponectin receptors are expressed in the hypothalamus of rats, and particularly appear to co-localise with POMC and NPY neurons (Guillod-Maximin et al. 2009).

In the present study, there is initial evidence that adiponectin production may be increased in the BACE1 AdKO mice. This could be attributable to the increase in FGF21 signalling, which will result in an increase in adiponectin production, which is well known to exert a number of peripheral effects to improve insulin sensitivity (Lin et al. 2013; Whitehead et al. 2006). Lack of adipocyte BACE1 may directly influence this process, by preventing cleavage of β-klotho, a co-receptor vital for FGF21 signalling functionality. Thus, adiponectin may be released at increased levels by BACE1 AdKO adipocytes, and this may have central implications as well as peripheral. In agreement with this, centrally injected adiponectin appears to lower body weight, without alterations in food intake, and is accompanied by increased oxygen consumption (Qi et al. 2004), thus

bearing a striking resemblance to the BACE1 AdKO phenotype. Interestingly, it has recently been reported that adiponectin is able to depolarise leptin receptor positive POMC neurons, and causes a suppression of inhibitory inputs to POMC neurons (Sun et al. 2016), thus increasing overall excitation of the neurons. This effect appears to be additive to the effect of leptin alone, and is dependent on intact PI3K signalling (Sun et al. 2016). These data are in agreement with the previous study, which demonstrated increased UCP1 expression in BAT and oxygen consumption was greater in mice treated with both leptin and adiponectin, rather than with either adipokine alone (Qi et al. 2004).

To test the hypothesis that adiponectin may be acting centrally in the present studies, one approach would be to use adiponectin receptor antagonists, administered centrally in BACE1 AdKO mice and the control groups, to see if this would mitigate any of the improvements in glucose homeostasis in the HF-fed model. Another alternative could use an alternative conditional knock-out model to remove BACE1 from the hypothalamus to see if this alters sympathetic output.

6.4 Therapeutic Implications

There are currently very few effective pharmacological treatments for obesity. The NHS recommends weight loss measures such as improving diet and increasing exercise, and in some cases of morbid obesity performs bariatric surgery to reduce food intake by physically shrinking the stomach (with a gastric band) or by joining the top of the stomach to the start of the small intestine (a gastric bypass) (NHS 2016).

There are currently only a few drugs which have been made available specifically for the treatment of obesity. One example is orlistat, which is a gastrointestinal lipase inhibitor (Padwal & Majumdar 2007), and therefore works by preventing fat absorption. Another is rimonobant, which acts as an antagonist of CB-1 cannabinoid receptors, but has since been withdrawn due to the significant increased risk of psychiatric side effects such as depression, anxiety (Christensen et al. 2007) associated with the

drug. Another drug which had been made available was sibutramine, which acted to supress appetite but was ultimately withdrawn also, due to increased risk of cardiovascular side effects (Comerma-Steffensen et al. 2014). All three of these drugs were found to reduce body weight compared to placebo treated control patients in meta-analyses, but the effects were relatively modest. Orlistat, the only drug of the three still available, reduced body weight by an average of 2.9kg, the lowest of the three drugs included (Padwal et al. 2003).

Other compounds that have been associated with weight loss include lorcaserin, a serotonergic antagonist (Shukla et al. 2015) and GLP-1 analogues such as liraglutide, which also improves glycemic control (Marre et al. 2009). However many of these drugs are often prescribed for conditions such as T2DM, rather than for obesity, which often occurs prior to development of the disease. Metformin, for example, which is the first line therapy for treatment of T2DM, is reported to induce weight loss in pre-diabetic patients (Knowler et al. 2002), but is currently not used as an anti-obesity drug. Others are not currently approved for use within the UK. Therefore, there is a pressing need to identify new compounds and targets which could effectively reduce the onset of obesity without severe side effects.

Numerous BACE1 inhibitor clinical trials have been performed by drug companies (Vassar 2014), which have been generally targeted towards reducing production of Aβ and preventing the occurrence of plaques associated with AD. Some human studies, however have been abandoned. In 2013, a phase II clinical trial by Eli Lilly was halted early due to abnormal liver biochemistry (Eli Lilly 2013). More recently a more advanced study by Merck was abandoned at the phase II/III phase, due to lack of efficacy in treating patients with mild to moderate AD (Mullard 2017). One explanation for this could be that it does not help patients with AD as the plaques have already caused significant neuronal damage by the point of intervention, and to this end trials taking place at an earlier stage of disease and still underway (Mullard 2017). There is no publicly available

data as to the impact of these drugs on body weight in humans, although any such data may be misleading as weight loss is associated with early-stage AD in any case (Gillette-Guyonnet et al. 2000).

The cost of developing a new drug is immense, reaching hundreds of millions of dollars per drug (Morgan et al. 2011), and the process has a high failure rate. Finding new purposes to drugs which fail in their initial aims would therefore be a highly attractive prospect for any drug development company. The data shown in the present study suggests that using a BACE1 inhibitor to target BACE1 in adipocytes could be a beneficial approach to limit the progression of obesity. Furthermore, in screening for compounds which inhibit BACE1, multiple compounds may have been discarded because they are unable to cross the BBB. It may be that such a drug would be hugely beneficial as they could lower BACE1 activity peripherally with the associated metabolic benefits without causing any side effects which could be mediated through central BACE1 reduction, such as hypomyelination of nerve fibres or increased propensity to seizures (Dominguez et al. 2005). Indeed, previous data from the lab does indicate that peripheral infusion of a BACE1 inhibitor can reverse weight gain induced by a HFD, and given the similarity of the phenotype of these mice to mice with BACE1 removed from adipocytes, it could be argued that the drug is already capable of gaining sufficient access to WAT to mediate its effects. However, the drug was found to have crossed the BBB, so some effects may have been mediated centrally.

The pharmacokinetics of such a drug targeting WAT would be an important consideration. The absorption of drugs into adipose tissue may be difficult, given the relatively low blood supply of adipose tissue compared to other tissues (Rang, H. P et al. 2007). Indeed, this problem may be further complicated as in obese individuals vascularisation of adipose tissue is significantly impaired (Fuster et al. 2016), particularly in visceral fat depots. Therefore, route of administration and dose of any drug targeting the adipose tissue must be carefully considered to firstly provide a high enough dose to result in a clinical effect, and secondly to prevent excessive

accumulation within the WAT if treatment is maintained for a long time. Higher doses also increase the possibility of inducing off- target effects. Indeed, in the present study it is suggested that novel substrates of BACE1, namely β-klotho, are of critical importance in mediating the phenotypes associated with loss of BACE1 in adipocytes. Consequently, it will be important to more fully understand any other peripheral substrates of BACE1 in mammals to eliminate the possibility of any such events. One possible way to tackle these issues would be to use a compound which inhibits BACE1, but cannot cross the BBB, and administer it to mice at varying doses. These mice could then be tested for the effects on body weight, and glucose homeostasis- whilst also being monitored for any signs of unwanted side effects.

6.5 Final Comments

The studies completed in this thesis reveal for the first time the importance of reducing adipocyte BACE1 in whole body metabolic health and provides further evidence that the use of BACE1 inhibitors may be beneficial in treating obesity. Taken together with previous work from the lab, this work also demonstrates that APP processing may be important in central modification of energy homeostasis but not peripheral.

Model / Parameter	BACE1 global knock-out	BACE1 AdKO	BACE1 inhibitor (peripheral M3)	Central $A\beta_{1-42}$ infusion	Peripheral $A\beta_{1-42}$ infusion
Body Weight	↓	↓	↓	↑	↑
Fat Mass	↓	↓	↓	Not tested	↔
Glucose sensitivity	↑	↑	↑	↓	↔
Insulin sensitivity	↑	↔	↑	↓	↔
Insulin Signalling	↑	Not tested	Not tested	Not tested	↔
Energy expenditure	↑	↑	↑	Not tested	Not tested
RER	↑	↔	↑	Not tested	Not tested
Food Intake	↔	↔	↔	↔	↔

Table 6.1 Summary of the major phenotypes of mice with altered BACE1 expression and increased $A\beta_{1-42}$ levels

Although there are some discrepancies between the models demonstrated and described in this thesis (summarised in table 6.1), taken together it broadly appears that reducing peripheral or central BACE1 improves metabolic health, whereas raising APP processing, particularly centrally worsens metabolic health.

Removal of adipocyte BACE1 appears to rely on substrates other than APP to mediate its effects, which suggests multiple mechanisms, dependent on BACE1 activity, may regulate energy homeostasis in a tissue dependent manner. Although significantly more work must be completed to fully elucidate such mechanisms, it seems clear that BACE1 activity is a vital regulator of energy homeostasis.

Chapter 7 - References

7.1 References

Abel, E.D. et al., 2001. Adipose-selective targeting of the GLUT4 gene impairs insulin action in muscle and liver. *Nature*, 409(Feb 2001), pp.729–733.

Aderinwale, O.G., Ernst, H.W. & Mousa, S. a, 2010. Current therapies and new strategies for the management of Alzheimer's disease. *American journal of Alzheimer's Disease and other Dementias*, 25(5), pp.414–24.

Ajuwon, K.M. & Spurlock, M.E., 2005. Palmitate Activates the NF- kB Transcription Factor and Induces IL-6 and TNF-alpha Expression in 3T3-L1 Adipocytes. *The Journal of Nutrition*, 135(8), pp.1841–1846.

Alkhouri, N. et al., 2009. Adipocyte Apoptosis, a Link between Obesity, Insulin Resistance, and Hepatic Steatosis. The Journal of Biological Chemistry, 285(5), pp.3428-3438.

Andersen, D.K. et al., 1978. Oral glucose augmentation of insulin secretion. Interactions of gastric inhibitory polypeptide with ambient glucose and insulin levels. *The Journal of Clinical Investigation*, 62(1), pp.152–61.

Araki, E. et al., 1994. Alternative pathway of insulin signalling in mice with targeted disruption of the IRS-1 gene. *Nature*, 372(6502), pp.186–190.

Araki, W., 2016. Post-translational regulation of the β-secretase BACE1. *Brain Res Bull*, pp.1–8.

Arita, Y. et al., 1999. Paradoxical Decrease of an Adipose-Specific Protein, Adiponectin, in Obesity. *Biochemical and Biophysical Research Communications*, 257(1), pp.79–83.

Aronoff, S.L. & Berkowitz, K., 2004. Glucose Metabolism and Regulation: Beyond Insulin and Glucagon. *Diabetes Spectrum*, 17(3).

Avramovich, Y., Amit, T. & Youdim, M.B.H., 2002. Non-steroidal anti-inflammatory drugs stimulate secretion of non-amyloidogenic precursor protein. *The Journal of Biological Chemistry*, 277(35), pp.31466–73.

Azzout-Marniche, D. et al., 2000. Insulin effects on sterol regulatory-

element-binding protein-1c (SREBP-1c) transcriptional activity in rat hepatocytes. *Biochem. J*, 350, pp.389–393.

Baier, L. et al., 2002. Positional cloning of an obesity/diabetes susceptibility gene(s) on chromosome 11 in Pima Indians. *Annals of the New York Academy of Sciences*, 967, pp.258–64.

Balakrishnan, K. et al., 2005. Plasma Aβ42 correlates positively with increased body fat in healthy individuals. *Journal of Alzheimer's Disease*, 8(3), pp.269–282.

Bartness, T.J. et al., 2014. Neural innervation of white adipose tissue and the control of lipolysis. *Frontiers in Neuroendocrinology*, 35(4), pp.473–93.

Bates, S.H. et al., 2003. STAT3 signalling is required for leptin regulation of energy balance but not reproduction. *Nature*, 421(6925), pp.856–9.

Bedse, G. et al., 2015. Aberrant insulin signaling in Alzheimer's disease: current knowledge. *Frontiers in Neuroscience*, 9, p.204.

Belfiore, A. et al., 2009. Insulin Receptor Isoforms and Insulin Receptor/Insulin-Like Growth Factor Receptor Hybrids in Physiology and Disease. *Endocrine Reviews*, 30(6), pp.586–623.

Benjannet, S. et al., 2001. Post-translational processing of beta-secretase (beta-amyloid-converting enzyme) and its ectodomain shedding. The pro- and transmembrane/cytosolic domains affect its cellular activity and amyloid-beta production. *The Journal of Biological Chemistry*, 276(14), pp.10879–87.

Bennett, B.D. et al., 2000. Expression analysis of BACE2 in brain and peripheral tissues. *The Journal of Biological Chemistry*, 275(27), pp.20647–51.

Benyoucef, S. et al., 2007. Characterization of insulin/IGF hybrid receptors: contributions of the insulin receptor L2 and Fn1 domains and the alternatively spliced exon 11 sequence to ligand binding and receptor activation. *The Biochemical Journal*, 403(3), pp.603–13.

Bevan, P., 2001. Insulin signalling. *Journal of Cell Science*, 114(8).

Biessels, G.-J. et al., 1998. Water maze learning and hippocampal synaptic plasticity in streptozotocin-diabetic rats: effects of insulin

treatment. *Brain Research*, 800, pp.125–135.

Biessels, G.J. et al., 2006. Risk of dementia in diabetes mellitus: a systematic review. *Lancet Neurology*, 5(1), pp.64–74.

Bitan, G. et al., 2003. Amyloid beta -protein (Abeta) assembly: Abeta 40 and Abeta 42 oligomerize through distinct pathways. *Proceedings of the National Academy of Sciences of the United States of America*, 100(1), pp.330–5.

Bjørbaek, C. et al., 1998. Identification of SOCS-3 as a potential mediator of central leptin resistance. *Molecular Cell*, 1(4), pp.619–25.

Bjorbak, C. et al., 2000. SOCS3 mediates feedback inhibition of the leptin receptor via Tyr985. *The Journal of Biological Chemistry*, 275(51), pp.40649–57.

Bloch, L. et al., 2009. Klotho is a substrate for alpha-, beta- and gamma-secretase. *FEBS letters*, 583(19), pp.3221–4.

Bodendorf, U. et al., 2001. A Splice Variant of beta -Secretase Deficient in the Amyloidogenic Processing of the Amyloid Precursor Protein. *Journal of Biological Chemistry*, 276(15), pp.12019–12023.

Bollen, M., Keppens, S. & Stalmans, W., 1998. Specific features of glycogen metabolism in the liver. *The Biochemical Journal*, 336(Pt 1), pp.19–31.

BonDurant, L.D. et al., 2017. FGF21 Regulates Metabolism Through Adipose-Dependent and -Independent Mechanisms. *Cell Metabolism*, 25(4), p.935–944.e4.

Boucher, J., Kleinridders, A. & Kahn, C.R., 2014. Insulin receptor signaling in normal and insulin-resistant states. *Cold Spring Harbor Perspectives in Biology*, 6(1).

Boudina, S. & Graham, T.E., 2014. Mitochondrial function/dysfunction in white adipose tissue. *Experimental Physiology*, 99(9), pp.1168–78.

Bourne, K.Z. et al., 2007. Differential regulation of BACE1 promoter activity by nuclear factor-κB in neurons and glia upon exposure to β-amyloid peptides. *Journal of Neuroscience Research*, 85(6), pp.1194–1204.

Bradford, M.M., 1976. A rapid and sensitive method for the quantitation of microgram quantities of protein utilizing the principle of protein-dye

binding. *Analytical Biochemistry*, 72(1–2), pp.248–254.

Broberger, C. et al., 1998. Hypocretin/orexin- and melanin-concentrating hormone-expressing cells form distinct populations in the rodent lateral hypothalamus: relationship to the neuropeptide Y and agouti gene-related protein systems. *The Journal of Comparative Neurology*, 402(4), pp.460–74.

Bruun, J.M. et al., 2005. Monocyte Chemoattractant Protein-1 Release Is Higher in Visceral than Subcutaneous Human Adipose Tissue (AT): Implication of Macrophages Resident in the AT. *The Journal of Clinical Endocrinology & Metabolism*, 90(4), pp.2282–2289.

Cannon, B. & Nedergaard, J., 2010. Nonshivering thermogenesis and its adequate measurement in metabolic studies. *Journal of Experimental Biology*, 214(2).

Capell, A. et al., 2000. Maturation and pro-peptide cleavage of beta-secretase. *The Journal of Biological Chemistry*, 275(40), pp.30849–54.

Carvalho, E. et al., 2005. Adipose-specific overexpression of GLUT4 reverses insulin resistance and diabetes in mice lacking GLUT4 selectively in muscle. *AJP: Endocrinology and Metabolism*, 289(4), pp.E551–E561.

Castan-Laurell, I. et al., 2012. Apelin, a promising target for type 2 diabetes treatment? *Trends in endocrinology and metabolism: TEM*, 23(5), pp.234–41.

Cevenini, E. et al., 2010. Age-related inflammation: the contribution of different organs, tissues and systems. How to face it for therapeutic approaches. *Current Pharmaceutical Design*, 16(6), pp.609–18.

Champy, M.-F. et al., 2008. Genetic background determines metabolic phenotypes in the mouse. *Mammalian Genome*, 19(5), pp.318–331.

Chang, C.I., Liao, J.C. & Kuo, L., 1998. Arginase modulates nitric oxide production in activated macrophages. *The American Journal of Physiology*, 274(1 Pt 2), pp.H342-8.

Chao, A.-C. et al., 2016. Hyperglycemia Increases the Production of Amyloid Beta-Peptide Leading to Decreased Endothelial Tight Junction. *CNS Neuroscience & Therapeutics*, 22(4), pp.291–297.

Charlwood, J. et al., 2001. Characterization of the glycosylation profiles of Alzheimer's beta -secretase protein Asp-2 expressed in a variety of cell lines. *The Journal of biological chemistry*, 276(20), pp.16739–48.

Chau, M.D.L. et al., 2010. Fibroblast growth factor 21 regulates energy metabolism by activating the AMPK–SIRT1– PGC-1α pathway. *Proceedings of the National Academy of Sciences*, 107(28), pp.12553–12558.

Chavez, J.A. et al., 2013. Ceramides and Glucosylceramides Are Independent Antagonists of Insulin Signaling. *The Journal of Biological Chemistry*, 289(2), pp.723–734.

Chen, C.-H. et al., 2012a. Increased NF-κB signalling up-regulates BACE1 expression and its therapeutic potential in Alzheimer's disease. *The International Journal of Neuropsychopharmacology*, 15(1), pp.77–90.

Chen, C.-H. et al., 2012b. Increased NF-κB signalling up-regulates BACE1 expression and its therapeutic potential in Alzheimer's disease. *The international journal of neuropsychopharmacology / official scientific journal of the Collegium Internationale Neuropsychopharmacologicum (CINP)*, 15(1), pp.77–90.

Chen, H. et al., 1996. Evidence that the diabetes gene encodes the leptin receptor: identification of a mutation in the leptin receptor gene in db/db mice. *Cell*, 84(3), pp.491–5.

Chen, M. et al., 1995. Platelets Are the Primary Source of Amyloid β-Peptide in Human Blood. *Biochemical and Biophysical Research Communications*, 213(1), pp.96–103.

Chen, Y. & Dong, C., 2009. Ab40 promotes neuronal cell fate in neural progenitor cells. *Cell Death and Differentiation*, 1694(10), pp.386–394.

Chobanyan-Jürgens, K. & Jordan, J., 2015. Autonomic nervous system activity and inflammation: good ideas, good treatments, or both? *American Journal of Physiology - Heart and Circulatory Physiology*, 309(12).

Chondronikola, M. et al., 2014. Brown Adipose Tissue Improves Whole-Body Glucose Homeostasis and Insulin Sensitivity in Humans.

Diabetes, 63(12).

Christensen, M.A. et al., 2004. Transcriptional regulation of BACE1, the beta-amyloid precursor protein beta-secretase, by Sp1. *Molecular and Cellular Biology*, 24(2), pp.865–74.

Christensen, R. et al., 2007. Efficacy and safety of the weight-loss drug rimonabant: a meta-analysis of randomised trials. *The Lancet*, 370(9600), pp.1706–1713.

Chua, S.C. et al., 1996. Phenotypes of mouse diabetes and rat fatty due to mutations in the OB (leptin) receptor. *Science*, 271(5251), pp.994–6.

Cinti, S. et al., 2005. Adipocyte death defines macrophage localization and function in adipose tissue of obese mice and humans. *Journal of Lipid Research*, 46(11), pp.2347–55.

Clarke, J.R. et al., 2015. Alzheimer-associated Aβ oligomers impact the central nervous system to induce peripheral metabolic deregulation. *EMBO Molecular Medicine*, 7(2), pp.190–210.

Clough, G. et al., 1995. A positive, individually ventilated caging system: a local barrier system to protect both animals and personnel. *Laboratory Animals*, 29(2), pp.139–151.

Comerma-Steffensen, S. et al., 2014. Cardiovascular effects of current and future anti-obesity drugs. *Current Vascular Pharmacology*, 12(3), pp.493–504.

Coskun, T. et al., 2008. Fibroblast Growth Factor 21 Corrects Obesity in Mice. *Endocrinology*, 149(12), pp.6018–6027.

Costantini, C. et al., 2007. A reversible form of lysine acetylation in the ER and Golgi lumen controls the molecular stabilization of BACE1. *Biochemical Journal*, 407(3).

Cummings, J.L., 2004. Alzheimer's Disease. *The New England Journal of Medicine*, 351(1), pp.56–67.

Cummins, T.D. et al., 2014. Metabolic remodeling of white adipose tissue in obesity. *AJP: Endocrinology and Metabolism*, 307(3), pp.E262–E277.

Cypess, A.M. et al., 2009. Identification and Importance of Brown Adipose Tissue in Adult Humans. *New England Journal of Medicine*,

360(15), pp.1509–1517.

Dadson, K., Liu, Y. & Sweeney, G., 2011. Adiponectin action: a combination of endocrine and autocrine/paracrine effects. *Frontiers in endocrinology*, 2, p.62.

Danforth, E., 2000. Failure of adipocyte differentiation causes type II diabetes mellitus? *Nature Genetics*, 26(1), pp.13–13.

Deane, R. et al., 2003. RAGE mediates amyloid-β peptide transport across the blood-brain barrier and accumulation in brain. *Nature Medicine*, 9(7), pp.907–913.

Diabetes UK, 2017a. Diabetes: the basics - Diabetes UK. Available at: https://www.diabetes.org.uk/Diabetes-the-basics/ [Accessed April 30, 2017].

Diabetes UK, 2017b. Facts and Stats October 2016. Available at: https://www.diabetes.org.uk/Documents/Position statements/DiabetesUK_Facts_Stats_Oct16.pdf [Accessed August 10, 2017].

Ding, X. et al., 2012. βKlotho Is Required for Fibroblast Growth Factor 21 Effects On Growth and Metabolism. *Cell Metabolism*, 16(3), pp.387–393.

Dominguez, D. et al., 2005. Phenotypic and biochemical analyses of BACE1- and BACE2-deficient mice. *The Journal of Biological Chemistry*, 280(35), pp.30797–806.

Dulloo, A.G. & Miller, D.S., 1984. Thermogenic drugs for the treatment of obesity: sympathetic stimulants in animal models. *British Journal of Nutrition*, 52, pp.179–196.

Duncan, R.E. et al., 2007. Regulation of Lipolysis in Adipocytes. *Annu Rev Nutr.*, 27, pp.79–101.

Ebeling, P., Koistinen, H.A. & Koivisto, V.A., 1998. Insulin-independent glucose transport regulates insulin sensitivity. *FEBS Letters*, 436(3), pp.301–303.

Edbauer, D. et al., 2003. Reconstitution of gamma-secretase activity. *Nature Cell Biology*, 5(5), pp.486–488.

Ehehalt, R. et al., 2003. Amyloidogenic processing of the Alzheimer β-amyloid precursor protein depends on lipid rafts. *The Journal of Cell*

Biology, 160(1).

Elchebly, M. et al., 1999. Increased Insulin Sensitivity and Obesity Resistance in Mice Lacking the Protein Tyrosine Phosphatase-1B Gene. *Science*, 283(5407).

Eli Lilly, 2013. Lilly Voluntarily Terminates Phase II Study for LY2886721, a Beta Secretase Inhibitor, Being Investigated as a Treatment for Alzheimer's Disease (NYSE:LLY). Available at: https://investor.lilly.com/releasedetail.cfm?ReleaseID=771353 [Accessed August 21, 2017].

Ellacott, K.L.J. et al., 2007. Obesity-Induced Inflammation in White Adipose Tissue Is Attenuated by Loss of Melanocortin-3 Receptor Signaling. *Endocrinology*, 148(12), pp.6186–6194.

Farris, W. et al., 2003. Insulin-degrading enzyme regulates the levels of insulin, amyloid beta-protein, and the beta-amyloid precursor protein intracellular domain in vivo. *Proceedings of the National Academy of Sciences of the United States of America*, 100(7), pp.4162–7.

Farzan, M. et al., 2000. BACE2, a beta -secretase homolog, cleaves at the beta site and within the amyloid-beta region of the amyloid-beta precursor protein. *Proceedings of the National Academy of Sciences of the United States of America*, 97(17), pp.9712–9717.

Fasshauer, M. & Blüher, M., 2015. Adipokines in health and disease. *Trends in Pharmacological Sciences*, 36(7), pp.461–470.

Fellmann, L. et al., 2013. Murine models for pharmacological studies of the metabolic syndrome. *Pharmacology & Therapeutics*, 137(3), pp.331–40.

Fewlass, D.C. et al., 2004. Obesity-related leptin regulates Alzheimer's Abeta. *FASEB journal : official publication of the Federation of American Societies for Experimental Biology*, 18(15), pp.1870–8.

Fiala, M. et al., 1998. Amyloid-beta Induces Chemokine Secretion and Monocyte Migration across a Human Blood- Brain Barrier Model. *Molecular Medicine*, 4, pp.480–489.

Finder, V.H. & Glockshuber, R., 2007. Amyloid-β aggregation. *Neurodegenerative Diseases*, 4(1), pp.13–27.

Findlay, J.A., Hamilton, D.L. & Ashford, M.L.J., 2015. BACE1 activity

impairs neuronal glucose oxidation: rescue by beta-hydroxybutyrate and lipoic acid. *Frontiers in Cellular Neuroscience*, 9, p.382.

Finer, N., 2003. Obesity. *Clinical Medicine*, 3(1), pp.23–27.

Fischer, K. et al., 2017. Alternatively activated macrophages do not synthesize catecholamines or contribute to adipose tissue adaptive thermogenesis. *Nature Medicine*, 23(5), pp.623–630.

Fisher, M. et al., 2010. Obesity Is a Fibroblast Growth Factor 21 Resistant State. *Diabetes*, 59(11), pp.2781–2789.

Fontana, L. et al., 2007. Visceral Fat Adipokine Secretion Is Associated With Systemic Inflammation in Obese Humans. *Diabetes*, 56(4), pp.1010–1013.

Freeman, L.R. et al., 2012. Mutant Amyloid precursor protein differentially alters adipose biology under obesogenic and non-obesogenic conditions. *PLoS ONE*, 7(8).

Friedman, J.M. & Halaas, J.L., 1998. Leptin and the regulation of body weight in mammals. *Nature*, 395(6704), pp.763–70.

Fuster, J.J. et al., 2016. Obesity-Induced Changes in Adipose Tissue Microenvironment and Their Impact on Cardiovascular Disease. *Circulation Research*, 118(11).

Gainsford, T. et al., 1996. Leptin can induce proliferation, differentiation, and functional activation of hemopoietic cells. *Proceedings of the National Academy of Sciences of the United States of America*, 93(25), pp.14564–8.

Gan, L. et al., 2012. TNF-α up-regulates protein level and cell surface expression of the leptin receptor by stimulating its export via a PKC-dependent mechanism. *Endocrinology*, 153(12), pp.5821–33.

Garthwaite, T.L. et al., 1980. A Longitudinal Hormonal Profile of the Genetically Obese Mouse*. *Endocrinology*, 107(3), pp.671–676.

Gautam, D. et al., 2006. A critical role for β cell M3 muscarinic acetylcholine receptors in regulating insulin release and blood glucose homeostasis in vivo. *Cell Metabolism*, 3(6), pp.449–461.

Ge, X. et al., 2011. Fibroblast Growth Factor 21 Induces Glucose Transporter-1 Expression through Activation of the Serum Response Factor/Ets-Like Protein-1 in Adipocytes. *Journal of Biological*

Chemistry, 286(40), pp.34533–34541.

Ghorbani, M. & Himms-Hagen, J., 1997. Appearance of brown adipocytes in white adipose tissue during CL 316,243-induced reversal of obesity and diabetes in Zucker fa/fa rats. *International journal of obesity and related metabolic disorders : journal of the International Association for the Study of Obesity*, 21(6), pp.465–75.

Gillette-Guyonnet, S. et al., 2000. Weight loss in Alzheimer disease. *The American Journal of Clinical Nutrition*, 71(2), p.637S–642S.

Giorgino, F. et al., 1997. Specific increase in p85alpha expression in response to dexamethasone is associated with inhibition of insulin-like growth factor-I stimulated phosphatidylinositol 3-kinase activity in cultured muscle cells. *The Journal of Biological Chemistry*, 272(11), pp.7455–63.

Green, H. & Kehinde, O., 1974. Sublines of Mouse 3T3 Cells That Accumulate Lipid. *Cell*, 1, pp.113–116.

Guillod-Maximin, E. et al., 2009. Adiponectin receptors are expressed in hypothalamus and colocalized with proopiomelanocortin and neuropeptide Y in rodent arcuate neurons. *Journal of Endocrinology*, 200(1), pp.93–105.

Guo, S., 2014. Insulin signaling, resistance, and the metabolic syndrome: insights from mouse models into disease mechanisms. *Journal of Endocrinology*, 220(2), pp.T1–T23.

Halaas, J.L. et al., 1997. Physiological response to long-term peripheral and central leptin infusion in lean and obese mice. *Proceedings of the National Academy of Sciences of the United States of America*, 94(16), p.8878.

Hamilton, D.L. et al., 2014. Altered amyloid precursor protein processing regulates glucose uptake and oxidation in cultured rodent myotubes. *Diabetologia*, 57(8), pp.1684–92.

Hannun, Y.A. & Obeid, L.M., 2008. Principles of bioactive lipid signalling: lessons from sphingolipids. *Nature Reviews Molecular Cell Biology*, 9(2), pp.139–150.

Hardy, J. & Higgins, G., 1992. Alzheimer's disease: the amyloid cascade hypothesis. *Science*, 256(5054).

Harms, M. & Seale, P., 2013. Brown and beige fat: development, function and therapeutic potential. *Nature Medicine*, 19(10), pp.1252–1263.

Harno, E. et al., 2013. Metabolic Pitfalls of CNS Cre-Based Technology. *Cell Metabolism*, 18(1), pp.21–28.

Harper, J.D. & Lansbury, P.T., 1997. Models of amyloid seeding in Alzheimer's disease and scrapie:Mechanistic Truths and Physiological Consequences of the Time-Dependent Solubility of Amyloid Proteins. *Annual Review of Biochemistry*, 66(1), pp.385–407.

Harte, A.L. et al., 2013. NFκB as a potent regulator of inflammation in human adipose tissue, influenced by depot, adiposity, T2DM status, and TNFα. *Obesity*, 21(11), pp.2322–2330.

He, Y. et al., 2012. Soluble oligomers and fibrillar species of amyloid β-peptide differentially affect cognitive functions and hippocampal inflammatory response. *Biochemical and Biophysical Research Communications*, 429(3–4), pp.125–130.

Hemming, M.L. et al., 2009. Identification of β-Secretase (BACE1) Substrates Using Quantitative Proteomics. *PLoS ONE*, 4(12).

Heneka, M.T., Kummer, M.P. & Latz, E., 2014. Innate immune activation in neurodegenerative disease. *Nature Reviews Immunology*, 14(7), pp.463–477.

Henley, D.B. et al., 2014. Safety profile of semagacestat, a gamma-secretase inhibitor: IDENTITY trial findings. *Current Medical Research and Opinion*, 30(10), pp.2021–2032.

Henriksen, E.J. & Dokken, B.B., 2006. Role of glycogen synthase kinase-3 in insulin resistance and type 2 diabetes. *Current Drug Targets*, 7(11), pp.1435–41.

Hickman, S.E., Allison, E.K. & El Khoury, J., 2008. Microglial Dysfunction and Defective β-Amyloid Clearance Pathways in Aging Alzheimer's Disease Mice. *Journal of Neuroscience*, 28(33).

Hill, B.G., 2015. Insights into an adipocyte whitening program. *Adipocyte*, 4(1), pp.75–80.

Hitt, B. et al., 2012. β-Site amyloid precursor protein (APP)-cleaving enzyme 1 (BACE1)-deficient mice exhibit a close homolog of L1

(CHL1) loss-of-function phenotype involving axon guidance defects. *The Journal of Biological Chemistry*, 287(46), pp.38408–25.

Hitt, B.D. et al., 2010. BACE1 - / - mice exhibit seizure activity that does not correlate with sodium channel level or axonal localization. *Molecular Neurodegeneration*, 5(31), pp.1–14.

Ho, L. et al., 2004. Diet-induced insulin resistance promotes amyloidosis in a transgenic mouse model of Alzheimer's disease. *The FASEB Journal*, 18(7), pp.902–4.

Hoffmeister, A. et al., 2013. Genetic and biochemical evidence for a functional role of BACE1 in the regulation of insulin mRNA expression. *Obesity (Silver Spring, Md.)*, 21(12), pp.E626-33.

Holland, W.L. et al., 2011. Lipid-induced insulin resistance mediated by the proinflammatory receptor TLR4 requires saturated fatty acid–induced ceramide biosynthesis in mice. *Journal of Clinical Investigation*, 121(5), pp.1858–1870.

Hotamisligil, G.S., 2006. Inflammation and metabolic disorders. *Nature*, 444(7121), pp.860–7.

Hotamisligil, G.S. et al., 1996. IRS-1-mediated inhibition of insulin receptor tyrosine kinase activity in TNF-alpha- and obesity-induced insulin resistance. *Science*, 271(5249), pp.665–8.

Hotamisligil, G.S., Shargill, N.S. & Spiegelman, B.M., 1993. Adipose Expression of Tumor Necrosis Factor-α: Direct Role in Obesity-Linked Insulin Resistance. *Science*, 259, pp.87–91.

Howard, J.K. et al., 2004. Enhanced leptin sensitivity and attenuation of diet-induced obesity in mice with haploinsufficiency of Socs3. *Nature Medicine*, 10(7), pp.734–738.

Hu, X. et al., 2006. Bace1 modulates myelination in the central and peripheral nervous system. *Nature neuroscience*, 9(12), pp.1520–5.

Huang-Doran, I. et al., 2010. Lipodystrophy: metabolic insights from a rare disorder. *Journal of Endocrinology*, 207, pp.245–255.

Huang, S. & Czech, M.P., 2007. The GLUT4 Glucose Transporter. *Cell Metabolism*, 5(4), pp.237–252.

Hui, X. et al., 2015. Adiponectin Enhances Cold-Induced Browning of Subcutaneous Adipose Tissue via Promoting M2 Macrophage

Proliferation. *Cell Metabolism*, 22(2), pp.279–290.

Huse, J.T. et al., 2000. Maturation and endosomal targeting of beta-site amyloid precursor protein-cleaving enzyme. The Alzheimer's disease beta-secretase. *The Journal of Biological Chemistry*, 275(43), pp.33729–37.

Hussain, I. et al., 1999. Identification of a Novel Aspartic Protease (Asp 2) as β-Secretase. *Molecular and Cellular Neuroscience*, 14, pp.419–427.

Iikuni, N. et al., 2008. Leptin and Inflammation. *Current Immunology Reviews*, 4(2), pp.70–79.

Iwaki, M. et al., 2003. Induction of adiponectin, a fat-derived antidiabetic and antiatherogenic factor, by nuclear receptors. *Diabetes*, 52(7), pp.1655–63.

Iwatsubo, T. et al., 1994. Visualization of A beta 42(43) and A beta 40 in senile plaques with end-specific A beta monoclonals: evidence that an initially deposited species is A beta 42(43). *Neuron*, 13(1), pp.45–53.

Jablonski, K.A. et al., 2015. Novel Markers to Delineate Murine M1 and M2 Macrophages M. A. Olszewski, ed. *PLOS ONE*, 10(12), p.e0145342.

Jalicy, S.M., 2015. *The Hypothalamic role of BACE1 in Energy Homeostasis*. PhD Thesis, University of Dundee.

Janson, J. et al., 2004. Increased risk of type 2 diabetes in Alzheimer disease. *Diabetes*, 53(2), pp.474–81.

Jiang, G. & Zhang, B.B., 2003. Glucagon and regulation of glucose metabolism. *Am J Physiol Endocrinol Metab*, 284, pp.E671–E678.

Jo, J. et al., 2009. Hypertrophy and/or Hyperplasia: Dynamics of Adipose Tissue Growth. *PLoS Computational Biology*, 5(3), p.e1000324.

Johnson, A.M.F. & Olefsky, J.M., 2013. The origins and drivers of insulin resistance. *Cell*, 152(4), pp.673–684.

Johnson, J.L., Chambers, E. & Jayasundera, K., 2013. Application of a Bioinformatics-Based Approach to Identify Novel Putative in vivo BACE1 Substrates. *Biomedical Engineering and Computational Biology*, 5, pp.1–15.

Jorissen, E. et al., 2010. The Disintegrin/Metalloproteinase ADAM10 Is Essential for the Establishment of the Brain Cortex. *Journal of Neuroscience*, 30(14), pp.4833–4844.

Julien, C. et al., 2010. High-fat diet aggravates amyloid-beta and tau pathologies in the 3xTg-AD mouse model. *Neurobiology of Aging*, 31(9), pp.1516–31.

Kamat, P.K., 2015. Streptozotocin induced Alzheimer's disease like changes and the underlying neural degeneration and regeneration mechanism. *Neural regeneration research*, 10(7), pp.1050–2.

Kamei, N. et al., 2006. Overexpression of monocyte chemoattractant protein-1 in adipose tissues causes macrophage recruitment and insulin resistance. *The Journal of biological chemistry*, 281(36), pp.26602–14.

Kanda, H. et al., 2006. MCP-1 contributes to macrophage infiltration into adipose tissue, insulin resistance, and hepatic steatosis in obesity. *The Journal of clinical investigation*, 116(6), pp.1494–505.

Kang, E.L. et al., 2010. Ubiquitin regulates GGA3-mediated degradation of BACE1. *The Journal of Biological Chemistry*, 285(31), pp.24108–19.

Kashiwagi, A. et al., 1985. The effects of short-term overfeeding on adipocyte metabolism in Pima Indians. *Metabolism: Clinical and Experimental*, 34(4), pp.364–70.

Kellerer, M. et al., 1997. Leptin activates PI-3 kinase in C2C12 myotubes via janus kinase-2 (JAK-2) and insulin receptor substrate-2 (IRS-2) dependent pathways. *Diabetologia*, 40(11), pp.1358–1362.

Kersten, S., 2001. Mechanisms of nutritional and hormonal regulation of lipogenesis. *EMBO reports*, 2(4), pp.282–6.

Khan, T. et al., 2009. Metabolic dysregulation and adipose tissue fibrosis: role of collagen VI. *Molecular and Cellular Biology*, 29(6), pp.1575–91.

Kharitonenkov, A. et al., 2005. FGF-21 as a novel metabolic regulator. *Journal of Clinical Investigation*, 115(6), pp.1627–1635.

Kiguchi, N. et al., 2009. Leptin enhances CC-chemokine ligand expression in cultured murine macrophage. *Biochemical and*

Biophysical Research Communications, 384(3), pp.311–315.

Kim, J.Y. et al., 2017. Palmitic Acid-BSA enhances Amyloid-β production through GPR40-mediated dual pathways in neuronal cells: Involvement of the Akt/mTOR/HIF-1α and Akt/NF-κB pathways. *Scientific Reports*, 7(1), p.4335.

Kim, T. & Tanzi, R.E., 1999. BACE Maps to Chromosome 11 and a BACE Homolog, BACE2, Reside in the Obligate Down Syndrome Region of Chromosome 21. *Science*, 286(November), p.1255a.

King, R.S. & Newmark, P. a., 2012. The cell biology of fat expansion. *The Journal of Cell Biology*, 196(5), pp.553–562.

Kitazume, S. et al., 2005. In Vivo Cleavage of 2,6-Sialyltransferase by Alzheimer β-Secretase. *Journal of Biological Chemistry*, 280(9), pp.8589–8595.

Kleinridders, A. et al., 2009. MyD88 signaling in the CNS is required for development of fatty acid-induced leptin resistance and diet-induced obesity. *Cell Metabolism*, 10(4), pp.249–59.

Klip, A. & Paquet, M.R., 1990. Glucose Transport and Glucose Transporters in Muscle and Their Metabolic Regulation. *Diabetes Care*, 13(3), pp.228–243.

Knight, Z.A. et al., 2010. Hyperleptinemia Is Required for the Development of Leptin Resistance K. Stadler, ed. *PLoS ONE*, 5(6), p.e11376.

Knowler, W.C. et al., 2002. Reduction in the Incidence of Type 2 Diabetes with Lifestyle Intervention or Metformin. *New England Journal of Medicine*, 346(6), pp.393–403.

Kohjima, M., Sun, Y. & Chan, L., 2010. Increased food intake leads to obesity and insulin resistance in the tg2576 Alzheimer's disease mouse model. *Endocrinology*, 151(4), pp.1532–40.

Kostrzewa, R.M. & Jacobowitz, D.M., 1974. Pharmacological Actions of 6-Hydroxydopamine. *Pharmacological Reviews*, 26(3).

Kotani, K. et al., 2004. GLUT4 glucose transporter deficiency increases hepatic lipid production and peripheral lipid utilization. *The Journal of Clinical Investigation*, 114(11), pp.1666–75.

Kraegen, E.W. et al., 1993. Glucose transporters and in viva glucose

uptake in skeletal and cardiac muscle: fasting, insulin stimulation and immunoisolation studies of GLUT1 and GLUT4. *Biochemical Journal*, 295, pp.287–293.

Krssak, M. et al., 1999. Intramyocellular lipid concentrations are correlated with insulin sensitivity in humans: a 1 H NMR spectroscopy study. *Diabetologia*, 42(1), pp.113–116.

Kubota, N. et al., 2002. Disruption of adiponectin causes insulin resistance and neointimal formation. *The Journal of Biological Chemistry*, 277(29), pp.25863–6.

Kuhn, P.-H. et al., 2010. ADAM10 is the physiologically relevant, constitutive α-secretase of the amyloid precursor protein in primary neurons. *The EMBO Journal*, 29(17), pp.3020–3032.

Kurosu, H. & Kuro-o, M., 2009. The Klotho gene family as a regulator of endocrine fibroblast growth factors. *Molecular and Cellular Endocrinology*, 299(1), pp.72–78.

Kwon, H. & Pessin, J.E., 2013. Adipokines mediate inflammation and insulin resistance. *Frontiers in Endocrinology*, 4(June), p.71.

de la Monte, S.M. & Wands, J.R., 2008. Alzheimer's Disease Is Type 3 Diabetes — Evidence Reviewed. *Journal of Diabetes Science and Technology*, 2(6), pp.1101–1113.

LaFerla, F.M., Green, K.N. & Oddo, S., 2007. Intracellular amyloid-beta in Alzheimer's disease. *Nature reviews. Neuroscience*, 8(7), pp.499–509.

Lafontan, M., 2014. Adipose tissue and adipocyte dysregulation. *Diabetes & Metabolism*, 40(1), pp.16–28.

Lammich, S. et al., 1999. Constitutive and regulated alpha-secretase cleavage of Alzheimer's amyloid precursor protein by a disintegrin metalloprotease. *Proceedings of the National Academy of Sciences of the United States of America*, 96(7), pp.3922–7.

Lammich, S. et al., 2004. Expression of the Alzheimer protease BACE1 is suppressed via its 5'-untranslated region. *EMBO reports*, 5(6), pp.620–625.

Lara-castro, C. et al., 2006. Adiponectin Multimeric Complexes and the Metabolic Syndrome Trait Cluster Cristina. *Diabetes*, 55(January),

pp.249–259.

Lawrence, T., 2009. The nuclear factor NF-kappaB pathway in inflammation. *Cold Spring Harbor perspectives in Biology*, 1(6), p.a001651.

Lee, H.-K. et al., 2009. The insulin/Akt signaling pathway is targeted by intracellular beta-amyloid. *Molecular Biology of the Cell*, 20(5), pp.1533–44.

Lee, H.J. et al., 2016. High glucose upregulates BACE1-mediated Aβ production through ROS-dependent HIF-1α and LXRα/ABCA1-regulated lipid raft reorganization in SK-N-MC cells. *Scientific Reports*, 6(1), p.36746.

Lee, K.N. et al., 2001. Regulation of leptin gene expression by insulin and growth hormone in mouse adipocytes. *Experimental & Molecular Medicine*, 33(4), pp.234–239.

Lee, K.Y. et al., 2013. Lessons on conditional gene targeting in mouse adipose tissue. *Diabetes*, 62(3), pp.864–74.

Lee, M.-J., Wu, Y. & Fried, S.K., 2013. Adipose tissue heterogeneity: implication of depot differences in adipose tissue for obesity complications. *Molecular aspects of Medicine*, 34(1), pp.1–11.

Lee, Y.-H. et al., 2008. Amyloid precursor protein expression is upregulated in adipocytes in obesity. *Obesity (Silver Spring, Md.)*, 16(7), pp.1493–500.

Lee, Y.-H. et al., 2009. Plasma Amyloid-β Peptide Levels Correlate with Adipocyte Amyloid Precursor Protein Gene Expression in Obese Individuals. *Neuroendocrinology*, 90(4), pp.383–390.

Lee, Y.H. et al., 2003. c-Jun N-terminal Kinase (JNK) Mediates Feedback Inhibition of the Insulin Signaling Cascade. *Journal of Biological Chemistry*, 278(5), pp.2896–2902.

Li, Y. et al., 2004. Protein kinase C Theta inhibits insulin signaling by phosphorylating IRS1 at Ser(1101). *The Journal of Biological Chemistry*, 279(44), pp.45304–7.

Li, Z. et al., 2007. SH2B1 Enhances Leptin Signaling by Both Janus Kinase 2 Tyr ^{813} Phosphorylation-Dependent and -Independent Mechanisms. *Molecular Endocrinology*, 21(9), pp.2270–2281.

Lichtenthaler, S.F., 2011. Alpha-secretase in Alzheimer?s disease: molecular identity, regulation and therapeutic potential. *Journal of Neurochemistry*, 116(1), pp.10–21.

Lin, Z. et al., 2013. Adiponectin Mediates the Metabolic Effects of FGF21 on Glucose Homeostasis and Insulin Sensitivity in Mice. *Cell Metabolism*, 17(5), pp.779–789.

Liu, L. et al., 2013. Palmitate induces transcriptional regulation of BACE1 and presenilin by STAT3 in neurons mediated by astrocytes. *Experimental neurology*, 248, pp.482–90.

Liu, Y. et al., 2011. Deficient brain insulin signalling pathway in Alzheimer's disease and diabetes. *The Journal of Pathology*, 225(1), pp.54–62.

Lo, K.A. & Sun, L., 2013. Turning WAT into BAT: a review on regulators controlling the browning of white adipocytes. *Bioscience reports*, 33(5).

Lucas, J.J. et al., 2001. Decreased nuclear beta-catenin, tau hyperphosphorylation and neurodegeneration in GSK-3beta conditional transgenic mice. *The EMBO journal*, 20(1–2), pp.27–39.

Luchsinger, J.A. & Gustafson, D.R., 2009. Adiposity, type 2 diabetes and Alzheimer's disease. *J Alzheimers Dis.*, 16(4), pp.693–704.

Lumeng, C.N., Bodzin, J.L. & Saltiel, A.R., 2007. Obesity induces a phenotypic switch in adipose tissue macrophage polarization. The *Journal of Clinical Ivestigation*, 117(1), pp.175-184.

Luo, Y. et al., 2003. BACE1 (β-secretase) knockout mice do not acquire compensatory gene expression changes or develop neural lesions over time. *Neurobiology of Disease*, 14(1), pp.81–88.

Luo, Y. et al., 2001. Mice deficient in BACE1, the Alzheimer's beta-secretase, have normal phenotype and abolished beta-amyloid generation. *Nature Neuroscience*, 4(3), pp.231–2.

M, H. et al., 2015. Omentin - a new adipokine with many roles to play. *Curr. Issues Pharm. Med. Sci*, 28(3), pp.176–180.

Macauley, S.L. et al., 2015. Hyperglycemia modulates extracellular amyloid-β concentrations and neuronal activity in vivo. *The Journal of Clinical Investigation*, 125(6), pp.2463–7.

Macklin, L. et al., 2017. Glucose tolerance and insulin sensitivity are impaired in APP/PS1 transgenic mice prior to amyloid plaque pathogenesis and cognitive decline. *Experimental Gerontology*, 88, pp.9–18.

Maeda, N. et al., 2002. Diet-induced insulin resistance in mice lacking adiponectin/ACRP30. *Nature Medicine*, 8(7), pp.731–737.

Maesako, M. et al., 2015. High Fat Diet Enhances β-Site Cleavage of Amyloid Precursor Protein (APP) via Promoting β-Site APP Cleaving Enzyme 1/Adaptor Protein 2/Clathrin Complex Formation. *PloS one*, 10(9), p.e0131199.

Maffei, M. et al., 1995. Leptin levels in human and rodent: Measurement of plasma leptin and ob RNA in obese and weight-reduced subjects. *Nature Medicine*, 1(11), pp.1155–1161.

Manning, B.D. & Cantley, L.C., 2007. AKT/PKB Signaling: Navigating Downstream. *Cell*, 129(7), pp.1261–1274.

Mao, X. et al., 2006. APPL1 binds to adiponectin receptors and mediates adiponectin signalling and function. *Nature Cell Biology*, 8(5), pp.516–523.

Markan, K.R. et al., 2017. FGF21 resistance is not mediated by downregulation of beta-klotho expression in white adipose tissue. *Molecular Metabolism, 6(6), pp.602-610*.

Marre, M. et al., 2009. Liraglutide, a once-daily human GLP-1 analogue, added to a sulphonylurea over 26 weeks produces greater improvements in glycaemic and weight control compared with adding rosiglitazone or placebo in subjects with Type 2 diabetes (LEAD-1 SU). *Diabetic Medicine*, 26(3), pp.268–278.

Martinez, F.O. & Gordon, S., 2014. The M1 and M2 paradigm of macrophage activation: time for reassessment. *F1000 Prime Reports*, 6, p.13.

Matsuzaki, T. et al., 2010. Insulin resistance is associated with the pathology of Alzheimer disease: The Hisayama Study. *Neurology*, 75(9), pp.764–770.

Mattson, D.L. & Krauski, K.R., 1998. Chronic Sodium Balance and Blood Pressure Response to Captopril in Conscious Mice. , pp.923–928.

McQuaid, S.E. et al., 2011. Downregulation of Adipose Tissue Fatty Acid Trafficking in Obesity A Driver for Ectopic Fat Deposition? *Diabetes*, 60, pp.47–55.

Meakin, P.J. et al., 2018. Bace1-dependent amyloid processing regulates hypothalamic leptin sensitivity in obese mice. *Scientific Reports*, 8(1), p.55.

Meakin, P.J., Harper, A.J., Hamilton, D.L., Gallagher, J., McNeilly, A.D., Burgess, L.A., et al., 2012. Reduction in BACE1 decreases body weight, protects against diet-induced obesity and enhances insulin sensitivity in mice. *The Biochemical Journal*, 441(1), pp.285–96.

Mestas, J. & Hughes, C.C.W., 2004. Of Mice and Not Men: Differences between Mouse and Human Immunology. *The Journal of Immunology*, 172(5).

Min, H. et al., 2017. Measurement of altered APP isoform expression in adipose tissue of diet-induced obese mice by absolute quantitative real-time PCR. *Animal Cells and Systems*, 21(2), pp.100–107.

Moitra, J. et al., 1998. Life without white fat: a transgenic mouse. *Genes & Development*, 12(20), p.3168.

Moloney, A.M. et al., 2010. Defects in IGF-1 receptor, insulin receptor and IRS-1/2 in Alzheimer's disease indicate possible resistance to IGF-1 and insulin signalling. *Neurobiology of Aging*, 31(2), pp.224–243.

Morgan, S. et al., 2011. The cost of drug development: A systematic review. *Health Policy*, 100, pp.4–17.

Morton, G.J. et al., 2005. Leptin regulates insulin sensitivity via phosphatidylinositol-3-OH kinase signaling in mediobasal hypothalamic neurons. *Cell Metabolism*, 2(6), pp.411–420.

Mössenböck, K. et al., 2014. Browning of White Adipose Tissue Uncouples Glucose Uptake from Insulin Signaling M. Kanzaki, ed. *PLoS ONE*, 9(10), p.e110428.

Mottillo, E.P. et al., 2017. FGF21 does not require adipocyte AMP-activated protein kinase (AMPK) or the phosphorylation of acetyl-CoA carboxylase (ACC) to mediate improvements in whole-body glucose homeostasis. *Molecular Metabolism*, 6, pp.471–481.

Mouton-Liger, F. et al., 2012. Oxidative stress increases BACE1 protein levels through activation of the PKR-eIF2α pathway. *Biochimica et Biophysica Acta*, 1822(6), pp.885–96.

Mullard, A., 2017. BACE inhibitor bust in Alzheimer trial. *Nature Reviews Drug Discovery*, 16(3), pp.155–155.

N, R. & Fain, J., 1968. Stimulation of Respiration in Brown Fat Cells by Epinephrine, Dibutyryl-3',5'-adenosine Monophosphate, and m-Chloro(carbonyl Cyanide)phenylhydrazone. *Journal of Biological Chemistry*, 243, pp.2843–2848.

Nedergaard, J. & Cannon, B., 2014. The Browning of White Adipose Tissue: Some Burning Issues. *Cell Metabolism*, 20(3), pp.396–407.

Nguyen, K.D. et al., 2011. Alternatively activated macrophages produce catecholamines to sustain adaptive thermogenesis. *Nature*, 480(7375), pp.104–8.

Nguyen, N.L.T. et al., 2014. Central sympathetic innervations to visceral and subcutaneous white adipose tissue. *American Journal of physiology. Regulatory, Integrative and Comparative Physiology*, 306(6), pp.R375-86.

NHS, NHS Choices- Obesity. Available at: http://www.nhs.uk/conditions/Obesity/Pages/Introduction.aspx [Accessed August 21, 2016].

Nicholls, D.G., Bernson, V.S. & Heaton, G.M., 1978. The identification of the component in the inner membrane of brown adipose tissue mitochondria responsible for regulating energy dissipation. *Experientia. Supplementum*, 32, pp.89–93.

Nihon Seikagakkai., Y. et al., 1996. Isolation and Characterization of GBP28, a Novel Gelatin-Binding Protein Purified from Human Plasma. *The Journal of Biochemistry*, 120(4), pp.803–812.

Nishimura, S. et al., 2009. CD8+ effector T cells contribute to macrophage recruitment and adipose tissue inflammation in obesity. *Nature Medicine*, 15(8), pp.914–920.

Niswender, K.D. et al., 2003. Insulin Activation of Phosphatidylinositol 3-Kinase in the Hypothalamic Arcuate Nucleus. *Diabetes*, 52(2).

Nitsch, R. et al., 1992. Release of Alzheimer amyloid precursor

derivatives stimulated by activation of muscarinic acetylcholine receptors. *Science*, 258(5080).

Nowak, K. et al., 2006. The transcription factor Yin Yang 1 is an activator of BACE1 expression. *Journal of Neurochemistry*, 96(6), pp.1696–1707.

O'Neill, S. & O'Driscoll, L., 2014. Metabolic syndrome: a closer look at the growing epidemic and its associated pathologies. *Obesity reviews : an official journal of the International Association for the Study of Obesity*.

Obregon, D. et al., 2012. Soluble amyloid precursor protein-α modulates β-secretase activity and amyloid-β generation. *Nature Communications*, 3, p.777.

Odegaard, J.I. et al., 2007. Macrophage-specific PPARgamma controls alternative activation and improves insulin resistance. *Nature*, 447(7148), pp.1116–20.

Ogawa, Y. et al., 2007. BetaKlotho is required for metabolic activity of fibroblast growth factor 21. *Proceedings of the National Academy of Sciences of the United States of America*, 104(18), pp.7432–7.

Ohashi, K. et al., 2010. Adiponectin promotes macrophage polarization toward an anti-inflammatory phenotype. *The Journal of Biological Chemistry*, 285(9), pp.6153–60.

Olefsky, J.M. & Glass, C.K., 2010. Macrophages, inflammation, and insulin resistance. *Annual review of Physiology*, 72, pp.219–46.

Oliverio, M. et al., 2016. Dicer1–miR-328–Bace1 signalling controls brown adipose tissue differentiation and function. *Nature Cell Biology*, 18(3), pp.328–336.

Oral, E.A. et al., 2002. Leptin-Replacement Therapy for Lipodystrophy. *New England Journal of Medicine*, 346(8), pp.570–578.

Orskov, C., Wettergren, A. & Holst, J.J., 1996. Secretion of the Incretin Hormones Glucagon-Like Peptide-1 and Gastric Inhibitory Polypeptide Correlates with Insulin Secretion in Normal Man Throughout the Day. *Scandinavian Journal of Gastroenterology*, 31(7), pp.665–670.

Ørtenblad, N., Westerblad, H. & Nielsen, J., 2013. Muscle glycogen

stores and fatigue. *The Journal of Physiology*, 591(18), pp.4405–13.

Ouchi, N. et al., 2011. Adipokines in inflammation and metabolic disease. *Nature reviews. Immunology*, 11(2), pp.85–97.

Ozcan, L. et al., 2009. Endoplasmic reticulum stress plays a central role in development of leptin resistance. *Cell Metabolism*, 9(1), pp.35–51.

Özcan, U. et al., 2004. Endoplasmic Reticulum Stress Links Obesity, Insulin Action, and Type 2 Diabetes. *Science*, 306(5695).

Padwal, R.S. et al., 2003. Long-term pharmacotherapy for obesity and overweight. In R. S. Padwal, ed. *Cochrane Database of Systematic Reviews*. Chichester, UK: John Wiley & Sons, Ltd.

Padwal, R.S. & Majumdar, S.R., 2007. Drug treatments for obesity: orlistat, sibutramine, and rimonabant. *The Lancet*, 369(9555), pp.71–77.

Park, S. et al., 2004. CCAAT/Enhancer Binding Protein and Nuclear Factor-Y Regulate Adiponectin Gene Expression in Adipose Tissue. *Diabetes*, 53(11).

Parker, M.W. et al., 1999. Crystal structure of the N-terminal, growth factor-like domain of Alzheimer amyloid precursor protein. *Nature Structural Biology*, 6(4), pp.327–331.

Pasarica, M. et al., 2009. Reduced Adipose Tissue Oxygenation in Human Obesity. *Diabetes*, 58(3).

Plucińska, K. et al., 2014. Knock-In of Human BACE1 Cleaves Murine APP and Reiterates Alzheimer-like Phenotypes. *The Journal of Neuroscience,* 34(32), pp.10710–28.

Plucińska, K. et al., 2016. Neuronal human BACE1 knockin induces systemic diabetes in mice. *Diabetologia*.

Polak, P. et al., 2008. Adipose-Specific Knockout of raptor Results in Lean Mice with Enhanced Mitochondrial Respiration. *Cell Metabolism*, 8(5), pp.399–410.

Prince, M, Knapp, M, G., M, McCrone, P, Prina, M, Comas-Herrera, A, Wittenberg, R. & Adelaja, B, Hu, B, King, D, Rehill, A and Salimkumar, D., 2014. Dementia UK: Update. Available at: https://www.alzheimers.org.uk/download/downloads/id/2323/dementia_uk_update.pdf [Accessed August 21, 2017].

Puglielli, L. et al., 2003. Ceramide stabilizes beta-site amyloid precursor protein-cleaving enzyme 1 and promotes amyloid beta-peptide biogenesis. *The Journal of Biological Chemistry*, 278(22), pp.19777–83.

Puig, K.L. et al., 2012. Amyloid precursor protein and proinflammatory changes are regulated in brain and adipose tissue in a murine model of high fat diet-induced obesity. *PLoS ONE*, 7(1).

Puigserver, P. et al., 1998. A cold-inducible coactivator of nuclear receptors linked to adaptive thermogenesis. *Cell*, 92(6), pp.829–39.

Qi, Y. et al., 2004. Adiponectin acts in the brain to decrease body weight. *Nature Medicine*, 10(5), pp.524–529.

Qiao, L.Y. et al., 1999. Identification of enhanced serine kinase activity in insulin resistance. *The Journal of Biological Chemistry*, 274(15), pp.10625–32.

R&D Systems, 2018. Proteome Profiler Mouse Adipokine Array Kit: R&D Systems. Available at: https://www.rndsystems.com/products/proteome-profiler-mouse-adipokine-array-kit_ary013 [Accessed January 21, 2018].

Rafii, M.S. & Aisen, P.S., 2009. Recent developments in Alzheimer's disease therapeutics. *BMC Medicine*, 7(1), p.7.

Rang, H. P et al., 2007. *Pharmacology* 6th ed., Elsevier.

Refolo, L.M. et al., 2000. Hypercholesterolemia Accelerates the Alzheimer's Amyloid Pathology in a Transgenic Mouse Model. *Neurobiology of Disease*, 7(4), pp.321–331.

Ring, S. et al., 2007. The Secreted β-Amyloid Precursor Protein Ectodomain APPsα Is Sufficient to Rescue the Anatomical, Behavioral, and Electrophysiological Abnormalities of APP-Deficient Mice. *Journal of Neuroscience*, 27(29).

Roberds, S.L. et al., 2001. BACE knockout mice are healthy despite lacking the primary β -secretase activity in brain : implications for Alzheimer ' s disease therapeutics. *Human Molecular Genetics*, 10(12), pp.1317–1324.

Roden, M. & Bernroider, E., 2003. Hepatic glucose metabolism in humans — its role in health and disease. *Best Practice & Research*

Clinical Endocrinology & Metabolism, 17(3), pp.365–383.

Roher, A.E. et al., 2009. Amyloid beta peptides in human plasma and tissues and their significance for Alzheimer's disease. *Alzheimer's & Dementia*, 5(1), pp.18–29.

Roher, A.E. et al., 2009. Amyloid beta peptides in human plasma and tissues and their significance for Alzheimer's disease. *Alzheimer's & Dementia : the Journal of the Alzheimer's Association*, 5(1), pp.18–29.

Rosen, E.D. & MacDougald, O. a, 2006. Adipocyte differentiation from the inside out. *Nature reviews. Molecular cell biology*, 7(December), pp.885–896.

Rosen, E.D. & Spiegelman, B.M., 2006. Adipocytes as regulators of energy balance and glucose homeostasis. *Nature*, 444(7121), pp.847–53.

Rossner, S. et al., 2006. Transcriptional and translational regulation of BACE1 expression--implications for Alzheimer's disease. *Progress in neurobiology*, 79(2), pp.95–111.

Ruan, H. & Dong, L.Q., 2016. Adiponectin signaling and function in insulin target tissues. *Journal of Molecular Cell Biology*, 8(2), pp.101–109.

Rui, L. et al., 2002. SOCS-1 and SOCS-3 block insulin signaling by ubiquitin-mediated degradation of IRS1 and IRS2. *Journal of Biological Chemistry*, 277(44), pp.42394–42398.

Saltiel, A.R. & Kahn, C.R., 2001. Insulin signalling and the regulation of glucose and lipid metabolism. *Nature*, 414(December), pp.799–806.

Sastre, M. et al., 2006. Nonsteroidal anti-inflammatory drugs repress beta-secretase gene promoter activity by the activation of PPARgamma *Proceedings of the National Academy of Sciences*, 103(2), pp.443–448.

Savage, D.B., 2009. Mouse models of inherited lipodystrophy. *Disease Models & Mechanisms*, 2(11–12).

Scherer, P.E. et al., 1995. A Novel Serum Protein Similar to C1q, Produced Exclusively in Adipocytes. *Journal of Biological Chemistry*, 270(45), pp.26746–26749.

Seale, P., Conroe, H.M., et al., 2011. Prdm16 determines the thermogenic program of subcutaneous white adipose tissue in mice. *Journal of Clinical Investigation*, 121(1), pp.96–105.

Seale, P., Conroe, H.M., et al., 2011. Prdm16 determines the thermogenic program of subcutaneous white adipose tissue in mice. *The Journal of clinical investigation*, 121(1), pp.96–105.

Shepherd, P.R. et al., 1993. Adipose cell hyperplasia and enhanced glucose disposal in transgenic mice overexpressing GLUT4 selectively in adipose tissue. *The Journal of biological chemistry*, 268(30), pp.22243–6.

Shimizu, I. et al., 2014. Vascular rarefaction mediates whitening of brown fat in obesity. *The Journal of Clinical Investigation*, 124(5), pp.2099–112.

Shoelson, S.E., Lee, J. & Goldfine, A.B., 2006. Inflammation and insulin resistance. *The Journal of Clinical Investigation*, 116(7), pp.1793–1801.

Shrestha, Y.B. et al., 2010. Central melanocortin stimulation increases phosphorylated perilipin A and hormone-sensitive lipase in adipose tissues. *AJP: Regulatory, Integrative and Comparative Physiology*, 299(1), pp.R140–R149.

Shukla, A.P., Kumar, R.B. & Aronne, L.J., 2015. Lorcaserin Hcl for the treatment of obesity. *Expert Opinion on Pharmacotherapy*, 16(16), pp.2531–2538.

Siddle, K., 2011. Signalling by insulin and IGF receptors: supporting acts and new players. *Journal of Molecular Endocrinology*, 47(1), pp.R1-10.

Sipe, L.M. et al., 2017. Differential sympathetic outflow to adipose depots is required for visceral fat loss in response to calorie restriction. *Nutrition & Diabetes*, 7(4), p.e260.

Skolnik, E.Y. et al., 1993. The function of GRB2 in linking the insulin receptor to Ras signaling pathways. *Science*, 260(5116), pp.1953–5.

Sohn, J.-W., 2015. Network of hypothalamic neurons that control appetite. *BMB Reports*, 48(4), pp.229–33.

Song, W.-J. et al., 2015. Enhancement of BACE1 Activity by p25/Cdk5-

Mediated Phosphorylation in Alzheimer's Disease. *PLOS ONE*, 10(8), p.e0136950.

Souza, S.C. et al., 2007. Perilipin regulates the thermogenic actions of norepinephrine in brown adipose tissue. *Journal of Lipid Research*, 48(6), pp.1273–1279.

Spalding, K.L. et al., 2008. Dynamics of fat cell turnover in humans. *Nature*, 453(7196), pp.783–787.

Speakman, J.R., 2013. Measuring Energy Metabolism in the Mouse – Theoretical, Practical, and Analytical Considerations. *Frontiers in Physiology*, 4, p.34.

Speakman, J.R. & Keijer, J., 2012. Not so hot: Optimal housing temperatures for mice to mimic the thermal environment of humans. *Molecular Metabolism*, 2(1), pp.5–9.

Stanford, K.I. et al., 2013. Brown adipose tissue regulates glucose homeostasis and insulin sensitivity. *The Journal of Clinical Investigation*, 123(1), pp.215–23.

Steen, E. et al., 2005. Impaired insulin and insulin-like growth factor expression and signaling mechanisms in Alzheimer's disease – is this type 3 diabetes? *Journal of Alzheimer's Disease*, 7, pp.63–80.

Stéphan, A., Laroche, S. & Davis, S., 2001. Generation of aggregated beta-amyloid in the rat hippocampus impairs synaptic transmission and plasticity and causes memory deficits. *The Journal of Neuroscience*, 21(15), pp.5703–14.

Stertz, L. et al., 2016. BACE1-Deficient Mice Exhibit Alterations in Immune System Pathways. *Molecular Neurobiology*, pp.1–9.

De Strooper, B. et al., 1998. Deficiency of presenilin-1 inhibits the normal cleavage of amyloid precursor protein. *Nature*, 391(6665), pp.387–390.

Stützer, I. et al., 2013. Systematic Proteomic Analysis Identifies β-Site Amyloid Precursor Protein Cleaving Enzyme 2 and 1 (BACE2 and BACE1) Substrates in Pancreatic β-Cells. *Journal of Biological Chemistry*, 288(15), pp.10536–10547.

Sukanto Sinha, John P. Anderson, Robin Barbour, Guriqbal S. Basi, Russell Caccavello, David Davis, Minhtam Doan, Harry F. Dovey,

Normand Frigon, Jin Hong, Kirsten Jacobson-Croak, Nancy Jewett, Pamela Keim, Jeroen Knops, Ivan Lieberburg, Michael Power, Hua, L.M.& V.J., 1999. Purification and cloning of amyloid precursor protein b -secretase from human brain. *Nature*, 705(November), pp.537–540.

Sun, J. et al., 2016. Adiponectin potentiates the acute effects of leptin in arcuate Pomc neurons. *Molecular metabolism*, 5(10), pp.882–91.

Sung, H.-K. et al., 2013. Adipose Vascular Endothelial Growth Factor Regulates Metabolic Homeostasis through Angiogenesis. *Cell Metabolism*, 17(1), pp.61–72.

Takahashi, K. et al., 2003. Adiposity elevates plasma MCP-1 levels leading to the increased CD11b-positive monocytes in mice. *The Journal of Biological Chemistry*, 278(47), pp.46654–60.

Takechi, R. et al., 2013. Probucol prevents blood-brain barrier dysfunction in wild-type mice induced by saturated fat or cholesterol feeding. *Clinical and Experimental Pharmacology and Physiology*, 40(1), pp.45–52.

Talukdar, S. et al., 2012. Neutrophils mediate insulin resistance in mice fed a high-fat diet through secreted elastase. *Nature Medicine*, 18(9), pp.1407–12.

Tang, L. et al., 2015. Sympathetic Nerve Activity Maintains an Anti-Inflammatory State in Adipose Tissue in Male Mice by Inhibiting TNF-α Gene Expression in Macrophages. *Endocrinology*, 156(10), pp.3680–94.

Taniguchi, C.M., Ueki, K. & Kahn, R., 2005. Complementary roles of IRS-1 and IRS-2 in the hepatic regulation of metabolism. *The Journal of Clinical Investigation*, 115(3), pp.718–27.

Tchkonia, T. et al., 2013. Mechanisms and metabolic implications of regional differences among fat depots. *Cell Metabolism*, 17(5), pp.644–56.

Teperino, R. et al., 2012. Hedgehog partial agonism drives Warburg-like metabolism in muscle and brown fat. *Cell*, 151(2), pp.414–26.

Tesco, G. et al., 2007. Depletion of GGA3 Stabilizes BACE and Enhances ?-Secretase Activity. *Neuron*, 54(5), pp.721–737.

Tharp, W.G. et al., 2016. Effects of glucose and insulin on secretion of amyloid-β by human adipose tissue cells. *Obesity*, 24(7), pp.1471–1479.

Thorens, B. & Mueckler, M., 2010. Glucose transporters in the 21st Century. *American Journal of Physiology - Endocrinology and Metabolism*, 298(2).

Tran, T.T. et al., 2008. Beneficial Effects of Subcutaneous Fat Transplantation on Metabolism. *Cell Metabolism*, 7(5), pp.410–420.

Trayhurn, P. & Beattie, J.H., 2017. Physiological role of adipose tissue: white adipose tissue as an endocrine and secretory organ. *Proceedings of the Nutrition Society*, 60, pp.329–339.

Ueki, K., Kondo, T. & Kahn, C.R., 2004. Suppressor of cytokine signaling 1 (SOCS-1) and SOCS-3 cause insulin resistance through inhibition of tyrosine phosphorylation of insulin receptor substrate proteins by discrete mechanisms. *Molecular and Cellular Biology*, 24(12), pp.5434–46.

Um, S.H. et al., 2004. Absence of S6K1 protects against age- and diet-induced obesity while enhancing insulin sensitivity. *Nature*, 431(7005), pp.200–205.

Unger, R., 1991. Diabetic hyperglycemia: link to impaired glucose transport in pancreatic beta cells. *Science*, 251(4998).

Vassar, R., 2014. BACE1 inhibitor drugs in clinical trials for Alzheimer's disease. *Alzheimer's Research & Therapy*, 6(9), p.89.

Vassar, R. et al., 1999. Beta-Secretase Cleavage of Alzheimer's Amyloid Precursor Protein by the Transmembrane Aspartic Protease BACE. *Science*, 286(5440), pp.735–741.

Vassar, R. et al., 2014. Function, therapeutic potential and cell biology of BACE proteases: current status and future prospects. *Journal of Neurochemistry*, 130(1), pp.4–28.

Vekrellis, K. et al., 2000. Neurons Regulate Extracellular Levels of Amyloid β-Protein via Proteolysis by Insulin-Degrading Enzyme. *Journal of Neuroscience*, 20(5).

Velliquette, R.A., T, O. & Vassar, R., 2006. Energy inhibition elevates beta-secretase levels and activity and is potentially amyloidogenic in

APP transgenic mice: possible early events in Alzheimer's disease pathogenesis. *Journal of Neuroscience*, 26(7), pp.2140–2142.

Virtanen, K.A. et al., 2009. Functional Brown Adipose Tissue in Healthy Adults. *New England Journal of Medicine*, 360(15), pp.1518–1525.

Virtue, S. & Vidal-Puig, A., 2013. Assessment of brown adipose tissue function. *Frontiers in Physiology*, 4, p.128.

Vitali, A. et al., 2012. The adipose organ of obesity-prone C57BL/6J mice is composed of mixed white and brown adipocytes. *Journal of Lipid Research*, 53(4), pp.619–29.

Wahli, W., Braissant, O. & Desvergne, B., 1995. Peroxisome proliferator activated receptors: transcriptional regulators of adipogenesis, lipid metabolism and more.... *Chemistry & Biology*, 2(5), pp.261–6.

Walter, J. et al., 2001. Phosphorylation regulates intracellular trafficking of beta-secretase. *The Journal of Biological Chemistry*, 276(18), pp.14634–41.

Wan, Z. et al., 2015. Role of amyloid b in the induction of lipolysis and secretion of adipokines from human adipose tissue. *Adipocyte*, 4(3), pp.212–216.

Wang, B., Wood, I.S. & Trayhurn, P., 2007. Dysregulation of the expression and secretion of inflammation-related adipokines by hypoxia in human adipocytes. *Pflugers Archiv : European journal of Physiology*, 455(3), pp.479–92.

Wang, Q. et al., 2011. Differential effect of weight loss with low-fat diet or high-fat diet restriction on inflammation in the liver and adipose tissue of mice with diet-induced obesity. *Atherosclerosis*, 219(1), pp.100–108.

Wang, Q.A. et al., 2013. Tracking adipogenesis during white adipose tissue development, expansion and regeneration. *Nature Medicine*, 19(10), pp.1338–44.

Wang, R. et al., 2013. Metabolic stress modulates Alzheimer's β-secretase gene transcription via SIRT1-PPARγ-PGC-1 in neurons. *Cell Metabolism*, 17(5), pp.685–94.

Wang, Y. et al., 2005. Comparison of abdominal adiposity and overall obesity in predicting risk of type 2 diabetes among men. *The*

American Journal of Clinical Nutrition, 81(3), pp.555–63.

Wang, Y. et al., 2014. Insulin-stimulated leptin secretion requires calcium and PI3K/Akt activation. *The Biochemical Journal*, 458(3), pp.491–8.

Wankhade, U.D. et al., 2016. Novel Browning Agents, Mechanisms, and Therapeutic Potentials of Brown Adipose Tissue. *BioMed research international*, 2016, p.2365609.

Weisberg, S.P. et al., 2006. CCR2 modulates inflammatory and metabolic effects of high-fat feeding. *The Journal of Clinical Investigation*, 116(1), pp.115–24.

Weisberg, S.P. et al., 2003. Obesity is associated with macrophage accumulation in adipose tissue. *Journal of Clinical Investigation*, 112(12), pp.1796–1808.

White, M.F. et al., 1998. Disruption of IRS-2 causes type 2 diabetes in mice. *Nature*, 391(6670), pp.900–904.

Whitehead, J.P. et al., 2006. Adiponectin – a key adipokine in the metabolic syndrome. *Diabetes, Obesity and Metabolism*, 8, pp.264–280.

Whitson, J.S., Selkoe, D.J. & Cotman, C.W., 1989. Amyloid beta protein enhances the survival of hippocampal neurons in vitro. *Science (New York, N.Y.)*, 243(4897), pp.1488–90.

WHO, 2017. Data and statistics.

WHO, 2016a. Diabetes. *WHO*. Available at: http://www.who.int/mediacentre/factsheets/fs312/en/ [Accessed June 30, 2017].

WHO, 2014. Obesity: Situations and Trends. Available at: http://www.who.int/gho/ncd/risk_factors/obesity_text/en/ [Accessed December 16, 2014].

WHO, 2016b. Obesity and overweight. *WHO*. Available at: http://www.who.int/mediacentre/factsheets/fs311/en/ [Accessed August 21, 2016].

Wilcox, G., 2005. Insulin and insulin resistance. *The Clinical Biochemist. Reviews*, 26(2), pp.19–39.

Willem, M. et al., 2006. Control of Peripheral Nerve Myelination by the -Secretase BACE1. *Science*, 314(5799), pp.664–666.

Winer, D.A. et al., 2011. B cells promote insulin resistance through modulation of T cells and production of pathogenic IgG antibodies. *Nature medicine*, 17(5), pp.610–7.

Won, J.C. et al., 2009. Central Administration of an Endoplasmic Reticulum Stress Inducer Inhibits the Anorexigenic Effects of Leptin and Insulin. *Obesity*, 17(10), pp.1861–1865.

Xie, L. et al., 2002. Alzheimer's β-Amyloid Peptides Compete for Insulin Binding to the Insulin Receptor. *Journal of Neuroscience*, 22(10).

Xu, A.W. et al., 2005. PI3K integrates the action of insulin and leptin on hypothalamic neurons. *The Journal of Clinical Investigation*, 115(4), pp.951–8.

Xu, H. et al., 2003. Chronic inflammation in fat plays a crucial role in the development of obesity-related insulin resistance. *Journal of Clinical Investigation*, 112(12), pp.1821–1830.

Xu, J. et al., 2009. Fibroblast Growth Factor 21 Reverses Hepatic Steatosis, Increases Energy Expenditure, and Improves Insulin Sensitivity in Diet-Induced Obese Mice. *Diabetes*, 58(1), pp.250–259.

Xu, W.L. et al., 2011. Midlife overweight and obesity increase late-life dementia risk: a population-based twin study. *Neurology*, 76(18), pp.1568–74.

Yamaguchi, N. et al., 2005. Adiponectin inhibits Toll-like receptor family-induced signaling. *FEBS Letters*, 579(30), pp.6821–6826.

Yan, R. et al., 2001. BACE2 Functions as an Alternative alpha-Secretase in Cells. *Journal of Biological Chemistry, 276(36), pp.34019-3427*

Yang, F. et al., 2015. Receptor for Advanced Glycation End-Product Antagonist Reduces Blood-Brain Barrier Damage After Intracerebral Hemorrhage. *Stroke*, 46(5), pp.1328–1336.

Yang, G. et al., 2009. Central role of ceramide biosynthesis in body weight regulation, energy metabolism, and the metabolic syndrome. *American Journal of Physiology - Endocrinology and Metabolism*, 297(1).

Yang, X. & Ruan, H.-B., 2015. Neuronal Control of Adaptive Thermogenesis. *Frontiers in Endocrinology*, 6, p.149.

Yates, S.L. et al., 2000. Amyloid beta and amylin fibrils induce increases in proinflammatory cytokine and chemokine production by THP-1 cells and murine microglia. *Journal of Neurochemistry*, 74(3), pp.1017–1025.

Ye, L. et al., 2013. Fat cells directly sense temperature to activate thermogenesis. *Proceedings of the National Academy of Sciences*, 110(30), pp.12480–12485.

Yoshida, T. et al., 1994. Anti-obesity and anti-diabetic effects of CL 316,243, a highly specific beta 3-adrenoceptor agonist, in yellow KK mice. *Life Sciences*, 54(7), pp.491–8.

Youssef-Elabd, E.M. et al., 2012. Acute and chronic saturated fatty acid treatment as a key instigator of the TLR-mediated inflammatory response in human adipose tissue, in vitro. *The Journal of Nutritional Biochemistry*, 23(1), pp.39–50.

Yuan, M. et al., 2001. Reversal of Obesity-and Diet-Induced Insulin Resistance with Salicylates or Targeted Disruption of Ikkβ. *Science*, 1673–1677(10), pp.251–2623.

Zabolotny, J.M. et al., 2002. PTP1B regulates leptin signal transduction in vivo. *Developmental Cell*, 2(4), pp.489–95.

Zaina, S. & Squire, S., 1998. The soluble type 2 insulin-like growth factor (IGF-II) receptor reduces organ size by IGF-II-mediated and IGF-II-independent mechanisms. *The Journal of Biological Chemistry*, 273(44), pp.28610–6.

Zhang, Q. et al., 1997. Insulin-like growth factor II signaling through the insulin-like growth factor II/mannose-6-phosphate receptor promotes exocytosis in insulin-secreting cells. *Proceedings of the National Academy of Sciences of the United States of America*, 94(12), pp.6232–7.

Zhang, X. et al., 2007. Hypoxia-inducible factor 1alpha (HIF-1alpha)-mediated hypoxia increases BACE1 expression and beta-amyloid generation. *The Journal of Biological Chemistry*, 282(15), pp.10873–80.

Zhang, Y. et al., 2012. Amyloid-β induces hepatic insulin resistance by activating JAK2/STAT3/SOCS-1 signaling pathway. *Diabetes*, 61(6),

pp.1434–1443.

Zhang, Y. et al., 2013. Amyloid-β induces hepatic insulin resistance in vivo via JAK2. *Diabetes*, 62(4), pp.1159–1166.

Zhang, Y. et al., 1994. Positional cloning of the mouse obese gene and its human homolog. *Nature*, 372, pp.425–432.

Zhou, Y. & Rui, L., 2013. Leptin signaling and leptin resistance. *Frontiers of Medicine*, 7(2), pp.207–22.

Zuchner, T., Perez-Polo, J.R. & Schliebs, R., 2004. Beta-secretase BACE1 is differentially controlled through muscarinic acetylcholine receptor signaling. *Journal of Neuroscience Research*, 77(2), pp.250–257.